LIGAND VARIATION IN MOLYBDENUM IMIDO ALKYLIDENE COMPLEXES: A SYNTHETIC, STRUCTURAL, AND CATALYTIC STUDY

by

ALEJANDRO G. LICHTSCHEIDL

B.S. (*summa cum laude*) in Chemistry
B.S. (*magna cum laude*) in Biochemistry and Molecular Biology
University of California Irvine, Irvine, CA
(2006)

Submitted to the Department of Chemistry
in Partial Fulfillment of the Requirements
for the Degree of

DOCTOR OF PHILOSOPHY

at the
MASSACHUSETTS INSTITUTE OF TECHNOLOGY
May 2012
[June 2012]

Signature of Author

Department of Chemistry
May 1st, 2012

Certified by

Richard R. Schrock
Frederick G. Keyes Professor of Chemistry
Thesis Supervisor

Accepted by

Robert W. Field
Haslam and Dewey Professor of Chemistry
Chairman, Departmental Committee on Graduate Students

This doctoral thesis has been examined by a Committee of the Department of Chemistry as follows:

Professor Christopher C. Cummins

Chairman

Professor Richard R. Schrock

Thesis Supervisor

Professor Mircea Dincă

Dedicated to the memory of

Consuelo Mendez

LIGAND VARIATION IN MOLYBDENUM IMIDO ALKYLIDENE COMPLEXES: A SYNTHETIC, STRUCTURAL, AND CATALYTIC STUDY

by

ALEJANDRO G. LICHTSCHEIDL

Submitted to the Department of Chemistry, May 2012 in
Partial Fulfillment of the Requirements for the Degree of
Doctor of Philosophy in Chemistry

ABSTRACT

Chapter 1

A general introduction is given.

Chapter 2

The biscarboxylate species, $Mo(NR)(CHCMe_2Ph)(O_2CPh_3)_2$ (R = 2,6-*i*-$Pr_2C_6H_3$, 2,6-$Me_2C_6H_3$, 2-*t*-BuC_6H_4, or 1-adamantyl) are compared to newly synthesized bis(terphenylcarboxylate) species, $Mo(NR)(CHCMe_2Ph)(O_2CTer)_2$ (Ter = 2,6-diphenyl-4-methylphenyl or 2,6-diphenyl-4-methoxyphenyl). Preparation of bis(terphenylcarboxylate) species was accomplished through protonolysis of $Mo(NR)(CHCMe_2R')(Me_2Pyr)_2$ with two equivalents of $TerCO_2H$ and one of them was characterized through X-ray crystallography. Photolysis experiments of many of the biscarboxylate complexes led to rate constants for the converstion of *anti* to *syn* species, which are much slower than bisalkoxide species. Trimethylphosphine adducts of selected triphenylacetate complexes have been isolated and studied in solution. Protonolysis of $Mo(NAr)(CHCMe_2R')(Me_2Pyr)_2$ (Ar = 2,6-*i*-$Pr_2C_6H_3$) with one equivalent of $TerCO_2H$ led to the isolation of a handful of monocarboxylate species, $Mo(NAr)(CHCMe_2Ph)(O_2CAr')(Me_2Pyr)$. An X-ray structure of one of them was also characterized. Several of the bis(triphenylacetate) complexes and all of the monocarboxylates are active initiators for the regioselective polymerization of diethyl dipropargylmalonate (DEPDM). In the case of the latter compounds, activity towards olefins is also observed and briefly mentioned.

Chapter 3

Monaryloxide pyrrolide (MAP) molybdenum imido alkylidene complexes of the type $Mo(NAr^X)(CHCMe_2R)(Me_2Pyr)(OR')$ (Me_2Pyr = 2,5-dimethylpyrrolide) have been prepared in which NAr^X is an *ortho*-substituted phenylimido group (X = Cl (NAr^{Cl}), CF_3 (NAr^{CF3}), *i*-Pr (NAr^{iPr}), *t*-Bu (NAr^{tBu}), mesityl (NAr^M), or TRIP (TRIP = triisopropylphenyl; NAr^T)) and OR' = O-2,3,5,6-$(C_6H_5)_4C_6H$ (OTPP), O-2,6-$(2,4,6\text{-}Me_3C_6H_2)_2C_6H_3$ (OHMT), or O-2,6-$(2,4,6\text{-}i\text{-}Pr_3C_6H_2)_2C_6H_3$ (OHIPT). The object was to explore to what extent relatively "large" NAr^M or NAr^T ligands would alter the performance of MAP catalysts in reactions that have been proposed to depend upon the relative size of the imido and OR' groups. Preliminary studies employing the

ring-opening metathesis polymerization of 5,6-dicarbomethoxynorbornadiene as a measure of selectivity suggest that a single *ortho*-substituent in the phenylimido group, even in an NAr^M or NAr^T group, does not produce any unique behavior and that the outcome of the ROMP reaction correlates with the overall relative size of the imido and OR' group. Single crystal X-ray structures of six species that contain the new NAr^M or NAr^T groups are reported.

Chapter 4

Several bipyridine adducts of molybdenum imido alkylidene bispyrrolide complexes of the type $Mo(NR)(CHCMe_2Ph)(Pyr)_2(bipy)$ (**9-15**; R = 2,6-*i*-$Pr_2C_6H_3$ (Ar), adamantyl (Ad), 2,6-$Me_2C_6H_3$ (Ar'), 2-ClC_6H_4 (Ar^{Cl}), 2-*i*-PrC_6H_4 (Ar^{iPr}), 2-*t*-BuC_6H_4 (Ar^{tBu}), 2-MesitylC_6H_4 (Ar^M), respectively; have been prepared using three different methods. Up to three isomers of the adducts are observed that are proposed to be the *trans* and two possible *cis* pyrrolide isomers of *syn* alkylidenes. Sonication of a mixture containing **9-15**, HMTOH (2,6-(2',4',6'-$Me_3C_6H_2)_2C_6H_3OH$), and $ZnCl_2$(dioxane) led to the formation of MAP species of the type $Mo(NR)(CHCMe_2Ph)(Pyr)(OHMT)$ (**16-22**), which were isolated by filtration and purified by recrystallization. DCMNBD (2,3-dicarbomethoxynorbornadiene) is polymerized employing **16-22** as initiators to yield >98% *cis,syndiotactic* poly(DCMNBD). Attempts to prepare bipy adducts of bisdimethylpyrrolide complexes led to the formation of imido alkylidyne complexes of the type $Mo(NR)(CHCMe_2R')(Me_2Pyr)(bipy)$ (Me_2Pyr = 2,5-dimethylpyrrolide); **23-28**) through a ligand-induced migration of an alkylidene α proton to a dimethylpyrrolide ligand. X-ray structures of $Mo(NAr)(CHCMe_2Ph)(Pyr)_2(bipy)$ (**9**), $Mo(NAr^{iPr})(CHCMe_2Ph)(Pyr)(OHMT)$ (**20**), $Mo(NAr)(CCMe_2Ph)(Me_2Pyr)(bipy)$ (**23**), $Mo(NAr')(CCMe_2Ph)(Me_2Pyr)(bipy)$ (**24**), $Mo(NAr^T)(CCMe_3)(Me_2Pyr)(bipy)$ (Ar^T = 2-(2',4',6'-*i*-$Pr_3C_6H_2)C_6H_4$, **28**) showed structures with the expected characteristic bond lengths and angles.

Chapter 5

The formation of $Mo(NAr)(CHCMe_2Ph)(OC(CF_3)_2(CH_3))(O_2CTer_{Me})$ (Ar = 2,6-*i*-$Pr_2C_6H_3$, O_2CTer_{Me} = 4,4'-dimethylterphenylcarboxylate, **1**) from $Mo(NR)(CHCMe_2Ph)(OC(CF_3)_2(CH_3))_2$ via protonolys with $Ter_{Me}CO_2H$, as well as formation of complexes of the general formula $Mo(NR)(CHCMe_2Ph)(OC(CF_3)_2(CH_3))(X)$ (R = 2,6-*i*$Pr_2C_6H_3$ (Ar), **2**; 2,6-$Me_2C_6H_3$ (Ar'), **3**; 2-*i*PrC_6H_4 (Ar^{iPr}), **4**; 1-adamantyl (Ad), **5**; X = 2,2',4,4',6,6'-hexamethylterphenoxide (HMTO)) (2,6-$Me_2C_6H_3$ (Ar'), **6**, 2-*i*PrC_6H_4 (Ar^{iPr}), **7**; X = 2,2',4,4',6,6'-hexamethylterphenylamine (HMT(H)N)) (R = 1-adamantyl, X = 2,2',4,4',6,6'-hexamethylterphenyl (HMT), **8**) via salt-metathesis of $Mo(NR)(CHCMe_2Ph)(OC(CF_3)_2(CH_3))_2$ with one equivalent of LiX is presented as an efficient synthetic route for the preparation of monoalkoxide monoanionic (MAX) complexes. The X-ray studies of **5**, **7**, and **8** show that complexes **5** and **8** have similar structures; whereas **7** differs considerably due to the overall spacial arrangement of the N(H)HMT in the complex, which is orthogonal to the arrangement of OHMT in **5** or HMT in **8**. The distance of the terphenyl backbone is shown to be one Angstrom shorter for **8**, in comparison to **5** and **7**, which results in failed attempts to prepare $Mo(NR)(CHCMe_2Ph)(OC(CF_3)_2(CH_3))$(HMT) complexes with bigger R groups. The catalytic reactivity complexes **1-8** is probed with diallyl ether (DAE), 1-hexene, 1-octene, and dicarbomethoxynorbornadiene (DCMNBD). For comparison, the same olefin-metathesis reactions are carried-out with the analogous monoanionic monopyrrolide (MXP) complexes of general formula $Mo(NR)(CHCMe_2Ph)(Pyr)(X)$ (Pyr = C_4H_4N, 2,5-$Me_2C_4H_2N$). Overall, the reactivity of MAX and MXP complexes differs least when *cis* or *trans*

bond formation is involved, and differs most when tacticity is considered, showing that during catalysis the transition states may differ significantly between the two kinds of complexes.

Appendix

The preparation of pure (*R*)-Mo(NAr)(CHCMe$_2$Ph)(Me$_2$Pyr)(OR*) (Ar = 2,6-*i*Pr$_2$C$_6$H$_3$, R*O = (1*S*,2*S*,4*R*)-2-(4-ClC$_6$H$_4$)-1,7,7-Me$_3$-bicyclo[2.2.1]heptan-2-oxide), Me$_2$Pyr = 2,5-Me$_2$C$_4$H$_2$N, **1**) and Mo(NAd)(CHCMe$_2$Ph)(OR$^+$)$_2$ (Ad = 1-adamantyl, R$^+$O = 3,3'-Br$_2$-2'-(OSi(Me$_2$)$_2$(*t*-Bu))-5,5',6,6',7,7',8,8'-H$_8$-[1,1'-binaphthalen]-2-oxide, **21**) are discussed. X-ray studies of both complexes are also presented. The polymerization of diethyl dipropargylmalonate (DEPDM) is probed with a variety of monoalkoxidemonopyrrolide (MAP) complexes, including **1**, that either contain PMe$_3$ bound to the metal center or not. In addition, a variety of bisalkoxide/bisphenoxide complexes, among them **21**, are also used to polymerize DEPDM.

Thesis Supervisor: Richard R. Schrock
Title: Frederick G. Keyes Professor of Chemistry

TABLE OF CONTENTS

LIST OF FIGURES

LIST OF TABLES

LIST OF SCHEMES

LIST OF ABBREVIATIONS

3,5-HIPTO	3,5-bis(2',4',6'-triisopropylphenyl)phen-1-oxide
Ad	1-adamantyl
Anal. Calcd	elemental analysis calculated
Anal. Found	elemental analysis found
Anti	alkylidene rotamer with alkyl group directed away from the imido group
Ar	2,6-diisopropylphenyl
Ar′	2,6-dimethylphenyl
Ar^{CF3}	2-(trifluoromethyl)phenyl
Ar^{Cl}	2-chlorophenyl
Ar^{iPr}	2-isopropylphenyl
Ar^{Ph}	2-biphenyl
Ar^{m}	3,5-dimethylphenyl
Ar^{M}	2-(2',4',6'-trimethylphenyl)phenyl
Ar^{tBu}	2-*t*ert-butylphenyl
Ar^{T}	2-(2',4',6'-triisopropylphenyl)phenyl
Bipy	2,2'-bipyridine
δC_{α}	^{13}C chemical shift in parts per million (ppm)
δH_{α}	^{1}H chemical shift in parts per million (ppm)
DAE	diallyl ether
DCMNBD	2,3-dicarbomethoxynorborna-1,5-diene
DEAPM	diethylester-2-allyl-2-propargylmalonate
DEDPM	diethylester-2,2-dipropargylmalonate
DFT	density functional theory
DIDPM	diisopropylester-2,2-dipropargylmalonate
DIPP	2,6-diisopropylphen-1-oxide
DME	1,2-dimethoxyethane
DTDPM	di-*tert*-butylester-2,2-dipropargylmalonate
ε	molar absorptivity coefficient
g	gram
h	hour
HIPT	2,6-bis(2',4',6'-triisopropylphenyl)phenyl
HIPTI	2,6-bis(2',4',6'-triisopropylphenyl)phenyl-2-iodide
HIPTO	2,6-bis(2',4',6'-triisopropylphenyl)phen-2-oxide
HMT	2,6-bis(2',4',6'-trimethylphenyl)phenyl
HMT(H)N	2,6-bis(2',4',6'-trimethylphenyl)phenyl-2-amide
HMTI	2,6-bis(2',4',6'-trimethylphenyl)phenyl-2-iodide
$HMTNH_2$	2,6-bis(2',4',6'-trimethylphenyl)phenyl-2-amine
HMTO	2,6-bis(2',4',6'-trimethylphenyl)phenoxide
HPLC	high performance liquid chromatography
J_{AB}	coupling constant between nuclei A and B
$k_{a/s}$	rate constant for the conversion of *anti*–alkylidene to *syn*-alkylidene rotamer
$k_{s/a}$	rate constant for the conversion of *syn*–alkylidene to *anti*–alkylidene rotamer
L	liter

M	molar
MAP	monoalkoxide monopyrrolide alkylidene imido molybdenum complex
MAX	monoalkoxide monoanionic ligand alkylidene imido molybdenum complex
Me	methyl
Mes	mesityl
Mesityl	2,4,6-trimethylphenyl
Me_2Pyr	2,5-dimethylpyrrolide
Me_4Pyr	2,3,4,5-tetramethylpyrrolide
min	minutes
mL	milliliter
mM	millimolar
mmol	millimole
mol	mole
MOCAP	monocarboxylate monopyrrolide alkylidene imido molybdenum complex
MXP	monoanianic ligand monopyrrolide alkylidene imido molybdenum complex
n-BuLi	*n*-butyl lithium
nm	nanometer
NMR	nuclear magnetic resonance
o	*ortho*
$OBITETBr_2$	3,3'-Br_2-2'-(OSi(Me_2)$_2$(*t*-Bu))-5,5',6,6',7,7',8,8'-H_8-[1,1'-binaphthalen]-2-oxide)
$OBITETX_2$	3,3'-X_2-2'-(OSi(Me_2)$_2$(*t*-Bu))-5,5',6,6',7,7',8,8'-H_8-[1,1'-binaphthalen]-2-oxide)
O-*i*Pr^{F6}	1,1,1,3,3,3-hexafluoroisopropoxide
OTf	triflate
OR_{F6}	hexafluoro-*tert*-butoxide
OR_{F9}	perfluoro-tert-butoxide
p	*para*
Ph	phenyl
pK_a	negative logarithm-base-ten of the acid dissociation constant
pK_b	negative logarithm-base-ten of the base dissociation constant
Pyr	pyrrolide
R*O	(1*S*,2*S*,4*R*)-2-(4-ClC_6H_4)-1,7,7-Me_3-bicyclo[2.2.1]heptan-2-oxide
R^+	Br_2BITET
RCM	ring closing metathesis
ROMP	ring opening metathesis polymerization
SP	square pyramid
Syn	alkylidene rotamer with alkyl group directed towards the imido group
TBS	*tert*-butyldimethylsilyl
TBP	trigonal bipyramid
Ter	2,6-terphenyl
Ter_{Me}	2,6-bis(4'-methylphenyl)phenyl
Ter_{OMe}	2,6-bis(4'-methoxyphenyl)phenyl
TIPT	2,2',6,6'-tetraisopropylterphenyl
TIPTI	2,2',6,6'-tetraisopropylterphenyl-2-iodide
TIPTO	2,2',6,6'-tetraisopropylterphen-2-oxide

TPP	2,3,5,6-tetraphenylphenoxide
Triflate	trifluoromethylsulfonate
TRIP	2,4,6-triisopropylphenyl
μg	microgram
μM	micromolar
μmol	micromole
UV-vis	ultraviolet and visible light
wk	weeks
X	anionic ligand

LIST OF COMPOUND NUMBERS

Compound Name of Formula

CHAPTER 2

1a	$Mo(NAr)(CHCMe_2Ph)(O_2CCPh_3)_2$*
1b	$Mo(NAd)(CHCMe_2Ph)(O_2CCPh_3)_2$*
1c	$Mo(NAr')(CHCMe_2Ph)(O_2CCPh_3)_2$*
1d	$Mo(NAr^{tBu})(CHCMe_3)(O_2CCPh_3)_2$*
2a	$Mo(NAr)(CHCMe_2Ph)(O_2CTer_{Me})_2$
2b	$Mo(NAr)(CHCMe_2Ph)(O_2CTer_{OMe})_2$
2c	$Mo(NAd)(CHCMe_2Ph)(O_2CTer_{Me})_2$
2d	$Mo(NAd)(CHCMe_2Ph)(O_2CTer_{OMe})_2$
3a	$Mo(NAr)(CHCMe_2Ph)(Me_2Pyr)(O_2CTRIP)$
3b	$Mo(NAr)(CHCMe_2Ph)(Me_2Pyr)(O_2CTer_{Me})$
3c	$Mo(NAr)(CHCMe_2Ph)(Me_2Pyr)(O_2CTer_{OMe})$
3d	$Mo(NAr)(CHCMe_2Ph)(Me_2Pyr)(O_2CHIPT)^{\#}$

CHAPTER 3

1	$Mo(NAr^{Cl})_2(Cl)_2(DME)$
2	$Mo(NAr^{M})_2(Cl)_2(THF)_2 \cdot 2THF$
3	$Mo(NAr^{T})_2(Cl)_2(DME)$
4	$Mo(NAr^{Cl})_2(CH_2CMe_2Ph)_2$
5	$Mo(NAr^{M})_2(CH_2CMe_2Ph)_2$
6	$Mo(NAr^{T})_2(CH_2CMe_3)_2$
7	$Mo(NAr^{T})_2(CH_3)_2$
8	$Mo(NAr^{Cl})(CHCMe_2Ph)(OTf)_2(DME)$
9	$Mo(NAr^{M})(CHCMe_2Ph)(OTf)_2(DME)$
10	$Mo(NAr^{T})(CHCMe_3)(OTf)_2(DME)$
11	$Mo(NAr^{Cl})(CHCMe_2Ph)(Me_2Pyr)_2$
12	$Mo(NAr^{CF3})(CHCMe_3)(Me_2Pyr)_2$
13	$Mo(NAr^{iPr})(CHCMe_2Ph)(Me_2Pyr)_2$
14	$Mo(NAr^{tBu})(CHCMe_3)(Me_2Pyr)_2$
15	$Mo(NAr^{tBu})(CHCMe_2Ph)(Me_2Pyr)_2$
16	$Mo(NAr^{M})(CHCMe_2Ph)(Me_2Pyr)_2$
17	$Mo(NAr^{T})(CHCMe_3)(Me_2Pyr)_2$
18	$Mo(NAr^{M})(CHCMe_2Ph)(OTPP)_2$
19	$Mo(NAr^{T})(CHCMe_2Ph)(Me_2Pyr)(OTPP)$
20	$Mo(NAr^{Cl})(CHCMe_2Ph)(Me_2Pyr)(OHMT)$
21	$Mo(NAr^{CF3})(CHCMe_3)(Me_2Pyr)(OHMT)$
22	$Mo(NAr^{CF3})(CHCMe_2Ph)(Me_2Pyr)(OHMT)$
23	$Mo(NAr^{iPr})(CHCMe_2Ph)(Me_2Pyr)(OHMT)$
24	$Mo(NAr^{tBu})(CHCMe_3)(Me_2Pyr)(OHMT)$
25	$Mo(NAr^{tBu})(CHCMe_2Ph)(Me_2Pyr)(OHMT)$

26	$Mo(NAr^{M})(CHCMe_2Ph)(Me_2Pyr)(OHMT)$
27	$Mo(NAr^{M})(CHCMe_2Ph)(Me_2Pyr)(OHIPT)$
28	$Mo(NAr^{T})(CHCMe_3)(Me_2Pyr)(OHMT)$
29	$Mo(NAr^{T})(CHCMe_3)(Me_2Pyr)(OHIPT)^{\#}$

CHAPTER 4

1	$[Mo(NAr^{Ph})(CHCMe_3)(Pyr)_2]_2$
2	$Mo(NAr)(CHCMe_2Ph)(OTf)_2(bipy)$
3	$Mo(NAd)(CHCMe_2Ph)(OTf)_2(bipy)$
4	$Mo(NAr')(CHCMe_2Ph)(OTf)_2(bipy)$
5	$Mo(NAr^{Cl})(CHCMe_2Ph)(OTf)_2(bipy)$
6	$Mo(NAr^{iPr})(CHCMe_2Ph)(OTf)_2(bipy)$
7	$Mo(NAr^{tBu})(CHCMe_2Ph)(OTf)_2(bipy)$
8	$Mo(NAr^{M})(CHCMe_2Ph)(OTf)_2(bipy)$
9	$Mo(NAr)(CHCMe_2Ph)(Pyr)_2(bipy)$
10	$Mo(NAd)(CHCMe_2Ph)(Pyr)_2(bipy)$
11	$Mo(NAr')(CHCMe_2Ph)(Pyr)_2(bipy)$
12	$Mo(NAr^{Cl})(CHCMe_2Ph)(Pyr)_2(bipy)$
13	$Mo(NAr^{iPr})(CHCMe_2Ph)(Pyr)_2(bipy)$
14	$Mo(NAr^{tBu})(CHCMe_2Ph)(Pyr)_2(bipy)$
15	$Mo(NAr^{M})(CHCMe_2Ph)(Pyr)_2(bipy)$
16	$Mo(NAr)(CHCMe_2Ph)(Pyr)(OHMT)$
17	$Mo(NAd)(CHCMe_2Ph)(Pyr)(OHMT)$
18	$Mo(NAr')(CHCMe_2Ph)(Pyr)(OHMT)$
19	$Mo(NAr^{Cl})(CHCMe_2Ph)(Pyr)(OHMT)$
20	$Mo(NAr^{iPr})(CHCMe_2Ph)(Pyr)(OHMT)$
21	$Mo(NAr^{tBu})(CHCMe_2Ph)(Pyr)(OHMT)$
22	$Mo(NAr^{M})(CHCMe_2Ph)(Pyr)(OHMT)$
23	$Mo(NAr)(\equiv CCMe_2Ph)(Me_2Pyr)(bipy)$
24	$Mo(NAr')(\equiv CCMe_2Ph)(Me_2Pyr)(bipy)$
25	$Mo(NAr^{CF3})(\equiv CCMe_2Ph)(Me_2Pyr)(bipy)$
26	$Mo(NAr^{iPr})(\equiv CCMe_2Ph)(Me_2Pyr)(bipy)$
27	$Mo(NAr^{M})(\equiv CCMe_2Ph)(Me_2Pyr)(bipy)$
28	$Mo(NAr^{T})(\equiv CCMe_2Ph)(Me_2Pyr)(bipy)$

CHAPTER 5

1	$Mo(NAr)(CHCMe_2Ph)(OF_6)(O_2CTer_{Me})$
2	$Mo(NAr)(CHCMe_2Ph)(OF_6)(OHMT)$
3	$Mo(NAr')(CHCMe_2Ph)(OF_6)(OHMT)$
4	$Mo(NAr^{iPr})(CHCMe_2Ph)(OF_6)(OHMT)$
5	$Mo(NAd)(CHCMe_2Ph)(OF_6)(OHMT)$
6	$Mo(NAr')(CHCMe_2Ph)(OF_6)(N(H)HMT)$
7	$Mo(NAr^{iPr})(CHCMe_2Ph)(OF_6)(N(H)HMT)$
8	$Mo(NAd)(CHCMe_2Ph)(OF_6)(HMT)$

9	$Mo(NAr^{m})(CHCMe_2Ph)(OF_6)(HMT)^{\#}$
10	$Mo(NAr')(CHCMe_2Ph)(OF_6)(HMT)^{\#}$
11	$Mo(NAr)(CHCMe_2Ph)(OF_6)(HMT)^{\#}$
12	$Mo(NAd)(CHCMe_2Ph)(OF_6)(TIPT)^{\#}$
13	$Mo(NAr')(CHCMe_2Ph)(OF_6)(TIPT)^{\#}$
14	$Mo(NAr)(CHCMe_2Ph)(OF_6)(TIPT)^{\#}$
15	$Mo(NAd)(CHCMe_2Ph)(OF_9)_2$
16	$Mo(NAd)(CHCMe_2Ph)(OF_9)(HMT)^{\#}$

APPENDIX

1	$Mo(NAr)(CHCMe_2Ph)(Me_2Pyr)(OR^*)$
2	$Mo(NAr)(CHCMe_2Ph)(Me_2Pyr)(OR^+)^*$
3	$Mo(NAr)(CHCMe_2Ph)(Me_2Pyr)(OF_6)^*$
3a	$Mo(NAr)(CHCMe_2Ph)(Me_4Pyr)(OF_6)(PMe_3)^*$
3b	$Mo(NAr)(CHCMe_2Ph)(Ph_2Pyr)(OF_6)^*$
3c	$Mo(NAr)(CHCMe_2Ph)(Ph_2Pyr)(OF_6)(PMe_3)^*$
3d	$Mo(NAr)(CHCMe_2Ph)(i\text{Pr}_2Pyr)(OF_6)^*$
3e	$Mo(NAr)(CHCMe_2Ph)(i\text{Pr}_2Pyr)(OF_6)(PMe_3)^*$
4	$Mo(NAr)(CHCMe_2Ph)(Me_2Pyr)(O\text{-}i\text{Pr})^*$
5	$Mo(NAr)(CHCMe_2Ph)(Me_2Pyr)(OAr)^*$
6	$Mo(NAr)(CHCMe_2Ph)(Me_2Pyr)(OSi(O\text{-}t\text{-}Bu)_3)^*$
7	$Mo(NAr)(CHCMe_2Ph)(Me_2Pyr)(OSiPh_3)^*$
8	$Mo(NAr)(CHCMe_2Ph)(Me_2Pyr)(O\text{-}2,4\text{-}(t\text{-}Bu)_2\text{-}6\text{-}BrC_6H_2)^*$
9	$Mo(NAr)(CHCMe_2Ph)(OR^+)_2^*$
10	$Mo(NAr)(CHCMe_2Ph)(OC(CH_3)_2(CF_3))_2^*$
11	$Mo(NAr)(CHCMe_2Ph)(OF_9)_2^*$
12	$Mo(NAr)(CHCMe_2Ph)(OC(CH_3)(C_6F_5)_2)_2^*$
13	$Mo(NAr)(CHCMe_2Ph)(OSi(CH_3)_2(t\text{-}Bu))_2^*$
14	$Mo(NAr)(CHCMe_2Ph)(OAr)_2^*$
15	$Mo(NAr')(CHCMe_2Ph)(OF_6)_2^*$
16	$Mo(NAr')(CHCMe_2Ph)(OAr)_2^*$
17	$Mo(NAr^{CF3})(CHCMe_2Ph)(OF_6)_2^*$
18	$Mo(NAr^{tBu})(CHCMe_2Ph)(OF_6)_2^*$
19	$Mo(NAr^{Ph})(CHCMe_2Ph)(OF_6)_2^*$
20	$Mo(NAd)(CHCMe_2Ph)(OF_6)_2^*$
21	$Mo(NAd)(CHCMe_2Ph)(OR^+)_2$

*compounds were previously reported by other researchers
compounds were only made *in situ*

CHAPTER 1

General Introduction

Olefin metathesis is a reaction wherein two alkene moieties react to exchange functional groups,[1] as depicted in equation 1. This reaction was the subject of the 2005 Nobel Prize in Chemistry, which was awarded to Y. Chauvin, R. R. Schrock, and R. H. Grubbs. Olefin metathesis was first observed as a minor reaction during the polymerization of ethylene in the presence of certain metals.[2] Early attempts to design a better catalytic system involved the use of MoO_3, WCl_6, $WOCl_4$, and Re_2O_7 in the presence of alkylating agents (e.g. AlR_3, LiR, SnR_4) or alumina in ethyl alcohol or chlorobenzene.[3] The systems mentioned above did yield high turnover numbers (100 TON/sec) for olefin metathesis but their lifetimes were short and the concentration of active species was too small to determine its nature. In addition, tolerance to functionalities was limited.

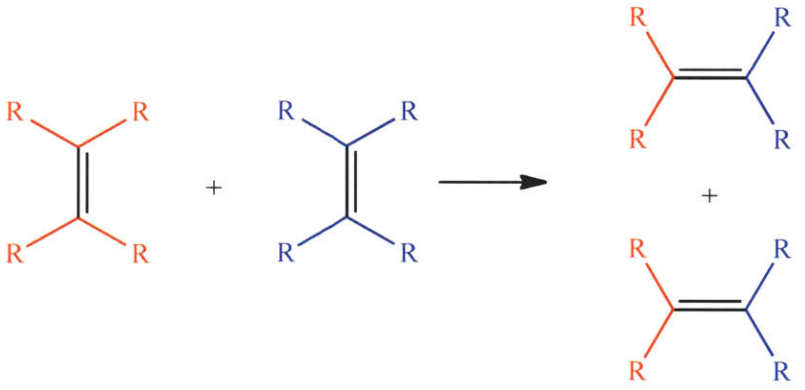

(1)

Y. Chauvin first proposed that the active species in the reaction had to involve a metal-carbon double bond and the reaction would proceed via a [2 + 2] addition of the olefin to the metal center forming a metallacyclobutane intermediate. The metallacyclobutane can then undergo a retro [2 + 2] reaction to reform the starting material or generate a new olefin, Scheme 1.[4]

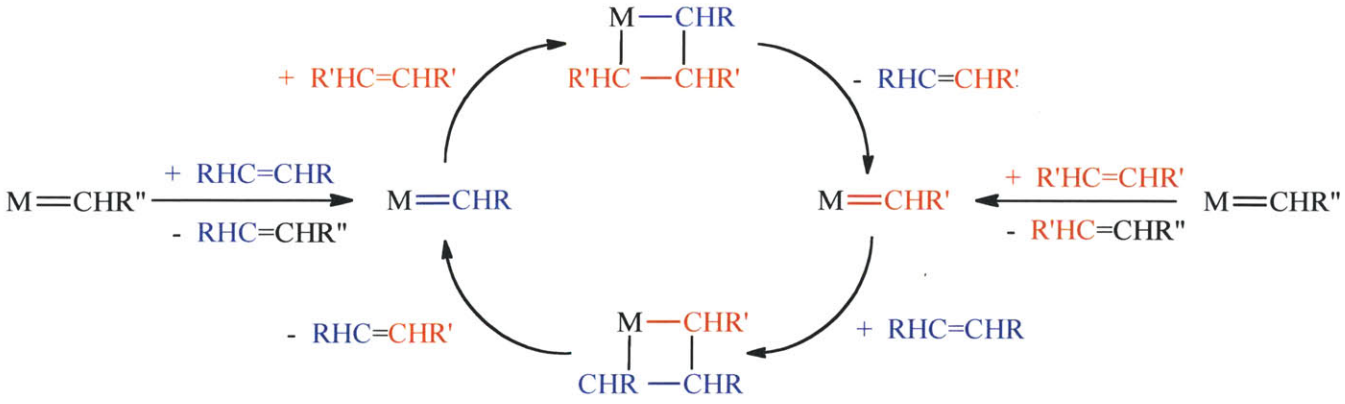

Scheme 1 – Chauvin's proposed mechanism for olefin metathesis.

Synthesis of the first metal carbon double bond (carbene) was accomplished by Fisher in 1964. The carbene was characterized by the presence of a π-donor group, as in $(CO)_5Cr{=}C(OMe)(Ph)$, which makes the carbene of singlet character.[19] A decade later, the first high-oxidation state transition metal carbon double-bond bearing no π-donor group (alkylidene) was prepared in 1974 by Schrock et. al. by treatment of $Ta(CH_2\text{-}t\text{-}Bu)_3(Cl)_2$ with two equivalents of $LiCH_2\text{-}t\text{-}Bu$ to generate $Ta(=CH\text{-}t\text{-}Bu)(CH_2\text{-}t\text{-}Bu)_3$.[5] Alkylidenes differ from carbenes in that the alkylidene has triplet character. Compounds related to tantalum alkylidenes did not react catalytically with olefins, but formed a metallacyclobutane that rearranged to form an olefin complex. Similarly, titanium alkylidene complexes were developed and investigated, were active only for ring-opening metathesis polymerization (ROMP) reactions.[6] Titanium and tantalum alkylidene complexes paved the way for the preparation of the better known Group VIB metal alkylidene complexes. Preparation of tungsten alkylidene oxo complexes like $WO(CH\text{-}t\text{-}Bu)Cl_2(PEt_3)_2$ was achieved by Schrock by treating $WO(O\text{-}t\text{-}Bu)_4$ with one equivalent of $Ta(CH\text{-}t\text{-}Bu)Cl_3(PEt_3)_2$.[20a] Similarly, Osborn prepared $M(O)(CH\text{-}t\text{-}Bu)(CH_2\text{-}t\text{-}Bu)(X)$ complexes from $M(O)(CH_2\text{-}t\text{-}Bu)_3(X)$ in the presence of a Lewis acid.[20b-c] Almost a decade later, Group VIB alkylidene imido of the general formula $M(NR)(CHR')(OR")_2$, where M = Mo, W; R = alkyl or phenyl; R' = *tert*-butyl, CMe_2Ph, $SiMe_3$; and R" = alkyl, phenyl were prepared. Complexes of this kind can react with olefins catalytically in a metathetical fashion. The metal in these catalysts are all in the highest oxidation state (+6), which makes the metal relatively Lewis acidic. The ancillary ligands serve to protect the metal sterically from intermolecular or intramolecular decomposition.[7]

Preparation of $M(NR)(CHR')(OR")_2$ species has been ongoing in the Schrock laboratory during the last 20 years of the 20th century. The best and most accessible route to catalysts of this type involves a four-step synthesis when M = Mo and a five-step synthesis when M = W. The overall synthetic scheme is shown in Scheme 2.[8]

In the case of M = W, the first step involves preparation of WO_2Cl_2 from WCl_6 by treatment with hexamethyldisiloxane. Preparation of WO_2Cl_2 is required since the next reaction cannot be carried out with Na_2WO_4. The next step is the preparation of $M(NR)_2Cl_2(DME)$ from WO_2Cl_2 (if M = W) or $(NH_4)_2Mo_2O_7$ (if M = Mo) by treatment with RNH_2, TMSCl, base in a coordinating solvent (DME), followed by alkylation with a Grignard reagent to form $M(NR)_2(CH_2R')_2$. Treatment of the latter with three equivalents of triflic acid (TfOH) in the presence of a coordinating solvent (DME) generates the alkylidene complex $M(NR)(CHR')(OTf)_2(DME)$. This alkylidene complex is often referred to as the universal catalyst precursor because treatment with two equivalents of LiOR" yields $M(NR)(CHR')(OR")_2$ complexes. Moreover, treatment of the universal precursor with one equivalent of chiral binaphtholate or biphenolate dianions yields the corresponding Mo(NR)(CHR')(diolate)

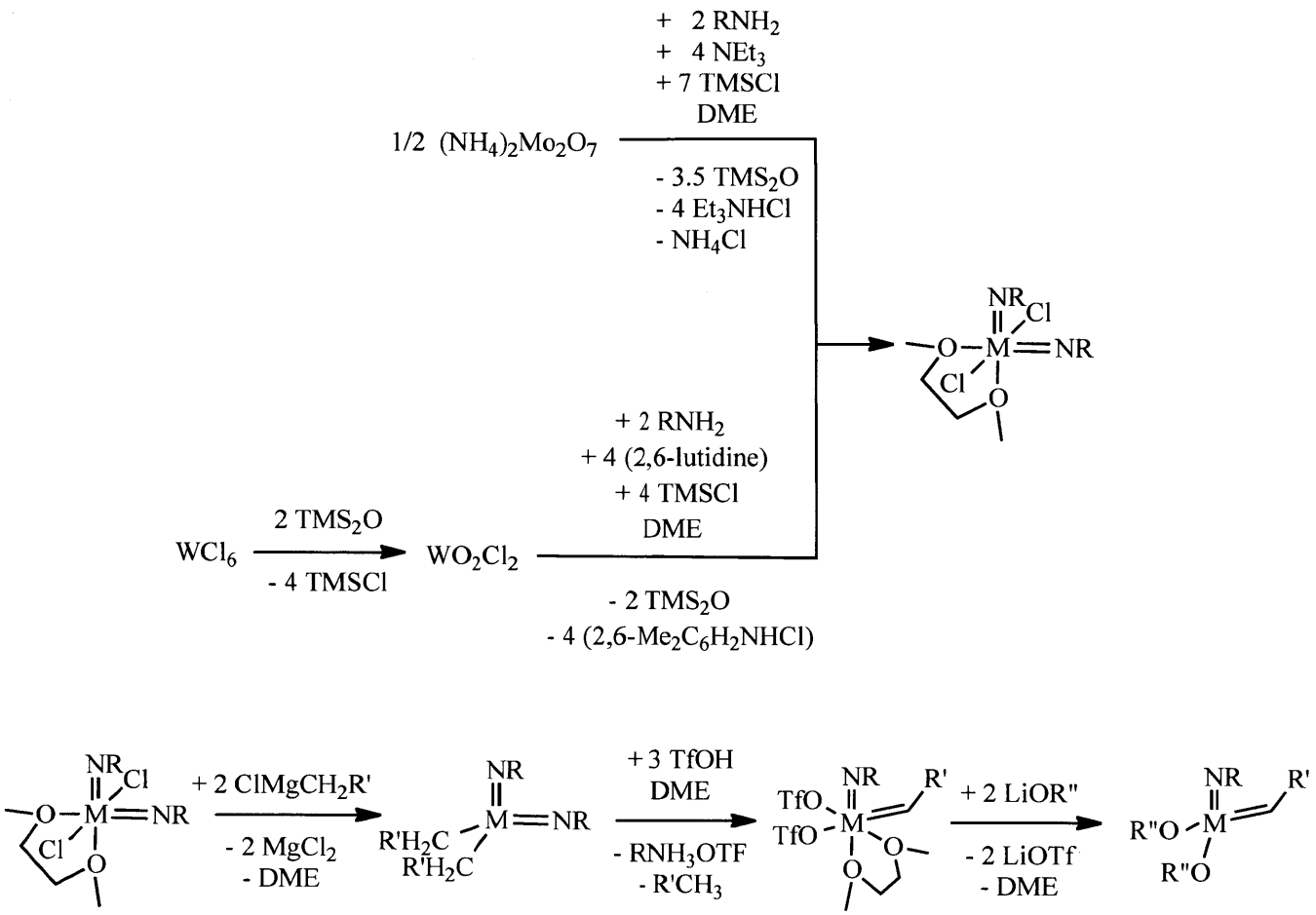

Scheme 2 – General synthetic route to $Mo(NR)_2Cl_2(DME)$, top, and bisalkoxide complexes, bottom.

complex. Enatiomerically pure biphenolate and binaphthalate complexes have been used to generate olefinic products containing a chiral center from achiral precursors.[9]

The presence of two different groups on the alkylidene ligand and competition for metal orbitals between the imido and the alkylidene ligands can generate two isomers. In one the R' group of the alkylidene points towards the imido ligand (*syn*) and in the other the R' group points away from the imido ligand (*anti*), Figure 1.[10] The *syn* species lies lower in energy, in part because of an agostic interaction that takes place between the metal center and the C-H bond of the alkylidene group. In the *anti* configuration, the alkylidene C-H bond points away and no such agostic interaction is present.[11] Experimentally, if the isomers are present in solution in millimolar concentrations, they can be observed and identified by measuring the J_{CH} coupling of the alkylidene α-carbon to the alkylidene α-proton in a simple ^1H NMR experiment. The J_{CH}

coupling in the *syn* species typically ranges between 110-130 Hz, while the J_{CH} coupling in the *anti* species is > 130 Hz. The J_{CH} value of 110-130 Hz is in agreement with the presence of an agostic interaction in the *syn* configuration.[10c] Additionally, X-ray structures of many complexes not only unambiguously show whether the complex is in the *syn* or *anti* configuration, but the shorter Mo=C bond length and larger Mo=C-R' bond angle of the *syn* species (in comparison to the *anti* isomer) are also consistent with the presence of an agostic interaction in *syn* complexes.[10c, 12]

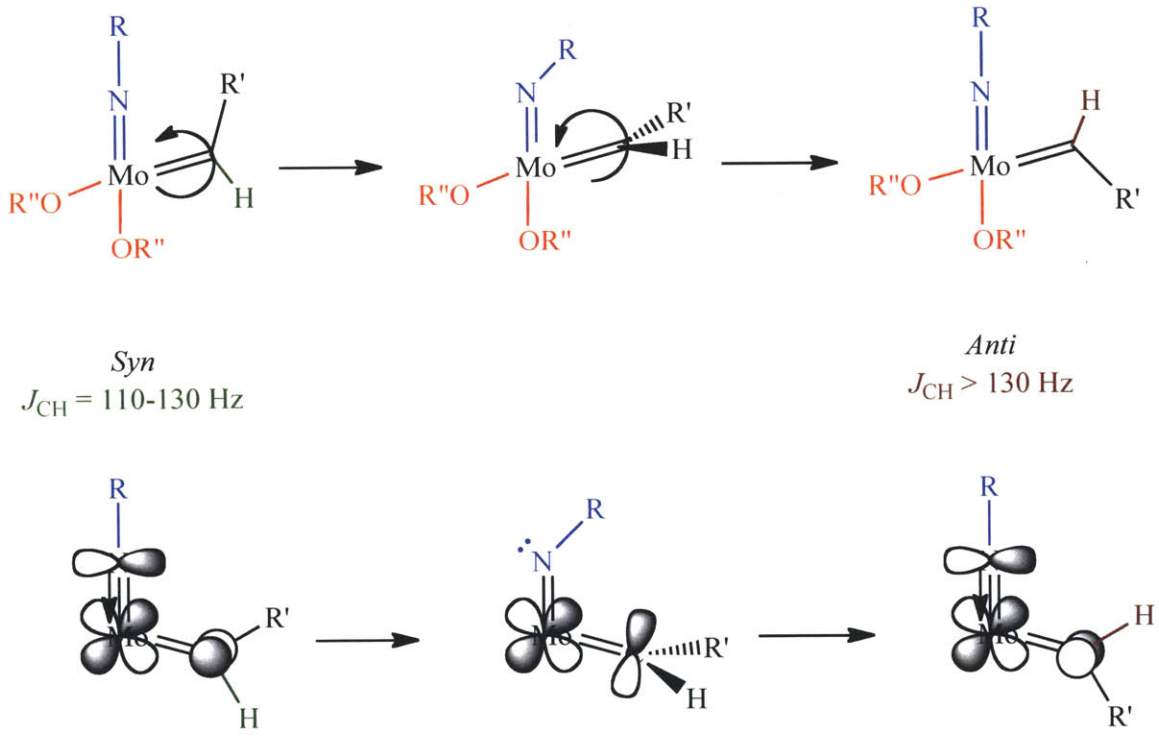

Figure 1 – Conversion of *syn* and *anti* isomers via rotation of the alkylidene group. An orbital diagram is shown at the bottom for clarity.

Interconversion of *syn* and *anti* isomers has been observed in solution for many $M(NR)(CHR')(OR")_2$ complexes.[10a] Typically, the equilibrium concentration of the *anti* species is too small to observe readily, but its concentration can be increased considerably by UV-vis photolysis of a solution of the complex at 360 nm at – 78 °C. Kinetic data of the nonequilibrium mixture can be obtained to determine the rate of conversion of *anti* to *syn*. It has been found that species where R" = $CMe(CF_3)_2$ or fluorinated alkyl convert at five orders of magnitude slower than species where R" = CMe_3 or nonfluorinated alkyl/phenyl.[10a] Conversion of one isomer to

another involves the loss of the metal-imido dative triple bond in order to allow free rotation of the alkylidene to take place (Figure 1).

Counting all the possible combinations of imido groups that can be used as ligands and multiplying that number by the vast combination of alkoxides and chiral diolates that can be used suggets that *in situ* preparation of catalysts for screening reactions would be desirable. For this reason catalyst precursors were sought that would generate active catalyst species without forming salts as byproducts. Ideally the precursor would have to be relatively stable, generate active catalysts efficiently (in solution), and produce byproducts that would not interfere with the catalytic reaction. Bispyrrolide complexes of the general formula $M(NR)(CHR')(Pyr)_2$, where Pyr = pyrrolide, were the first complexes that satisfied most of the criteria mentioned above,[13a] while complexes where Pyr = 2,5-dimethylpyrrolide, satisfied all the requirements and criteria.[13b] Bispyrrolide complexes where Pyr = 2,5-diisopropylpyrrolide, 2,5-diphenylpyrrolide, 2,3,4,5-tetramethylpyrrolide, and 2-indolyl were prepared as well,[13c-d] but those where Pyr = pyrrolide and 2,5-dimethylpyrrolide have been the most widely used in the Schrock and Hoveyda laboratories.

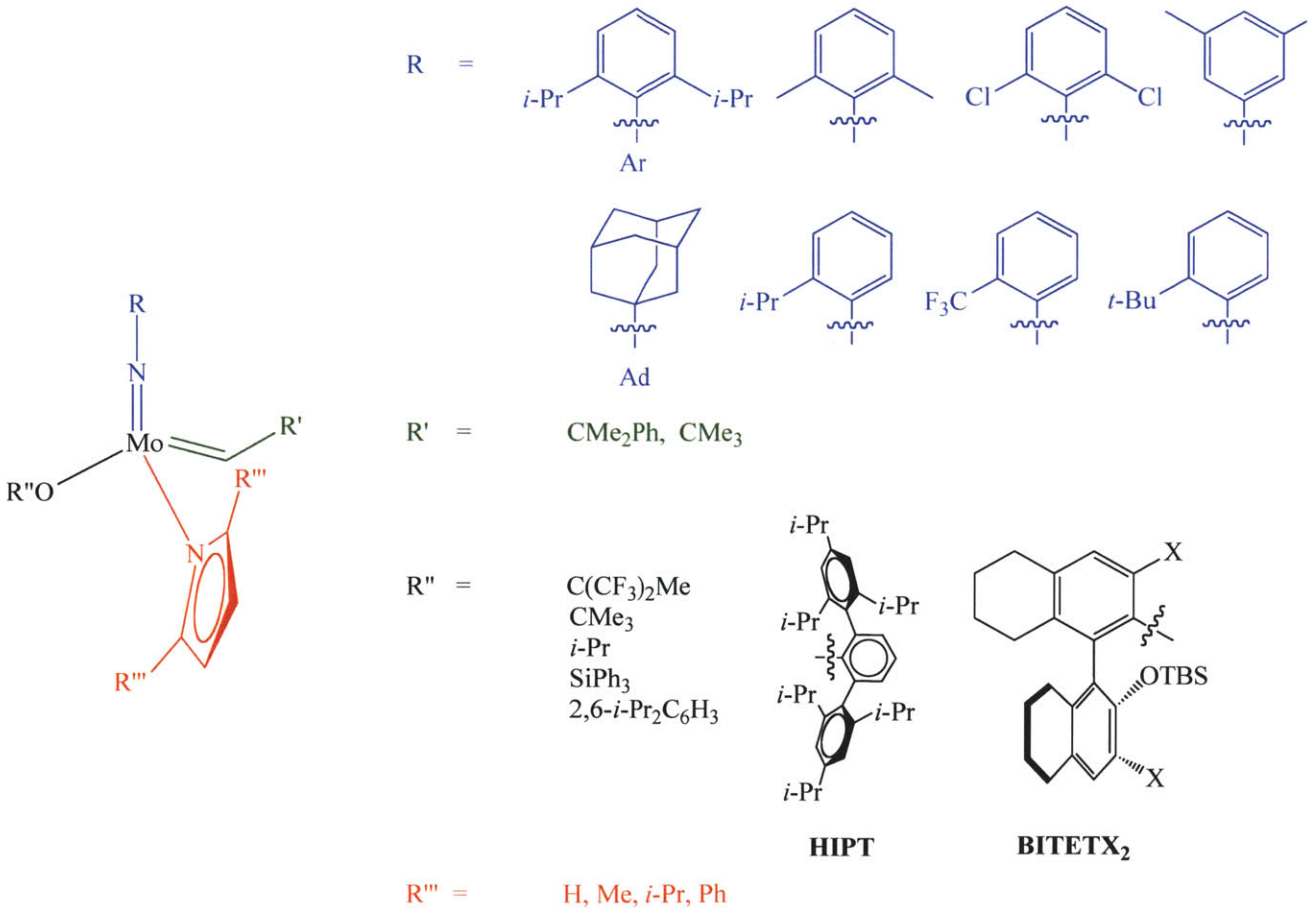

Figure 2 – General structure of MAP catalysts (left), typical ligands used are shown on the right.

Treatment of M(NR)(CHR')(Pyr)$_2$ complexes with one equivalent of R"OH (where R = alkyl or aryl) allowed synthesis of monoalkoxide monopyrrolide (MAP) complexes (Figure 2).[14, 15] Apart from work presented in this thesis, the majority of MAP catalysts synthesized in the past are those where the imido ligand is 2,6-*i*-$Pr_2C_6H_3N$ (ArN) or 1-adamantyl (AdN). MAP catalysts, where R = Ar or Ad, have been shown to be effective for the ring closing metathesis (RCM) of enyne substrates,[13c, 14a] the *Z*-selective polymerization of 2,3-dicarbomethoxynorbornadiene (DCMNBD) and 2,3-dicarbomethoxynorbornene (DCMNB),[10b,14b-c] Development of *Z*-selective catalysts was first achieved with Mo(NAd)(CHCMe$_2$Ph)(Pyr)(OHIPT), where Ad = 1-adamantyl, Pyr = pyrrolide, and OHIPT = 2,6-bis(2',4',6'-triisopropylphenyl)phenoxide. The large OHIPT ligand ensures that incoming olefins would only bind so that the olefin substituents would point away from the OHIPT ligand and toward the small imido group, thus yielding *cis* olefin product (see Figure 4). This catalyst has been employed to form *Z*-selective products.[10b, 14b-c]

MAP complexes where the phenoxide ligand is chiral are of special interest because diastereomers are formed that can potentially have different reactivity. The best studied diastereomeric MAP catalysts are complexes of the type M(NAr)(CHCMe$_2$Ph)(Me$_2$Pyr)(OBITETX$_2$), where M = Mo or W, Ar = 2,6-*i*-PrC_6H_3, Me$_2$Pyr = 2,5-dimethylpyrrolide, OBITETX$_2$ = 3,3'-X$_2$-5,5',6,6',7,7',8,8'-octahydro-1,1'-bi-2'-(*tert*-butyldimethylsilloxide)naphtha-2-ol, and X = halide (shown in Figure 2).[15] M(NAr)(CHCMe$_2$Ph)(Me$_2$Pyr)(OBITET**Br**$_2$) diastereomers can be isolated from one another and their reactions with olefins showed that the configuration at the metal changes with each metathesis reaction.[15] Inversion of configuration at the metal during a single metathesis reaction is required by the principle of microscopic reversibility. DFT calculations suggest that inversion at the metal does take place and that species where all ligands are different (e.g. MAP) are in many cases more efficient catalysts than bisalkoxides catalysts. In particular, catalysts of the type M(NR)(CHR')(X)(Y), where X is a good sigma-donor ligand and Y is a poor one, are predicted to have lower activation barriers for olefin coordination and olefin dissociation.[16] Diastereomeric MAP complexes have been shown to be highly selective for the asymmetric RCM of a desired intermediate in the total synthesis of (-)-quebrachamine.[15b-c]

A method to evaluate whether or not the inversion of configuration at the metal center affects selectivity during olefin metathesis reactions is the ring opening metathesis polymerization (ROMP) of DCMNBD, which can yield up to four regular structures. Regular poly(DCMNBD) can have *cis* or *trans* olefin bonds and have either isotactic or syndiotactic structures (Figure 3). Examination of the polymer structure by NMR methods gives information about what happens during insertion of the monomer and propagation of the polymer chain.

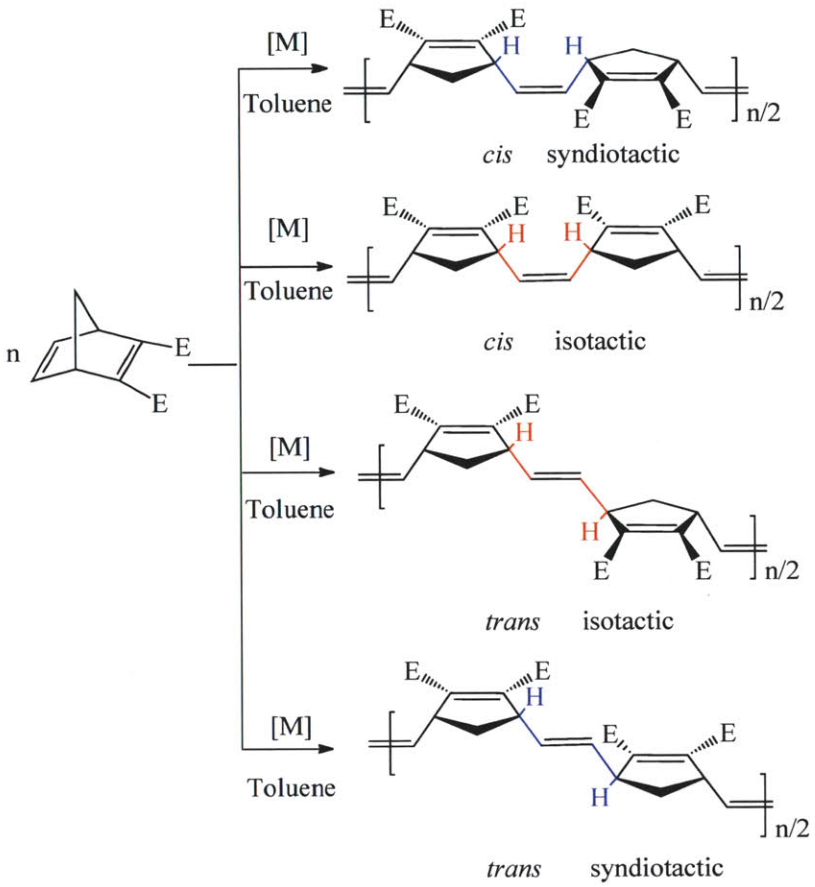

Figure 3 – Four regular structures for poly(DCMNBD).

Poly(DCMNBD) that is formed employing Mo(NR)(CHCMe$_2$Ph)(Me$_2$Pyr)(OBITET**Br**$_2$) is atactic and contains only 70 % of *cis* bonds. On the other hand, when Mo(NAd)(CHCMe$_2$Ph)(Pyr)(OHIPT) is used, poly(DCMNBD) is isolated as a regular polymer with *cis*-syndiotactic structure.[14b] Figure 4 shows the proposed mechanism for formation of *cis*-syndiotactic poly(DCMNBD). In step **1** *syn* binding of DCMNBD to *syn*-(*R*)-Mo(NAd)(CHCMe$_2$Ph)(Pyr)(OHIPT) results in an intermediate molybdacyclobutane that contains all bulky subsituents pointing toward the imido ligand. Opening of the metallacyclobutane yields *syn*-(*S*)-Mo(NAd)(CHR')(Pyr)(OHIPT). In step **2** a second molecule of monomer binds *syn* to *syn*-(*S*)-Mo(NAd)(CHR')(Pyr)(OHIPT) from the opposite face of the catalyst and yields, upon collapse of the metallacyclobutane ring, a propagating chain with alternating tacticity. In addition, the configuration at the metal returns to (*R*). Finally, steps **1** and **2** are repeated consecutively yielding *cis*-syndiotactic poly(DCMNBD). It is worth noting

that in each insertion step the monomer is expected to bind *trans* to the pyrrolide, as suggested by Eisenstein[16] and inversion of configuration is required to get syndiotactic polymer, which is in agreement with experimental results.[15] Likewise, formation of a new olefin is also expected to occur *trans* to the pyrrolide, which is the reason the metal configuration changes during each metathesis step.

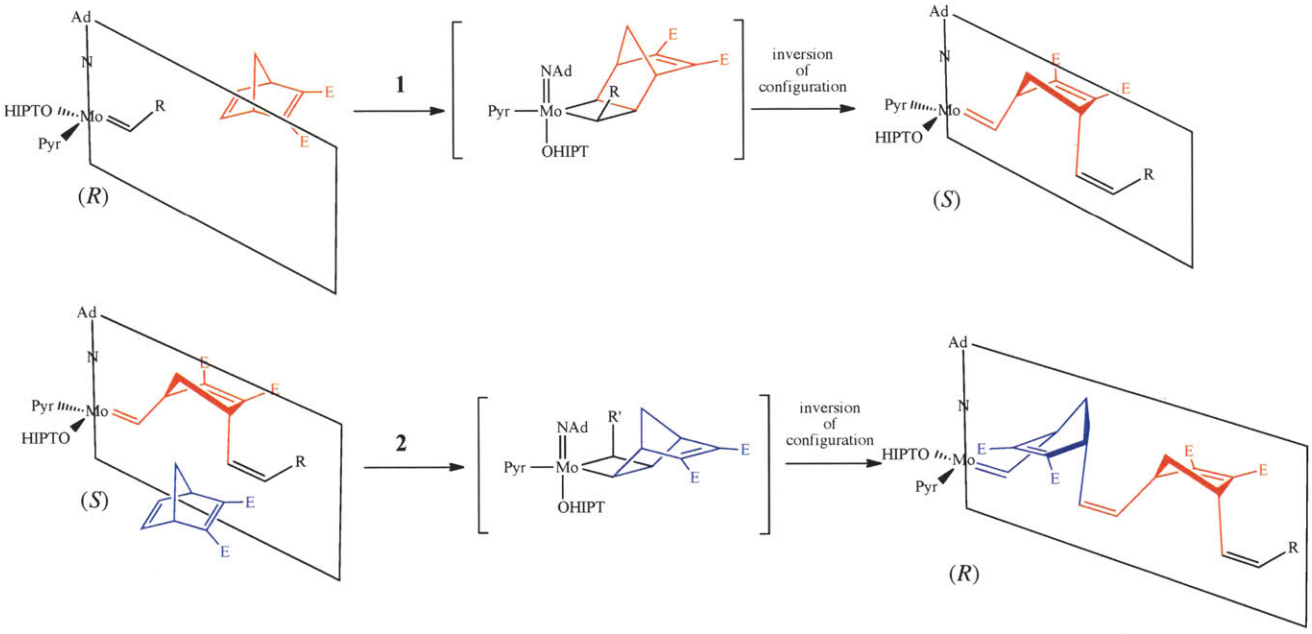

Figure 4 – Proposed mechanism for ROMP of DCMNBD with Mo(NAd)(CHR)(Pyr)(OHIPT): (**1**) *syn* binding of 1st DCMNBD monomer from the back face of catalyst, and (**2**) *syn* binding of 2nd DCMNBD monomer from the front face of the catalyst yielding *cis*-syndiotactic polymer.

Two other regular poly(DCMNBD) structures have been obtained with other catalysts. *Cis*-isotactic-poly(DCMNBD) can be made with Mo(NAr)(CHCMe$_2$Ph)(diolate*) catalysts and the polymer structure is proposed to result from enantiomorphic-site control.[17a] *Trans*-syndiotactic-poly(DCMNBD) can be made with Mo(NAr)(CHCMe$_2$Ph)(O-*t*-Bu)$_2$ (Figure 5).[17b] The *trans*, syndiotactic structure is suggested to arise by *syn*-binding of DCMNBD to *anti*-Mo(NAr)(CHCMe$_2$Ph)(O-*t*-Bu)$_2$ (step **A**) to generate the *syn*-first-insertion product (step **B**), followed by conversion to the *anti*-first-insertion product (step **C**) before *syn*-binding of a second molecule of DCMNBD (step **D**).[18] The tacticity of the polymer is expected to arise the same

way as depicted in Figure 4; however, since the catalyst is C_s symmetric, invertion at the metal will have no effect on the selectivity. Instead, insertion of subsequent monomer is directed via chain-end control.

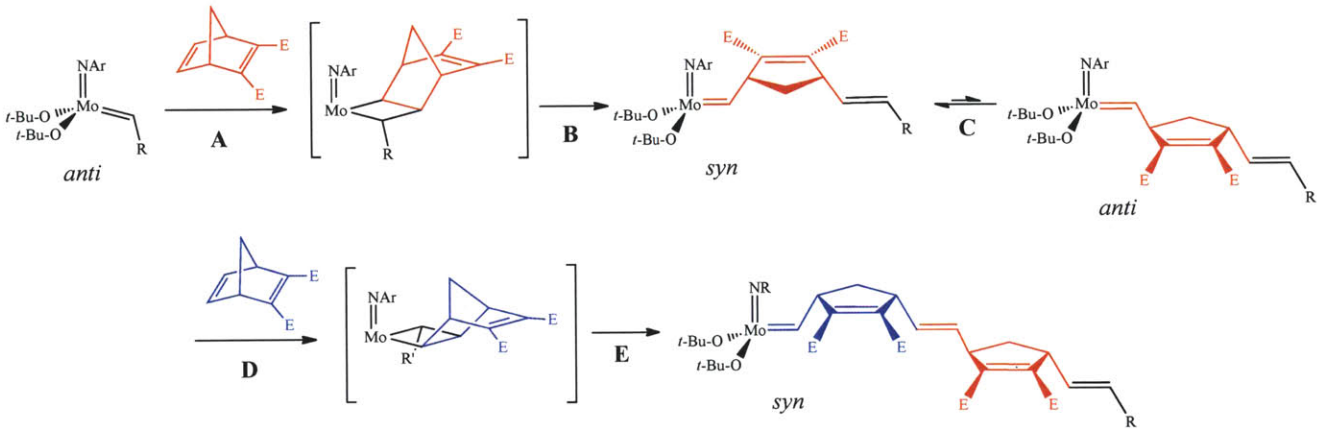

Figure 5 – Proposed mechanism for ROMP of DCMNBD with Mo(NAr)(CHR)(O-*t*-Bu)$_2$: (**A**) *Syn*-binding of DCMNBD, (**B**) Propagation, (**C**) *syn* to *anti* interconversion, (**D**) *syn* binding of 2nd DCMNBD monomer, and (**E**) Propagation.

The reactions depicted in Figures 4 and 5 are excellent examples of how ROMP of DCMNBD can be used to elucidate and deduce how substrates bind to the metal and what happens to the catalyst during subsequent metathesis reactions. Due to the aforementioned attributes, DCMNBD is used in this thesis to test the selectivity of a wide variety of catalytically active complexes.

The dissertation will present the synthesis, characterization, and catalytic activity of biscarboxylate and monocarboxylate monopyrrolide complexes (Chapter 2), MAP complexes containing *ortho*-substituted phenyl imido ligands (Chapter 3), MAP complexes that contain the unsubstituted-pyrrolide ligand with a small variety of imido ligands (Chapter 4), and monoalkoxide monoanionic (MAX) complexes where the anionic ligand is a carboxylate, a phenoxide, an amide, or a terphenyl group (Chapter 5). The appendix will survey the polymerization of 4,4-diethyldipropargylmalonate (DEDPM) to form polyconjugated polymer containing ring structures with MAP and bisalkoxide catalysts.

REFERENCES

1. Calderon, N. *Acc. Chem. Res.* **1972**, *5*, 127.
2. Ziegler, K.; Holzkamp, E.; Breil, H.; Martin, H. *Angew. Chem.* **1955**, *67*, 426.
3. (a) Banks, R. L.; Bailey, G. C. *Ind. Eng. Chem. Prod. Res. Dev.* **1964**, *3*, 170. (b) Natta, G.; Dall'Asta, G.; Bassi, I. W.; Carella, G. *Makromol. Chem.* **1966**, *91*, 87. (c) Calderon, N.; Chen, H. Y.; Scout, K. W. *Tetl. Lett.* **1967**, *8*, 3327.
4. (a) Hérisson, J.-L.; Chauvin, Y. *Makromol. Chem.* **1971**, *141*, 161. (b) Chauvin, Y. *Angew. Chem. Int. Ed.* **2006**, *45*, 3740.
5. Schrock, R. R. *J. Am. Chem. Soc.* **1974**, *96*, 6796.
6. Schrock, R. R. *Acc. Chem. Res.* **1978**, *12*, 98.
7. (a) Fox, H. H.; Schofield, M. H.; Schrock, R. R. *Organometallics* **1994**, *13*, 2804. (b) Feldman, J.; Schrock, R. R. *Prog. Inorg. Chem.* **1991**, *39*, 1.
8. (a) Schrock, R. R.; DePue, R. T.; Feldman, J.; Schaverien, C. J.; Dewan, J. C.; Liu, A. H. *J. Am. Chem. Soc.* **1988**, *110*, 1423. (b) Schrock, R. R.; DePue, R. T.; Feldman, J.; Yap, K. B.; Yang, D. C.; Davis, W. M.; Park, L.; DiMare, M.; Schofield, M. *Organometallics* **1990**, *9*, 2262. (c) Schrock, R. R.; Murdzek, J. S.; Bazan, G. C.; Robbins, J.; DiMare, M.; O'Regan, M. *J. Am. Chem. Soc.* **1990**, *112*, 3875. (d) Oskam, J. H.; Fox, H. H.; Yap, K. B.; McConville, D. H.; O'Dell, R.; Lichtenstein, B. J. Schrock, R. R. *J. Organomet. Chem.* **1993**, *459*, 185. (e) Fox, H. H.; Yap, K. B.; Robbins, J.; Cai, S.; Schrock, R. R. *Inorg. Chem.* **1992**, *31*, 2287.
9. (a) Totland, K. M.; Boyd, T. J.; Lavoie, G. G.; Davis, W. M.; Schrock, R. R. *Macromolecules* **1996**, *29*, 6114. (b) Zhu, S. S.; Cefalo, D. R.; La, D. S.; Jamieson, J. Y.; Davis, W. M.; Hoveyda, A. H.; Schrock, R. R. *J. Am. Chem. Soc.* **1999**, *121*, 8251. (c) Alexander, J. B.; Schrock, R. R.; Davis, W. M.; Hultzsch, K. C.; Hoveyda, A. H.; Houser, J. H. *Organometallics* **2000**, *19*, 3700. (d) Hultzsch, K. C.; Bonitatebus, P. J. Jr.; Jernelius, J. A.; Schrock, R. R.; Hoveyda, A. H. *Organometallics* **2001**, *20*, 4705. (e) Tsang, W. C. P.; Schrock, R. R.; Hoveyda, A. H. *Organometallics* **2001**, *20*, 4705. (f) Schrock, R. R.; Jamieson, J. Y.; Dolman, S. J.; Miller, S. A.; bonitatebus, P. J. Jr.; Hoveyda, A. H. *Organometallics* **2002**, *21*, 409.
10. (a) Oskam, J. H.; Schrock, R. R. *J. Am. Chem. Soc.* **1993**, *115*, 11831. (b) Flook, M. M.; Gerber, L. C. H.; Debelouchina, G. T.; Schrock, R. R. *Macromolecules*, **2010**, *43*, 7515. (c) Dr. Smaranda C. Marinescu, Ph.D. Thesis (MIT, 2011).
11. (a) Brookhart, M.; Green, M. L. H.; Wong, L. *Prog. Inorg. Chem.* **1988**, *36*, 1. (b) Cundari, T. R.; Gordon, M. S. *J. Am. Chem. Soc.* **1991**, *113*, 5231. (c) Cundari, T. R.; Gordon, M. S. *Organometallics* **1992**, *11*, 55.

12. (a) Schrock, R.R.; Hoveyda, A. H. *Angew. Chem. Int. Ed.* **2003**, *42*, 4592. (b) Gerber, L. C. H.; Schrock, R. R.; Müller, P. Takase, M. K. *J. Am. Chem. Soc.* **2011**, *133*, 18142.
13. (a) Hock, A. S.; Schrock, R. R.; Hoveyda, A. H. *J. Am. Chem. Soc.* **2006**, *128*, 16373. (b) Singh, R; Czekelius, C.; Schrock, R. R.; Müller, P. *Organometallics*, **2007**, *26*, 2528. (c) Marinescu, S. C.; Singh, R.; Hock, A. S.; Wampler, K. M.; Schrock, R. R.; Müller, P. *Organometallics* **2008**, *27*, 6570. (d) King, A. J. H. Ph.D. Thesis, 2010, Massachusetts Institute of Technology.
14. (a) Singh, R.; Schrock, R. R.; Müller, P.; Hoveyda, A. H. *J. Am. Chem. Soc.* **2007**, *129*, 12654. (b) Flook, M. M.; Jiang, A. J.; Schrock, R. R.; Müller, P.; Hoveyda, A. H. *J. Am. Chem. Soc.* **2009**, *131*, 7962. (c) Flook, M. M.; Ng, V. W. L.; Schrock, R. R. *J. Am. Chem. Soc.* **2011**, *133*, 1784.
15. (a) Marinescu, S. C.; Schrock, R. R.; Li, B.; Hoveyda, A. H. *J. Am. Chem. Soc.* **2009**, *131*, 58. (b) Malcomson, S. J.; Meek, S. J.; Sattely, E. S.; Schrock, R. R.; Hoveyda, A. H. *Nature* **2008**, *456*, 933. (c) Sattely, E. S.; Meek, S. J.; Malcolmson, S. J.; Schrock, R. R.; Hoveyda, A. H. *J. Am. Chem. Soc.* **2009**, *131*, 943. (d) Ibrahem, I; Yu, M.: Schrock, R. R.; Hoveyda, A. H. *J. Am. Chem. Soc.* **2009**, *131*, 3844. (e) Jiang, A. J.; Simpson, J. H.; Müller, P.; Schrock, R. R. *J. Am. Chem. Soc.* **2009**, *131*, 7770. (f) Meek, S. J.; Malcomson, S. J.; Li, R.; Schrock, R. R.; Hoveyda, A. H. *J. Am. Chem. Soc.* **2009**, *131*, 16407. (g) Jiang, A. J.; Zhao, Y.; Schrock, R. R.; Hoveyda, A. H. *J. Am. Chem. Soc.* **2009**, *131*, 16630. (h) Lee, Y.-J.; Schrock, R. R.; Hoveyda, A. H. *J. Am. Chem. Soc.* **2009**, *131*, 10652. (i) Marinescu, S. C.; Schrock, R. R.; Müller, P.; Hoveyda, A. H. *J. Am. Chem. Soc.* **2009**, *131*, 10840.
16. Poater, A.; Solans-Monfort, X.; Clot, E.; Coperet, C. ; Eisenstein, O. *J. Am. Chem. Soc.* **2007**, *129*, 8207.
17. (a) McConville, D. H.; Wolf, J. R.; Schrock, R. R. *J. Am. Chem. Soc.* **1993**, *115*, 4413. (b) Bazan, G. C.; Khosravi, E.; Schrock, R. R.; Feast, W. J.; Gibson, V. C.; O'Regan, M. B.; Thomas, J. K.; Davis, W. M. *J. Am. Chem. Soc.* **1990**, *112*, 8378.
18. Schrock, R. R.; Lee, J. K.; O'Dell, R.; Oskam, J. H. *Macromolecules* **1995**, *28*, 5933.
19. (a) Fischer, E. O. *Pure Appl. Chem.* **1970**, *24*, 407. (b) Fischer, E. O. *Pure Appl. Chem.* **1972**, *30*, 353. (c) Fischer, E. O.; Maasbol, A. *Angew. Chem. Int. Ed.* **1964**, *3*, 580. (d) Fischer, E. O.; Kreis, G.; Kreiter, C. G.; Müller, J.; Huttner, G.; Lorenz, H. *Angew. Chem. Int. Ed. Engl.* **1973**, *12*, 564.
20. (a) Wengrovius, J. H.; Schrock, R. R.; Churchill, M. R.; Missert, J. R.; Youngs, W. J. *J. Am. Chem. Soc.* **1980**, *102*, 4515. (b) Kress, J. R.; Russell, M. J. M.; Wesolek, M. G.; Osborn, J. A. *J. Chem. Soc. Chem. Comm.* **1980**, *10*, 431. (c) Kress, J. ; Wesolek, M.; Ny, J-P. L.; Osborn, J. A. *J. Chem. Soc. Chem. Comm.* **1981**, *20*, 1039.

CHAPTER 2

Molybdenum Imido Alkylidene Complexes Containing Carboxylate Ligands and their Application for the Ring-Closing Metathesis Polymerization of 4,4-Di-substitutedheptadi-1,6-yne

INTRODUCTION

Tungsten and molybdenum high oxidation state alkylidene complexes of the type $M(NR)(CHR')(OR'')_2$ (M = Mo or W; R, R′, and R″ = various bulky alkyl or aryl groups)[1] have proven useful for a variety of catalytic metathesis reactions. Examples include the living ring-opening metathesis polymerization (ROMP) of strained olefins,[2] the polymerization of monoalkynes or dialkynes to yield polyenes,[3] and the ring-closing metathesis (RCM) of dienes.[1b, 1d, 4] Molybdenum-based compounds have been proposed to be less sensitive to functionalities than tungsten-based species and therefore have been preferred.[5] Unsubstituted tungstacyclobutane complexes also in some cases have been found to be relatively stable toward loss of ethylene, whereas observable molybdacyclobutanes are rare;[6] turnover frequencies with Mo catalysts therefore can be higher than with W catalysts in certain circumstances. One valuable asset of $M(NR)(CHR')(OR'')_2$ catalysts is their modularity. Variation of the NR and OR″ ligands can lead to different reactivities and selectivities, often dramatically so, especially in stereoselective ROMP of strained olefins and asymmetric metathesis reactions. We have reported the synthesis of Mo(NR)(CHR′)(pyrrolide)(OR″) species[7] through addition of R"OH to $Mo(NR)(CHR')(pyrrolide)_2$ species,[8] where the pyrrolide is the parent pyrrolide (NC_4H_4 = Pyr) or 2,5-dimethylpyrrolide ($NC_4Me_2H_2$ = Me_2Pyr). The Mo(NR)(CHR′)(pyrrolide)(OR″) species are potentially even more highly variable as well as chiral at the metal center. Preliminary results suggest that some enyne metathesis reactions are successful with Mo(NR)(CHR′)(Pyr)(OR″) species.[7]

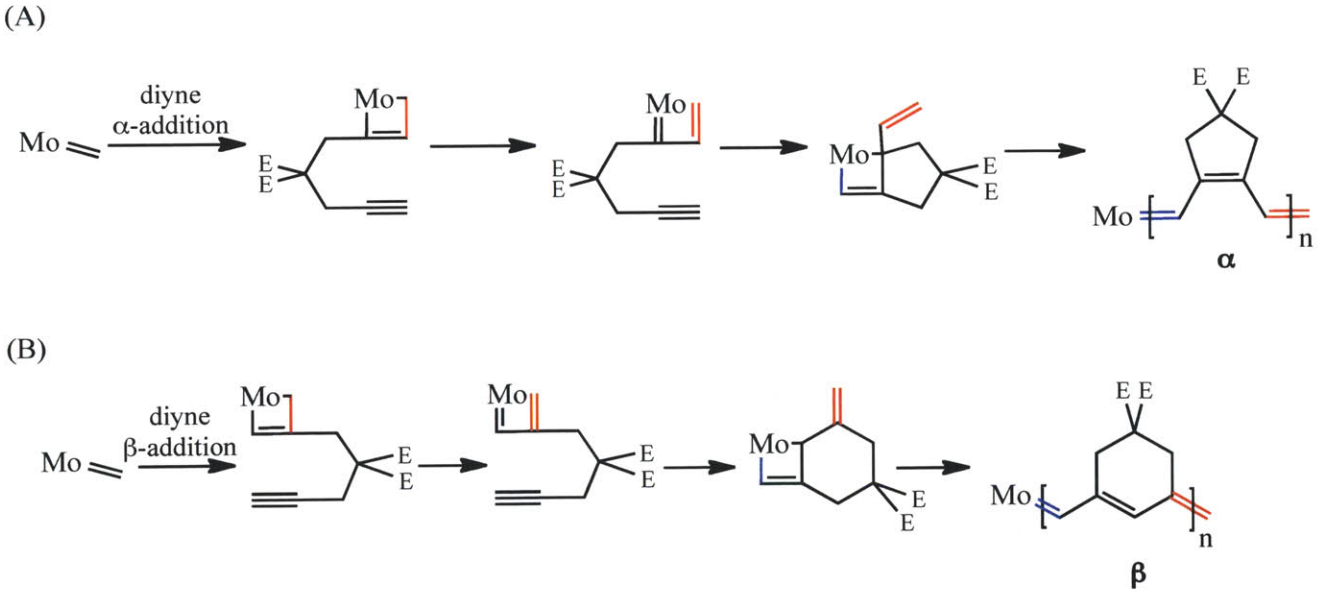

Scheme 1 – Structure of propagating polymer unit as a result of **(A)** α–addition or **(B)** β–addition of the diyne substrate.

An important feature of polymerization reactions involving terminal alkynes is the (presumably irreversible) addition of the alkyne to place the alkyne substituent in either an α or a β position in the metallacyclobutene intermediate, the rearrangement of which yields either a disubstituted (**A**) or monosubstituted alkylidene (**B**, Scheme 1). If both addition pathways are operative, the resulting polyenes will contain a mixture of five-membered rings (as a consequence of α-addition) or six-membered rings (as a consequence of β-addition) as the repeat unit. Several Mo[3e, 9] and Ru[10] catalysts are known that are capable of producing polyenes that contain 95% five-membered rings, while we reported (in a preliminary fashion) the synthesis and polymerization behavior of some molybdenum imido alkylidene complexes that contain two carboxylate ligands that serve as initiators for the living polymerization of diethyl dipropargylmalonate to give polyenes that contain >98% six-membered rings.[11] In this chapter we describe some further studies of biscarboxylates or monocarboxylates and 1,6-heptadiyne aimed at the synthesis of polymers that contain a high fraction of six-membered rings.

RESULTS AND DISCUSSION

2.1 Molybdenum imido alkylidene biscarboxylate complexes

2.1.1 Synthesis of Bisbenzoate Complexes

Preparation of isolable biscarboxylate complexes was achieved in the past in our laboratory using the sterically demanding triphenylacetate ligand.[11] Carboxylate ligands smaller than triphenylacetate tended to give "ate" complexes or ill-defined (possibly oligomeric) species that could not be isolated. Isolable complexes were prepared from bistriflate precursors through salt metathesis reactions with sodium triphenylacetate (equation 1; Ar = 2,6-*i*-$Pr_2C_6H_3$, Ar′ = 2,6-$Me_2C_6H_3$, Ad = 1-adamantyl, Ar^{tBu} = 2-*t*-BuC_6H_4) by Dr. Z. J. Tonzetich.

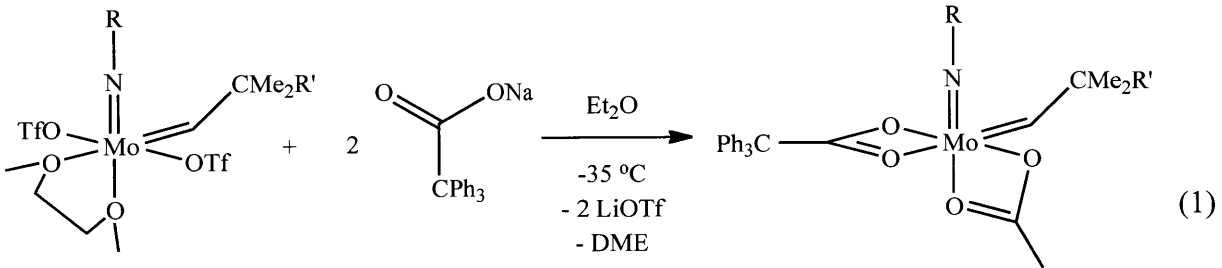

(1)

1a R = Ar, R' = Ph
1b R = Ad, R' = Ph
1c R = Ar', R' = Ph
1d R = Ar^{tBu}, R' = Me

A single crystal X-ray study of **1d** revealed it to be a distorted six-coordinate 18 electron species in which both carboxylates are bound κ^2.[11] However, both are bound somewhat asymmetrically with Mo-O distances of 2.136 Å and 2.261 Å for one carboxylate and 2.090 Å and 2.336 Å for the other carboxylate. The longer Mo-O bonds are *trans* to the Mo=C (2.336 Å) or the Mo=N bond (2.261Å). The carboxylates are technically inequivalent in this structure, although all biscarboxylate complexes show time-averaged C_s symmetry in solution at room temperature, consistent with fluxional coordination geometry on the NMR time scale that may or may not involve intermediates that contain at least one κ^1 carboxylate.

Attempts to prepare bisbenzoate complexes utilizing commercially available carboxylates did not yield isolable products. This behavior is similar to what occurs in the reaction between bistriflate complexes and small acetate ligands. However, we found that "ate" complexes can be avoided and bisbenzoate complexes prepared if 2,6-terphenylcarboxylates[12] are employed. The two chosen terphenylcarboxylates contain *p*-methyl or *p*-methoxy substituents in the phenyl ring bound in the 2 and 6 positions in the benzoate backbone, (O_2CTer_{Me}) and (O_2CTer_{OMe}), respectively (Figure 1).

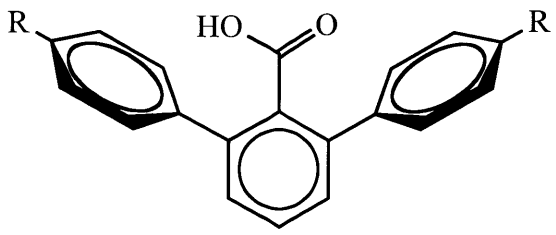

$Ter_{Me}CO_2H$: R = Me
$Ter_{OMe}CO_2H$: R = OMe

Figure 1 – Terphenylcarboxylic acids used for synthesis of carboxylate complexes.

The chosen method of synthesis consisted of addition of two equivalents of the acid to $Mo(NR)(CHCMe_2Ph)(Me_2Pyr)_2$ (Me_2Pyr = 2,5-dimethylpyrrolide; equation 2).[8] The complexes can also be prepared via salt-metathesis starting from the corresponding bistriflate precursor and two equivalents of NaO_2CTer. However, the more complicated work-up involves recrystallization of the compounds because the initial product obtained from the reaction is relatively impure. In the case of complexes that contain the adamantylimido ligand (discussed below), the product of the salt metathesis reaction could not be obtained in a pure form suitable for further studies. The resulting bisbenzoates, $Mo(NAr)(CHCMe_2Ph)(O_2CTer_{Me})_2$ (**2a**) and

$Mo(NAr)(CHCMe_2Ph)(O_2CTer_{OMe})_2$ (**2b**) (equation 2) were isolated in yields between 50 and 60%. Similarly, bisbenzoate alkylidene complexes containing the adamantylimido group, $Mo(NAd)(CHCMe_2Ph)(O_2CTer_{Me})_2$ (**2c**) and $Mo(NAd)(CHCMe_2Ph)(O_2CTer_{OMe})_2$ (**2d**), were obtained in yields ranging between 40 and 70% (equation 2). The ^1H NMR spectra of all compounds suggest that a mirror plane is present on the NMR time scale as a consequence of rapid carboxylate interconversion. Only a *syn* isomer is observed for each with δH_α, δC_α, and J_{CH} values similar to other carboxylates described earlier. The resonances corresponding to the alkyl groups of the imido substituents, as well as to the alkyl groups of the carboxylate, are sharp, again consistent with a plane of symmetry being present on the NMR time scale.

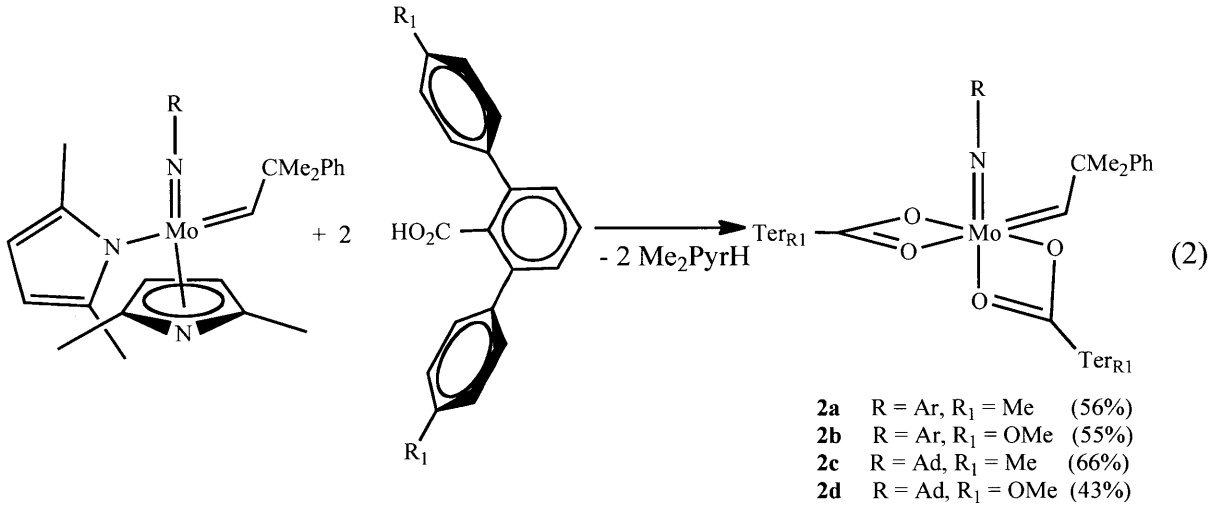

(2)

2a R = Ar, R_1 = Me (56%)
2b R = Ar, R_1 = OMe (55%)
2c R = Ad, R_1 = Me (66%)
2d R = Ad, R_1 = OMe (43%)

Crystals of **2a** were grown from a saturated methylene chloride solution layered with diethyl ether. The structure is shown in Figure 2. (See Table 3 for details.) The structure is best described as a distorted octahedron, with both carboxylate groups bound to the metal in a κ^2,κ^2 fashion, similar to the biscarboxylate described in the preliminary communication.[11] The alkylidene is in the *syn* orientation. The most interesting features are again long Mo(1)-O(1) and Mo(1)-O(3) bond lengths (2.2867(16) Å and 2.3186(16) Å, respectively), i.e., those *trans* to the imido and alkylidene groups, respectively. In the solid state the two carboxylates are inequivalent, but equivalent in solution on the NMR time scale.

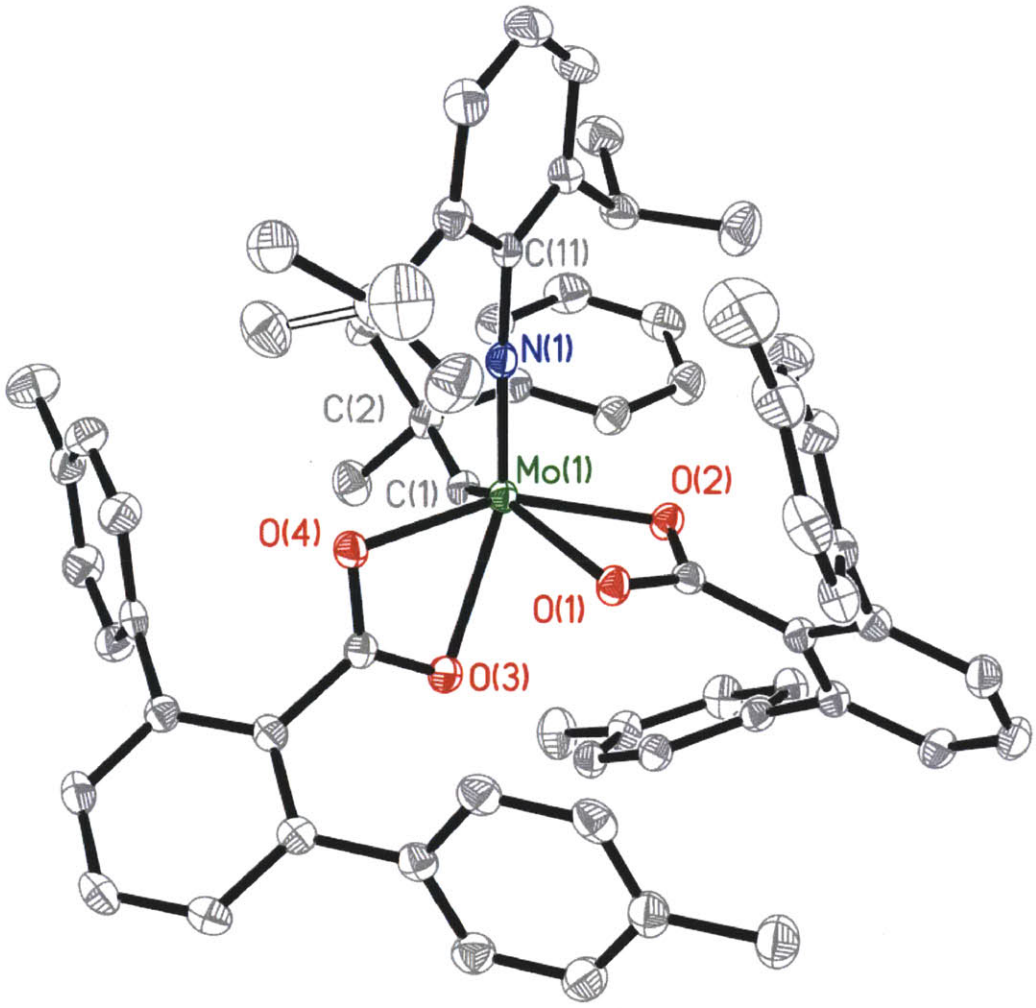

Figure 2 – The solid state structure of **2a** (50% probability ellipsoids). Selected bond lengths (Å) and bond angles (°): Mo1-N1 = 1.7247(16), Mo(1)-C(1) = 1.902(2), Mo(1)-O(1) = 2.2867(16), Mo(1)-O(2) = 2.1160(14), Mo(1)-O(3) = 2.3186(16), Mo(1)-O(4) = 2.1252(14), Mo(1)-N(1)-C(11) = 174.15(13), Mo(1)-C(1)-C(2) = 145.18(14).

2.1.2 Observation of *Anti* Isomers

The UV-vis spectrum of **1a** is shown in Figure 3. The absorption maximum at 324 nm ($\varepsilon \approx$ 15000 $M^{-1}cm^{-1}$) is similar to what was found for Mo(NAr)(CH-*t*-Bu)$(OR)_2$ complexes in which R = *t*-Bu, $CMe_2(CF_3)$, or $CMe(CF_3)_2$.[13] This absorption is ascribed to the M-N_{imido} $\pi \rightarrow \pi^*$ transition, in part because a photostationary mixture of *syn* and *anti* isomers (equation 3) can be formed through irradiation of samples with 366 nm light in toluene. Rates of interconversion of *syn* and *anti* alkylidene isomers in bisalkoxide complexes vary by several orders of magnitude,

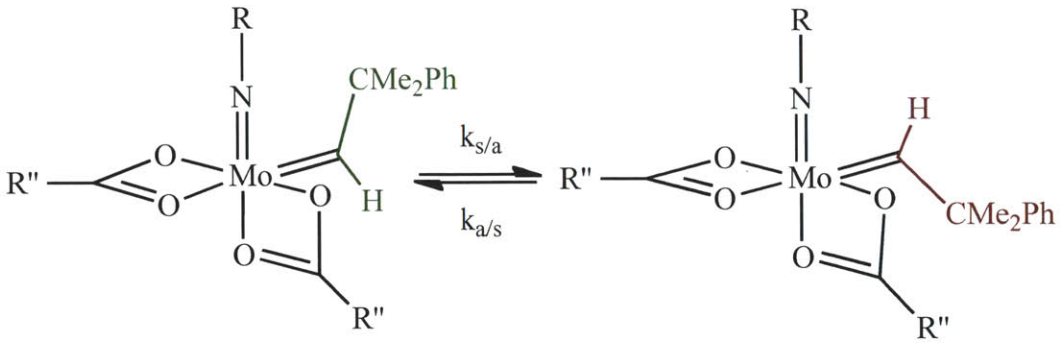

Syn
J_{CH} = 120-130 Hz

Anti
J_{CH} = 130-140 Hz

(3)

with the slowest rates being found for alkylidene complexes that contain relatively electron-withdrawing alkoxides such as $OCMe(CF_3)_2$.[13, 14] Interconversion of *syn* and *anti* isomers appears to be most facile in 14e species. For example, the base (e.g. PMe_3) in a 16e adduct of $Mo(NAr)(CH\text{-}t\text{-}Bu)[OCMe(CF_3)_2]_2$ must be lost before *syn* and *anti* isomers can interconvert. A coordinating solvent such as THF will also hinder alkylidene rotation to a significant degree in

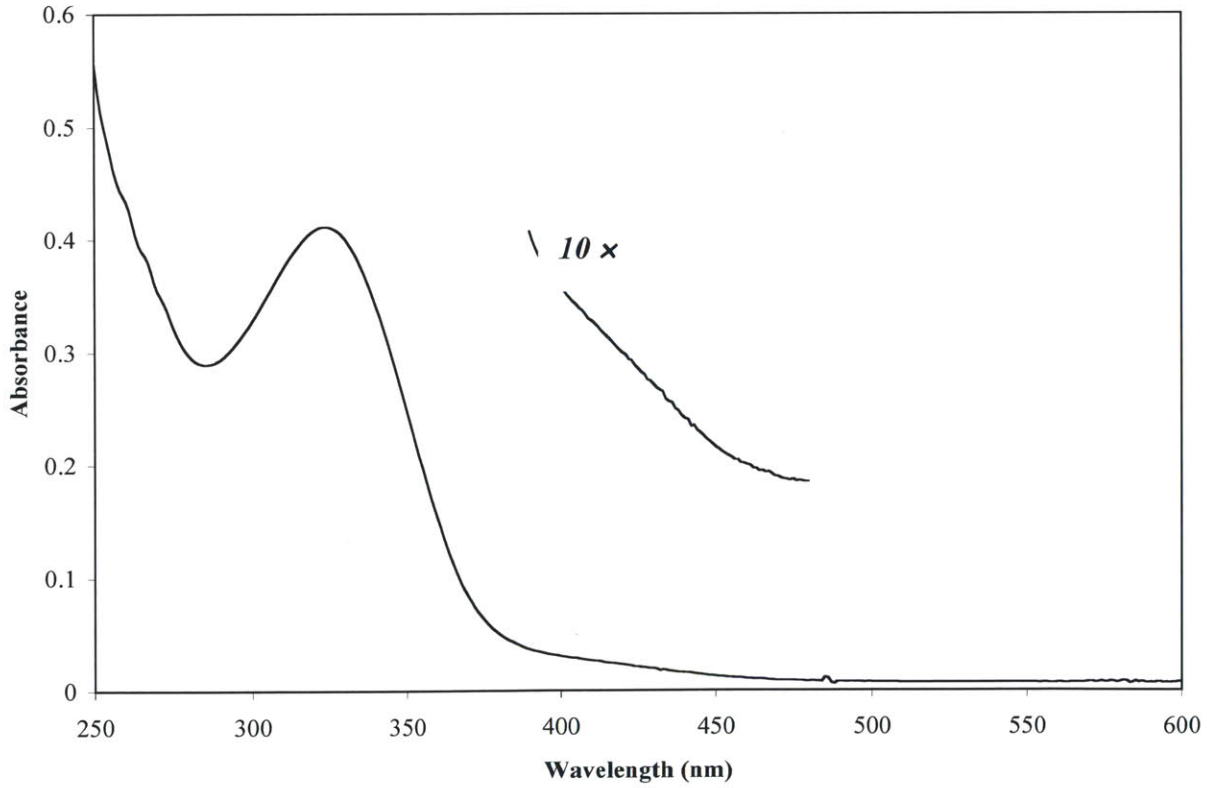

Figure 3 - Electronic absorption spectrum of $Mo(NAr)(CHCMe_2Ph)(O_2CCPh_3)_2$ (**1a**) at 23 °C in methylene chloride (33.9 μM).

$Mo(NR)(CHR')(OR'')_2$ species on the basis of slower rates and negative values for the activation entropy for *syn*/*anti* interconversion in THF.[15] Since *syn* and *anti* isomers can have dramatically different reactivities,[14] the rate of interconversion of *syn* and *anti* isomers and the position of that equilibrium can have important consequences in terms of metathesis with such species.

Photolysis of a sample of **1a** in toluene-d_8 at 366 nm for 3 h at 22 °C yielded a mixture containing 16% of a new species in which δH_α = 13.93 ppm and J_{CH} = 138 Hz, characteristic of an *anti* isomer. At 22 °C the *anti* isomer was found to convert to the *syn* isomer in a first order manner with $k_{a/s} = (8.30 \pm 0.93) \times 10^{-6}$ s^{-1} ($t_{1/2}$ = 23.2 h). A sample of **1b** irradiated in toluene-d_8 at 366 nm for 2 h at 22 °C produced a mixture containing 28% of an *anti* species (δH_α = 13.99 ppm, J_{CH} = 140 Hz) that reverted back to the *syn* isomer at 22 °C with $k_{a/s} = (3.08 \pm 0.14) \times 10^{-4}$ s^{-1} ($t_{1/2}$ = 39 minutes). Finally, a sample of **1d** irradiated in toluene-d_8 at 366 nm for 2 h at 22 °C produced a mixture containing 17% of an *anti* species (δH_α = 13.90 ppm, J_{CH} = 137 Hz) that reverted to the *syn* isomer at 0 °C with $k_{a/s} = (1.55 \pm 0.12) \times 10^{-5}$ s^{-1} and at room temperature with $k_{a/s} = (3.62 \pm 0.74) \times 10^{-3}$ s^{-1}. Therefore, at room temperature the relative rates of conversion of *anti* to *syn* isomers are **1d** > **1b** > **1a** with $t_{1/2}$ ranging from ~1 day (for **1a**) to ~3 minutes (for **1d**).

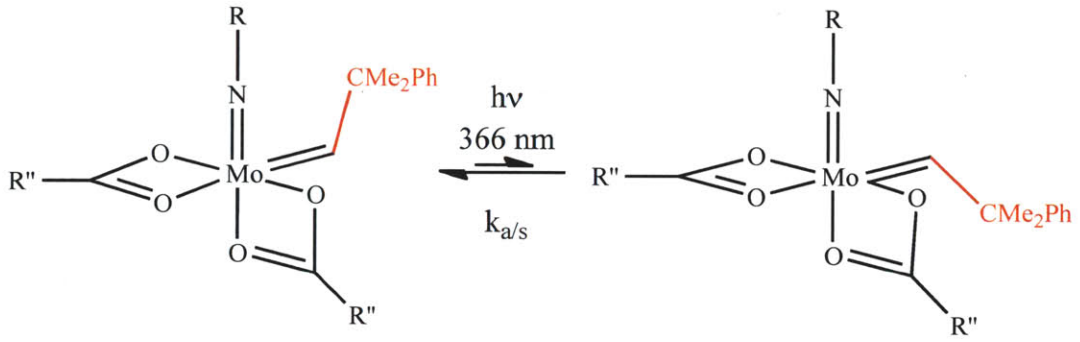

(4)

Syn/*anti* isomerization reactions of bisbenzoate complexes were studied briefly for **2a** and **2c**. A sample of **2a** in toluene-d_8 was photolyzed at 22 °C with 366 nm light for 2 hours. The resulting mixture contained 7% of the *anti* species (δH_α = 13.6 ppm, J_{CH} = 137 Hz), and 93% of the *syn* species (δH_α = 13.4 ppm, J_{CH} = 126 Hz). The rate constants for the *anti* to *syn* conversion of **2a** at 22 °C and 0 °C in toluene-d_8 were found to be $(5.31 \pm 1.14) \times 10^{-4}$ s^{-1} and $(1.28 \pm 0.11) \times 10^{-5}$ s^{-1} respectively. Photolysis of a solution of **2c** in toluene-d_8 at room temperature for 2 hours yielded a mixture of 9% *anti* (δH_α = 13.9 ppm, J_{CH} = 140 Hz) and 91% *syn* (δH_α = 13.2 ppm, J_{CH} = 124 Hz) isomers. However, unlike **2a**, which proved to have a short half-life for conversion of *anti* to *syn*, *anti*-**2c** was virtually unchanged after four hours at 22 °C. Only after 16 hours at 22

°C did the amount of the *anti* species decrease to ~3% (30% of the initial amount). All data are summarized in Table 1.

Table 1 – Analysis of Photolyzed Biscarboxylate Complexes in C_7D_8.

[Mo]	***Syn* Species**			***Anti* Species**			Photolysis time at RT	Rates of Conversion from *Anti* to *Syn* (sec^{-1})	
	ppm	J_{CH} (Hz)	%	ppm	J_{CH} (Hz)	%		RT	0 °C
1a	13.84	123	84	13.93	138	16	3 h	$(8.30\pm0.93)\cdot10^{-6}$	-------
1b	13.80	123	72	13.99	140	28	2 h	$(3.08\pm0.14)\cdot10^{-4}$	-------
1d	13.77	120	83	13.90	137	17	2 h	$(3.62\pm0.74)\cdot10^{-3}$	$(1.55\pm0.12)\cdot10^{-5}$
2a	13.40	126	93	13.60	137	7	2 h	$(5.31\pm1.14)\cdot10^{-4}$	$(1.28\pm0.11)\cdot10^{-5}$
2c	13.20	124	91	13.90	140	9	2 h	-------	------

2.1.3 Trimethylphosphine adducts of triphenylacetate complexes

Base adducts of imido alkylidene complexes often can serve as models of the first adduct formed when a substrate approaches the metal center in a catalytic reaction.[12] Although the 18-electron biscarboxylates are unlikely to bind a Lewis base if the κ^2,κ^2 configuration is maintained, compounds **1b-d** do react readily with PMe_3 to give mono-adducts (**1b·PMe$_3$** - **1d·PMe$_3$**, equation 5). Compound **1a** does not bind PMe_3 strongly enough to isolate the adduct, presumably because of the greater steric demands of the 2,6-diisopropylphenyl imido ligand.

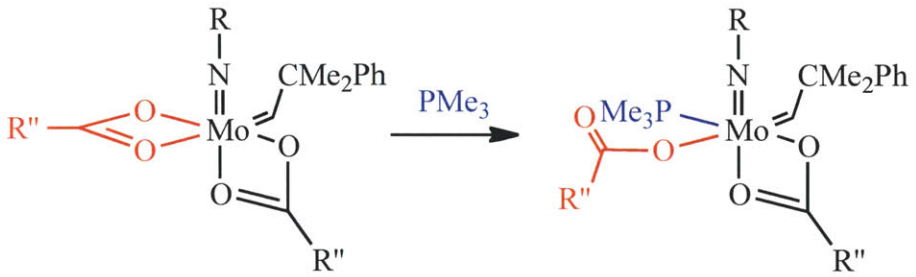

(5)

The phosphine adducts were initially isolated and characterized by Dr. F. J. Schattenmann and Dr. Z. J. Tonzetich through crystallization from a mixture of methylene chloride and

pentane. They found that the alkylidene protons in **1b·PMe$_3$** - **1d·PMe$_3$** are coupled to phosphorus by 5-6 Hz, which is consistent with the phosphine not dissociating rapidly on the NMR time scale. Coupling constants of 5-6 Hz are analogous to those found in various phosphine adducts of imido alkylidene bisalkoxide complexes.[12] NMR spectra of **1c·PMe$_3$** and **1d·PMe$_3$** reveal that the carboxylates are inequivalent, consistent with one being κ^2 and the other being κ^1, as depicted in equation 5, and shown to be the case in the solid state structure of **1d·PMe$_3$**. **1b·PMe$_3$** has equivalent carboxylate ligands on the NMR time scale. The methyl groups of the neophylidene ligand are inequivalent in **1b·PMe$_3$**, which suggests that the carboxylates must equilibrate without generating a mirror plane that passes through the β carbon of the alkylidene ligand.

Proton NMR spectra of freshly crystallized **1b·PMe$_3$**, **1c·PMe$_3$**, and **1d·PMe$_3$** show only the *syn* isomer. However, over a period of several days the *anti* isomers appear. For example, when a solution of freshly prepared *syn*-**1d·PMe$_3$** was kept at -35 °C for a period of 2 days and the crystals collected, NMR spectroscopy in C_6D_6 showed them to be a mixture of 41% of the *anti* isomer (δH_α = 13.8 ppm, J_{CH} = 135 Hz) and 59% of the *syn* isomer (δH_α = 13.1 ppm, J_{CH} = 116 Hz). After this solution was left at room temperature for 6 days, the mixture consisted of 64% of the *anti* species and 36% of the *syn* species (Figure 4). No further change was observed after 3 weeks; therefore the two appear to be at equilibrium at this point. This general behavior is analogous to that of Mo(NAr)(CH-t-Bu)[OCMe(CF$_3$)$_2$]$_2$(PMe$_3$), which can be isolated as a *syn* isomer that slowly converts over a period of days in solution into the *anti* isomer (completely), a process that is believed to require loss of trimethylphosphine followed by (inherently slow) *syn* to *anti* rotation about the Mo=C bond in intermediate Mo(NAr)(CH-t-Bu)[OCMe(CF$_3$)$_2$]$_2$.[12]

Overall the structure is reminiscent of the structure of a typical adduct of a bisalkoxide species such as Mo(NAr)(CH-*t*-Bu)[OCMe(CF$_3$)$_2$]$_2$(PMe$_3$).[12] One can imagine that if a terminal alkyne were to bind to the metal in the same position as the trimethylphosphine, the steric influence of the t-butyl group in the imido substituent combined with that of the bidentate triphenylacetate ligand could direct the terminal alkyne substituent (if large enough) to point in a direction that would yield the β–substituted metallacyclobutene intermediate (Scheme 1).

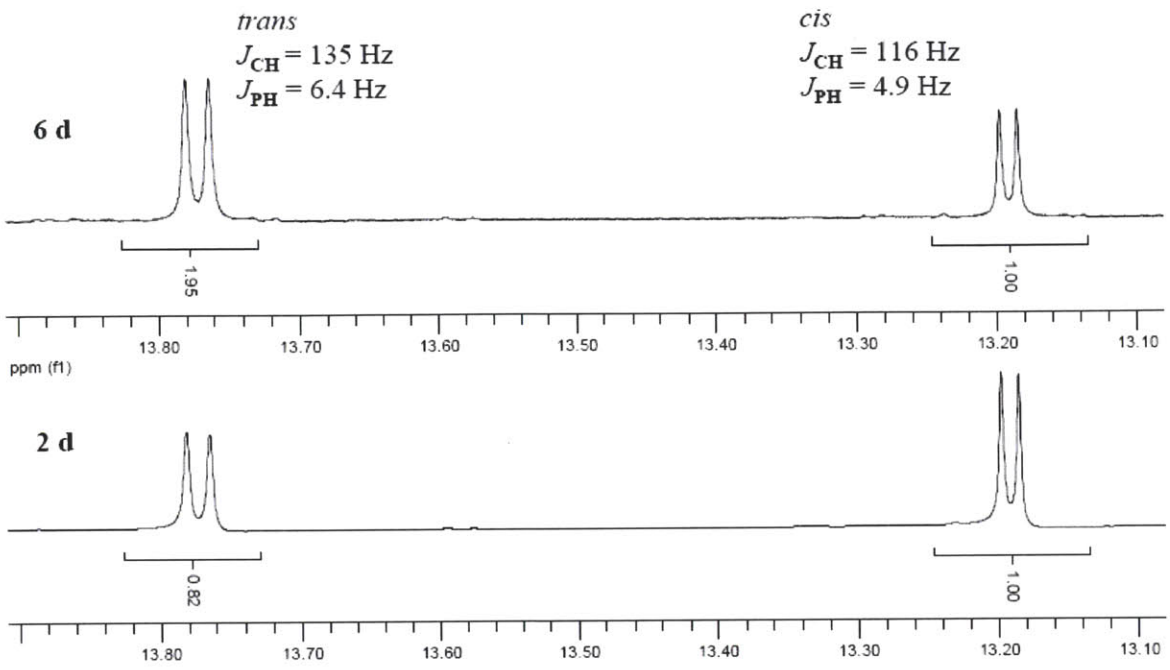

Figure 4 – Alkylidene region in the ^{1}H NMR of **1d-PMe$_3$** after 2 days (bottom) and 6 days (top) of being dissolved in C_6D_6.

2.1.4 Cyclopolymerization of 1,6-heptadiynes

None of the biscarboxylate species reported here react readily with olefins, even ethylene or norbornene. However, several are competent, though slow, catalysts for the cyclopolymerization of diethyl dipropargylmalonate (DEDPM). Compound **1a** is an impractically slow initiator, presumably because of the steric demands of the diisopropylphenylimido ligand. Catalysts **1b** and **1d** produce polymers that contain >98% six-membered rings, according to ^{13}C NMR spectra, which reveal resonances for quaternary carbons in five-membered rings at 57-58 ppm and in six-membered rings at 54-55 ppm.[3d] ^{13}C NMR spectra are much more convenient to obtain, even in the absence of any relaxation agent such as Cr(acac)$_3$, when the quaternary carbon is ^{13}C-labeled. Typical spectra of polymers that contain mostly six-membered rings are shown in Figure 5. Compound **1c** is also an initiator for the cyclopolymerization of DEDPM, but does not show any advantages over initiators **1b** and **1d**. Polymers prepared with initiators **1a** and **1c** contained only 35% or 90% six-membered rings, according to ^{13}C NMR studies. All polymers prepared with initiators **1a-d** that contain up to 125 equiv of DEDPM are soluble in toluene, dichloromethane, and THF, but sparingly soluble in pentane and diethyl ether. Polymers that

contain exclusively five-membered rings[9c] are known to dissolve only in relatively polar solvents (e.g., CH_2Cl_2 and THF). Unlike polymers that contain all five-membered rings, those that contain all six-membered rings may not be stereoregular in terms of the E/Z configuration in the exocyclic double bond, since the ^{13}C quaternary carbon method is not likely to be sensitive enough to detect different E/Z configurations. Different E/Z configurations also may contribute to greater structural disorder and therefore higher solubilities of polymers that contain a significant fraction of six-membered rings.

DEDPM can be cyclopolymerized with initiators **2a-2d**, although more slowly than with initiators of type **1**. Polymerization of 10 equivalents of ^{13}DEDPM (in which the quaternary carbon is ^{13}C-labeled) by **2a** or **2b**, produced polymer (~80%) only after ~1 week at room temperature. The amount of β product was ~70% overall when either **2a** or **2b** was employed. Similarly, when 20 equivalents of ^{13}DEDPM were added to **2c** or **2d**, the reactions were still slower than with initiators of type **1**. For example, after 74 hours 86% of the starting material was consumed when **2c** was employed (83% β product) and 60% when **2d** was employed (77% β product).

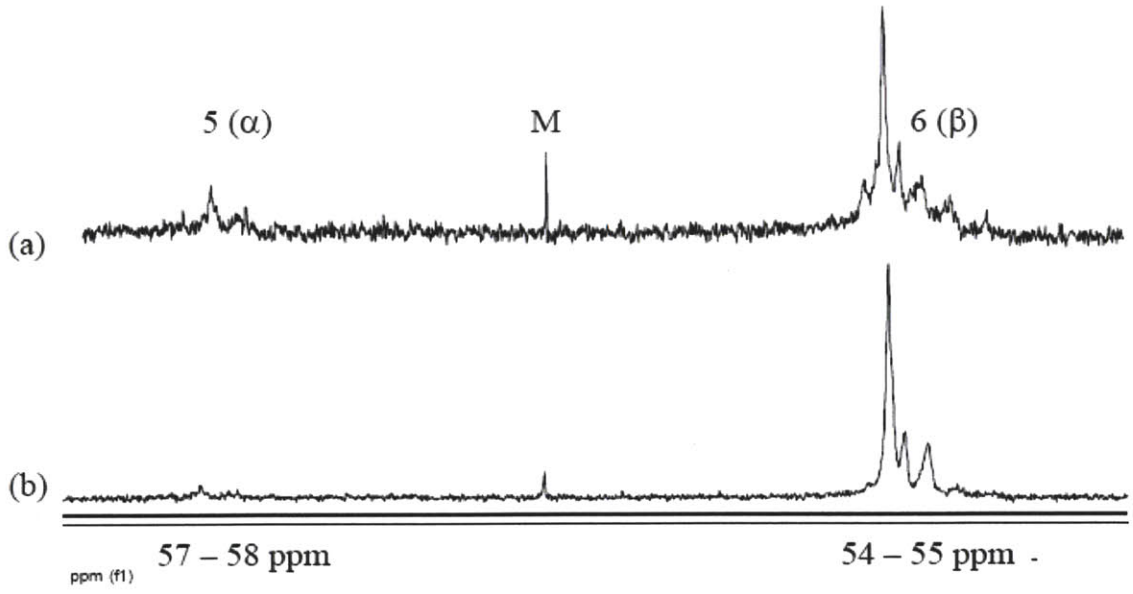

Figure 5 – ^{13}C NMR spectra of polymers prepared from (quaternary ^{13}C-labeled) DEDPM (M) using initiators **2c** (a) and **1b** (b).

2.2 Molybdenum imido alkylidene monocarboxylate complexes

2.2.1 Synthesis of monocarboxylate complexes

As opposed to the ease of preparation of the biscarboxylate complexes, it was found that reactions between $Mo(NR)(CHCMe_2Ph)(Me_2Pyr)_2$ and one equivalent of aliphatic carboxylic acid tends to yield a mixture of biscarboxylate, starting material, and very little monocarboxylate. This is even true for the most sterically-hindered conditions (e.g. R = Ar, acid = Ph_3CCO_2H). Likewise, reactions between aromatic carboxylic acids and $Mo(NR)(CHCMe_2Ph)(Me_2Pyr)_2$, where R ≠ Ar, lead to mixtures containing mostly biscarboxylate species.

Fortunately, when the imido group is Ar the preparation and isolation of monocarboxylate complexes $Mo(NAr)(CHCMe_2Ph)(Me_2Pyr)(O_2CR")$ is possible when R" = 2,4,6-triisopropylphenyl (TRIP), Ter_{Me}, Ter_{OMe}, or 2,6-(2',4',6'-*i*-$Pr_3C_6H_2)_2C_6H_3$ (HIPT). Thus, reaction between $Mo(NAr)(CHCMe_2Ph)(Me_2Pyr)_2$ and one equivalent of $R"CO_2H$ at -35 °C gave the desired complexes, after recrystallization, in modest yields (equation 6). The low yield of **3a** is due to formation of 5-10% of biscarboxylate, which can be removed only by multiple recrystallizations. Complex **3d** was prepared only *in situ* in C_6D_6 at RT because purification by recrystallization was not possible.

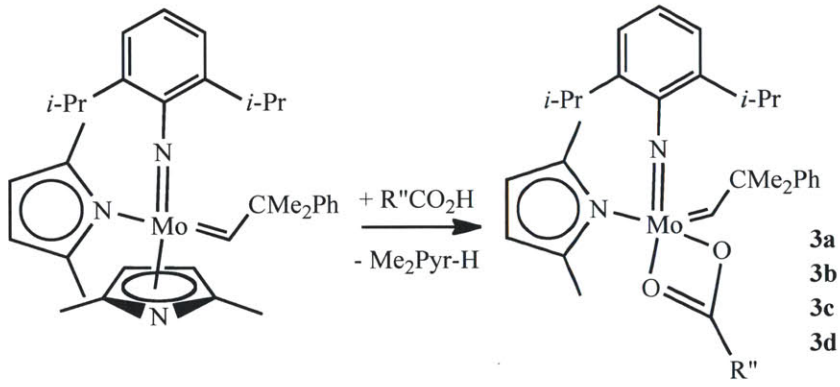

3a R" = TRIP (24%)
3b R" = Ter_{Me} (40%)
3c R" = Ter_{OMe} (47%)
3d R" = HIPT (*in situ*)

(6)

Proton NMR of all complexes show only one alkylidene peak with J_{CH} values ranging between 120-123 Hz, all in agreement with the presence of the *syn* species. With the exception of **3a**, the spectra of all complexes exhibit broad resonances corresponding to the pyrrolide and phenylimido ligands at RT. The ^1H NMR spectrum of **3b** was studied further under variable temperature from 20 °C down to – 10 °C and the aromatic and aliphatic regions of the spectra are shown in Figure 6.

The signals corresponding to the pyrrolide and imido ligands begin to decoalesce at 15 °C and the maximum number of inequivalent peaks is clearly observed at 10 °C, while between 0 °C

and – 10 °C they are all well defined. For example, the broad peaks at 5.6 ppm and 1.9 ppm (pyrrolide) split into two sharp signals each, suggesting two different environments for this ligand. Likewise, the very broad signals corresponding to the isopropyl groups of the phenylimido ligand sharpen into two peaks for the methine protons and 4 peaks for the methyl protons, suggesting the molecule is C_1-symmetric.

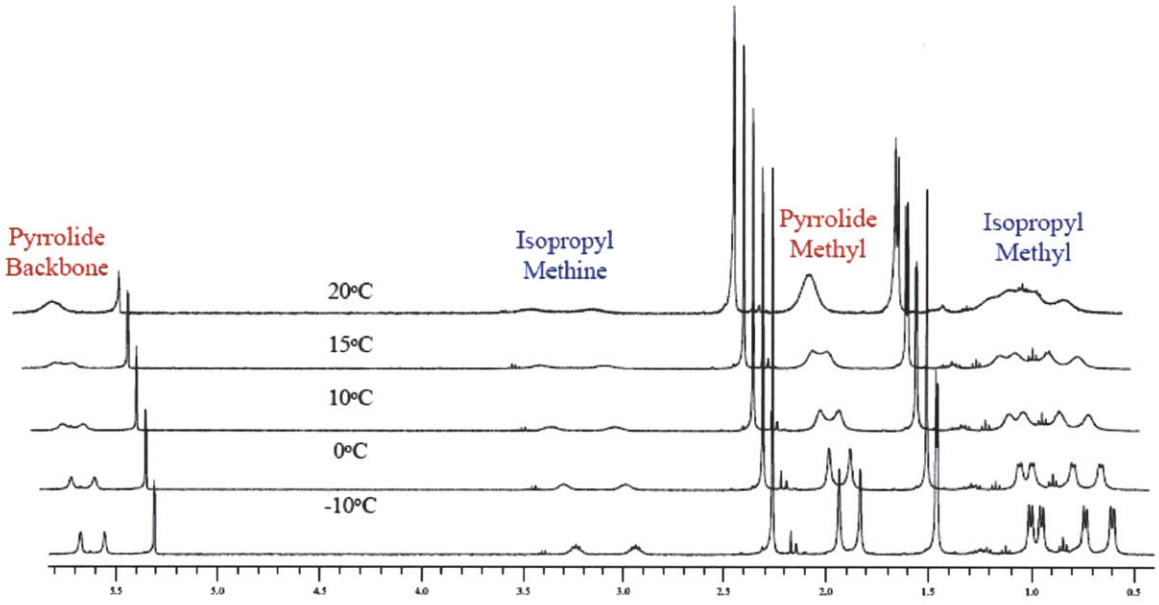

Figure 6 – VT ^{1}H NMR of **3b** in CD_2Cl_2 from 20°C (top) to -10°C (bottom). Only the region containing the broad pyrrolide and isopropyl peaks is shown.

A typical temperature range for decoalescence of broad signals in the ^{1}H NMR spectra of bispyrrolide complexes is – 40 °C and – 80 °C.[8] The fact that for **3b** the decoalescence temperature occurs at much higher values suggests that this complex is more crowded and that there is a significant amount of steric interactions between the ligands in the complex.

The structure of **3b**, as determined in an X-ray study, is shown in Figure 7. The molecule crystallizes in the orthorhombic space group Pbca. The structure can be best described as a distorted square pyramid, with the alkylidene ligand located in the apical position. The largest bond angles of the square pyramid correspond to N(1)-Mo(1)-O(2) (145.06(6)°) and N(2)-Mo(1)-O(1) (144.92(5)°), while the shortest correspond to C(1)-Mo(1)-O(1) (93.71(6)°) and O(1)-Mo(1)-O(2) (59.32(4)°).

The Mo(1)-N(1) and Mo(1)-C(1) bond lengths, as well as the Mo(1)-C(1)-C(2) and Mo(1)-N(1)-C(11) bond angles are similar to monoalkoxide-monopyrrolide (MAP) species prepared in the past.[7] One of the *iso*propyl groups on the phenyl imido ligand is disordered. Overall, the

structure is consistent with having an asymmetrical environment around the metal center; as suggested by the low temperature ^{1}H NMR experiments (*vide supra*).

The carboxylate ligand binds κ^2 to the metal center with similar Mo-O bond distances (~ 2.2 Å), with a Mo-O bond *trans* to the imido ligand and the other *trans* to the pyrrolide. The pyrrolide is found to be bound η^1 to the metal with a Mo(1)-N(2) distance of 2.0481(14)°, consistent with what has been found with many MAP complexes.[7] The κ^2-η^1 configuration makes the catalyst a 16-electron complex. The other alternative, a κ^1-η^5 configuration, would produce an electronically saturated, probably relatively unreactive, 18-electron species.

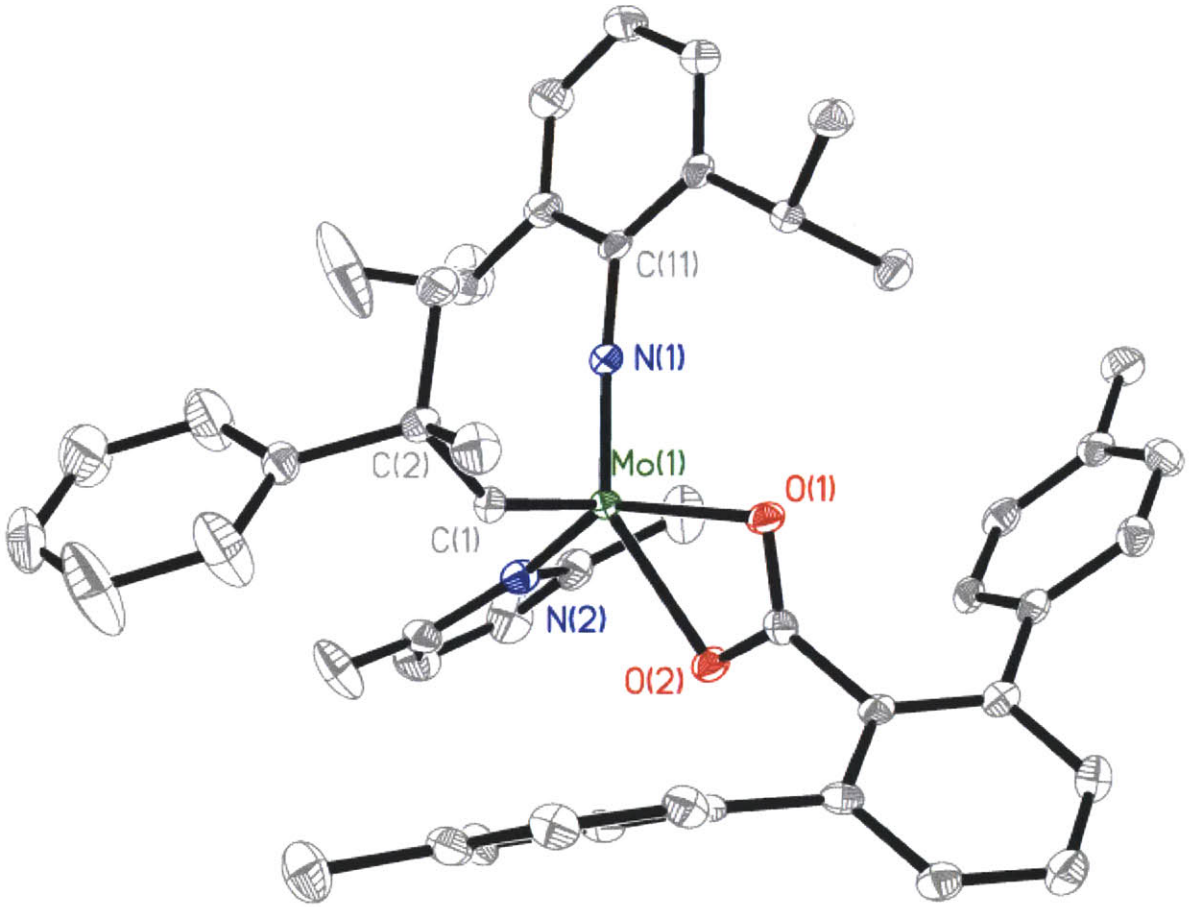

Figure 7 – The solid state structure of **3b** (50% probability ellipsoids). Selected bond lengths (Å) and bond angles (°): Mo1-N1 = 1.7284(14), Mo(1)-C(1) = 1.8690(17), Mo(1)-O(1) = 2.2066(12), Mo(1)-O(2) = 2.1874(11), Mo(1)-N(2) = 2.0481(14), Mo(1)-N(1)-C(11) = 175.73(13), Mo(1)-C(1)-C(2) = 144.25(13), N(1)-Mo(1)-C(1) = 100.48(7), N(1)-Mo(1)-N(2) = 103.88(6), N(1)-Mo(1)-O(1) = 101.51(6), N(1)-Mo(1)-O(2) = 145.06(6), N(2)-Mo(1)-C(1) = 104.92(7), N(2)-Mo(1)-O(1) = 144.92(5), N(2)-Mo(1)-O(2) = 86.30(5), C(1)-Mo(1)-O(1) = 93.71(6), C(1)-Mo(1)-O(2) = 109.13(6), O(1)-Mo(1)-O(2) = 59.32(4).

2.2.2 Reactivity Studies: Ethylene

The 16-electron monocarboxylate complexes do react with olefins, a property that is not shared with biscarboxylate catalysts. For example, treatment of **3b** with ethylene at RT in C_6D_6 was monitored during a period of 5 days by ^1H NMR spectroscopy. After 10 minutes of exposure to 1 atmosphere of ethylene no appreciable reaction takes place; however, after 17 h two doublets (13.05 ppm and 13.95 ppm, $J_{HH} = 4.0$ Hz) characteristic of the methylidene species are present with most of the starting material consumed. After 1 day no starting material remains and only the methylidene doublets are observed. Unfortunately, the stability of the methylidene complex is limited, presumably due to inadequate steric protection present around the metal center. As a result, the methylidene species decomposes to uncharacterizable products.

Since decomposition of monocarboxylate catalysts takes place under ethylene, olefin metathesis reactions that generate ethylene also suffer from decomposition (Scheme 2). For instance, when 5 mol% of **3b** is used for the metathesis of 1-hexene, the catalyst begins to decompose as ethylene is evolved from the system. After standing the sample for 2 days at RT, the alkylidene peak of the original catalyst has disappeared and the amount of 5-decene vs. 1-hexene remains 2:1 (see Chapter 5, Section 5.2 for further studies).

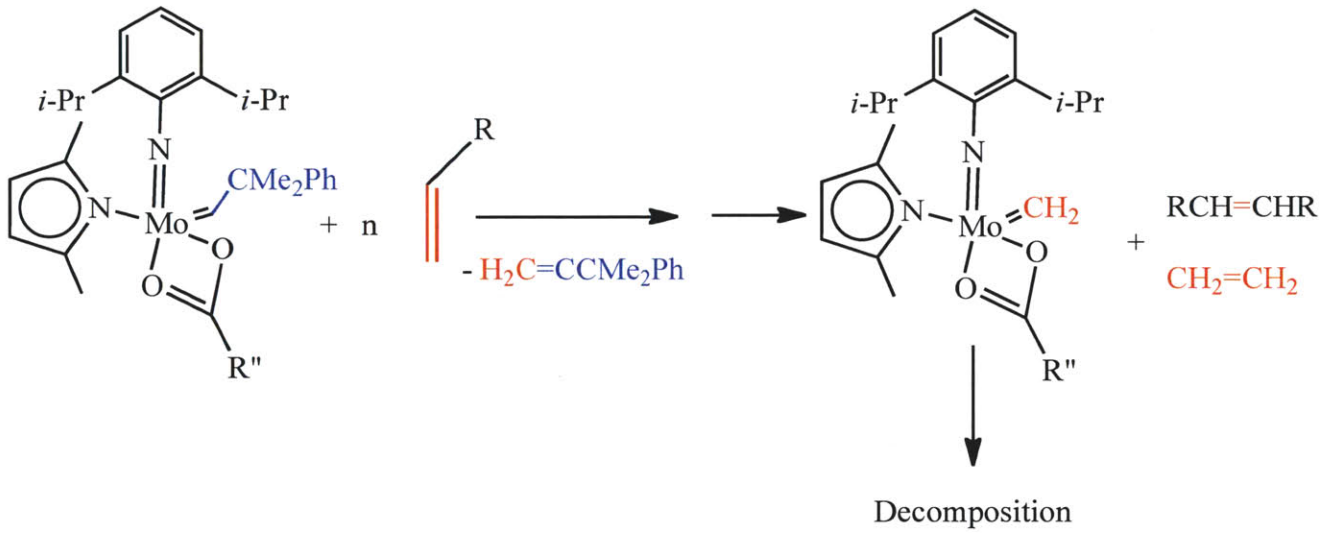

Scheme 2 – Pathway showing reaction between complexes **3a-c** and terminal olefins, and fate of the catalysts upon formation of methylene species.

2.2.3 Reactivity studies: Ring-closing metathesis reactions

Although olefin metatheses that evolves ethylene in the process is detrimental to the stability of the catalyst, reactions that do not form ethylene tend to preserve the catalyst longevity; therefore, these reactions are more efficiently catalyzed. For instance, the ring closing methatesis, RCM, of enyne substrates like diethyl(allylpropargylmalonate) (DEAPM) and the ring closing metathesis polymerization (RCMP) of DEDPM (shown in Scheme 3) gives products within a reasonable amount of time for some catalysts, shown in Table 2.

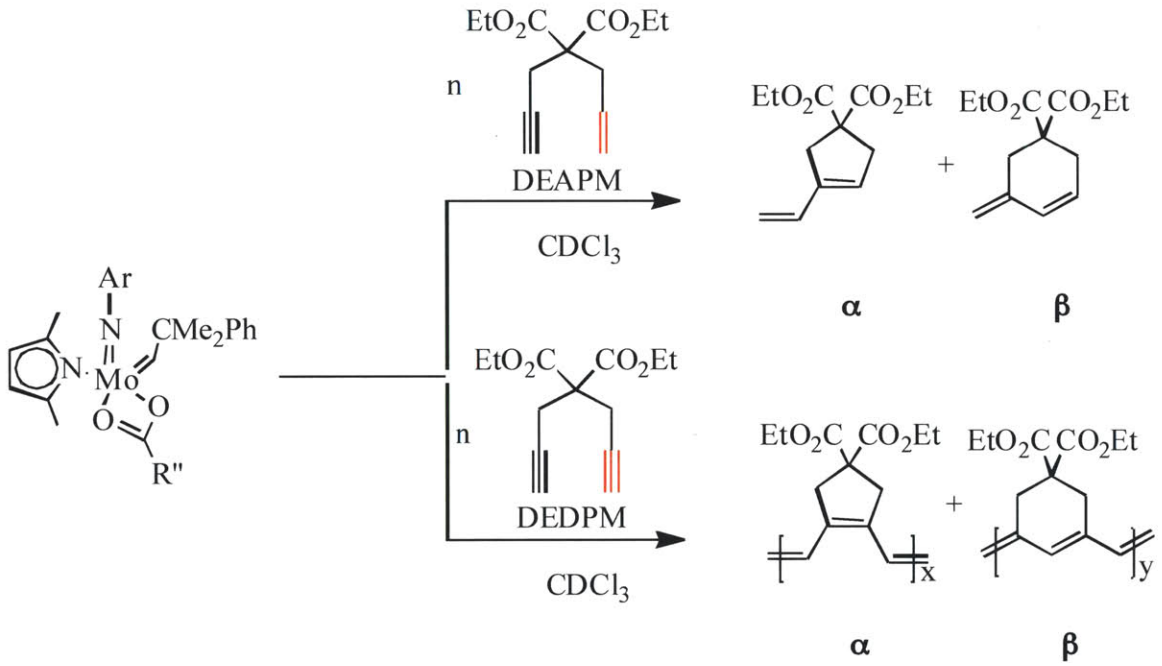

Scheme 3 – Possible products formed during RCM of DEAPM (top) and RCMP of DEDPM (bottom) with complexes **3a-d**.

RCM of 20 equivalents of DEAPM with catalysts **3a-c** is accomplished after 2 h at RT, while **3d** requires 3 days to reach completion at the same temperature. The slower reactivity of **3d** is attributed to the greater steric bulk of the carboxylate ligand, which hinders the substrate access to the metal center more than either $TRIPCO_2$ or $Ter_{Me}CO_2$. Surprisingly, none of the catalysts have any selectivity for β–product formation and form roughly equal amounts of five-membered and six-membered rings in the polymer. This result contrasts those obtained with MAP species, which tend to be selective for β–product formation.[7] Some of these reactions are discussed in Appendix A.

Table 2 - RCM of DEAPM and RCMP of DEDPM with catalysts **3a-d**.						
Catalyst	RCM of 20 eq. DEAPM			RCMP of 50 eq. DEDPM		
	α	β	Time	α	β	Time
3a	45%	55%	2 h	5%	93%	30 m
3b	52%	48%	2 h	14%	86%	30 m
3c	52%	48%	2 h	27%	73%	30 m
3d	59%	41%	3 d	14%	86%	19 h

On the other hand, RCMP of DEDPM with catalysts **3a-d** give polymer that contains a high content of six-membered rings (73-95%), with **3a** being the most selective. Catalysts **3b** and **3d** yield polymer with slightly lower 6-membered rings (86%), while **3c** is the least selective of the group. Figure 8 shows the quaternary carbon region of the ^{13}C NMR spectra for the polymers made with catalysts **3a** and **3b**. Polymerization of 25 equivalents of DEDPM with complexes **3a-c** is done within 30 min, whereas the reaction takes 19 hours to reach completion when complex **3d** is used. This result also parallels with the reactivity of RCM of DEAPM observed above. Thus, monocarboxylates with carboxylates smaller than $HIPTCO_2$ are very fast and efficient catalysts for the polymerization of DEDPM. This implies that the isopropyl groups of $TRIPCO_2$ may provide more steric guidance for substrate-binding than the phenyl rings of Ter_{Me} and Ter_{OMe}. In the case of **3d**, substrate-binding may be too unfavorable and may require significant ligand rearrangement (e.g. κ^2 to κ^1), which allows for α-binding to occur more frequently. Interestingly, when MAP species that are selective for RCM of DEAPM are used for RCMP of DEDPM, the β-selectivity is lost and there is either no preference for either ring structure or if there is any it is biased towards 5-membered ring formation. All of this data can be found in Appendix A. From the results provided in this section we can say that electronics may play a bigger role for β-selectivity of DEAPM, whereas sterics may be more important to get high β-selectivity in the polymerization of DEDPM.

A closer study of poly(DEDPM) formed with catalysts **3a-b** was undertaken by analyzing the UV-vis spectra of the isolated polymers, as shown in Figure 9. The polymers produced with catalyst **3a** (25mer, 50mer, 75mer, and 125mer) have absorption maxima that approach 533 nm as the size of the polymer becomes larger; whereas, polymers produced with **3b** (75mer, 100mer, and 125mer) have absorption maxima that approach 544 nm.

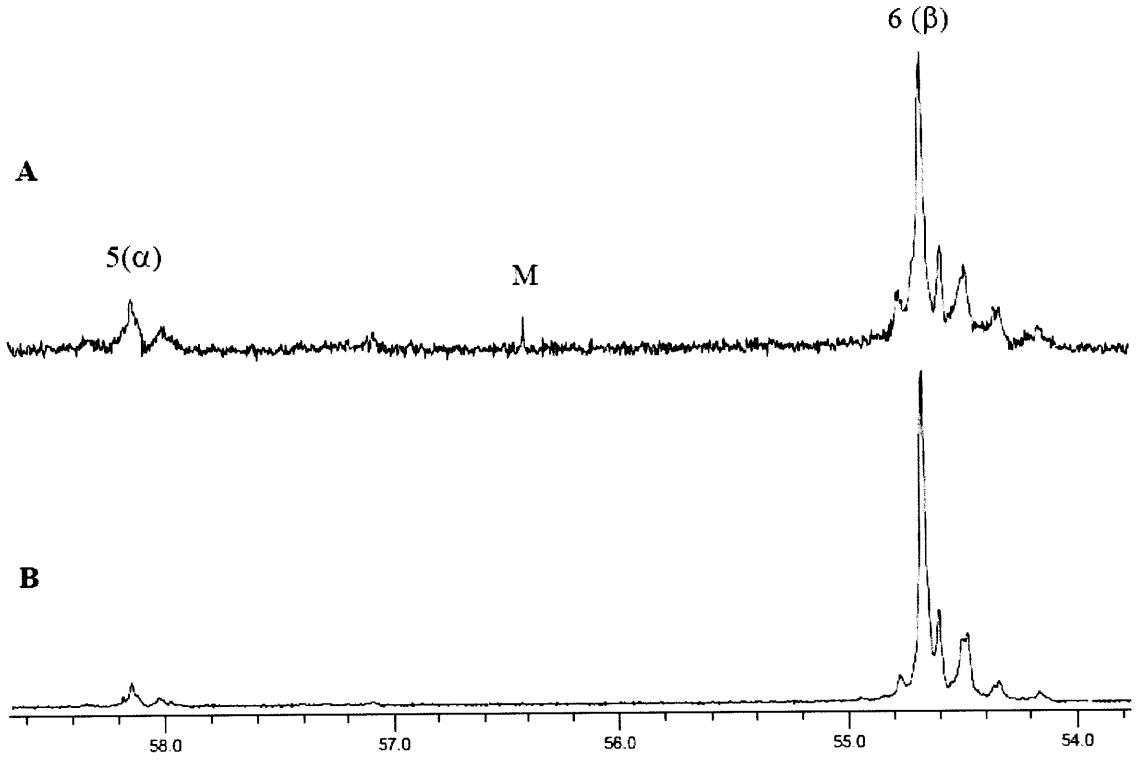

Figure 8 – ^{13}C NMR spectra of polymers prepared from (quaternary ^{13}C-labeled) DEDPM (M) using initiators **3b** (**A**) and **3a** (**B**).

Buchmeiser reported in the past that poly(DEDPM) containing exclusively all or greater than 95% six-membered structures has a maximum UV-vis absorption at 533 nm, while that of pure α polymer has a maximum absorption at 600 nm.[10e] Our results corroborate Buchmeiser's statement because polymer containing 95% six-membered rings (as indicated by ^{13}C NMR; Table 2) has a maximum at 533 nm and polymer containing only 86% six-membered rings (Figure 9B) has a maximum absorption peak red-shifted closer to the 600 nm limit. In addition, a shoulder is observed in the spectra of all polymers prepared with catalyst **3b** (Figure 9A). This shoulder corresponds to fine electronic absorption deriving from short 5-membered ring repeats throughout the polymer. This feature is absent in the UV-vis spectrum of the polymer made with catalyst **3a** (Figure 9B). In a polymer containing > 95% 6-membered rings, the probability of having high number of 5-membered ring repeats is low.

Polymerization of 100 equivalents of monomers containing bulkier ester groups (Figure 10), di*iso*propylesterdipropargylmalonate (DIDPM) or di*tert*butylesterdipropargylmalonate (DTDPM), with catalyst **3a** was performed to test the catalyst's overall selectivity. The resulting isolated polymers were examined by UV-vis. The spectrum of a 2.0 μg/ml poly(DIDPM)

solution in CH_2Cl_2 shows an absorption band at 533 nm, which correlates well with the results obtained with DEDPM and a polymer containing ~ 95% β polymer.

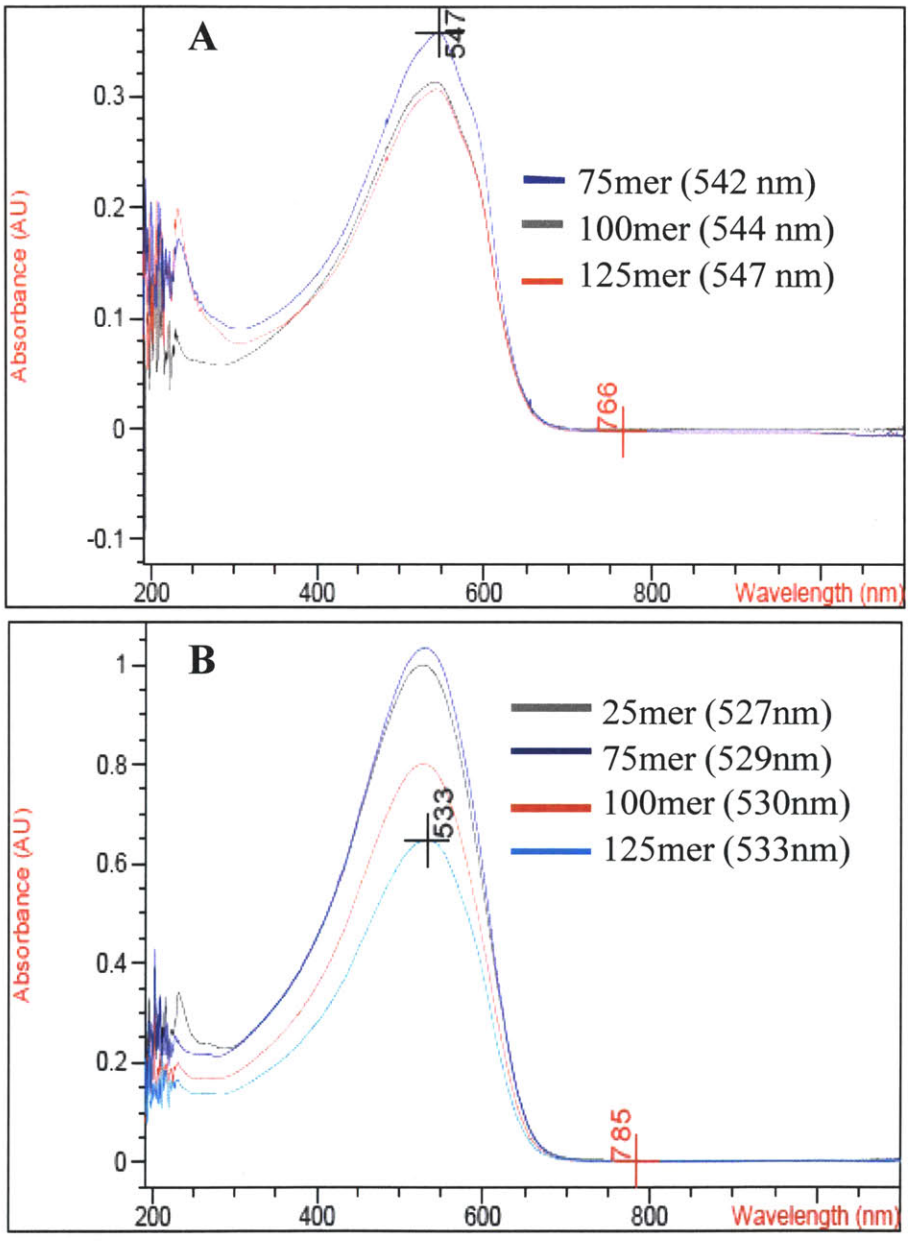

Figure 9 - UV-vis spectra of isolated poly(DEDPM) in CH_2Cl_2 prepared by reaction of 25, 50, 75, and 100 equivalents of DEDPM and catalysts **3b** (**A**) and **3a** (**B**). Absorption maxima are listed in parenthesis.

Unfortunately, the polymer is not soluble enough to get a good ^{13}C NMR spectrum. In the case of poly(DTDPM), a 1.2 μg/ml solution in the same solvent exhibits an absorption band around 540 nm, suggesting that the amount of β product has been diminished to about 86% (see Figures 8A and 9A). This polymer is soluble in $CDCl_3$ and ^{13}C NMR data can be obtained. In this case, the quaternary carbon region is in agreement with the UV-vis data and measures up to 86% six-membered rings present in the polymeric structure. These results point out that increasing the size of the ester groups effects the selectivity of monomer binding and, consequently, ring-size formation along the propagating unit of the polymer.

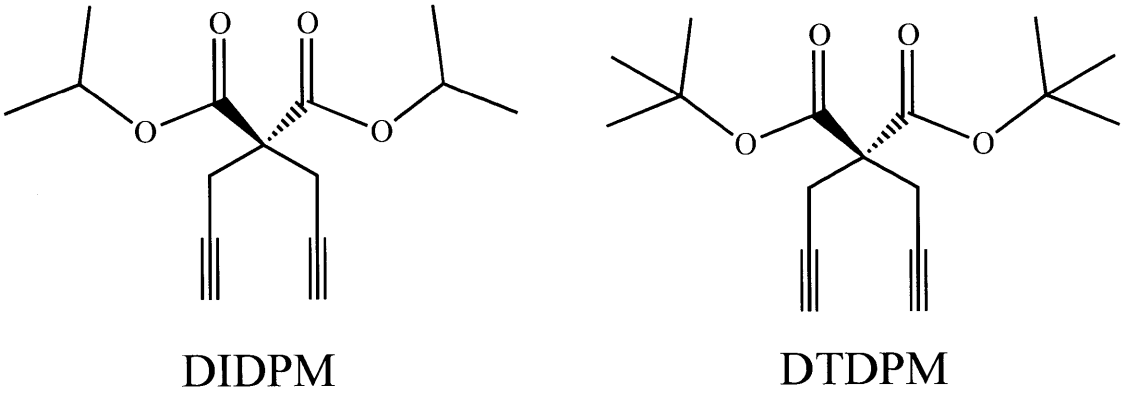

Figure 10 – Molecular structures of DIDPM and DTDPM monomers.

CONCLUSIONS

The ability to prepare and isolate stable, well-defined, carboxylate complexes depends critically on the steric bulk of the carboxylate. Carboxylates that possess smaller substituents result in "ate" complexes or formation of ill-defined oligomeric species. Binding of the carboxylates in a κ^2 fashion is favored, which yields a metal center that is less reactive than bisalkoxides or MAP species. In the case of biscarboxylates, the complexes are unreactive towards olefins but in the right circumstances will react with terminal alkynes, possibly through an unsaturated (κ^1, κ^1 or κ^1, κ^2) intermediate. On the other hand, monocarboxylates react with terminal olefins such as ethylene because they have a vacant site for substrate binding; however, their stability in the presence of ethylene is limited. Luckily, ring closing reactions that do not evolve ethylene are catalyzed effectively by these catalysts. Such is the case with DEAPM and

DEDPM, in the former no binding selectivity is observed, whereas in the latter selective for β-binding is observed.

As stated above, the utility of the carboxylate species lies in their ability to selectively polymerize DEDPM to give a polymer that contains all six-membered rings. Unfortunately, larger ester groups in the dipropargylmalonate lead to polymers that do not contain exclusively six-membered rings. Terphenylcarboxylates provide almost too much steric protection at the metal center in biscarboxylate complexes but perhaps too little in monocarboxylates. Both of these outcomes have a negative impact on the selectivity of six-membered ring formation. Still, it is somewhat surprising that polymer that contains only six-membered rings can form at all, since α,β disubstituted metallacyclobutene intermediates would appear less sterically crowded than α,α' disubstituted metallacyclobutene intermediates, all else being equal. Therefore we have little hope that many examples will arise in which only six-membered rings are formed from 1,6-heptadiynes. In contrast, formation of 1,6-heptadiyne polymers that contain only five-membered rings through formation of α,α' disubstituted metallacyclobutene intermediates seems to hold more promise.[3e, 9b] Such polymers also do not contain opportunities for E/Z isomerism and are relatively linear and rigid.

EXPERIMENTAL

All manipulations were performed in oven-dried (200 °C) glassware under an atmosphere of nitrogen on a dual-manifold Schlenk line or in a Vacuum Atmospheres glovebox. HPLC grade organic solvents were sparged with nitrogen and dried by passage through activated alumina prior to use, then stored over 4 Å Linde-type molecular sieves. Benzene-d_6 was dried over sodium/benzophenone ketyl and vacuum-distilled. Methylene chloride-d_2 was dried over CaH_2, vacuum distilled and stored over 4 Å Linde-type molecular sieves. NMR spectra were recorded on Varian spectrometers operating at 300 or 500 MHz and Bruker spectrometers operating at 400 MHz. Chemical shifts for ^1H and ^{13}C spectra were referenced to the residual $^1H/^{13}C$ resonances of the deuterated solvent (^1H: C_6D_6, δ 7.16; CD_2Cl_2, δ 5.32; ^{13}C: C_6D_6, δ 128.39; CD_2Cl_2, δ 54.00) and are reported as parts per million relative to tetramethylsilane. UV-vis spectra were recorded on an Agilent 8453 diode array spectrometer. Elemental analyses were performed by H. Kolbe Microanalytical Laboratory, Mülheim an der Ruhr, Germany.

Mo(NR)($CHCMe_2Ph$)($OTf)_2$(DME) species (where R = 2,6-*i*-$Pr_2C_6H_3$ (Ar), 2,6-$Me_2C_6H_3$ (Ar'), 1-adamantyl (Ad), and 2-*t*-BuC_6H_4 (Ar"))[15] and Mo(NAr)($CHCMe_2Ph$)($Me_2Pyr)_2$[17] were prepared according to published procedures. Syntheses of Mo(NAr)($CHCMe_2Ph$)($O_2CCPh_3)_2$, Mo(NAr)($CHCMe_2Ph$)($O_2CCMePh_2)_2$, Mo(NAr")(CH-*t*-Bu)($O_2CCPh_3)_2$, and Mo(NAd)($CHCMe_2Ph$)($O_2CCPh_3)_2$ have been reported in a preliminary fashion.[11] $Ter_{Me}CO_2H$ and $Ter_{OMe}CO_2H$ were prepared as described in the literature.[12] All carboxylate salts were prepared by addition of NaH to a THF solution of the corresponding acid (Aldrich) followed by crystallization from THF/pentane. All other reagents were purchased from commercial vendors and used as received.

Mo(NAr)($CHCMe_2Ph$)($O_2CTer_{Me})_2$ (2a). Mo(NAr)($CHCMe_2Ph$)($Me_2Pyr)_2$ (0.295 g, 0.495 mmol) was dissolved in a minimal amount of diethyl ether and the solution was placed at -35 °C for 1 h. $Ter_{Me}CO_2H$ (0.299 g, 0.990 mmol) was dissolved in a minimal amount of ether and the solution was placed at -35 °C for 1 h. At the end of the cooling period, the solution containing the carboxylic acid was added to the other dropwise. The reaction was stirred at RT for 30 min. The volatiles were removed and the sample was triturated with pentane for 1 h until an orange powder was obtained. The powder was isolated by filtration. The powder was redissolved in diethyl ether and placed at -35 °C for 12 h to yield pure orange product upon filtration (0.279 g, 56%): ^1H NMR (400 MHz, CD_2Cl_2) δ 13.13 (s, 1H, MoC*H*CMe_2Ph, J_{CH} = 124.8 Hz), 7.60-6.80 (m, 30H, aromatics), 3.17 (m, 2H, C*H*Me_2), 2.19 (s, 12H, Ter_{Me} *Me*), 1.30 (s, 6H, MoCHC*Me*$_2$Ph), 0.835 (d, 12H, CH*Me*$_2$); ^{13}C NMR (100 MHz, CD_2Cl_2) δ 309 (Mo*C*HCMe_2Ph), 185 (*C*O_2), 152.5, 150.3, 148.9, 143.0, 138.6, 136.8, 131.6, 130.3, 129.9,

129.3, 128.5, 128.3, 128.1, 126.2, 126.0, 122.9, 55.7, 31.3, 28.6, 23.4, 21.2. Anal. Calcd for $C_{65}H_{65}MoNO_4$: C, 76.40; H, 6.31; N, 1.39. Found: C, 76.31; H, 6.32; N, 1.42.

A small sample (0.030 g) of the pure compound was dissolved in a saturated solution of methylene chloride and ether was layered on top at RT to yield small crystals suitable for diffraction.

Mo(NAr)(CHCMe$_2$Ph)(O$_2$CTer$_{OMe}$)$_2$ (2b). Prepared as for **2a** from Mo(NAr)(CHR)(Me$_2$Pyr)$_2$ (0.250 g, 0.420 mmol) and Ter$_{OMe}$CO$_2$H (0.281 g, 0.840 mmol). The volatiles were removed from the reaction mixture and the sample was triturated with pentane for 1 h until an orange powder was obtained. The powder was isolated by filtration and recrystallized from ether at -35 °C (0.248 g, 55%): ^{1}H NMR (400 MHz, CD_2Cl_2) δ 13.14 (s, 1H, MoC*H*CMe$_2$Ph, J_{CH} = 123.28 Hz), 7.8-6.4 (m, 30H, aromatics), 3.59 (s, 12H, TerO*Me*), 3.24 (m, 2H, C*H*Me$_2$Ph), 1.29 (s, 6H, MoCHC*Me$_2$*), 0.85 (d, 12H, CH*Me$_2$*); ^{13}C NMR (100 MHz, CD_2Cl_2) δ 307.0 (Mo*C*HCMe$_2$Ph), 185.3 (*C*O$_2$), 159.1, 142.7, 133.7, 130.3, 129.8, 128.3, 126.1, 122.9, 114.4, 113.6, 105.8, 55.2, 28.6, 23.4, 14.1, 12.8. Anal. Calcd for $C_{65}H_{65}MoNO_8$: C, 71.83; H, 5.93; N, 1.31. Found: C, 71.80; H, 5.86; N, 1.33.

Mo(NAd)(CHCMe$_2$Ph)(O$_2$CTer$_{Me}$)$_2$ (2c). Prepared as for **2a** from Mo(NAd)(CHR)(Me$_2$Pyr)$_2$ (0.288 g, 0.509 mmol) and Ter$_{Me}$CO$_2$H (0.308 g, 1.02 mmol). After complete addition of the carboxylic acid, the off-white product precipitated out and was collected by filtration, washed twice with diethyl ether, and dried *in vacuo* (0.330 g, 66%): ^{1}H NMR (400 MHz, $CDCl_3$) δ 13.04 (s, 1H, MoC*H*CMe$_2$Ph, J_{CH} = 123.88 Hz), 7.42 (t, 2H, terphenyl), 7.33-7.14 (m, 17H, aromatics), 6.90 (d, 8H, terphenyl), 2.18 (s, 12H, *p-tolylMe*), 1.93 (s br, 3H, *CH* Ad), 1.64 (s br, 6H, *CH* Ad), 1.49 (s, 6H, *CH Ad*); ^{13}C NMR (100 MHz, $CDCl_3$) δ 307.3, 185.7 (*C*O$_2$), 150.7, 141.9, 138.4, 136.6, 132.9, 129.9, 129.3, 129.2, 128.9, 128.4, 126.6, 126.0, 51.4, 43.3, 35.9, 31.4, 29.5, 21.3. Anal. Calcd for $C_{62}H_{61}MoNO_4$: C, 75.98; H, 6.27; N, 1.43. Found: C, 75.88; H, 6.35; N, 1.41.

Mo(NAd)(CHCMe$_2$Ph)(O$_2$CTer$_{OMe}$)$_2$ (2d). Prepared as for **2a** from Mo(NAd)(CHR)(Me$_2$Pyr)$_2$ (0.250 g, 0.442 mmol) and Ter$_{OMe}$CO$_2$H (0.296 g, 0.885 mmol). The volatiles were removed and the sample was triturated with pentane for a few minutes. The white powder was isolated and dried by vacuum filtration (0.200 g, 43%): ^{1}H NMR (400 MHz, $CDCl_3$) δ 13.09 (s, 1H, MoC*H*CMe$_2$Ph, J_{CH} = 123.40 Hz), 7.46 (t, 2H, terphenyl), 7.32-7.14 (m, 12H, aromatics), 6.63 (d, 8H, terphenyl), 3.58 (s, 12H, TerO*Me*), 1.89 (s br, 3H, *CH Ad*), 1.60 (s, 6H, *CH Ad*), 1.49 (s, 6H, *CH Ad*); ^{13}C NMR (100 MHz, $CDCl_3$) δ 306.4, 185.8 (*C*O$_2$), 159.0, 150.4, 141.6, 133.6, 132.8, 130.1, 129.9, 129.2, 128.5, 128.4, 126.6, 126.1, 55.2, 51.3, 43.5, 35.9,

31.3, 29.5. Anal. Calcd for $C_{62}H_{61}MoNO_8$: C, 71.32; H, 5.89; N, 1.34. Found: C, 71.31; H, 5.95; N, 1.36.

Mo(NAr)(CHCMe$_2$Ph)(Me$_2$Pyr)(O$_2$CTRIP) (3a). Mo(NAr)(CHCMe$_2$Ph)(Me$_2$Pyr)$_2$ (0.225 g, 0.378 mmol) was dissolved in a minimal amount of ether and placed at -35 °C for 1 h. TRIPCO$_2$H (0.094 g, 0.378 mmol) was dissolved in a minimal amount of ether and placed at -35 °C for 1 h. At the end of the cooling period, the solution containing the carboxylic acid was added to the solution containing the precatalyst dropwise and it was left stirring at RT for 30 min. At the end of the reaction period, the volatiles were removed and the sample was triturated with pentane for 1 h until an orange powder precipitated. The powder was isolated by filtration and it was redissolved in ether and placed at - 35 °C for 12 h to yield a precipitate. This product was once again redissolved in diethyl ether and crystallized out at -35 °C to yield orange product upon filtration (0.031 g, 12%): ^{1}H NMR (400 MHz, CD_2Cl_2) δ 13.62 (s, 1H, MoC*H*, J_{CH} = 121.5 Hz), 7.48-7.00 (m, 10H, aromatics), 5.721 (s br, 2H, Me$_2$C$_4$*H*$_2$N), 3.04-2.82 (sept, 5H, C*H*Me$_2$), 2.19 (s br, 6H, *Me*$_2$C$_4$H$_2$N), 1.77 (s, 3H, MoCHC*Me*$_2$Ph), 1.76 (s, 3H, MoCHC*Me*$_2$Ph), 1.25 (d, 6H, TripCH*Me*$_2$), 1.23 (d, 6H, TripCH*Me*$_2$), 1.2-1.1 (m, 18H, Trip CH*Me*$_2$ + imido (CH*Me*$_2$)$_2$); ^{13}C NMR (100 MHz, CD_2Cl_2) δ 297.6 (MoCH), 191.4 (*C*O$_2$), 152.6, 151,9, 151.5, 151.1, 150.3, 148.8, 147.6, 146.3, 145.4, 131.5, 128.5, 128.4, 128.3, 126.5, 126.1, 123.2, 121.1, 107.6, 105.8, 65.9, 55.7, 34.7, 31.9, 31.6, 29.2, 28.4 (br), 24.2, 23.8, 23.3 (br), 15.3. Anal. Calcd for $C_{44}H_{60}MoN_2O_2$: C, 70.95; H, 8.12; N, 3.76. Found: C, 70.66; H, 8.00; N, 3.67.

Mo(NAr)(CHCMe$_2$Ph)(Me$_2$Pyr)(O$_2$CTer$_{Me}$) (3b). Prepared as for **3a** from Mo(NAr)(CHCMe$_2$Ph)(Me$_2$Pyr)$_2$ (0.422 g, 0.709 mmol) and Ter$_{Me}$CO$_2$H (0.214 g, 0.709 mmol) to yield an orange solid upon filtration (0.115 g, 34%). Pure **3b** (0.030 g) was dissolved in a saturated solution of 1:1 methylene chloride/diethyl ether and placed at -35 °C over a few days to yield crystals suitable for diffraction: ^{1}H NMR (400 MHz, CD_2Cl_2) δ 12.99 (s, 1H, MoC*H*, J_{CH} = 122.78 Hz), 7.60-7.00 (m, 19H, aromatics), 5.64 (s br, 2H, Me$_2$C$_4$*H*$_2$N), 3.19 (d, 2H, C*H*Me$_2$), 2.30 (s, 6H, *Ter*$_{Me}$CO$_2$), 1.97 (s br, 6H, *Me*$_2$C$_4$H$_2$N), 1.50 (d, 6H, MoCHC*Me*$_2$), 0.87 (m, 12H, CH*Me*$_2$); ^{13}C NMR (100 MHz, CD_2Cl_2) δ 301.3 (MoCHCMe$_2$Ph), 189.8 (*C*O$_2$), 152.0, 149.7 (br), 148.0, 140.2, 137.8, 137.7, 133.7, 132.3, 129.9, 129.4, 129.2, 129.0, 128.4, 128.1, 126.4, 126.2, 123.4 (br), 122.8 (br), 107.2, 55.9 (MoCHC*M*e$_2$Ph), 31.9, 29.2, 27.2 (br), 24.0 (br), 22.6, 17.8 (br), 14.1. Anal. Calcd for $C_{50}H_{56}MoN_2O_2$: C, 73.67; H, 6.81; N, 3.51. Found: C, 73.56; H, 6.86; N, 3.48.

Mo(NAr)(CHCMe$_2$Ph)(Me$_2$Pyr)(O$_2$CTer$_{OMe}$) (3c). Prepared as for **3a** from Mo(NAr)(CHCMe$_2$Ph)(Me$_2$Pyr)$_2$ (0.520 g, 0.873 mmol) and Ter$_{OMe}$CO$_2$H (0.292 g, 0.873 mmol)

to yield pure orange product upon filtration (0.340 g, 47%): ^{1}H NMR (400 MHz, CD_2Cl_2) δ 12.93 (s, 1H, MoC*H*, J_{CH} = 120.25 Hz), 7.64-6.72 (m, 19H, aromatics), 5.68 (s br, 2H, $Me_2C_4H_2N$), 3.73 (s, 6H, O*Me*), 3.20 (d br, 2H, C*H*Me_2), 1.88 (d br, 6H, $Me_2C_4H_2N$), 1.52 (d, 6H, MoCHCMe_2Ph), 0.90 (m, 12H, CHMe_2); ^{13}C NMR (100 MHz, CD_2Cl_2) δ 301.1 (MoCHCMe$_2$Ph), 189.9 (CO_2), 159.6, 152.0, 148.0, 141.4, 139.9, 133.8, 133.7, 132.8, 130.3, 129.9, 129.1, 128.4, 128.3, 128.1, 126.4, 126.2, 125.2, 122.8 (br), 114.4, 114.0, 107.3, 56.0, 55.5, 55.4, 55.2, 32.0, 28.9, 24.1 (br), 23.4 (br). Anal. Calcd For $C_{50}H_{56}MoN_2O_4$: C, 70.83; H, 6.55; N, 3.37. Found: C, 70.67%; H, 6.69; N, 3.53.

***In situ* preparation of Mo(NAr)(CHCMe$_2$Ph)(Me$_2$Pyr)(O$_2$CHIPT) (3d).** Mo(NAr)(CHCMe$_2$Ph)(Me$_2$Pyr)$_2$ (0.010 g, 16.8 mmol) and HIPTCO$_2$H (0.009 g, 17.1 mmol) were dissolved in $CDCl_3$ (0.7 ml) and charged to a J-Young tube. A new alkylidene peak formed within 30 min of mixing: ^{1}H NMR (400 MHz, $CDCl_3$) δ 13.53 (s, 1H, MoC*H*), 7.50-7.00 (m, 15H, aromatics), 6.08 (s br, 1H, $Me_2C_4H_2N$), 5.96 (s br, 1H, $Me_2C_4H_2N$), 3.13 (m, 2H, C*H*Me_2), 3.06 (m, 2H, C*H*Me_2), 2.97 (m, 2H, C*H*Me_2), 2.04 (s, 6H, $Me_2C_4H_2N$), 1.91 (s, 3H, CHCMe_2Ph), 1.75 (s, 3H, CHCMe_2Ph), 1.55-1.25 (overlapping peaks, 48H, various CHMe_2).

Photolysis Experiments

Mo(NAr)(CHCMe$_2$Ph)(O$_2$CCPh$_3$)$_2$ (1a). In a sample irradiated in toluene-d$_8$ at 366 nm for 3 h at 22 °C a mixture containing 16% *anti* was formed (δH_α = 13.93 ppm, J_{CH} = 138.4 Hz). At 22 °C conversion of *anti* to *syn* was found to take place in a first order manner with $k_{a/s}$ = (8.30 ± 0.93) x 10^{-6} s^{-1}.

Mo(NAd)(CHCMe$_2$Ph)(O$_2$CCPh$_3$)$_2$ (1b).

A sample of **1c** irradiated in toluene-d$_8$ at 366 nm for 2 h at 22 °C produced a mixture containing 28% *anti* (δH_α = 13.99 ppm, J_{CH} = 140.0 Hz). At 22 °C conversion of *anti* to *syn* was found to take place in a first order manner with $k_{a/s}$ = (3.08 ± 0.14) x 10^{-4} s^{-1}.

Mo(NAr^{tBu})(CH-*t*-Bu)(O$_2$CCPh$_3$)$_2$ (1d). A sample of **1d** irradiated in toluene-d$_8$ at 366 nm for 2 h at 22 °C produced a mixture containing 17% *anti* (δH_α = 13.90 ppm, J_{CH} = 136.9 Hz). At 0 °C conversion of *anti* to *syn* was found to take place in a first order manner with $k_{a/s}$ = (1.55 ± 0.12) x 10^{-5} s^{-1} and at room temperature with $k_{a/s}$ = (3.62 ± 0.74) x 10^{-3} s^{-1} ($t_{1/2} \approx 3$ min).

Mo(NAr)(CHCMe$_2$Ph)(O$_2$CTer$_{Me}$)$_2$ (2a). A sample of **5a** irradiated in toluene-d$_8$ at 366 nm for 2 h at 22 °C produced a mixture containing 7% of the *anti* species (δH_α = 13.6 ppm, J_{CH} =

137 Hz). At 0 °C conversion of *anti* to *syn* was found to take place in a first order manner with $k_{a/s} = (1.28 \pm 0.11) \times 10^{-5}$ s^{-1} and at room temperature $k_{a/s} = (5.31 \pm 1.14) \times 10^{-4}$ s^{-1}.

General procedure for polymerizations. In a representative example, 3.01 mL of a stock solution of **1d** (6.76 mM in toluene) was diluted with 3.0 mL of toluene. To the stirring catalyst solution was added 1.00 mL of a stock solution of DEDPM (0.406 M in toluene) via syringe. Within 30 seconds the reaction solution became deep red. After 6 hours, 20 μL of benzaldehyde was added. The mixture was stirred for an additional three hours and then poured into 100 mL of hexanes causing precipitation of the polymer as a deep red powder. Pertinent spectroscopic features of the polymer are as follows: ^{1}H NMR (300 MHz, $CDCl_3$) δ 6.2 (br, 1, C*H*), 5.9 (br, 1, CH), 4.2 (m, CH_2CH$_3$), 3.2 (br, 2, ring-CH_2), 2.9 (br, 2, ring-CH_2), 1.2 (t, CH$_2$CH_3); ^{13}C NMR (75 MHz, $CDCl_3$) δ 171.0 (*C*O$_2$), 134.3, 133.9, 132.9, 131.7 (4 vinylic-*C*), 61.8 (OCH_2CH$_3$), 54.6 (C_{quat}), 35.0 (ring-*C*H$_2$), 32.2 (ring-*C*H$_2$), 14.0 (OCH$_2$*C*H$_3$). Minor additional resonances for the polymer backbone proton and carbon atoms can be detected in polymers containing all six-membered rings. We attribute these minor resonances to *cis*/*trans* isomerism at the exocyclic double bond.

Description of X-ray Studies. Low temperature diffraction data were collected on a Siemens Platform three-circle diffractometer coupled to a Bruker-AXS Smart Apex CCD detector with graphite-monochromated Mo Kα radiation (λ = 0.71073 Å), performing φ- and ω-scans. All structures were solved by direct methods using SHELXS and refined against F^2 on all data by full-matrix least squares with SHELXL-97.[16] All non-hydrogen atoms were refined anisotropically. Coordinates for the hydrogen atoms on C_α of the alkylidene groups were taken from the difference Fourier synthesis and subsequently refined semi-freely with the help of distance restraints. All other hydrogen atoms were included in the model at geometrically calculated positions and refined using a riding model. The isotropic displacement parameters of all hydrogen atoms were fixed to 1.2 times the *U* value of the atoms they are linked to (1.5 times for methyl groups). A disordered isopropyl group in the structures of **2a** was refined with the help of similarity restraints on 1-2 and 1-3 distances and displacement parameters as well as rigid bond restraints for anisotropic displacement parameters. For details of data and refinement statistics see Tables 3 and 4.

Table 3. Crystal data and structure refinement for **2a**.

Reciprocal net identification code	**08026**	
Empirical formula	C64 H63 Mo N O4	
Formula weight	1006.09	
Temperature	100(2) K	
Wavelength	0.71073 Å	
Crystal system	Triclinic	
Space group	$P\bar{1}$	
Unit cell dimensions	a = 12.194(6) Å	α= 88.751(9)°
	b = 12.241(6) Å	β= 76.586(9)°
	c = 20.290(11) Å	γ = 66.079(9)°
Volume	2684(2) $Å^3$	
Z	2	
Density (calculated)	1.245 Mg/m^3	
Absorption coefficient	0.292 mm^{-1}	
F(000)	1056	
Crystal size	0.25 x 0.20 x 0.10 mm^3	
Theta range for data collection	1.04 to 28.28°	
Index ranges	-16<=h<=15, -16<=k<=16, -27<=l<=26	
Reflections collected	48967	
Independent reflections	13298 [R(int) = 0.0371]	
Completeness to theta = 28.28°	99.8 %	
Absorption correction	Semi-empirical from equivalents	
Max. and min. transmission	0.9713 and 0.9305	
Refinement method	Full-matrix least-squares on F^2	
Data / restraints / parameters	13298 / 100 / 665	
Goodness-of-fit on F^2	1.027	
Final R indices [I>2sigma(I)]	R1 = 0.0342, wR2 = 0.0804	
R indices (all data)	R1 = 0.0441, wR2 = 0.0860	
Largest diff. peak and hole	0.939 and -0.633 $e.Å^{-3}$	

Table 4. Crystal data and structure refinement for **3b**.

Reciprocal net identification code	**08017**	
Empirical formula	C49 H54 Mo N2 O2	
Formula weight	798.88	
Temperature	100(2) K	
Wavelength	0.71073 Å	
Crystal system	Orthorhombic	
Space group	Pbca	
Unit cell dimensions	a = 17.2200(14) Å	α= 90°
	b = 13.3951(11) Å	β= 90°
	c = 35.799(3) Å	γ = 90°
Volume	8257.6(12) $Å^3$	
Z	8	
Density (calculated)	1.285 Mg/m^3	
Absorption coefficient	0.359 mm^{-1}	
F(000)	3360	
Crystal size	0.25 x 0.25 x 0.07 mm^3	
Theta range for data collection	2.01 to 30.03°	
Index ranges	-24<=h<=24, -18<=k<=18, -50<=l<=50	
Reflections collected	216789	
Independent reflections	12070 [R(int) = 0.0685]	
Completeness to theta = 30.03°	100.0 %	
Absorption correction	Semi-empirical from equivalents	
Max. and min. transmission	0.9753 and 0.9157	
Refinement method	Full-matrix least-squares on F^2	
Data / restraints / parameters	12070 / 286 / 551	
Goodness-of-fit on F^2	1.043	
Final R indices [I>2sigma(I)]	R1 = 0.0339, wR2 = 0.0731	
R indices (all data)	R1 = 0.0529, wR2 = 0.0838	
Largest diff. peak and hole	0.732 and -0.634 $e.Å^{-3}$	

REFERENCES

(1) (a) Schrock, R. R. *Chem. Rev.* **2002**, *102*, 145. (b) Schrock, R. R.; Hoveyda, A. H. *Angew. Chem. Int. Ed.* **2003**, *42*, 4592. (c) Schrock, R. R. in *Handbook of Metathesis*, Grubbs, R. H., Ed. Wiley-VCH: Weinheim, 2003; Vol. 1, pp 8. (d) Schrock, R. R.; Czekelius, C. C. *Adv. Syn. Catal.* **2007**, *349*, 55.

(2) (a) *Handbook of Metathesis. Applications in Polymer Synthesis*, Grubbs, R. H., Ed., Wiley-VCH: Weinheim, 2003; Vol. 3. (b) Schrock, R. R. In *Metathesis Polymerization of Olefins and Polymerization of Alkynes*, Imamoglu, Y., Ed. Kluwer: 1998; p 357. (c) Schrock, R. R. *Acc. Chem. Res.* **1990**, *23*, 158.

(3) (a) Masuda, T. *J. Poly. Sci. A* **2007**, *45*, 165. (b) Schrock, R. R.; Luo, S.; Zanetti, N.; Fox, H. H. *Organometallics* **1994**, *13*, 3396. (c) Schrock, R. R.; Luo, S.; Lee, J. C. J.; Zanetti, N. C.; Davis, W. M. *J. Am. Chem. Soc.* **1996**, *118*, 3883. (d) Fox, H. H.; Schrock, R. R. *Organometallics* **1992**, *11*, 2763. (e) Anders, U.; Nuyken, O.; Buchmeiser, M. R. *J. Mol. Catal. A* **2004**, *213*, 89. (f) Buchmeiser, M. *Adv. Polym. Sci.* **2005**, *176*, 142. (g) Fox, H. H.; Wolf, M. O.; O'Dell, R.; Lin, B. L.; Schrock, R. R.; Wrighton, M. S. *J. Am. Chem. Soc.* **1994**, *116*, 2827. (h) Buchmeiser, M. R. *Monatshefte fuer Chemie* **2003**, *134*, 327. (i) Anders, U.; Krause, J. O.; Wang, D.; Nuyken, O.; Buchmeiser, M. R. *Designed Monomers and Polymers* **2004**, *7*, 151. (j) Mayershofer, M. G.; Nuyken, O.; Buchmeiser, M. R. *Macromolecules* **2006**, *39*, 2452.

(4) R. R. Schrock in *Handbook of Metathesis. Applications in Organic Synthesis*, Grubbs, R. H., Ed., Wiley-VCH: Weinheim, 2003; Vol. 2.

(5) (a) Schrock, R. R.; Murdzek, J. S.; Bazan, G. C.; Robbins, J.; DiMare, M.; O'Regan, M. *J. Am. Chem. Soc.* **1990**, *112*, 3875. (b) Schrock, R. R. *Chem. Rev.* **2002**, *102*, 145.

(6) Feldman, J.; Schrock, R. R. *Prog. Inorg. Chem.* **1991**, *39*, 1.

(7) Singh, R.; Schrock, R. R.; Müller, P.; Hoveyda, A. H. *J. Am. Chem. Soc.* **2007**, *129*, 12654.

(8) Hock, A. S.; Schrock, R. R.; Hoveyda, A. H. *J. Am. Chem. Soc.* **2006**, *128*, 16373.

(9) (a) Anders, U.; Nuyken, O.; Buchmeiser, M. R.; Wurst, K. *Angew. Chem., Int. Ed. Engl.* **2002**, *41*, 4044. (b) Anders, U.; Nuyken, O.; Buchmeiser, M. R.; Wurst, K. *Macromolecules* **2002**, *35*, 9029. (c) Krause, J. O.; Wang, D.; Anders, U.; Weberskirch, R.; Zarka, M. T.; Nuyken, O.; Jaeger, C.; Haarer, D.; Buchmeiser, M. R., *Macromol. Symp.* **2004**, *217*, 179. (d) Adamchuk, J.; Schrock, R. R.; Tonzetich, Z. J.; Müller, P. *Organometallics* **2006**, *25*, 2364.

(10) (a) Krause, J. O.; Nuyken, O.; Buchmeiser, M. R. *Chem. Eur. J.* **2004**, *10*, 2029. (b) Yang, L.; Mayr, M.; Wurst, K.; Buchmeiser Michael, R. *Chem. Eur. J.* **2004**, *10*, 5761. (c) Halbach,

T. S.; Krause, J. O.; Nuyken, O.; Buchmeiser, M. R. *Macromol. Rapid. Commun.* **2005**, *26*, 784. (d) Halbach, T. S.; Mix, S.; Fischer, D.; Maechling, S.; Krause, J. O.; Sievers, C.; Blechert, S.; Nuyken, O.; Buchmeiser, M. R. *J. Org. Chem.* **2005**, *70*, 4687. (e) Mayershofer, M. G.; Nuyken, O.; Buchmeiser, M. R. *Macromolecules* **2006**, *39*, 3484.

(11) Schattenmann, F. J.; Schrock, R. R.; Davis, W. M. *J. Am. Chem. Soc.* **1996**, *118*, 3295.

(12) (a) DU, C. –J. F.; Hart, H.; Ng, K. –K. D. *J. Org. Chem.* **1986**, *51*, 3162. (b) Saednya, A.; Hart, H. *Synthesis* **1996**, 1455.

(13) Oskam, J. H.; Schrock, R. R. *J. Am. Chem. Soc.* **1993**, *115*, 11831.

(14) Oskam, J. H.; Schrock, R. R. *J. Am. Chem. Soc.* **1992**, *114*, 7588.

(15) Oskam, J. H.; Fox, H. H.; Yap, K. B.; McConville, D. H.; O'Dell, R.; Lichtenstein, B. J.; Schrock, R. R. *J. Organometal. Chem.* **1993**, *459*, 185.

(16) Sheldrick, G. M. *Acta Cryst.* **2008**, *A64*, 112.

(17) Singh, R.; Czekelius, C.; Schrock, R. R.; Müller, P. *Organometallics* **2007**, *26*, 2528.

CHAPTER 3

Molybdenum Monoaryloxide Pyrrolide Alkylidene Complexes that Contain Mono-*ortho*-substituted Phenyl Imido Ligands

INTRODUCTION

High oxidation state molybdenum and tungsten imido alkylidene complexes[1] with the generic formula M(NR)(CHR')(X)(Y) (where X and Y are monoanionic ligands, initially both alkoxides) were first prepared approximately 25 years ago.[2] Unlike an oxo ligand, which was present in the first high oxidation state Group 6 complexes to be discovered,[3] the isoelectronic imido ligand can retard bimolecular decomposition of alkylidenes for steric reasons. Imido ligands also are available in many steric and electronic variations. Phenylimido ligands have been popular, especially 2,6-disubstituted versions (2,6-i-$Pr_2C_6H_3$, 2,6-$Me_2C_6H_3$, 2,6-$Cl_2C_6H_3$,, etc). 2-Substituted imido ligands are less common, while those with no *ortho* substituents are rare; one example is N-3,5-$Me_2C_6H_3$.[4, 14] Complexes that contain phenylimido ligands with progressively less steric protection in *ortho* positions are more difficult to prepare and the resulting imido alkylidene complexes appear to be less stable toward what is presumed to be bimolecular decomposition.

In the last several years new types of Mo and W imido alkylidene complexes that have the formula M(NR)(CHR')(OR")(Pyr), where Pyr is a pyrrolide or substituted pyrrolide ligand and OR" usually is an aryloxide, have been prepared and explored.[1a, 5] These MonoAryloxidePyrrolide (MAP) species can be viewed as third generation high oxidation state imido alkylidene catalysts (after "first generation" bisalkoxides and "second generation" biphenolates and binaphtholates[1]). MAP species have many features of fundamental interest. MAP species contain a stereogenic metal center, MAP species have proven to be much more efficient (higher turnover) than bisalkoxide catalysts in many cases, and MAP species can be engineered to be highly Z selective for the coupling of terminal olefins.[6] MAP species also have been the subject of detailed calculations.[7]

We have begun to explore the consequences of increasing the size of imido groups in MAP complexes to the point that their size approaches or exceeds that of sterically demanding O-2,6-(2,4,6-$Me_3C_6H_2)_2C_6H_3$ (OHMT) or O-2,6-(2,4,6-*i*-$Pr_3C_6H_2)_2C_6H_3$ (OHIPT) ligands that have been employed in order to enforce Z selective reactions.[8, 9] Phenylimido ligands that are *mono*substituted in the *ortho* position, N-2-XC_6H_4 species, especially those in which X is mesityl (NAr^M) or triisopropylphenyl (NAr^T), could prove to be interesting variations of MAP catalysts. The syntheses of NAr^M and NAr^T species and a comparison of them with NAr^{Cl}, NAr^{CF3}, NAr^{iPr}, and NAr^{tBu} species are the subject of this paper. The main questions we wanted to answer are in what way, if any, compounds that contain NAr^M or NAr^T ligands differ from those that contain NAr^{Cl}, NAr^{CF3}, NAr^{iPr}, or NAr^{tBu} ligands in some test reactions that may be sensitive to the size of X in N-2-XC_6H_4 MAP species.

RESULTS AND DISCUSSION

3.1 Synthesis, characterization and structural studies of catalyst precursors

3.1.1 Dichloro bisimido complexes

Anilines that contain either a Mes (2,4,6-trimethylphenyl) or a TRIP (2,4,6-triisopropylphenyl) substituent were prepared as shown in equation 1. These preparations are adaptations of known literature reports;[10, 11] no palladium-catalyzed step is required. The overall isolated yields of these new crystalline anilines are 81% for $Ar^{M}NH_2$ and 45% for $Ar^{T}NH_2$, respectively.

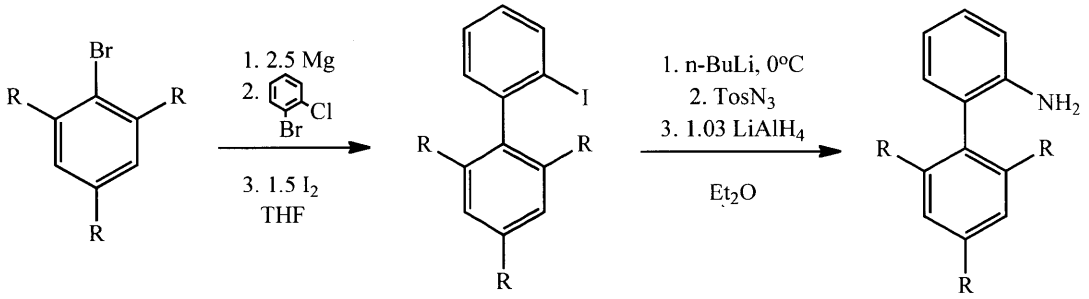

(1)

Bisimido dichloride complexes in which the imido ligand is NAr^{Cl}, NAr^{M}, or NAr^{T} could be prepared by the standard method shown in equation 2. When a mixture of two equivalents of $Ar^{M}NH_2$, Na_2MoO_4, NEt_3, and TMSCl in DME is heated at 60 °C overnight, an orange product is formed, but the DME adduct could not be isolated in crystalline form. However, recrystallization of the crude DME adduct from a mixture of pentane and THF led to red, crystalline **2** in 84% isolated yield. A proton NMR spectrum of **2** shows that a total of four equivalents of THF are present, as confirmed through elemental analysis. We propose that two equivalents of THF are present as solvent of crystallization (*vide infra*) and that THF exchange is fast on the NMR timescale at room temperature.

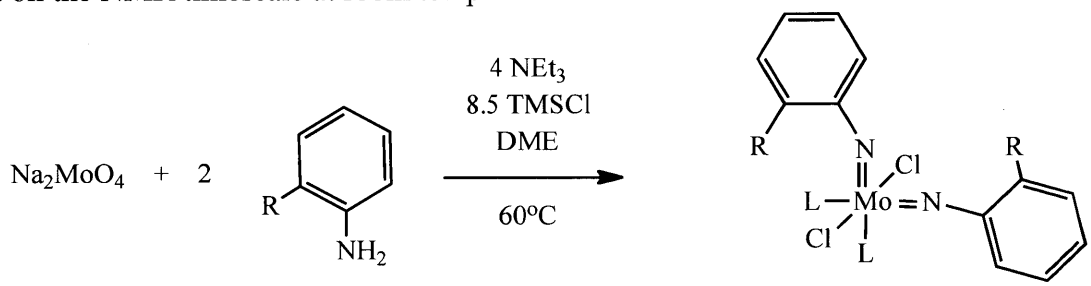

(2)

The result of X-ray structural studies of **2** and **3** are shown in Figures 1 and 2, respectively. As proposed, crystals of **2** contain two THF molecules of crystallization (shown in Figure 1). The imido ligands in both **2** and **3** are bent at the imido nitrogen; the smaller Mo-N-C angle in **3** (149.39(10)°) versus **2** (160.05(19)° and 156.4(2)°) can be attributed to the greater steric demand of the TRIP group in **3** compared to the Mes group in **2**. Other bond distances and angles are similar to other complexes of this general type that have been crystallographically characterized.[1]

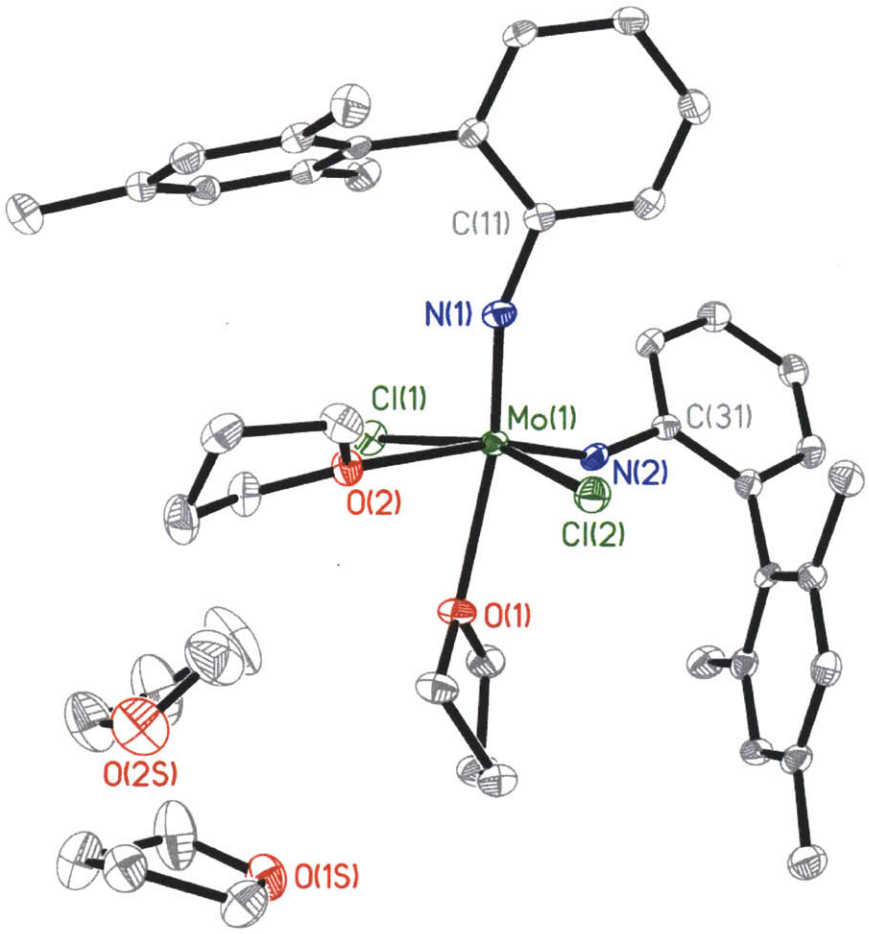

Figure 1. The solid state structure of **2** (50% probability ellipsoids). Selected bond lengths (Å) and angles (°): Mo(1)-N(1) = 1.750(2), Mo(1)-N(2) = 1.7535(19), Mo(1)-O(1) = 2.3138(18), Mo(1)-O(2) = 2.3394(6), Mo(1)-Cl(1) = 2.3863(9), Mo(1)-Cl(2) = 2.4119(9), N(1)-Mo(1)-N(2) = 102.95(10), C(11)-N(1)-Mo(1) = 160.05(19), C(31)-N(2)-Mo(1) = 156.4(2), Cl(1)-Mo(1)-Cl(2) = 160.63(3).

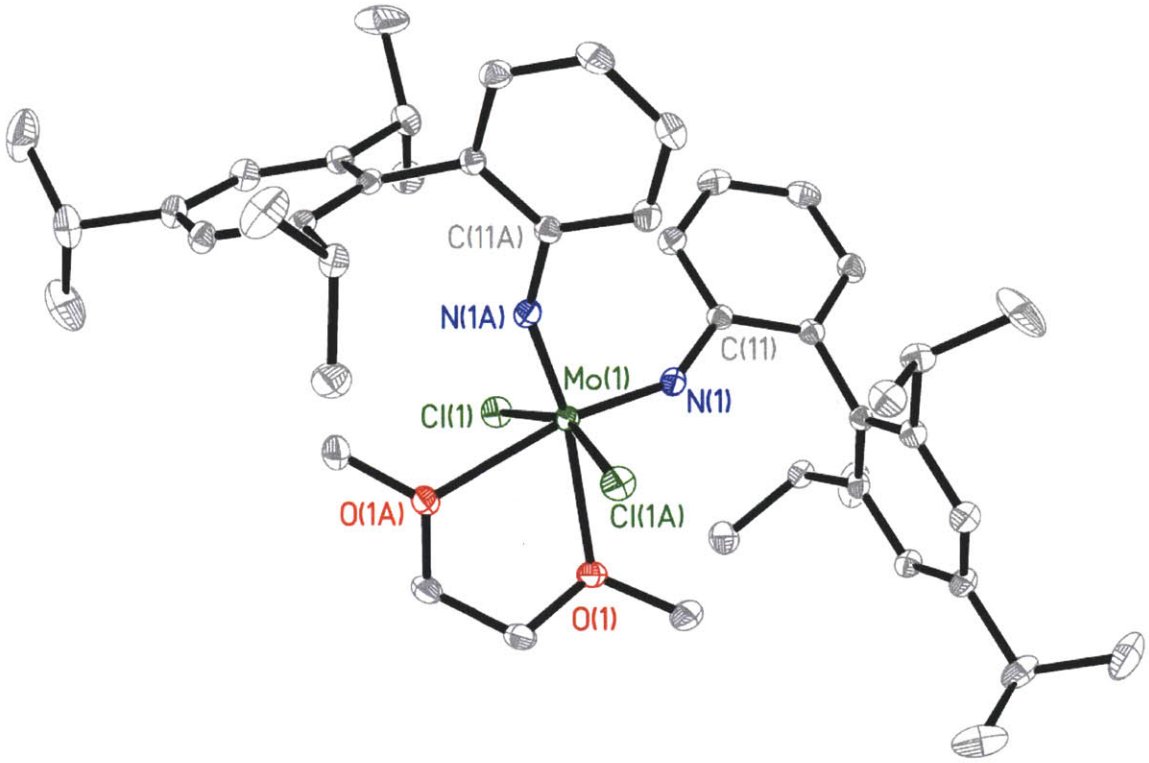

Figure 2. The solid state structure of **3** (50% probability ellipsoids). Selected bond lengths (Å) and angles (°): Mo(1)-N(1) = 1.7522(12), Mo(1)-O(1) = 2.3381(11), Mo(1)-Cl(1) = 2.4023(4), N(1)-Mo(1)-N(2) = 101.44(8), C(11)-N(1)-Mo(1) = 149.39(10), Cl(1)-Mo(1)-Cl(2) = 159.37(2).

3.1.2 Dialkyl bisimido complexes

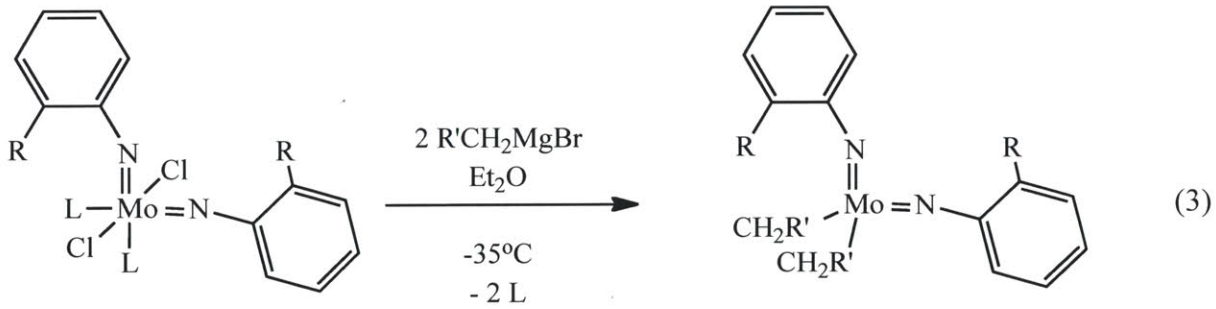

(3)

1
2
3
3

R = Cl, R' = CMe_2Ph **4** (68%)
R = Mes, R' = CMe_2Ph **5** (74%)
R = TRIP, R' = CMe_3 **6** (50%)
R = TRIP, R' = H **7** (50%)

Treatment of compounds **1**, **2** and **3** with 2 equivalents of a) neopentyl Grignard, b) neophyl Grignard, and c) methyl Grignard yield different results, Table 1. Some of the differences are mainly attributed to crystal packing differences of the compounds, while others are explained in

terms of complex stability towards decomposition. Compounds that were isolated were all red-orange in color and include $Mo(NAr^{Cl})_2(CH_2CMe_2Ph)_2$ (**4**), $Mo(NAr^{M})_2(CH_2CMe_2Ph)_2$ (**5**), $Mo(NAr^{T})_2(CH_2CMe_3)_2$ (**6**), and $Mo(NAr^{T})_2(CH_3)_2$ (**7**), equation 3. The yields are all listed in Table 1 and range from moderate to good. The compounds are stable indefinitely at -35°C, even in solution.

Table 1- Outcomes of the reactions between complexes **1**, **2**, and **3** with various alkyl Grignard reagents.

Complex	$ClMgCH_2CMe_2Ph$	$ClMgCH_2$-*t*-Bu	$BrMgCH_3$
1	Orange solid (68 %)	Oil	Decomposition
2	Orange solid (74 %)	Oil	Decomposition
3	Decomposition	Orange-red solid (50 %)	Orange-red solid (50 %)

One interesting observation is that when **3** reacts with neophyl Grignard the product is not stable and decomposes, which is probably a result of having a more exposed lone pair on the imido group and the ligands being too bulky to avoid unwanted interactions. On the other hand, decomposition also does occur when **1** or **2** is reacted with MeMgBr, suggesting that both the $Ar^{Cl}N$ and the $Ar^{M}N$ groups are not big enough to protect the complex from unwanted side-reactions. Either decomposition has not been studied any further. To gain some insight of how the $Ar^{T}N$ groups protect the metal sphere and to get an overall depiction of the geometry of dialkyl complexes, the crystal structure of **7** was obtained and it is presented in Figure 3. The compound crystallizes in the monoclinic space group $P2_1/c$ and it is tetrahedral. One amazing feature observed in the crystal as well as in solution is that even compound **7** that has the smallest alkyl group possible, is solvent-free. The angle between the alkyl groups is 116.8° and the Mo(1)-N(1)-C(11) angle is 160°, which is similar to compound **2** but 10° higher than compound **3**. This fact hints compound **7** is less crowded than **3**, which is expected for a solvent-free complex. In addition, the TRIP groups both point down towards the methyl groups, thus protecting the small ligands and the exposed metal center. This feature is what aids in making this complex stable and isolable.

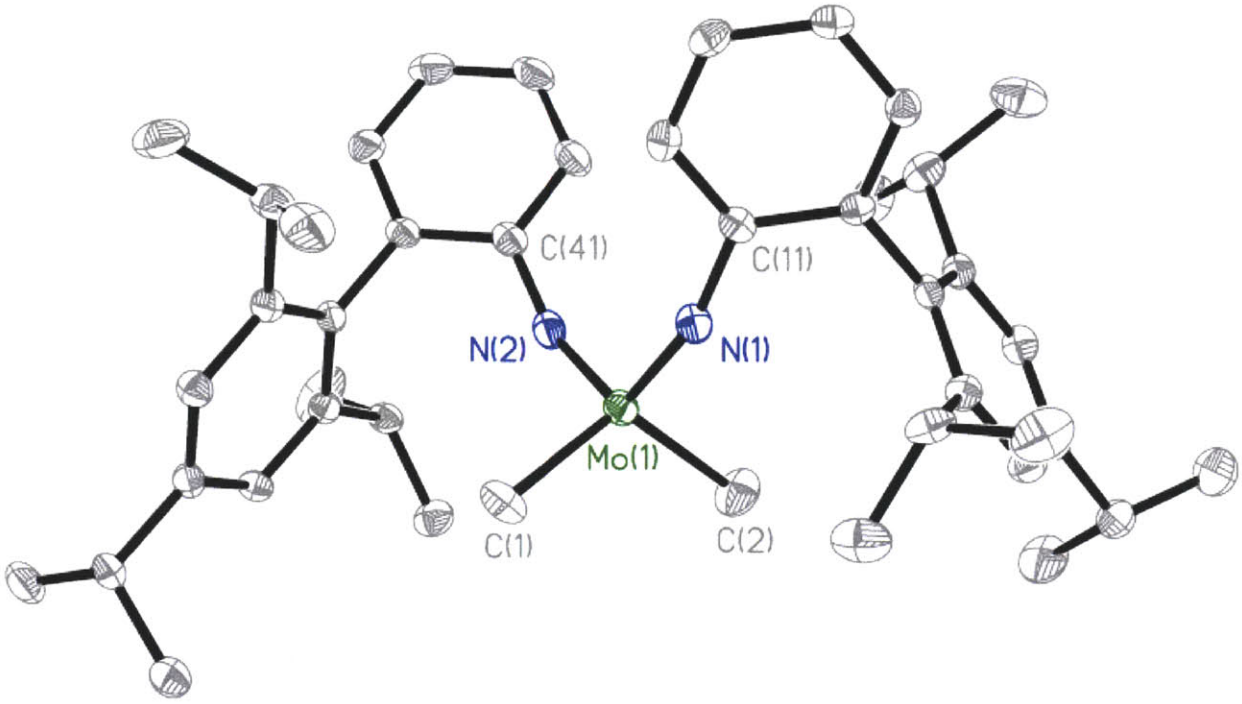

Figure 3- The solid state structure of **7** (50% probability ellipsoids). Selected bond lengths (Å) and angles (°) are given: Mo(1)-N(1) = 1.7530(18), Mo(1)-N(2) = 1.7543(19), Mo(1)-C(1) = 2.127(2), Mo(1)-C(2) = 2.121(2), N(1)-Mo(1)-N(2) = 109.46(8), C(11)-N(1)-Mo(1) = 158.19(16), C(41)-N(2)-Mo(1) = 155.35(2), C(1)-Mo(1)-C(2) = 116.85(11)

3.1.3 Alkylidene imido bistriflate complexes

Compounds **4-6** were then treated with three equivalents of triflic acid to yield **8**, **9** and **10** smoothly (equation 4); however, decomposition took place when **7** was treated with TfOH in the same manner. Attempts to isolate any product were unsuccessful and further reactions with **7** were not pursued. Among the more stable complexes (**8-10**), separation of **9** from the anilinium triflate byproduct was difficult. So far, trituration with diethyl ether is the only way to remove all anilinium triflate; the isolated yield of **9** (28%) suffers as a consequence of it being partially soluble in ether. Similarly, although the reaction between **6** and triflic acid yields **10** smoothly, separation of **10** from the anilinium triflate is again problematic; the isolated yield of **10** is only 47%. Bistriflate complexes that contain NAr^{CF3}, NAr^{iPr}, and NAr^{tBu} imido groups have been reported previously.[4] Details can be found in the experimental section.

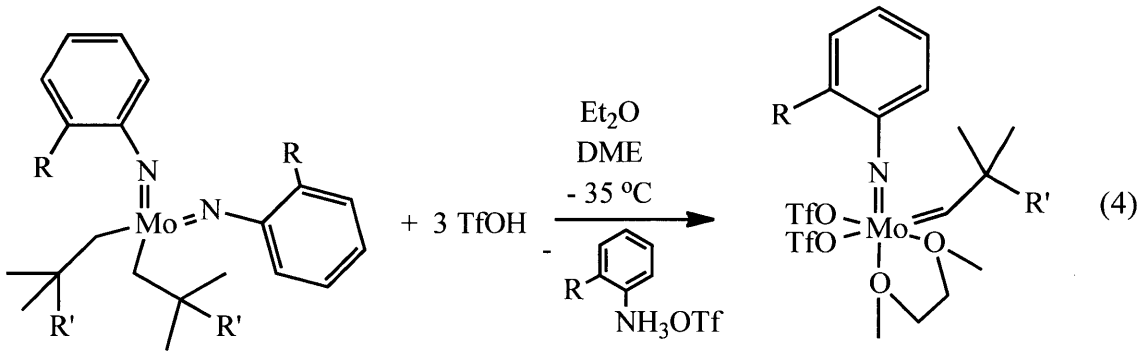

(4)

R = Cl,	R' = Ph	**4**
R = Mes,	R' = Ph	**5**
R = TRIP,	R' = Me	**6**

8 (43%)
9 (28%)
10 (47%)

Bistriflate complexes that contain NAr^{CF3}, NAr^{iPr}, NAr^{tBu}, and NAr^{Cl} groups all show resonances for two isomers in solution. Fluorine NMR spectra suggest that these isomers contain triflate ligands that are either *cis*, as shown in equation 4, or *trans* with respect to one another. Proton NMR data suggest that they are *syn* isomers (J_{CH} = 125±3 Hz), in which the alkylidene group points toward the imido group, as shown in equation 4. In contrast, ^{1}H NMR spectra (in C_6D_6) of both **9** and **10** each show more than the expected two alkylidene resonances, and ratios of the isomers vary depending upon conditions. The three most prominent resonances for **9** have J_{CH} values that range from 122 to 129 Hz; for **10** (Figure 4a) they range from 122 to 126 Hz. All J_{CH} values that can be measured are characteristic of *syn* species. Two isomers of the mixture are isolated upon recrystallizing the compound from diethyl ether at -35 °C. Proton and fluorine NMR spectra (Figure 4b) are consistent with these isomers of **10** being *cis* (84%) and *trans* (16%) species. *Cis* and *trans* mixtures of bistriflate complexes have been observed in other circumstances.[12]

The observation of more than two isomers suggests several possibilities. One or more of the adducts loses DME in the solid state, one or more of the isomers is actually not a solvent adduct, or the large mesityl and TRIP substituents give rise to isomers in which the mesityl or TRIP substituents limit free rotation of the imido phenyl group about the Mo=N axis on the NMR time scale giving rise up to six isomers (Figure 5). Spectra in the alkylidene region did not change significantly when several equivalents of DME were added and the amount of DME in a complex mixture could not be measured accurately through integraton. Therefore, we cannot determine the exact reason for isomer formation. Unfortunately, multiple elemental analyses of **9** and **10** as mixtures of four isomers were variable, as were elemental analyses of the mixture of *cis* and *trans* isomers shown in Figure 4b.

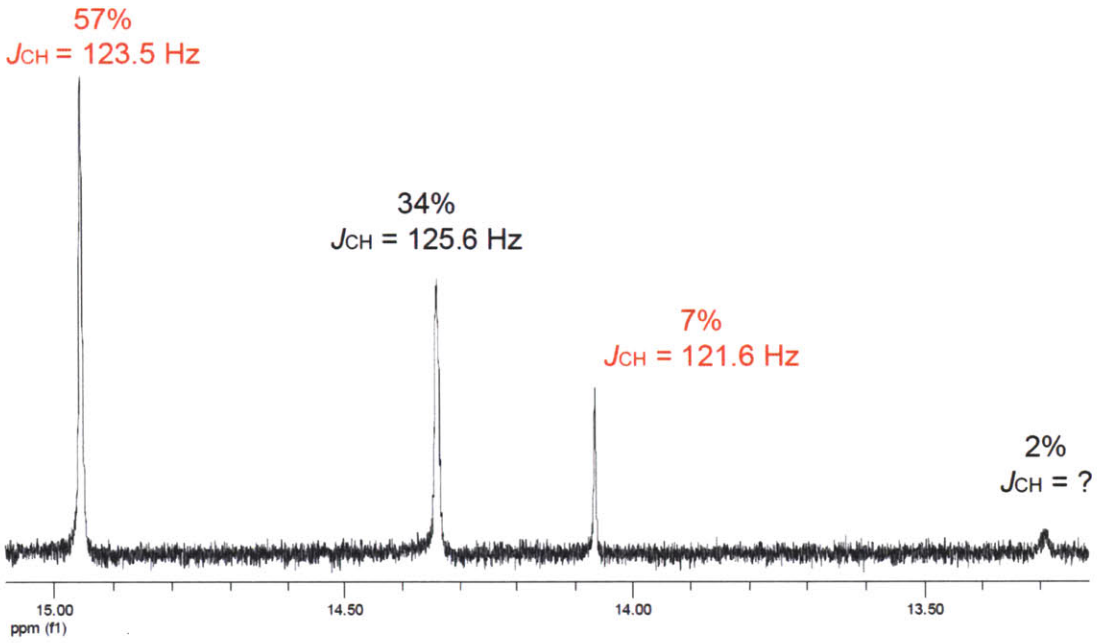

Figure 4a - The four alkylidene proton resonances in the ^{1}H NMR spectrum of **10**.

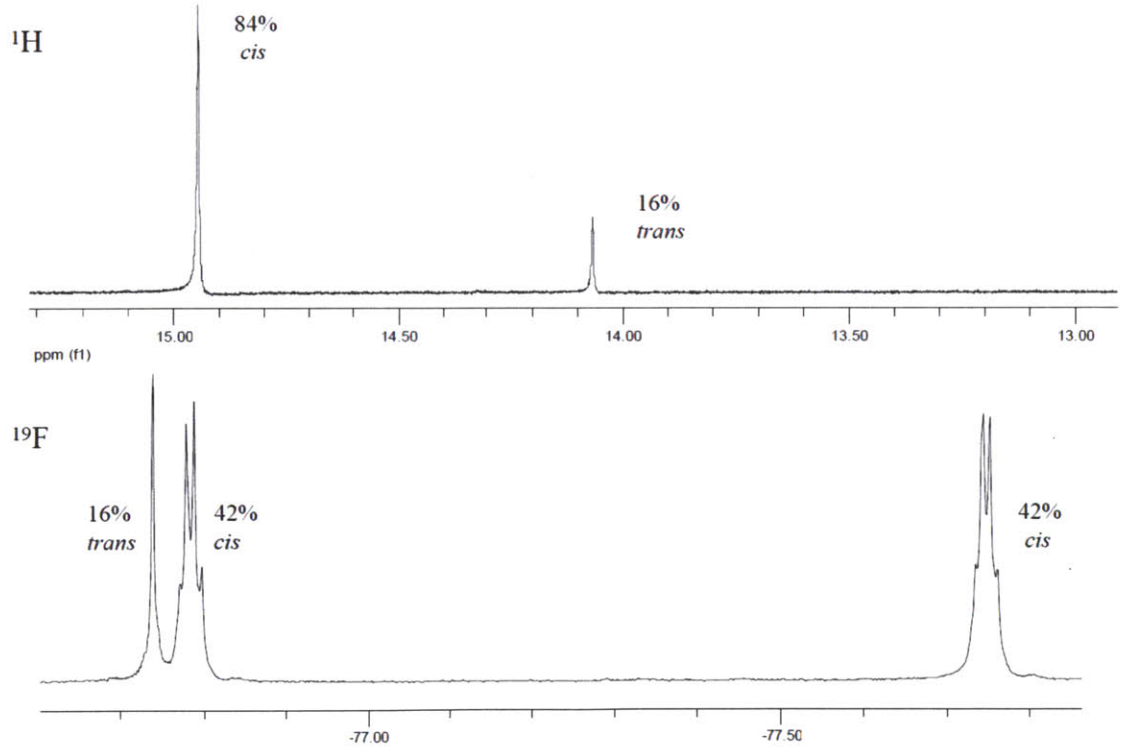

Figure 4b - The ^{1}H (top) and ^{19}F (bottom) NMR spectra of two of the isomers of **10**.

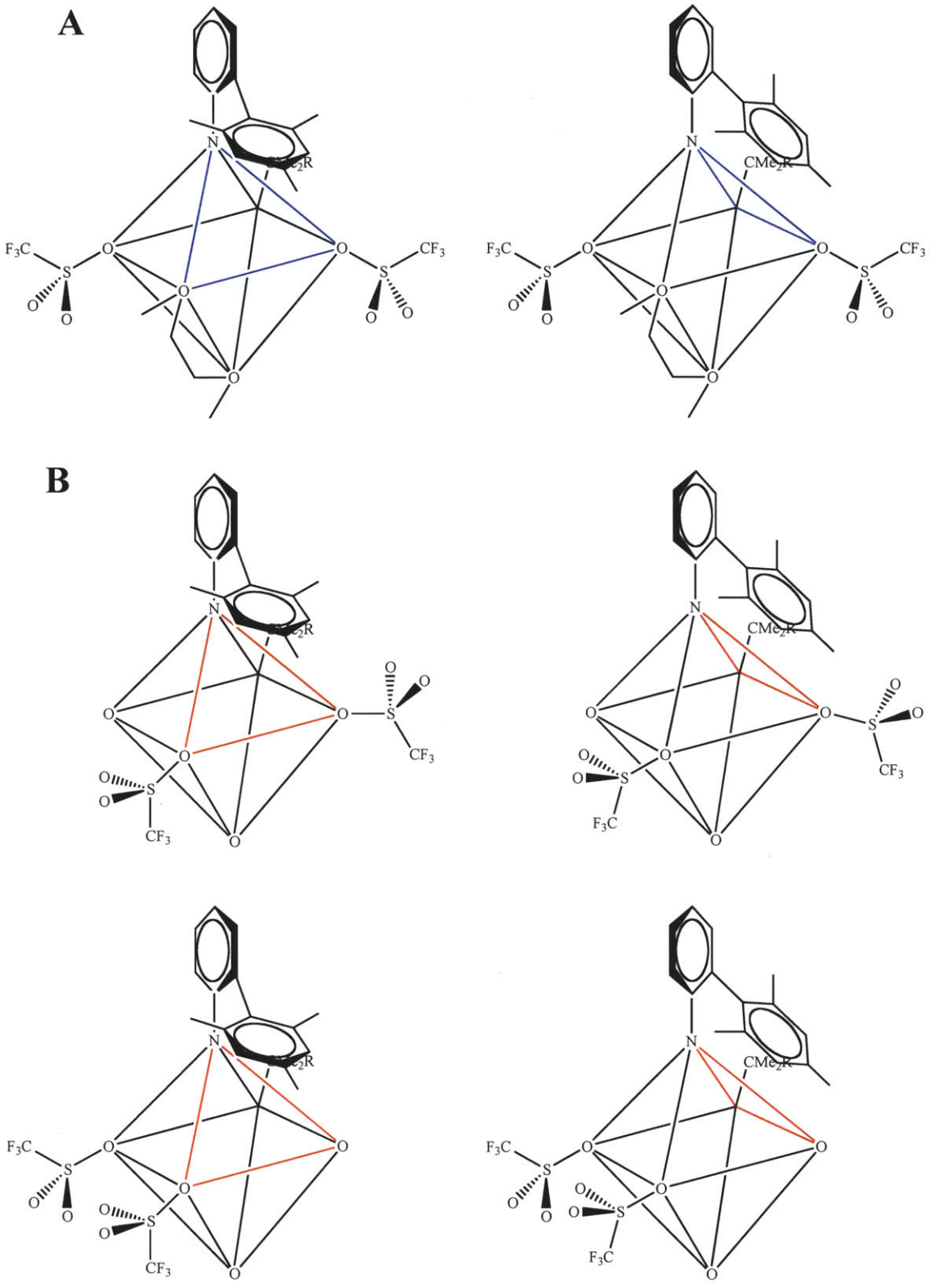

Figure 5 - Octahedron diagram of all *trans*- (**A**) and *cis*- (**B**) bistriflate isomers possible that result from restricted rotation of the imido ligand around the metal center.

3.1.4 Alkylidene imido bispyrrolide complexes

Treatment of the bistriflate complexes with two equivalents of Li-2,5-$Me_2C_4H_2N$ led to bispyrrolide compounds in yields ranging from 36% to 85% (equation 5). The neophylidene analog of **12** has been reported previously. The low isolated yield of **17** we propose is the result of its poor crystallinity. Proton NMR spectra of complexes **11-17** exhibit a single alkylidene peak and broad peaks corresponding to fluxional pyrrolide ligands, behavior which is analogous to other bispyrrolide compounds of this general type.[13]

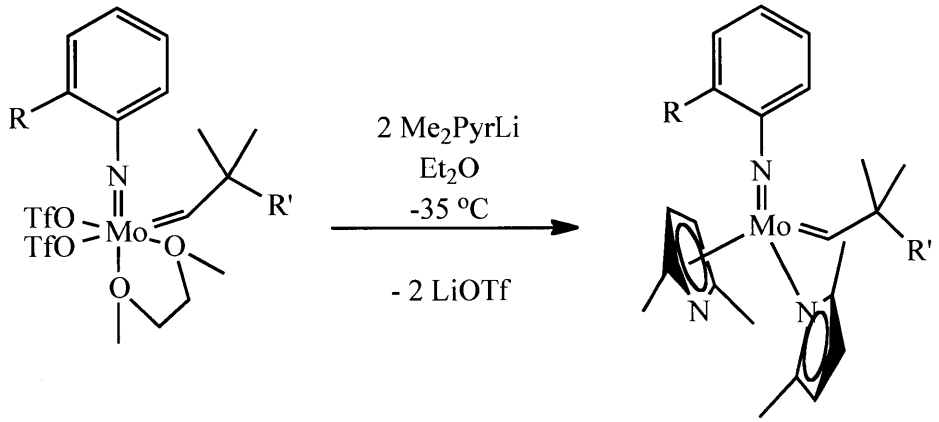

(5)

11 R = Cl, R' = Ph; (57%)
12 R = CF_3, R' = Me; (53%)
13 R = *i*-Pr, R' = Ph; (59%)
14 R = *t*-Bu, R' = Me; (82%)
15 R = *t*-Bu, R' = Ph; (68%)
16 R = Mes, R' = Ph; (85%)
17 R = TRIP, R' = Me; (36%)

An X-ray study of **16** was undertaken and it is shown in Figure 6. The compound crystallizes out in the monoclinic space group $P2_1/n$. The pyrrolide ligands are bound η^1 and η^5 to the metal respectively, as it was expected. The alkylidene group is observed as *syn* in this structure. In addition, the Mo(1)-N(1)-C(11) bond is nearly planar and the Mes group is placed on top of the η^5-bound pyrrolide parallel to it. It is quite interesting to note that the Mes group points away from the alkylidene group, creating a pseudo-small imido group around the N(imido)-C-N(η^1-pyrrolide) face of the complex.

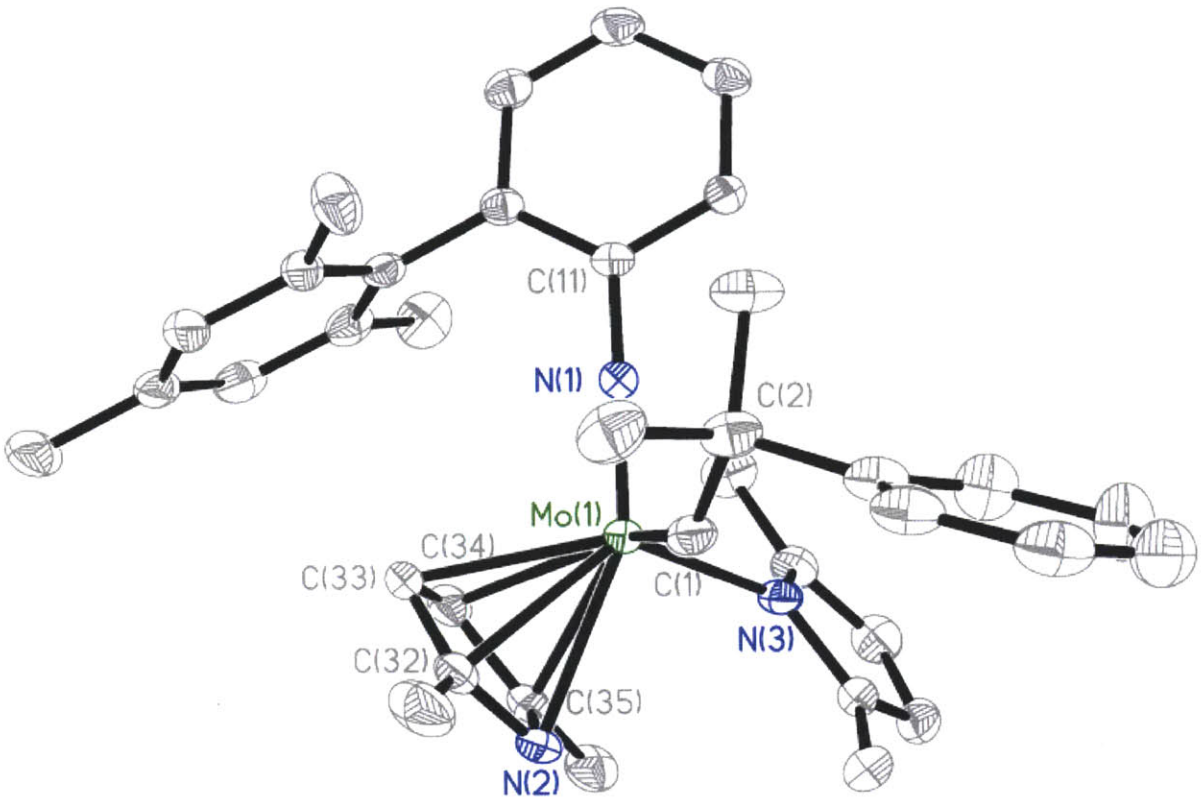

Figure 6 - The solid state structure of **16** (50% probability ellipsoids). Selected bond lengths (Å) and angles (°): Mo(1)-N(1) = 1.7340(16), Mo(1)-C(1) = 1.940(2), Mo(1)-N(2) = 2.4117(17), Mo(1)-N(3) = 2.1134(17), Mo(1)-C(32) = 2.391(2), Mo(1)-C(33) = 2.376(2), Mo(1)-C(34) = 2.458(2), Mo(1)-C(35) = 2.458(2), C(11)-N(1)-Mo(1) = 175.40(15), C(2)-C(1)-Mo(1) = 139.84(15).

3.2 Synthesis, characterization, and structural studies of alkylidene imido monoaryloxide monopyrrolide catalysts

3.2.1 Catalyst complexes that contain small alkoxide or aryloxide ligands

Addition of *t*-BuOH, $(CF_3)_2MeCOH$, or Ph_3SiOH to complexes **11-17** led to formation of bisalkoxide complexes as the only observable product, instead of the desired MAP species. Since N-2,6-*i*-$Pr_2C_6H_3$ (NAr) monoalkoxide pyrrolide (MAP) species that contain *t*-butoxide, hexafluoro-*t*-butoxide, or triphenylsiloxide can be obtained in good yields in similar reactions,[5a] these findings suggest that NAr^M and NAr^T ligands offer less steric protection toward rapid protonation of the second pyrrolide than bispyrrolides that contain the NAr ligand.

Addition of one equivalent of 2,3,5,6-tetraphenylphenol (TPPOH) to **16** led to a mixture that contains 25% **16**, 50% of a MAP product, and 25% of the bisphenoxide. The bisphenoxide species (**18**) could be prepared (in 55% yield) from the bistriflate as shown in equation 6. Since

18 would appear to be a relatively crowded species, an X-ray structural determination (Figure 7) was carried out.

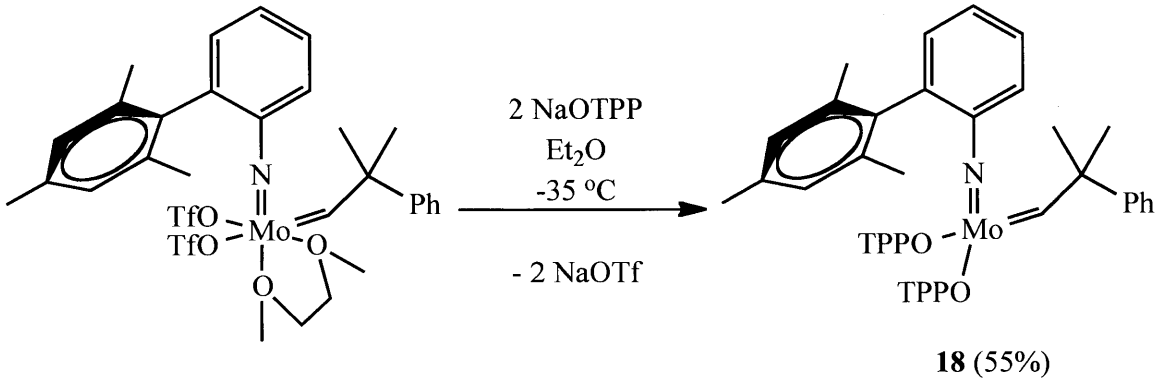

18 (55%) (6)

Compound **18** is a distorted tetrahedron with the smallest and largest angles being 99.29(12)° (N(1)-Mo(1)-C(1)) and 120.85(9)° (N(1)-Mo(1)-O(2)). The Mo(1)-O(1)-C(31) and Mo(1)-O(2)-C(61) bond angles (147.00(17)° and 148.18(16)°, respectively) are relatively large in view of the crowded coordination sphere. The Mo(1)-N(1)-C(11) bond angle is close to 180° (173.13(19)°) The ready formation of **18** confirms that 2,3,5,6-tetraphenoxide ligands are operationally not as large as one might think, as has been found in other circumstances.[14] In contrast, the reaction between **17** and one equivalent of TPPOH yields only Mo(NAr^T)(CH-*t*-Bu)(Me$_2$Pyr)(OTPP) (**19**; equation 7), i.e., increasing the bulk of the imido group (from Ar^M to Ar^T) decreases the rate of formation of the bisphenoxide, and therefore allows the synthesis of the MAP species.

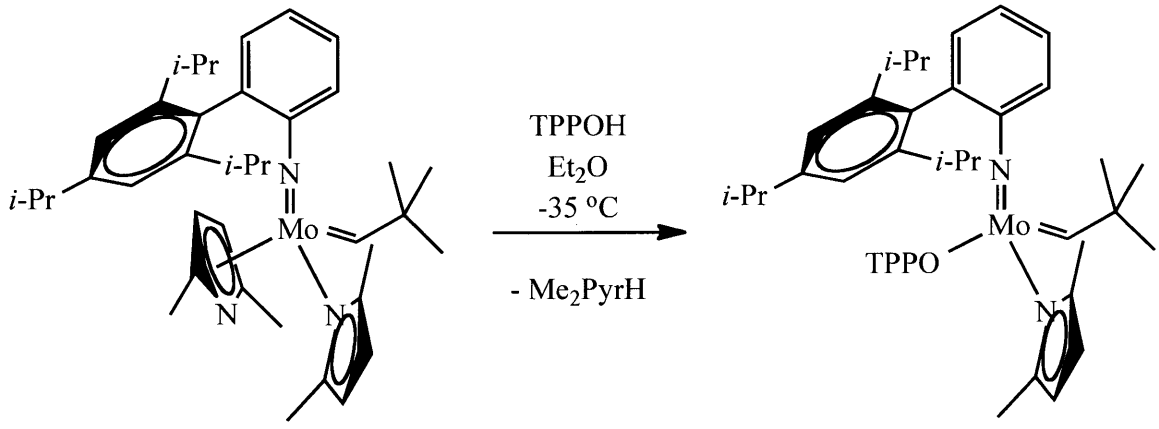

19 (44%) (7)

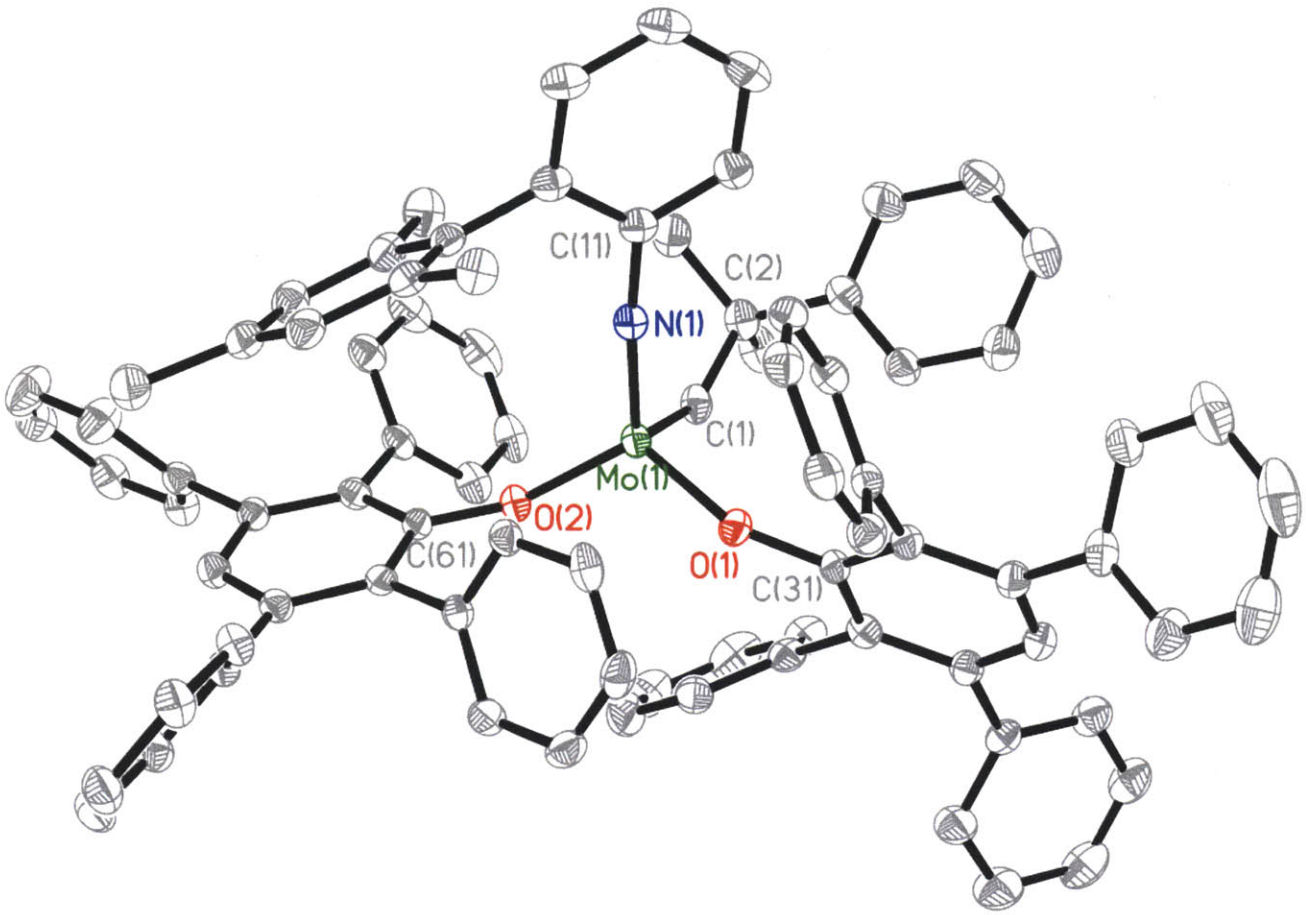

Figure 7 - The solid state structure of **18** (50% probability ellipsoids). Selected bond lengths (Å) and angles (°): Mo(1)-N(1) = 1.732(2), Mo(1)-C(1) = 1.880(3), Mo(1)-O(1) = 1.9402(18), Mo(1)-O(2) = 1.9303(17), Mes-TPP = 4.343, C(11)-N(1)-Mo(1) = 173.13(19), C(2)-C(1)-Mo(1) = 141.8(2), C(31)-O(1)-Mo(1) = 147.00(17), C(61)-O(2)-Mo(1) = 148.18(16).

3.2.2 Catalysts that contain bulky aryloxide ligands

Hexamethylterphenol (HMTOH) reacts readily at 22 °C with **11-17** to generate the MAP product in modest to good yields (equation 8). However, reactions between HMTOH or hexaisopropylterphenol (HIPTOH) with **16** and **17** are slow. Therefore, their preparation must be carried out at high temperatures in toluene for hours to days, depending on the phenol. The reactions at 110 °C between **16** or **17** and one equivalent of HMTOH to give **26** and **28**, respectively, required 18 h, while that between **16** and one equivalent of HIPTOH to give **27** required 5 days. Reaction between **17** and HIPTOH required 14 days at 80 °C to give 97% of the desired product. These data show that reactions between HMTOH and **16** or **17** clearly take place more readily. It is noteworthy to note that the MAP products do not decompose under the relatively harsh conditions required to prepare **26-29**. The isolated yields of **26-28** are modest

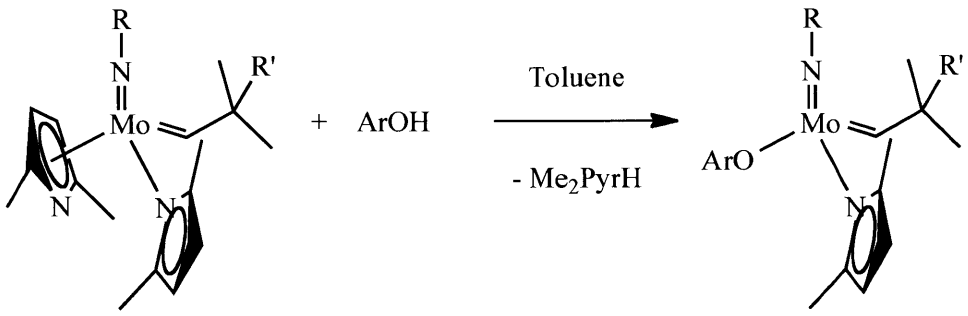

(8)

20	$R = Ar^{Cl}$,	R' = Ph,	Ar = HMT	(40%)
21	$R = Ar^{CF3}$,	R' = Me,	Ar = HMT	(76%)
22	$R = Ar^{CF3}$,	R' = Ph,	Ar = HMT	(75%)
23	$R = Ar^{iPr}$,	R' = Ph,	Ar = HMT	(48%)
24	$R = Ar^{tBu}$,	R' = Me,	Ar = HMT	(68%)
25	$R = Ar^{tBu}$,	R' = Ph,	Ar = HMT	(67%)
26	$R = Ar^{M}$,	R' = Ph,	Ar = HMT	(51%)
27	$R = Ar^{M}$,	R' = Ph,	Ar = HIPT	(35%)
28	$R = Ar^{T}$,	R' = Me,	Ar = HMT	(57%)
29	$R = Ar^{T}$,	R' = Me,	Ar = HIPT	(*in-situ*)

(35-57%), the lowest corresponding to **27** as a consequence of its high solubility in solvents like pentane and tetramethylsilane. Complexes **26** and **28** are more crystalline than **27**, which is mirrored in their yields. Due to the long times required for reactions between **17** and HIPTOH and possible complications during purification, **29** could not be isolated, but had to be prepared *in situ*. All reactions benefit from being run under more concentrated conditions, but a large excess of HMTOH or HIPTOH cannot be employed without creating problems with isolation of the desired product. The structures of highly crystalline **26** and **28** are shown in Figures 8 and 9, respectively. Both are distorted tetrahedra, with angles at the metal ranging from 102.97(5)° to 117.48(5)° and 101.41(12)° to 116.40(10)°, respectively. The Mo-N-C(imido) and the Mo(1)-C(1)-C(2) angles are similar in the two complexes and are similar to analogous angle in other complexes of this general type.

On the other hand, the Mo(1)-O(1)-C(41) angle of **26** is 158.89(9)°, which is 10° larger than the Mo-O-C angle in either **28** or **18**, but not uncommon among MAP complexes containing either HMTO or HIPTO. In both **26** and **28** the Mes and TRIP groups point away from the alkylidene and therefore would not seem to block an olefin from binding to the metal. In **26** an additional feature worth mentioning is a possible π-stacking interaction between the mesityl ring of the NAr^{M} ligand and the pyrrolide ring beneath it. However, this interaction is very weak due to a long distance between them (3.837 Å from the centroid of the mesityl ring to the centroid of the pyrrolide ring).[16]

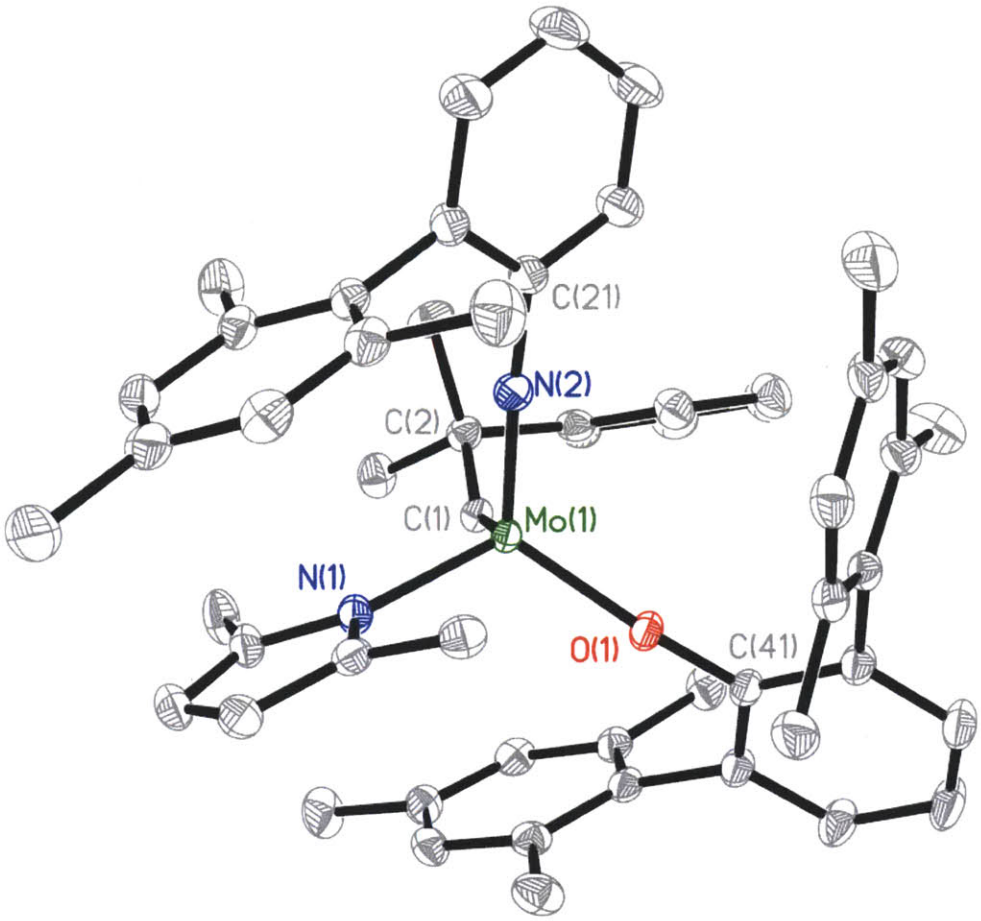

Figure 8 - The solid state structure of **26** (50% probability ellipsoids). Selected bond lengths (Å) and angles (°): Mo(1)-C(1) = 1.8752(13), Mo(1)-N(1) = 2.0230(11), Mo(1)-N(2) = 1.7302(11), Mo(1)-O(1) = 1.8997(9), Mes-Pyr = 3.837, C(21)-N(2)-Mo(1) = 175.50(10), C(2)-C(1)-Mo(1) = 146.02(10), C(41)-O(1)-Mo(1) = 158.89(9).

Compounds **26-29** show different number of isomers in solution, as evidenced by their respective ^{1}H NMR spectra. A trend is clearly observed between the overall steric hindrance at the metal center and the number of isomers observed in solution; the greater the steric hindrance the higher the number of isomers present. Thus, **26**, which has the smallest combination of imido and aryloxide ligands (among these four catalysts), has only one isomer, while **28**, which contains the slightly larger NAr^{T} imido group has two isomers. In the case where the aryloxide is HIPTO there are four isomers present in both NAr^{M} and NAr^{T} imido complexes. These findings can be rationalized in terms of steric crowding overall. As steric crowding around the metal increases, restricted rotation results in locking of the ligands on the NMR time scale in various positions that give rise to more than the expected number of isomers. On this basis we

can propose that complex **18** (two observable isomers) is less crowded than **27** or **29** but more crowded than **26**.

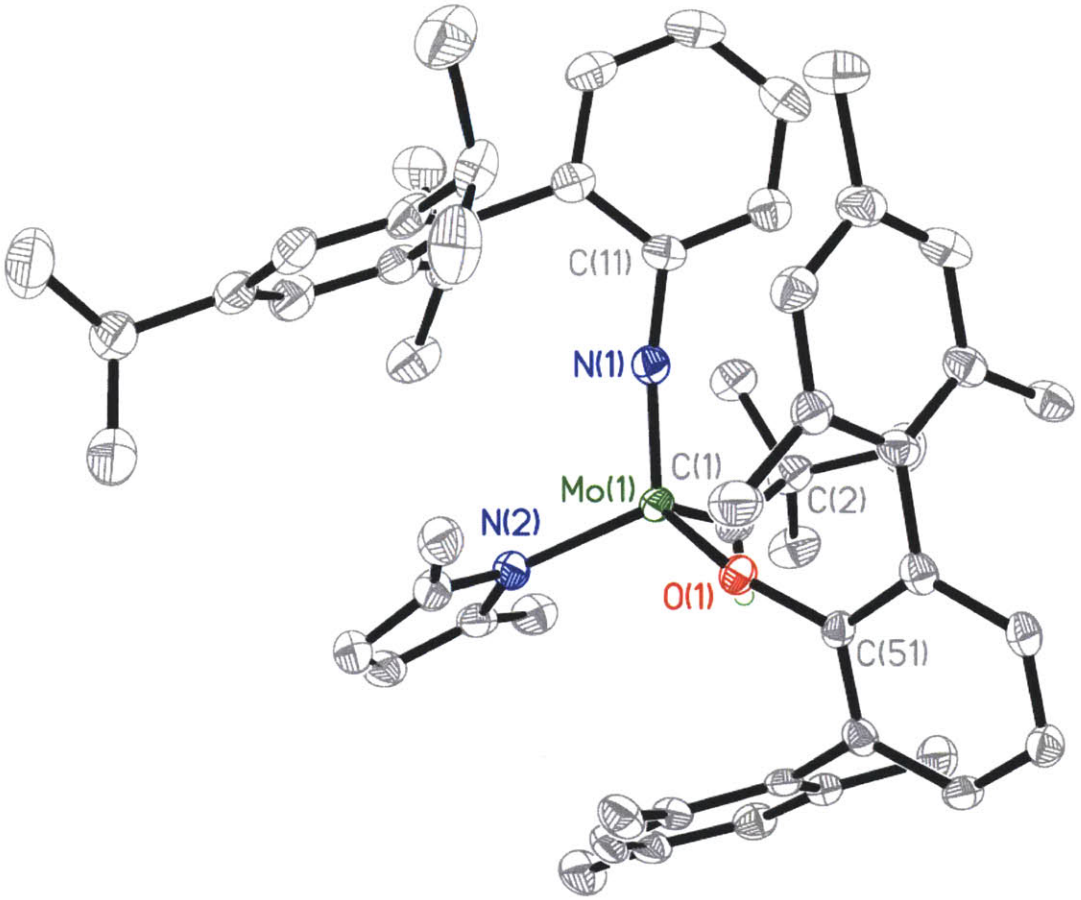

Figure 9 - The solid state structure of **28** (50% probability ellipsoids). Selected bond lengths (Å) and angles (°): Mo(1)-C(1) = 1.862(3), Mo(1)-N(1) = 1.736(2), Mo(1)-N(2) = 2.037(2), Mo(1)-O(1) = 1.9103(19), C(11)-N(1)-Mo(1) = 170.9(2), C(2)-C(1)-Mo(1) = 147.5(2), C(51)-O(1)-Mo(1) = 147.32(19).

3.3 Reactivity studies of MAP catalysts

The ROMP of 2,3-dicarbomethoxynorbornadiene (DCMNBD),[5h] shown in equation 9, has been employed as a means of judging the stereospecificity (*cis/trans* selectivity and *tacticity*) of a MAP metathesis catalyst.[15] Therefore, all MAP catalysts (**19-28** plus **29** prepared *in situ*) were treated with 25-100 equivalents of monomer and the resulting polymer was isolated and analyzed by NMR methods. The results are summarized in Table 2.

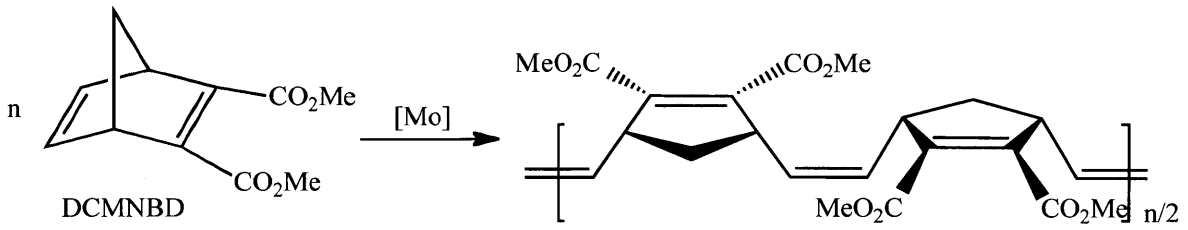

(9)

All ROMP reactions are relatively fast. The use of **19** as an initiator fails to deliver a highly structured polymer, presumably as a consequence of the imido group being too large relative to the aryloxide (OTPP). There is a drop in *cis*-selectivity from >98% to ~70% in MAP species **24-26** when the imido ligand is larger than NAr^{iPr}. However, increasing the size of the phenoxide from HMTO to HIPTO (with initiator **27**), again leads to a polymer that is >93% *cis,syndiotactic*. Initiators **28** and **29** are again unsuccessful, presumably because NAr^{T} is operationally too large, even when the aryloxide is OHMT or OHIPT.

Table 2. ROMP of DCMNBD with MAP initiators **19-29** in toluene at 22 °C.

Catalyst	**[Catalyst] (mM)**	**DCMNBD Equivalents**	**Reaction Time**	**Polymer Structure**
19	12	50	1 h	50% *cis*
20	1.9	100	1 h	> 98% *cis, syndio*
21	5.5	50	1 h	> 98% *cis, syndio*
22	5.6	50	1 h	> 98% *cis, syndio*
23	1.9	100	1 h	> 98% *cis, syndio*
24	5.8	50	1 h	76% *cis*
25	5.2	50	1 h	66% *cis*
26	13	25	1 h	69% *cis*
27	48	25	1 h	> 93% *cis,syndio*
28	13	25	1 h	77% *cis*
29	62	25	1 h	83% *cis*

A lower *cis*-selectivity has also been observed when Mo(NAr)(CHCMe$_2$Ph)(Pyr)(OHIPT) is employed as an initiator in place of Mo(NAd)(CHCMe$_2$Ph)(Pyr)(OHIPT) (Ad = adamantyl and Ar = 2,6-*i*-Pr$_2$C$_6$H$_3$).[5h] The fact that **27** is as Z-selective as Mo(NAd)(CHCMe$_2$Ph)(Pyr)(OHIPT) and **20-23** is surprising since it suggests that NAr^M is in the same category as NAr^{Cl}, NAr^{CF3}, and NAr^{iPr} imido ligands as far as producing polymers that have a high *cis,syndiotactic* content, that is, NAr^M is operationally relatively "small."

CONCLUSION

We have found that MAP catalysts that contain NAr^M and NAr^T ligands can be prepared through traditional synthetic routes that have been employed to prepare catalysts that contain NAr^{Cl}, NAr^{CF3}, NAr^{iPr}, and NAr^{tBu} imido groups. We were surprised to find that no imido ligands investigated in this report have properties that lead to unusual behavior in ROMP polymerization of DCMNBD. We conclude that a single ortho substituent in the 2-substituted imido groups explored here can point away from the C-M-N$_{imido}$ face where the olefin is proposed to bind, leaving no substituent to impede approach of the olefin. Therefore, complexes that contain a 2-substituted imido ligand behave like much smaller imido groups in reactions that have been explored so far. The results reported here seem to imply that any attempt to employ a highly sterically demanding phenyl imido group will lead to unique metathesis behavior only if that catalyst contains a 2,6-disubstituted phenylimido ligand such as 2,6-dimesitylphenyl imido.[8]

EXPERIMENTAL

General. All reactions and manipulations of air and moisture sensitive compounds were handled in oven-dried glassware (150 °C, 2 hr) under a N_2 atmosphere either in a dual Schlenk line or in a Vacuum Atmosphere glove box. HPLC grade solvents (benzene, toluene, diethyl ether, tetrahydrofuran, pentane, and methylene chloride), were purge with N_2 and passed through activated alumina and stored over molecular sieves 12 hours prior to use. 1,2-dimethoxyethane was dried in an oven-dried Schlenk flask with sodium and benzophenone ketal, vacuum-transferred into another oven-dried Schlenk flask and stored over molecular sieves 12 hours prior to use. Na_2MoO_4 and $ClMgCH_2CMe_2Ph$ were purchased from Sigma-Aldrich, magnesium turnings, *o*-$BrClC_6H_4$, MesBr, TRIPBr, I_2, NaN_3, Tosyl chloride, $LiAlH_4$, TMSCl, NEt_3, TfOH, and *n*-butyllithium were bought from VWR and used as received. 2,5-dimethylpyrrole was bought from VWR, dried on CaH_2, vacuum-distilled, and degassed prior to use. *t*-$BuCH_2Cl$ was bought from Alfa Aesar, washed with 95% H_2SO_4/5% HNO_3 to remove olefin impurities and dried over $MgSO_4$ before use. Tosyl azide[17], lithium 2,5-Me_2Pyrrolide[24], neopentyl Grignard[25], TPPOH[26], HMTOH and HIPTOH[23], and DCMNBD[22] were prepared according to literature reports. All proteo ligands were placed under high vacuum for 12 hours before use. $Mo(NR)_2Cl_2DME$ (R = Ar^{CF3}, Ar^{iPr}, Ar^{tBu})[4a-b], $Mo(NR)(CHCMe_2Ph)(OTf)_2DME$ (R = Ar^{iPr}, R = Ar^{tBu})[4a] and $Mo(NR)(CHCMe_3)(OTf)_2DME$ (R = Ar^{CF3}, R = Ar^{tBu})[4c-d] were prepared according to literature procedures. All deuterated solvents (d_6-benzene, d_8-toluene, and d_2-dichloromethane) were stored over molecular sieves 12 hours prior to use. All the recorded NMR spectra were done with Bruker 400 MHz and Varian 500 MHz spectrometers. Elemental analyses were performed by Midwest Microlab, LLC.

1-Iodo-2-(2',4',6'-$Me_3C_6H_2$)C_6H_4 (Ar^MI). Magnesium powder (15.3 g, 0.628 mol) of was placed in a 500 mL Schlenk flask in the oven (120 °C) overnight. The flask was sealed with a septum and 300 mL of dry THF was added. A few crystals of iodine were added, a refluxed condenser was attached, and the mixture was heated to 75 °C until the color of the solution changed from pale yellow to colorless. Mesityl bromide (50.0 g, 0.251 mol) was added slowly and the mixture was refluxed overnight. *Ortho*-bromochlorobenzene (29.4 mL, 0.251 mol) was added slowly and refluxing was continued for 12 h. Finally, the flask was cooled to 0 °C and iodine (70.1 g, 276 mmol) was added in small chunks, and the solution was stirred at room temperature for 30 min. Excess I_2 was quenched through addition of a saturated solution of Na_2SO_3 and the product was extracted with 50 mL of diethyl ether four times. The ether layer was dried with $MgSO_4$ and the mixture was filtered. The ether was removed from the filtrate *in vacuo* and the solid product was washed with hexane and dried on a frit under a vacuum to yield

colorless solid (68.7 g, 85% yield): ^{1}H NMR (400 MHz, $CDCl_3$) δ 7.95 (dd, 1H, CIC*H*), 7.42 (td, 1H, CICHC*H*), 7.15 (dd, 1H, CCC*H*), 7.04 (td, 1H, CCCHC*H*), 6.96 (s, 2H, MesC*H*), 2.36 (s, 3H, *p*-C*H*$_3$), 1.94 (s, 6H, *o*-C*H*$_3$); ^{13}C NMR (100 MHz, $CDCl_3$) δ 145.9, 141.0, 139.0, 137.2, 135.4, 129.7, 128.5, 128.4, 128.0, 100.8, 21.2 (*p*-*C*H$_3$), 20.3 (*o*-*C*H$_3$). Anal. Calcd for $C_{15}H_{15}I$: C, 55.92; H, 4.69. Found: C, 56.32; H, 4.72.

1-Iodo-2-(2',4',6'-i-Pr$_3$C$_6$H$_2$)C$_6$H$_4$ (Ar^{T}I). The procedure was similar to that described above for the synthesis of Ar^{M}I. The reagents consist of magnesium powder (10.7 g, 441 mmol), 2,4,6-triisopropylbromide (50.0 g, 177 mmol), *ortho*-bromochlorobenzene (20.6 mL, 177 mmol), and iodine (67.2 g, 265 mmol). The solid product was washed with hexane and dried on a a frit under vacuum to yield colorless solid (69.0 g, 96%) of Ar^{T}I: ^{1}H NMR (400 MHz, $CDCl_3$) δ 7.96 (dd, 1H, CIC*H*), 7.39 (td, 1H, CICHC*H*), 7.21 (dd, 1H, CCC*H*), 7.06 (s, 2H, Trip C*H*), 7.04 (td, 1H, CCCHC*H*), 2.97 (sept, 1H, p-C*H*(CH$_3$)$_2$), 2.34 (sept, 2H, *o*-C*H*(CH$_3$)$_2$), 1.32 (d, 6H, *o*-CH(C*H*$_3$)$_2$), 1.23 (d, 6H, *o*-CH(C*H*$_3$)$_2$), 1.02 (d, 6H, *p*-CH(C*H*$_3$)$_2$); ^{13}C NMR (100 MHz, $CDCl_3$) δ 150.6, 148.4, 145.8, 145.6, 139.1, 138.7, 130.4, 128.2, 127.7, 102.3, 34.2 (*p*-*C*H(CH$_3$)$_2$), 30.6 (*o*- *C*H(CH$_3$)$_2$), 24.9 (*p*-CH(*C*H$_3$)$_2$), 24.1 (*o*-CH(*C*H$_3$)), 23.5 (*o*-CH(*C*H$_3$). Anal. Calcd For $C_{21}H_{27}I$: C, 62.07; H, 6.70. Found: C, 62.47; H, 6.79.

1-Azido-2-(2',4',6'-Me$_3$C$_6$H$_2$)C$_6$H$_4$ (Ar^{M}N$_3$). Ar^{M}I (60.0 g, 186 mmol) was suspended in pentane (300 mL) in a 1L Schlenk flask. The suspension was cooled to 0 °C, Li-*n*-Bu (2.93 M in hexane, 63.6 ml, 186 mmol) was added dropwise, and the solution was stirred as it was allowed to warm to RT overnight. The mixture was cooled to 0 °C again and 40.4 g (205 mmol) of TosN$_3$ was added dropwise. The solution started to turn orange and it left stirring at RT for 12 h. The reaction was quenched by adding water and the organics were collected via extraction three times with diethyl ether. The ether extracts were combined and dried with $MgSO_4$. The mixtures were filtered and the solvent was removed *in vacuo*. The crude red product was purified by column chromatography on alumina (3:1 hexanes: Et_2O) to yield a red oil (39.5 g, 89%). This compound was compared to known literature reports via oxidation of the aniline[18] and found to be the same: ^{1}H NMR (400 MHz, $CDCl_3$) δ 7.44 (td, 1H, CCCHC*H*), 7.30 (dd, 1H, CN$_3$C*H*), 7.24 (td, 1H, CN$_3$CHC*H*), 7.14 (dd, 1H, CCC*H*), 7.01 (s, 2H, Mes C*H*), 2.39 (s, 3H, *p*-C*H*$_3$), 2.03 (s, 6H, *o*-C*H*$_3$). IR (KBr) ν 2958, 2923, 2861, 2119 (s, N$_3$ asymm), 1613, 1574, 1474 (m, N$_3$ symm) 1443, 1377, 1305, 1286, 1249, 1005, 850, 754, 720, 704, 649, 583.

1-N$_3$-2-(2',4',6'-*i*-Pr$_3$C$_6$H$_2$)C$_6$H$_4$ (Ar^{T}N$_3$). This compound was prepared as described for Ar^{M}N$_3$ from Ar^{T}I (50.0 g, 123 mmol) in THF (500 ml) in a 1L Schlenk flask, Li-*t*-Bu (1.70 M in hexane, 145 mL, 246 mmol), and TosN$_3$ (24.2 g, 123 mmol). The crude product was purified by

column chromatography on alumina (3:1 hexanes: Et_2O) to yield 33.3 g (84% by total mass) of a red oil containing 60% of the product (56% accounting for only Ar^TN_3) and 40% of 2,4,6-*i*-Pr_3biphenyl. This mixture was used without further purification.

1-NH_2-2-(2',4',6'-$Me_3C_6H_2$)C_6H_4 (Ar^MNH_2). Ar^MN_3 (10.3 g, 43.4 mmol) was added slowly to an Et_2O solution (500 ml) of $LiAlH_4$ (1.65 g, 43.4 mmol). The solution became green and it was left refluxing overnight. The reaction was quenched by adding small amounts of water until the fizzing stopped. The mixture was extracted three times with Et_2O and the combined extracts were dried over $MgSO_4$. The $MgSO_4$ was removed through filtration and the solvent was removed to yield a crude solid product, which was recrystallized from a mixture of ethyl acetate and hexane to yield a slightly colored solid (8.39 g, 91%): ^{1}H NMR (400 MHz, $CDCl_3$) δ 7.18 (td, 1H, CCCHC*H*), 6.99 (s, 2H, Mes C*H*), 6.94 (dd, 1H, CNH_2C*H*), 6.84 (td, 1H, CNH_2CHC*H*), 6.79 (dd, 1H, CCC*H*), 3.42 (s br, 2H, NH_2), 2.35 (s, 3H, *p*-CH_3), 2.04 (s, 6H, *o*-CH_3); ^{13}C NMR (100 MHz, $CDCl_3$) δ 143.5, 137.0, 136.9, 134.8, 129.9, 128.4, 128.0, 126.1, 118.4, 114.9, 21.0 (*p*-CH_3), 20.1 (*o*-CH_3). Anal. Calcd For $C_{15}H_{17}N$: C, 85.26; H, 8.11; N, 6.63. Found: C, 85.47; H, 8.15; N, 6.57.

1-NH_2-2-(2',4',6'-*i*-$Pr_3C_6H_2$)C_6H_4 (Ar^TNH_2). Ar^TN_3 (33.3 g of a 3:2 mixture of **Ar^TN_3**, 62.1 mmol, and 2,4,6-*i*-Pr_3biphenyl) was added slowly to a diethyl ether solution (500 ml) of $LiAlH_4$ (4.32 g, 114 mmol). The solution turned green and was left refluxing overnight. The reaction was quenched by adding small amounts of water until the fizzing stopped. The product was extracted three times with diethyl ether, and the combined ether extracts were dried over $MgSO_4$. The magnesium sulfate was removed via filtration and the solvent was removed *in vacuo* to yield a crude product, which was purified via silica column chromatography using a 1:9 Et_2O/hexanes as the eluting solvent. The desired fraction had a R_f value of 0.29 and was collected to yield 14.7 g of pure product upon removal of solvent (80% accounting only for 62.1 mmol of Ar^TN_3): ^{1}H NMR (400 MHz, $CDCl_3$) δ 7.16 (td, 1H, CCCHC*H*), 7.09 (s, 2H, Trip C*H*), 6.95 (dd, 1H, CNH_2C*H*), 6.78 (td, 1H, CNH_2CHC*H*), 6.74 (dd, 1H, CCC*H*), 3.41 (s br, 2H, NH_2), 2.94 (sept, 1H, *p*-$(CH_3)_2C$*H*), 2.62 (sept, 2H, *o*-$(CH_3)_2C$*H*), 1.31 (d, 6H, CHMe_2), 1.14 (d, 6H, CHMe_2), 1.06 (d, 6H, CHMe_2); ^{13}C NMR (100 MHz, $CDCl_3$) δ 148.3, 147.5, 144.4, 132.6, 130.8, 127.9, 125.6, 121.1, 117.9, 114.5, 34.3 (*p*-$(CH_3)_2C$*H*), 30.4 (*o*-$(CH_3)_2C$*H*), 24.7 (*p*-$(CH_3)_2$CH), 24.1, 24.0. Anal. Calcd for $C_{21}H_{29}N$: C, 85.37; H, 9.89; N, 4.74. Found: C, 85.49; H, 9.91; N, 4.70.

Mo(NAr^{Cl})$_2Cl_2$DME (1) Triethylamine (33.0 mL, 235 mmol), trimethylchlorosilane (64.0 mL, 500 mmol) and 2-chloroaniline (15.0 g, 118 mmol) were added to a stirred slurry of sodium

molybdate (12.1 g, 58.8 mmol) in dimethoxyethane (200 ml). The resulting orange-red mixture was stirred for 36 h at 65 °C. The salts were filtered over celite and washed with benzene until the washings were colorless. Removal of solvent from the filtrate yielded the crude product in quantitative yield. The product was recrystallized from a mixture of toluene/pentane to give analytically pure red microcrystalline solids (25.1 g, 84%): ^{1}H NMR (500 MHz, C_6D_6) δ 7.62 (d, 2H, *Ar*, J = 8.0 Hz), 6.97 (d, 2H, *Ar*, J = 8.0 Hz), 6.61 (t, 2H, *Ar*, J = 7.5 Hz), 6.39 (t, 2H, *Ar*, $J \sim$ 7.5 Hz), 3.59 (s, 6H, *dme*), 3.19 (s, 4H, *dme*); ^{13}C NMR (125 MHz, C_6D_6) δ 153.8 (*C*–N), 129.4, 127.3, 125.9, 71.2 (br, *dme*), 63.6 (br, *dme*). Anal. Calcd for $C_{16}H_{18}N_2Cl_2O_2Mo$: C, 37.82; H, 3.57; N, 5.51. Found: C, 38.08; H, 3.72; N, 5.22.

$Mo(NAr^M)_2Cl_2(THF)_2$•2THF (2). Na_2MoO_4 (4.87 g, 23.7 mmol), Ar^MNH_2 (10.0 g, 47.3 mmol), NEt_3 (13.2 ml, 94.6 mmol), and TMSCl (25.5 ml, 201 mmol) were dissolved in dry DME (300 ml) in a sealed Schlenk flask. The reaction was stirred at 60 °C overnight. The salts were filtered off from the deep red solution and rinsed with benzene. The solvent was removed from the filtrate at 60 °C under reduced pressure. The crude product was triturated with THF and the excess solvent was removed *in vacuo*. The mixture was dissolved in a mixture of THF and pentane and left to crystallize at – 35 °C; red crystalline solid (13.6 g, 84%) was collected upon filtration. A sample (0.100 g) was dissolved in a THF/pentane solution and the solution was stood at -35 °C for a couple of days to produce red crystals suitable for X-ray diffraction: ^{1}H NMR (400 MHz, C_6D_6) δ 7.98 (d, 2H, CNC*H*), 6.99 (t, 2H, CNCHC*H*), 6.90-6.82 (m, 8H, imido), 3.59 (m, 16H, OCH_2), 2.19 (s, 6H, *o*-CH_3), 2,16 (s, 3H, *p*-CH_3), 1.35 (m, 16H, OCH_2CH_2); ^{13}C NMR (100 MHz, C_6D_6) δ 155.4, 137.0, 136.5, 136.4, 132.6, 130.1, 130.0, 128.3, 127.9, 127.5, 69.4 (OCH_2), 25.6 (*o*-CH_3), 21.3 (*p*-CH_3), 21.1 (OCH_2CH_2). Anal. Calcd For $C_{46}H_{62}Cl_2MoN_2O_4$: C, 63.23; H, 7.15; N, 3.21. Found: C, 63.34; H, 7.13; N, 3.19.

$Mo(NAr^T)_2Cl_2(DME)$ (3). The procedure was similar to that of **1** employing Na_2MoO_4 (3.48 g, 16.9 mmol), Ar^TNH_2 (10.0 g, 33.8 mmol), NEt_3 (9.40 ml, 67.5 mmol), and TMSCl (20.0 ml, 158 mmol) in dry DME (300 ml). Upon removal of benzene/DME, the crude is washed with pentane and collected on a frit under reduced pressure to yield red solid (11.2 g, 79%). A sample (0.100 g) was dissolved in a Et_2O/CH_2Cl_2 solution and the solution was stood at -35 °C for a couple of days to produce red crystals suitable for X-ray diffraction: ^{1}H NMR (400 MHz, C_6D_6) δ 8.18 (d, 2H, CNC*H*), 7.14 (s, 4H, Trip C*H*), 7.05 (d, 2H, CCC*H*), 6.96 (t, 2H, CCCHC*H*), 6.79 (t, 2H, CNC*H*), 2.98-2.72 (m, 16H, $(CH_3)_2CH$ + DME), 1.42 (d, 12H, $CH(CH_3)_2$), 1.23 (d, 12H, $CH(CH_3)_2$), 1.11 (d, 12H, $CH(CH_3)_2$); ^{13}C NMR (100 MHz, C_6D_6) δ 155.8, 148.6, 147.6, 134.8, 132.3, 131.2, 131.1, 128.1, 127.9, 127.2, 70.6 (DME CH_2), 62.5 (DME CH_3), 34.9 ($(CH_3)_2CH$),

31.0 ($(CH_3)_2CH$), 25.4 ($CH(CH_3)_2$), 24.4 ($CH(CH_3)_2$), 23.6 ($CH(CH_3)_2$). Anal. Calcd for $C_{46}H_{64}Cl_2MoN_2O_2$: C, 65.47; H, 7.64; N, 3.32. Found: C, 65.19; H, 7.52: N, 3.28.

$Mo(NAr^{Cl})_2(CH_2CMe_2Ph)_2$ (4) Neophylmagnesium chloride (0.50 M in ether, 39.4 mL, 20 mmol) was added slowly to a chilled suspension of **1** (5.00 g, 10.0 mmol) in ether (100 mL). After stirring for 18 h, the mixture was filtered through celite. The solvent was removed *under vacuo* from the filtrate to give a dark-red oil. Pentane was added to the oil and stirred vigorously until precipitation of an orange product occurred. The precipitated solids were filtered, washed with cold pentane and dried *under vacuo*. Yields: 4.10 g (68%): ^{1}H NMR (500 MHz, C_6D_6) δ 7.38 (d, 4H, *Ar*, J = 7.5 Hz), 7.16 (t, 4H, *Ar*, J = 7.5 Hz), 7.10 (dd, 2H, *Ar*, J = 7.5, 1.5 Hz), 7.04 (t, 2H, *Ar*, J = 7.5 Hz), 6.92 (dd, 2H, *Ar*, J = 7.5, 1.5 Hz), 6.70 (t, 2H, *Ar*, J = 7.5 Hz), 6.51 (t, 2H, *Ar*, J = 7.5 Hz), 2.03 (s, 4H), 1.47 (s, 12H); ^{13}C NMR (125 MHz, C_6D_6) δ 153.8, 150.9, 129.7, 128.7, 128.4, 127.9, 127.0, 126.4, 126.24, 126.20, 125.9, 82.2, 41.0, 32.71, 32.66. Anal. Calcd for $C_{32}H_{34}N_2Cl_2Mo$: C, 62.65; H, 5.59; N, 4.57. Found: C, 62.43; H, 5.60; N, 4.55.

$Mo(NAr^{M})_2(CH_2CMe_2Ph)_2$ (5). The synthesis was essentially the same as for **4** employing **2** (3.33 g, 4.89 mmol) and $ClMgCH_2CMe_2Ph$ (0.50 M in Et_2O, 19.6 ml, 9.8 mmol) to yield orange solid product (2.86 g, 74%): ^{1}H NMR (400 MHz, C_6D_6) δ 7.20-7.08 (m, 10H, aromatics), 7.04 (dd, 2H, aromatics), 6.99 (td, 2H, aromatics), 6.93-6.83 (m, 8H, aromatics), 2.23 (s, 6H, *p*-CH_3), 2.11 (s, 12H, *o*-CH_3), 1.30 (s, 12H, CMe_2Ph), 1.07 (s, 4H, $MoCH_2$); ^{13}C NMR (100 MHz, C_6D_6) δ 155.8, 151.5, 137.3, 136.7, 136.5, 134.2, 130.0, 128.6, 128.5, 127.6, 126.3, 126.1, 125.9, 125.4, 78.4 (CH_2CMe_2Ph), 39.7 ($MoCH_2CMe_2Ph$), 32.4 ($CH_2C(CH_3)_2Ph$), 21.2 (Mes CH_3), 21.0 (Mes CH_3). Anal. Calcd for $C_{50}H_{56}MoN_2$: C, 76.90; H, 7.23; N, 3.59. Found: C, 76.86; H, 7.31; N 3.60.

$Mo(NAr^{T})_2(CH_2CMe_3)_2$ (6). The synthesis was essentially the same as for **4** employing **3** (6.31 g, 7.45 mmol) and $ClMgCH_2CMe_3$ (2.73 M in Et_2O, 5.47 ml, 14.9 mmol), but the compound was further purified by recrystallization from pentane at – 35 °C to yield orange-red **6** (3.11 g, 50%): ^{1}H NMR (400 MHz, C_6D_6) δ 7.54 (dd, 1H, imido), 7.22 (dd, 1H, imido), 7.20 (s, 2H, TRIP *CH*), 7.03 (td, 1H, imido), 6.86 (td, 1H, imido), 2.85 (sept, 3H, $(CH_3)_2CH$), 1.57 (s, 2H, *CH_2t-Bu*), 1.35 (d, 6H, $CH(CMe_3)_2$), 1.30 (d, 6H, $CH(CMe_3)_2$), 1.14 (d, 6H, $CH(CMe_3)_2$), 0.99 (s, 9H, CH_2CMe_3); ^{13}C NMR (100 MHz, C_6D_6) δ 156.3, 148.9, 148.3, 148.2, 147.0, 145.0, 135.5, 133.8, 133.0, 131.6, 130.9, 128.5, 127.9, 127.7, 125.4, 124.8, 121.4, 120.8, 118.1, 114.7, 80.3 (CH_2CMe_3), 34.9, 34.8, 34.2, 33.6, 31.0, 30.8, 25.6, 24.9, 24.5, 24.4, 24.3, 23.9. Anal. Calcd for $C_{52}H_{76}MoN_2$: C, 75.69; H, 9.28; N, 3.40. Found: C, 75.77; H, 9.08; N, 3.47.

$Mo(NAr^T)_2(CH_3)_2$ (7). The synthesis was essentially the same as for **4** employing **3** (0.361 g, 0.428 mmol), $ClMgCH_3$ (3.00 M in THF, 0.29 ml, 0.87 mmol), but the compound was further purified by recrystallization from pentane at – 35 °C to yield orange-red **7** as a solid (0.152 g, 50%). **7** (0.060 g) was redissolved in a pentane/Et_2O solution and left undisturbed at -35 °C for a few days to yield orange crystals suitable for X-ray diffraction: ^1H NMR (400 MHz, C_6D_6) δ 7.37 (d, 2H, CNC*H*), 7.20 (s, 4H, Trip C*H*), 7.11 (d, 2H, CCC*H*), 6.96 (t, 2H, CCCHC*H*), 6.87 (t, 2H, CNCHC*H*),2.92 (m, 4H, C*H*$(CH_3)_2$), 2.84 (m, 2H, C*H*$(CH_3)_2$), 1.28 (d, 12H, CH(C*H*$_3)_2$), 1.25 (d, 12H, CH(C*H*$_3)_2$), 1.16 (d, 12H, CH(C*H*$_3)_2$), 0.70 (s, 6H, MoC*H*$_3$); ^{13}C NMR (100 MHz, C_6D_6) δ 155.5, 148.5, 147.1, 135.1, 133.6, 130.9, 127.9, 126.8, 125.2, 120.8, 36.4 (Mo*C*H_3), 34.9, 31.1, 25.0 (CH_2C*Me*$_3$), 24.4 (CH_2C*Me*$_3$), 24.1 (CH_2C*Me*$_3$). Anal. Calcd For $C_{44}H_{60}MoN_2$: C, 74.13; H, 8.48; N, 3.93. Found: C, 73.93; H, 8.39; N 3.90.

$Mo(NAr^{Cl})(CHCMe_2Ph)(OTf)_2(DME)$ (8). **4** (2.00 g, 3.26 mmol) was suspended in ether (100 mL) and cooled to – 30 °C. Triflic acid (1.47 g, 9.78 mmol) was added slowly into the chilled suspension to yield a yellowish-brown solution. The resulting mixture was allowed to warm gradually to room temperature and stirred for 18 h. The solution was then evacuated to dryness and extracted with benzene. The triflate salts were removed via filtration through celite and the benzene was removed *under vacuo*. Addition of pentane to the residue gave microanalytically pure pale yellow needles (1.03 g, 43%): ^1H NMR (500 MHz, C_6D_6) (Major isomer 70%) δ 14.01 (s, 1H, *syn* Mo=C*H*, J_{CH} = 121.5 Hz), 7.82 (dd, 1H, *Ar*, *J* = 8.0, 1.0 Hz), 7.62 (d, 2H, *Ar*, *J* = 7.5 Hz), 7.44 (d, 1H, *Ar*, *J* = 7.5 Hz), 7.09 (t, 2H, *Ar*, *J* = 7.5 Hz), 6.77 (t, 1H, *Ar*, *J* = 7.5 Hz), 6.58 (t, 1H, *Ar*, *J* = 7.5 Hz), 6.46 (t, 1H, *Ar*, *J* = 7.5 Hz), 3.43 (s, 3H, *dme*), 3.24 (br s, 2H, *dme*), 2.89 (s, 3H, *dme*), 2.86 (br s, 2H, *dme*), 1.80 (s, 6H, C*Me*$_2$Ph); (Minor isomer 30%) δ 15.00 (s, 1H, *syn* Mo=C*H*, J_{CH} = 127.0 Hz), 8.10 (d, 1H, *Ar*, *J* = 8.0 Hz), 7.07 (t, 2H, *Ar*, *J* = 7.5 Hz), 6.86–6.90 (overlapping peaks, 2H, *Ar*), 6.75 (t, 2H, *Ar*, *J* = 7.5 Hz), 6.69 (t, 1H, *Ar*, *J* = 7.5 Hz), 6.54 (t, 1H, *Ar*, *J* = 7.5 Hz), 3.24 (m, 1H, *dme*), 3.14 (s, 3H, *dme*), 3.11(m, 1H, *dme*), 3.04 (s, 3H, *dme*), 2.96 (m, 1H, *dme*), 2.47 (m, 1H, *dme*), 1.97 (s, 3H, C*Me*$_2$Ph), 1.51 (s, 3H, C*Me*$_2$Ph); ^{13}C NMR (125 MHz, C_6D_6) δ 334.0 (Mo=*C*, minor isomer), 326.2 (Mo=*C*, major isomer), 151.9, 151.7, 148.6, 146.4, 132.4, 132.2, 132.1, 130.3, 129.7, 129.4, 128.9, 128.7, 127.3, 126.9, 126.8, 126.7, 124.0, 121.9, 121.6, 121.4, 119.4, 118.9, 116.4, 77.3, 73.7, 70.0, 69.7, 64.4, 62.4, 62.0, 61.5, 58.8, 31.2, 30.6, 30.5, 29.5, 28.8. Anal. Calcd for $C_{22}H_{26}NS_2ClF_6O_8Mo$: C, 35.61; H, 3.53; N, 1.89. Found: C, 35.66; H, 3.58; N, 1.71.

$Mo(NAr^M)(CHCMe_2Ph)(OTf)_2$DME (9). The synthesis was essentially the same as for **8** employing **5** (9.70 g, 12.4 mmol), dimethoxyethane (5.00 ml, 48.1 mmol), and TfOH (5.59 g, 37.3 mmol). The crude product was precipitated through addition of pentane and triturated with

Et_2O overnight to give clean product (2.88 g, 28%): ^1H NMR (400 MHz, C_6D_6) δ 15.41 (s, 0.2H, MoC*H*, J_{CH} = 128 Hz), 14.6 (s, 1H, MoC*H*, J_{CH} = 129 Hz), 13.4 (s, 0.6H, 0.02H, MoC*H*, J_{CH} = 122 Hz), 12.9 (s, 0.02H, MoC*H*), 8,42 (d, 1, aromatic), 7.86 (d, 1, aromatic), 7.51-6.74 (m, 9H, aromatics), 6.68-6.52 (m, 3H, aromatics), 3.43-3.01 (various s, 20H, DME), 2.28-1.61 (various singlets, 30H, aliphatics); ^{13}C NMR (100 MHz, C_6D_6) δ 330.7 (Mo*C*H), 319.9 (Mo*C*H), 315.4 (Mo*C*H), 154.5, 154.1, 149.9, 148.8, 146.8, 138.4, 138.0, 137.7, 137.6, 137.5, 136.6, 136.3, 136.2, 136.1, 135.9, 135.7, 134.2, 133.8, 131.9, 131.7, 131.6, 130.2, 129.1, 128.9, 128.8, 128.5, 126.8, 126.7, 126.4, 126.4, 75.5, 74.4, 70.2, 66.0, 61.3, 59.2, 57.2, 32.5, 31.1, 30.9, 30.4, 30.0, 29.5, 29.1, 28.4, 21.5, 21.3, 21.2, 20.9, 20.8, 20.6, 20.5; ^{19}F NMR (376 MHz, C_6D_6) δ – 76.7 (*trans*), - 77.0 (*cis*), - 77.9 (*cis*).

Mo(NAr^T)(CHCMe$_3$)(OTf)$_2$DME (10). The synthesis was essentially the same as for **8** employing **6** (2.01 g, 2.44 mmol), dimethoxyethane (1.00 ml, 9.62 mmol), and TfOH (1.10 g, 7.33 mmol). The crude was triturated with benzene for 2 h. The yellow solid product was collected in 2 crops (overall yield: 0.973 g, 47%): ^1H NMR (400 MHz, C_6D_6) δ 14.9 (s, 1H, MoC*H*, J_{CH} = 124 Hz), 14.3 (s, 0.6H, MoC*H*, J_{CH} = 126 Hz), 14.0 (s, 0.12H, MoC*H*, J_{CH} = 122 Hz), 13.2 (s, 0.03H, MoC*H*), 8.69 (d, 1H, aromatic), 8.51 (d, 0.03H, aromatic), 8.36 (d, 0.12H, aromatic), 8.12 (d, 0.6H, aromatic), 7.86 (d, 1H, aromatic), 7.40-6.70 (m, 11H, aromatics), 3.52 (s, 3H, DME C*H*$_3$), 3.50 (s, 2H, DME C*H*$_2$), 3.45 (s, 2H, DME C*H*$_2$), 3.31 (s, 3H, DME C*H*$_3$), 3.0-2.3 (various multiplets, 10H, (CH$_3$)$_2$C*H*), 1.50 (s, 1.1H, CHC*Me*$_3$), 1.32 (s, 9H, CHC*Me*$_3$), 1.23 (s, 5.4H, CHC*Me*$_3$), 1.41-1.34 (2 d, 3), 1.20-0.70 (m, 30H); ^{13}C NMR (100 MHz, C_6D_6) δ 334.8 (Mo*C*H), 322.4 (Mo*C*H), 310.4 (Mo*C*H), 154.9, 154.5, 150.2, 149.9, 149.5, 149.4, 148.8, 148.6, 147.6, 147.5, 146.3, 137.5, 136.1, 135.6, 134.8, 134.2, 134.1, 133.2, 132.9, 132.7, 132.5, 131.5, 131.4, 128.9, 128.8, 128.6, 128.5, 128.1, 127.9, 122.2, 121.8, 121.5, 121.0, 120.9, 120.8, 120.7, 119.0, 118.6, 78.4, 77.6, 76.1, 75.5, 70.0, 69.7, 65.9, 61.1, 60.9, 54.4, 52.7, 52.1, 34.8, 34.7, 34.6, 31.2, 31.1, 31.0 30.7, 30.6, 30.3, 26.3, 25.7, 25.6, 25.2, 24.4, 24.1, 24.0, 23.5, 23.4, 23.0, 22.4, 22.2, 15.6; ^{19}F NMR (376 MHz, C_6D_6) δ – 76.7 (s, 1), - 76.8 (m, 1.7), -76.9 (s, 0.09), - 77.7 (m, 3).

Mo(NAr^{Cl})(CHCMe$_2$Ph)(2,5-Me$_2$Pyr)$_2$ (11). **8** (1.00 g, 1.35 mmol) was dissolved in toluene (20 mL) and cooled to – 30 °C. Li(2,5-Me$_2$Pyr) (0.300, 2.97 mmol, 2.20 equivalents) was added portion wise to the suspension. The reaction was subsequently warmed to and stirred at room temperature for 24 h. The volatiles were then removed *under vacuo*. Benzene was added to the residue, and the mixture was filtered through Celite in order to remove LiOTf. The filtrate was evacuated to dryness yielding a dark orange-brown oil. The oil was triturated repeatedly with pentane until an orange-brown solid was obtained. The product was filtered, washed with

cold pentane and dried *under vacuo*. The crude product was extracted with tetramethylsilane and the solvent evaporated to give bright orange microcrystalline solids (0.420 g, 57%): ^{1}H NMR (500 MHz, C_6D_6) δ 13.19 (s, 1H, *syn* Mo=C*H*, J_{CH} = 131.0 Hz), 7.31 (d, 2H, *Ar*, J = 8.0 Hz), 7.00 (t, 2H, *Ar*, J = 8.0 Hz), 6.94 (dd, 1H, *Ar*, J = 8.0, 1.0 Hz), 6.89 (m, 2H, *Ar*), 6.55 (t, 1H, *Ar*, J = 8.0 Hz), 6.47 (t, 1H, *Ar*, J = 8.0 Hz), 2.11 (br s, 12H, *Pyr*), 1.59 (s, 6H, C*Me*$_2$Ph); ^{13}C NMR (125 MHz, C_6D_6) δ 315.2 (Mo=*C*), 152.1, 149.7, 136.0 (br), 130.0, 129.6, 129.1, 127.2, 126.0, 106.6 (br), 57.9, 31.6 (br), 17.9 (br). Anal. Calcd for $C_{28}H_{32}ClMoN_3$: C, 62.05; H, 5.95; N, 7.75. Found: C, 61.80; H, 5.83; N, 7.68.

Mo(NAr^{CF3})(CHCMe$_3$)(2,5-Me$_2$Pyr)$_2$ (12). Mo(NAr^{CF3})(CHCMe$_3$)(OTf)$_2$(DME) (2.37 g, 3.32 mmol) was dissolved in Et_2O and the solution was cooled to – 35 °C for 1 h before addition of 2,5-$Me_2C_4H_2NLi$ (0.672 g, 6.65 mmol) in one portion. The reaction was stirred overnight at RT. The solvent was removed *in vacuo*. A minimum of CH_2Cl_2 was added and the mixture was passed through a frit to remove LiOTf salts. The salts were washed with CH_2Cl_2 until they were colorless. The solvent was removed from the filtrate *in vacuo* to yield an oily crude product. A minimal amount of Et_2O and pentane were added to triturate the product for 30 min. The mixture was stored at – 35 °C overnight to yield an orange solid (0.930 g, 53%): ^{1}H NMR (400 MHz, C_6D_6) δ 13.5 (s, 1H, MoC*H*CMe$_3$, J_{CH} = 131.8 Hz), 7.21 (d, 1H, Ar), 7.11 (d, 1H, Ar), 6.71 (t, 1H, Ar), 6.50 (t, 1H, Ar), 6.4-5.6 (br s, 4H, $Me_2C_4H_2N$), 2.15 (s br, 12H, *Me*$_2$C$_4$H$_2$N), 1.19 (s, 9H, MoCHC*Me*$_3$); ^{13}C NMR (100 MHz, C_6D_6) δ 322.3 (MoCHCMe$_3$), 152.6, 132.5, 131.8, 125.9, 125.6 (q, *C*F$_3$), 122.4, 122.1, 106.4, 52.2 (MoCHCMe$_3$), 32.8 (MoCHC*Me*$_3$), 18.2 (br, Pyr *C*H$_3$). Anal. Calcd for $C_{24}H_{30}F_3MoN_3$: C, 56.14; H, 5.89; N, 8.18. Found: C, 55.88; H, 5.73; N, 8.02.

Mo(NAr^{iPr})(CHCMe$_2$Ph)(2,5-Me$_2$Pyr)$_2$ (13). The synthesis was essentially the same as for **11** employing Mo(NAr^{iPr})(CHCMe$_2$Ph)(OTf)$_2$(DME) (1.00 g, 1.34 mmol) and 2,5-$Me_2C_4H_2NLi$ (0.300 g, 2.97 mmol). The crude product was recrystallized from a concentrated solution of pentane at – 30 °C to give orange-red blocks of crystals (0.440 g, 59%): ^{1}H NMR (500 MHz, C_6D_6) δ 13.11 (s, 1H, *syn* Mo=C*H*, J_{CH} = 130.0 Hz), 7.31 (d, 2H, *Ar*, J = 7.5 Hz), 7.10 (overlapping peaks, 3H, *Ar*), 6.98–7.01 (overlapping peaks, 2H, *Ar*), 6.88 (t, 1H, *Ar*, J = 7.5 Hz), 6.80 (t, 1H, *Ar*, J = 7.5 Hz), 5.95 (br s, 4H, *Pyr*), 3.47 (sept, 1H, ^{i}*Pr*, J = 7.0 Hz), 2.07 (br s, 12H, *Pyr*), 1.65 (s, 6H, C*Me*$_2$Ph), 1.10 (d, 6H, CH*Me*$_2$); ^{13}C NMR (125 MHz, C_6D_6) δ 312.8 (Mo=*C*), 153.6, 149.2, 144.2, 129.4, 128.4, 127.5, 126.8, 126.3, 126.0, 125.9, 106.1 (br), 57.5, 31.7, 31.6, 27.9, 27.6, 23.8, 17.8 (br). Anal. Calcd for $C_{31}H_{39}N_3Mo$: C, 67.74; H, 7.15; N, 7.65. Found: C, 67.47; H, 6.97; N, 7.48.

Mo(NAr^{tBu})(CHCMe$_3$)(2,5-Me$_2$Pyr)$_2$ (14). The synthesis was essentially the same as for **12** employing Mo(NAr^{tBu})(CHCMe$_3$)(OTf)$_2$(DME) (4.25 g, 6.06 mmol) and 2,5-Me$_2$C$_4$H$_2$NLi (1.226 g, 12.1 mmol) to yield red orange solid (2.50 g, 82%): ^{1}H NMR (400 MHz, C$_6$D$_6$) δ 13.5 (s, 1H, MoC*H*CMe$_3$, J_{CH} = 125.9 Hz), 7.38 (d, 1H, Ar), 7.01 (d, 1H, Ar), 6.76 (t, 1H, Ar), 6.67 (t, 1H, Ar), 6.60-5.20 (d br, 4H, Me$_2$C$_4$*H*$_2$N), 2.25 (s br, 12H, *Me*$_2$C$_4$H$_2$N), 1.30 (s, 9H, *Ar*^{tBu}), 1.20 (s, 9H, MoCHC*Me*$_3$); ^{13}C NMR (100 MHz, C$_6$D$_6$) δ 319.0 (Mo*C*HCMe$_3$), 154.8, 141.8, 134.8, 127.1, 126.9, 125.7, 110.2 (br, Pyr *C*H), 102.9 (br, Pyr *C*H), 65.9, 52.9, 35.7, 32.8, 29.8. Anal. Calcd for C$_{27}$H$_{39}$MoN$_3$: C, 64.66; H, 7.84; N, 8.38. Found: C, 64.31; H, 7.66; N, 8.36.

Mo(NAr^{tBu})(CHCMe$_2$Ph)(2,5-Me$_2$Pyr)$_2$ (15). The synthesis was essentially the same as for **12** employing Mo(NAr^{tBu})(CHCMe$_2$Ph)(OTf)$_2$(DME) (4.10 g, 5.36 mmol) and 2,5-Me$_2$C$_4$H$_2$NLi (1.08 g, 10.7 mmol) to yield orange solid (3.00 g, 68%): ^{1}H NMR (400 MHz, C$_6$D$_6$) δ 13.3 (s, 1H, MoC*H*CMe$_2$Ph J_{CH} = 129.7 Hz), 7.42 (d, 1H, Ar), 7.31 (d, 2H, Ph), 7.10 (t, 2H, Ph), 7.04 (dd, 1H, Ar), 7.00 (t, 1H, Ph), 6.79 (t, 1H, Ar), 6.71 (t, 1H, Ar), 6.60-5.20 (d br, 4H, Me$_2$C$_4$*H*$_2$N), 2.40-1.70 (s br, 12H, *Me*$_2$C$_4$H$_2$N), 1.65 (s, 6H, MoCHC*Me*$_2$Ph), 1.31 (s, 9H, Ar^{tBu}); ^{13}C NMR (100 MHz, C$_6$D$_6$) δ 314.2 (Mo*C*HCMe$_2$Ph), 154.9, 149.0, 142.0, 134.9, 128.5, 127.2, 126.9, 126.6, 126.2, 125.8, 110.2 (s br, Pyr *C*H), 103.0 (br, Pyr *C*H), 59.3, 35.7, 29.8, 18.7 (br, Pyr *C*H$_3$), 16.3 (br, Pyr *C*H$_3$), 13.1. Anal. Calcd for C$_{32}$H$_{41}$MoN$_3$: C, 68.19; H, 7.33; N, 7.46. Found: C, 67.95; H, 7.31; N, 7.31.

Mo(NAr^{M})(CHCMe$_2$Ph)(2,5-Me$_2$Pyr)$_2$ (16). The synthesis was essentially the same as for **12** employing **9** (2.01 g, 2.43 mmol) and 2,5-Me$_2$C$_4$H$_2$NLi (0.493 g, 4.88 mmol) to yield orange solid (1.25 g, 82%): ^{1}H NMR (400 MHz, C$_6$D$_6$) δ 13.1 (s, 1H, MoC*H*CMe$_2$Ph J_{CH} = 123.9 Hz), 7.40-6.60 (m, 11H, aromatics), 6.60-3.00 (br s, 4H, Me$_2$C$_4$*H*$_2$N), 2.50-1.20 (br singlets, 27H, aliphatics); ^{13}C NMR (100 MHz, C$_6$D$_6$) δ 312. 0 (Mo*C*HCMe$_2$Ph), 153.7, 149.2, 137.8, 136.9, 136.1, 136.0, 130.3, 130.1, 128.4, 127.9, 127.0, 126.8, 126.2, 109.9 (pyr *C*H), 106.6,102.3 (pyr *C*H), 58.2, 31.9, 22.7, 20.9, 18.6, 14.2, 13.0. Anal. Calcd for C$_{39}$H$_{37}$MoN$_3$: C, 71.02; H, 6.93; N, 6.72. Found: C, 70.77; H, 7.03; N, 6.64. Crystals suitable for X-ray diffraction were obtained through recrystallization from toluene.

Mo(NAr^{T})(CHCMe$_3$)(2,5-Me$_2$Pyr)$_2$ (17). The synthesis was essentially the same as for **12** employing **10** (0.253 g, 0.298 mmol) and 2,5-Me$_2$C$_4$H$_2$NLi (0.060 g, 0.594 mmol). The crude product was too soluble to recrystallize from pentane or tetramethylsilane even after a period of weeks at – 35 °C. Therefore, the solvent was simply removed to give a product with only solvents as impurities (0.070 g, 36%): ^{1}H NMR (400 MHz, C$_6$D$_6$) δ 13.2 (s, 1H, MoC*H*CMe$_3$ J_{CH} = 129.0), 7.27 (d, 1H, CNC*H*), 7.13 (s, 2H, Trip C*H*), 6.95 (d, 1H, CCC*H*), 6.8-6.7 (m, 2H,

aromatics), 6.60 (s, 2H, pyrrolide C*H*), 2.79 (sept, 2H, $(CH_3)_2CH$), 2.64-2.0 (br s, 7H, $(CH_3)_2CH$ + pyrrolide CH_3), 1.26 (br d, 6H, *o*-$(CH_3)_2CH$), 1.24 (s, 9H, $CHCMe_3$), 1.20 (d, 6H, *p*-$(CH_3)_2CH$), 0.96 (br d, 6H, *o*-$(CH_3)_2CH$); ^{13}C NMR (100 MHz, C_6D_6) δ 316.8 ($MoCHCMe_3$), 154.8, 150.2, 135.3, 134.7, 132.0, 131.4, 128.3, 126.2, 121.0 (pyrrolide *C*H), 110.0 (pyrrolide *C*H) 106.9, 53.0, 35.9, 33.5, 30.8, 24.5 (br s, pyrrolide CH_3), 19.4 (pyrrolide CH_3), 13.1.

$Mo(NAr^M)(CHCMe_2Ph)(OTPP)_2$ (18). A solution of TPPOH (0.103 g, 0.258 mmol) in Et_2O (5.00 ml) was cooled to -35 °C and *n*-BuLi (1.60 M in hexane, 0.16 ml, 0.26 mmol) was added slowly. The mixture was stirred at RT for 1 h and cooled to -35 °C for 1 hour. The mixture was added to a -35 °C Et_2O solution of **9** (0.106 g, 0.128 mmol). After 1 h the solvent was removed *in vacuo*. The crude product was redissolved in dichloromethane, the insoluble salts were removed by filtration, and the solvent was removed *in vacuo*. The product was triturated with pentane and collected on a frit as an orange solid (0.084 g, 55%): ^1H NMR (400 MHz, C_6D_6) δ 10.75 (s, 1H, $MoCHCMe_2Ph$ J_{CH} = 123 Hz minor), 10.60 (s, 1.45H, $MoCHCMe_2Ph$ J_{CH} = 122 Hz major), 7.50-6.50 (m, 106H, aromatics), 3.31 (q, 14H, OCH_2), 2.24 (s, 4.5H, *para Mes* major), 2.20 (s, 3H, aromatics *para Mes*), 2.00 (s, 9H, *ortho Mes* major), 1.95 (s, 9H, $MoCHCMe_2Ph$ major), 1.87 (s, 6H, *ortho Mes*), 1.72 (s, 6H, *ortho Mes*), 1.58 (s, 3H, $MoCHCMe(CH_3)Ph$ minor), 1.50 (s, 3H, $MoCHCMe(CH_3)Ph$ minor), 1.17 (t, 21H, OCH_2CH_3); ^{13}C NMR (100 MHz, C_6D_6) δ 290.2 ($MoCHCMe_3$), 288.2 ($MoCHCMe_3$), 163.8, 161.8, 156.0, 151.1, 148.8, 148.6, 147.1, 146.7, 146.4, 142.9, 142.3, 142.1, 141.9, 141.7, 138.1, 137.0, 136.5, 134.6, 134.0, 133.9, 133.8, 133,1, 133.6 131.9, 131.5, 130.9, 130.2, 130.1, 129.8, 129.7, 128.7, 128.1, 127.2, 126.8, 126.6, 126.5, 126.4, 126.1, 125.6, 124.8, 121.3, 121.1, 120.5, 108.3, 106.5, 49.4, 48.9, 34.8, 31.3, 30.8, 27.0, 25.6, 25.4, 24.2, 22.7, 21.7. Anal. Calcd for $C_{89}H_{79}MoNO_3$: C, 81.82; H, 6.09; N, 1.07. Found: C, 81.87; H, 6.31; N, 1.09.

A sample of **18** suitable for an X-ray study was obtained by layering a solution of Et_2O with pentane and placing the mixture at -35 °C for several days.

$Mo(NAr^T)(CHCMe_3)(2,5\text{-}Me_2Pyr)(OTPP)$ (19). Compound **17** (0.200 g, 0.309 mmol) was dissolved in Et_2O and the solution was placed at – 35 °C for 1 h before addition of TPPOH (0.123 g, 0.309 mmol) in one portion. The reaction was allowed to warm up to RT and stirred for 2 h. The solvent was removed *in vacuo* and the crude product was triturated with pentane and collected on a frit (0.128 g, 44%): ^1H NMR (400 MHz, C_6D_6) δ 10.87 (s, 1H, $MoCHCMe_3$, J_{CH} = 116.0 Hz), 7.40-6.30 (m, 27H, aromatics), 5.89 (s, 2H, C*H*Pyrr), 2.92 (m, 1H, $CH(CH_3)_2$), 2.81 (m, 1H, $CH(CH_3)_2$), 2.70 (m, 1H, $CH(CH_3)_2$), 1.80 (s, 6H, *Me*Pyrr), 1.40 (d, 6H, *para* $CH(CH_3)_2$), 1.28 (d, 3H, *ortho* $CH(CH_3)_2$), 1.23 (d, 3H, *ortho* $CH(CH_3)_2$), 1.10 (s, 9H, $MoCHCMe_3$), 0.97 (d, 3H, *ortho* $CH(CH_3)_2$), 0.93 (d, 3H, *ortho* $CH(CH_3)_2$); ^{13}C NMR (100

MHz, C_6D_6) δ 288.3 (Mo*C*HCMe$_3$), 161.8, 156.0, 151.1, 148.8, 148.6, 147.1, 146.7, 146.4, 142.9, 142.3, 142.1, 141.9, 141.7, 138.1, 137.1, 136.5, 134.6, 134.0, 133.1, 133.1, 131.9, 131.5, 130.9, 130.3, 130.2, 129.8, 129.7, 128.7, 127.4, 127.2, 126.8, 126.6, 125.6, 124.8, 121.4, 121.3, 121.1, 120.7, 48.6, 34.8, 31.3, 30.9, 30.7, 27.0, 25.6, 25.4, 24.4, 22.7, 21.7. Anal. Calcd for $C_{62}H_{66}MoN_2O$: C, 78.29; H, 6.99; N, 2.95. Found: C, 77.94; H, 6.67; N, 2.91.

Mo(NAr^{Cl})(CHCMe$_2$Ph)(2,5-Me$_2$Pyr)(OHMT) (20). **11** (0.102 g, 0.188 mmol) and HMTOH (0.065 g, 0.197 mmol) were dissolved in benzene (15.0 ml) in a round-bottom flask and stirred at RT for 18 h. The resultant reaction mixture was evacuated to dryness. The brown oily residue was triturated several times with pentane until orange solids were formed. The pale orange solids were filtered, washed with cold pentane and dried *under vacuo*. Microanalytically pure product can be recrystallized from a mixture of toluene and pentane (0.059 g, 40%): ^{1}H NMR (500 MHz, C_6D_6) δ 11.34 (s, 1H, *syn* Mo=C*H*, J_{CH} = 123.5 Hz), 7.30 (d, 2H, *Ar*, J = 8.0 Hz), 7.08 (t, 2H, *Ar*, J = 7.5 Hz), 6.88–6.99 (overlapping peaks, 5H, *Ar*), 6.83 (s, 2H, *Ar*), 6.77 (s, 2H, *Ar*), 6.71–6.75 (overlapping peaks, 2H, *Ar*), 6.51 (m, 1H, *Ar*), 6.07 (s, 2H, *Pyr*), 2.14 (s, 6H), 2.05–2.06 (overlapping peaks, 12H), 2.02 (s, 6H), 1.62 (s, 3H), 1.42 (s, 3H); ^{13}C NMR (125 MHz, C_6D_6) δ 292.6 (Mo=*C*), 158.4, 153.4, 148.9, 136.7, 135.6, 134.6, 131.8, 131.2, 130.0, 129.7, 129.3, 128.5, 128.4, 127.4, 126.8, 126.6, 126.2, 122.7, 109.2, 109.0, 54.6, 32.4, 32.3, 29.8, 29.7, 21.9, 21.3, 21.1, 20.3, 17.1. Anal. Calcd for $C_{46}H_{49}ClMoN_2O$: C, 71.08; H, 6.35; N, 3.60. Found: C, 71.04; H, 6.44; N, 3.44.

Mo(NAr^{CF3})(CHCMe$_3$)(2,5-Me$_2$Pyr)(OHMT) (21). The synthesis was essentially the same as for **20** employing **12** (0.101 g, 0.197 mmol) and HMTOH (0.065 g, 0.197 mmol) yielding an orange solid (0.113 g, 76%): ^{1}H NMR (400 MHz, C_6D_6) δ 11.2 (s, 1H, MoC*H*CMe$_3$, J_{CH} = 120.8 Hz), 7.22 (s, 2H, HMTO), 7.18 (d, 1H, Ar), 7.10-6.96 (m, 3H, HMTO + Ar), 6.92-6.86 (overlapping peaks, 3H, HMTO), 6.69 (d, 1H, Ar), 6.66 (t, 1H, Ar), 6.10 (s, 2H, C*H*Pyr), 2.27-2.23 (overlapping peaks, 12H, *Me*), 2.17-2.10 (overlapping peaks, 12H, *Me*), 1.14 (s, 9H, Ar$^{t\text{Bu}}$); ^{13}C NMR (100 MHz, C_6D_6) δ 292.6 (Mo=*C*), 159.1, 137.2, 136.8, 136.6, 136.5, 135.5, 132.0, 131.4, 130.5, 130.3, 129.2, 128.5, 126.3, 122.5, 108.9, 106.5, 48.7, 31.7, 21.4, 21.3, 20.5; ^{19}F NMR (376 MHz, C_6D_6) δ – 60.4. Anal. Calcd for $C_{42}H_{47}F_3MoN_2O$: C, 67.37; H, 6.33; N, 3.74. Found: C, 66.97; H, 6.01; N, 3.59.

Mo(NAr^{CF3})(CHCMe$_2$Ph)(2,5-Me$_2$Pyr)(OHMT) (22). The synthesis was essentially the same as for **20** employing Mo(NAr^{CF3})(CHCMe$_2$Ph)(2,5-Me$_2$Pyr)$_2$ (0.209 g, 0.363 mmol) and HMTOH (0.120 g, 0.363 mmol) to yield a red solid (0.220 g, 75%): ^{1}H NMR (400 MHz, C_6D_6) δ 11.2 (s, 1H, MoC*H*CMe$_2$Ph, J_{CH} = 122.5 Hz), 7.24 (d, 2H, HMTO), 7.13-7.03 (overlapping,

3H, HMTO + Ar), 7.01-6.87 (overlapping, 5H, HMTO + Ar), 6.82 (s, 2H, HMTO), 6.76 (s, 2H, HMTO), 6.65 (d, 1H, Ar), 6.60 (t, 1H, Ar), 6.03 (s, 2H, C*H*Pyr), 2.16 (s, 6H, HMTO *Me*), 2.05 (s, 6H, HMTO *Me*), 2.03, (s br, 6H, Pyr *Me*), 1.99 (s, 6H, HMTO *Me*), 1.60 (s, 3H, MoCHC*Me*$_2$Ph), 1.40 (s, 3H, MoCHC*Me*$_2$Ph); ^{13}C NMR (100 MHz, C_6D_6) δ 291.2 (Mo=*C*), 158.5, 148.7, 136.8, 136.7, 136.5, 135.5, 131.8, 131.7, 130.7, 130.2, 129.2, 128.5, 128.4, 126.6, 126.4, 126.3, 122.6, 108.9, 55.1, 32.4, 29.6, 21.3, 21.1, 20.3; ^{19}F NMR (376 MHz, C_6D_6) δ – 60.2. Anal. Calcd for $C_{47}H_{49}F_3MoN_2O$: C, 69.62; H, 6.09; N, 3.45. Found: C, 69.72; H, 6.12; N, 3.50.

Mo(NAr^{iPr})(CHCMe$_2$Ph)(2,5-Me$_2$Pyr)(OHMT) (23). The synthesis was essentially the same as for **20** employing **13** (0.100 g, 0.182 mmol) and HMTOH (0.060 g, 0.182 mmol); yielding orange solid (0.068 g, 48%): ^{1}H NMR (500 MHz, C_6D_6) δ 11.32 (s, 1H, *syn* Mo=C*H*, J_{CH} = 122.5 Hz), 7.29 (d, 2H, J = 7.5 Hz, *Ar*), 7.13 (t, 2H, J = 7.5 Hz, *Ar*), 6.91–7.02 (overlapping peaks, 7H, *Ar*), 6.84–6.87 (overlapping peaks, 3H, *Ar*), 6.80 (s, 2H, *Ar*), 6.02 (br s, 2H, *Pyr*), 3.22 (sept, 1H, J = 6.5 Hz, *^{i}Pr*), 2.30-1.74 (overlapping peaks, 30H, OHMT Me + Pyr Me), 1.65 (s, 3H), 1.45 (s, 3H), 1.01 (d, 3H, J = 7.0 Hz), 0.82 (d, 3H, J = 7.0 Hz); ^{13}C NMR (125 MHz, C_6D_6) δ 291.0 (Mo=*C*), 158.5, 154.9, 148.8, 147.4, 136.8, 136.6, 135.7, 131.7, 130.0, 129.3, 128.5, 126.6, 126.3, 125.8, 122.4, 109.0, 54.7, 32.7, 29.8, 27.7, 27.5, 23.9, 23.7, 22.8, 21.9, 21.4, 21.2, 20.3. Anal. Calcd for $C_{49}H_{56}MoN_2O$: C, 74.98; H, 7.19; N, 3.57. Found: C, 74.80; H, 6.81; N, 3.54.

Mo(NAr^{tBu})(CHCMe$_3$)(2,5-Me$_2$Pyr)(OHMT) (24). The synthesis was essentially the same as for **20** employing **14** (0.161 g, 0.321 mmol) and HMTOH (0.106 g, 0.321 mmol); yielding orange solid (0.161 g, 68%): ^{1}H NMR (400 MHz, C_6D_6) δ 11.3 (s, 1H, *syn* Mo=C*H*, J_{CH} = 118.7 Hz), 7.07 (d, 1H, Ar), 7.03-6.85 (overlapping, 4H, HMTO + Ar), 6.82 (s, 4H, HMTO), 6.57 (d, 1H, Ar), 6.20-5.90 (d br, 2H, C*H*Pyr), 2.38 (s br, 3H, Pyr *Me*), 2.23 (s, 6H, HMTO *Me*), 2.21 (s, 6H, HMTO *Me*), 2.16 (s, 6H, HMTO *Me*), 1.89 (s br, 3H, Pyr *Me*), 1.12 (s, 9H, *Ar^{tBu}*), 1.08 (s, 9H, MoCHC*Me$_3$*); ^{13}C NMR (100 MHz, C_6D_6) δ 290.7 (Mo=*C*), 159.8, 156.4, 145.4, 136.8, 136.6, 136.4, 135.6, 134.3, 131.4, 130.4, 129.2, 128.7, 127.4, 126.6, 126.3, 122.1, 108.9 (br, *C*HPyr), 49.5, 35.7, 31.9, 30.7, 21.6, 21.4, 20.8. Anal. Calcd for $C_{45}H_{56}MoN_2O$: C, 73.35; H, 7.66; N, 3.80. Found: C, 73.47; H, 7.86; N, 3.57.

Mo(NAr^{tBu})(CHCMe$_2$Ph)(2,5-Me$_2$Pyr)(OHMT) (25). The synthesis was essentially the same as for **20** employing **15** (0.315 g, 0.559 mmol) and HMTOH (0.184 g, 0.557 mmol); yielding orange solid (0.300 g, 67%): ^{1}H NMR (400 MHz, C_6D_6) δ 11.3 (s, 1H, *syn* Mo=C*H*, J_{CH} = 120.2 Hz), 7.23 (d, 2H, Ph), 7.11 (t, 2H, Ph), 7.08 (d, 1H, Ar), 7.20-6.86 (overlapping, 5H,

HMTO + Ar), 6.83 (s, 2H, HMTO), 6.77 (s, 2H, HMTO), 6.66 (d, 1H, Ar), 6.20-5.80 (d br, 2H, C*H*Pyr), 2.36 (s br, 3H, Pyr *Me*), 2.19 (s, 6H, HMTO *Me*), 2.10 (s, 6H, HMTO *Me*), 2.03 (s, 6H, HMTO *Me*), 1.74 (s br, 3H, Pyr *Me*), 1.61 (s, 3H, MoCHC*Me*$_2$Ph), 1.47 (s, 3H, MoCHC*Me*$_2$Ph), 1.11 (s, 9, *Ar*^{tBu}); ^{13}C NMR (100 MHz, C_6D_6) δ 289.2 (Mo=*C*), 159.1, 156.3, 148.7, 145.4, 137.2, 136.8, 136.7, 136.5, 135.6, 134.3, 131.6, 130.4, 129.2, 128.6, 128.4, 126.6, 126.5, 126.4, 126.3, 122.5, 109.2 (br, *C*HPyr), 55.7, 35.7, 32.8, 30.8, 29.8 21.4, 21.2, 20.7. Anal. Calcd for $C_{50}H_{58}MoN_2O$: C, 75.17; H, 7.32; N, 3.51. Found: C, 74.80; H, 7.20; N, 3.45.

Mo(NAr^M)(CHCMe$_2$Ph)(2,5-Me$_2$Pyr)(OHMT) (26). Compound **16** (0.050 g, 0.080 mmol) and HMTOH (0.026 g, 0.080 mmol) were dissolved in toluene (0.70 ml) and the mixture was heated in a Teflon-sealed Schlenk flask to 110 °C for 18 h. Then, the reaction was cooled to RT and the solvent was removed *in vacuo*. The crude product was redissolved in minimal amount of pentane and store at -35 °C yielding crystalline red product (0.035 g, 51%): ^{1}H NMR (400 MHz, C_6D_6) δ 10.93 (s, 1H, MoC*H*CMe$_2$Ph), 7.40-6.40 (m, 18H, aromatics), 6.20-5.60 (s br, 2H, C*H*Pyr), 2.23-2.17 (overlapping peaks, 15H, Pyr*Me*$_2$ + Ar^M), 2.07-2.01 (overlapping peaks, 18H, *Mes*-HMTO), 1.80 (s, 3H, MoCH(CH$_3$)*CH$_3$*), 1.69 (s, 3H, MoCH(*CH$_3$*)CH$_3$); ^{13}C NMR (100 MHz, C_6D_6) δ 290.3 (Mo*C*HCMe$_2$Ph), 158.1, 155.5, 149.0, 136.9, 136.7, 136.7, 136.6, 136.5, 136.2, 135.7, 135.4, 134.8, 131.7, 131.3, 130.0, 129.5, 129.2, 128.8, 128.5, 128.4, 127.3, 126.6, 126.2, 53.9, 32.6, 29.7, 21.3, 21.1, 20.4, 20.1. Anal. Calcd for $C_{55}H_{60}MoN_2O$: C, 76.72; H, 7.02; N, 3.25. Found: C, 77.09; H, 7.27; N, 3.00.
Red crystals suitable for X-ray diffraction were obtained by dissolving the product in Et_2O, layering the ether solution with pentane, and storing the sample at -35 °C for several days.

Mo(NAr^M)(CHCMe$_2$Ph)(2,5-Me$_2$Pyr)(OHIPT) (27). The synthesis was similar to that of **26** employing **16** (0.061 g, 0.097 mmol) and HIPTOH (0.049 g, 0.098 mmol) and heating for 5 days. Purification required dissolution in TMS, storing at – 35 °C for a few days and filtering to remove unreacted HIPTOH. Upon removal of solvent from the filtrate clean **27** was collected as an orange powder (0.035 g, 35%): ^{1}H NMR (400 MHz, C_6D_6) *δ* 13.12 (s, 0.01H, MoC*H*), 12.18 (s, 1H, MoC*H*), 11.13 (s, 0.04H, MoC*H*), 10.14 (s, 0.07H, MoC*H*) 7.50-6.60 (m, 25H, aromatics), 6.50-6.10 (br s, 3.8H, *H*$_2$C$_4$Me$_2$N), 3.4-2.8 (m, 11.4H), 2.25-2.10 (various s, H$_2$C$_4$*Me*$_2$N + MoCHC*Me*$_2$Ph, 22.8H), 1.90-1.70 (various s, 11.2H *o-Mes*), 1.62-1.60 (various s, 5.7H, *p-Mes*); ^{13}C NMR (100 MHz, C_6D_6) δ 290.4 (Mo*C*HCMe$_2$Ph), 160.2, 155.3, 149.5, 148.2, 147.5, 147.3, 147.2, 147.1, 137.3, 137.0, 136.4, 135.6, 135.4, 134.6, 133.0, 131.6, 131.1, 130.6, 128.1, 127.9, 126.5, 121.8, 121.3, 121.0, 108.8, 106.5, 53.2, 34.4, 31.1, 31.0, 30.8, 30.6, 29.2, 26.2, 25.6, 24.6, 24.2, 24.0, 23.7, 23.4, 21.5, 21.1, 19.8 Anal. Calcd for $C_{67}H_{84}MoN_2O$: C, 78.18; H, 8.23; N, 2.72. Found: C, 78.28; H, 8.30; N, 2.40.

Mo(NAr^T)(CHCMe$_3$)(2,5-Me$_2$Pyr)(OHMT) (28). The synthesis was the same as that of **26** employing **17** (0.103 g, 0.016 mmol) and HMTOH (0.052 g, 0.016 mmol) yielding orange crystals (0.080 g, 57%): ^{1}H NMR (400 MHz, C_6D_6) δ 10.91 (s, 1H, MoC*H*), 10.85 (s, 0.17H, MoC*H*), 7.25-7.00 (overlapping peaks, 4.5H, Ar + HMTO), 7.00-6.81 (overlapping peaks, 7H, Ar + HMTO), 6.80 (s, 2H, HMTO), 6.70 (s, 2H, HMTO), 5.81 (s br, 2H, *H*$_2$C$_4$Me$_2$N), 2.83 (m, 2H, *CH*Me$_2$), 2.43 (m, 1H, *CH*Me$_2$), 2.11 (s, 6H, HMTO *Me*), 2.08 (s, 6H, HMTO *Me*), 2.06 (s, 6H, HMTO *Me*), 1.65 (s, 6H, H$_2$C$_4$*Me*$_2$N), 1.30 (d, 6H, CH*Me*$_2$), 1.29 (d, 6H, CH*Me*$_2$), 1.19 (d, 3H, CH*Me*$_2$), 1.17 (s, 9H, MoCHC*Me*$_3$), 1.15 (d, 3H, CH*Me*$_2$); ^{13}C NMR (100 MHz, C_6D_6) δ 288.2 (Mo*C*HCMe$_3$), 158.9, 155.9, 148.6, 146.7, 146.4, 137.2, 136.8, 136.5, 136.0, 135.9, 135.0, 134.2, 134.0, 132.0, 131.6, 131.4, 131.3, 130.0, 129.9, 129.4, 128.8, 127.1, 125.3, 122.2, 121.2, 121.0, 106.5, 48.4, 34.6, 31.8, 30.7, 30.5, 25.9, 25.7, 24.4, 24.3, 21.8, 21.4, 21.2, 21.1, 20.6, 20.5. Anal. Calcd for $C_{56}H_{70}MoN_2O$: C, 76.16; H, 7.99; N, 3.17. Found: C, 76.23; H, 7.99; N, 3.14. Red crystals suitable for X-ray diffraction were obtained by dissolving the product in pentane, and storing the sample at -35 °C for several days.

***In situ* preparation of (NAr^T)(CHCMe$_3$)(2,5-Me$_2$Pyr)(OHIPT) (29).** **17** (0.020 g, 0.031 mmol) and HIPTOH (0.015 g, 0.031 mmol) were dissolved in C_6D_6 (0.70 ml) and heated for 14 days at 80 °C: ^{1}H NMR (400 MHz, C_6D_6) δ 12.23 (s, 0.04H, MoC*H*), 11.80 (s, 1H, MoC*H*), 11.66 (s, 0.05H, MoC*H*), 9.85 (s, 0.5H, MoC*H*), 7.30-6.70 (m, 19.5H, aromatics), 6.50-6.10 (br s, 3H, *H*$_2$C$_4$Me$_2$N), 3.10-2.50 (m, 13.5H, C*H*Me$_2$), 1.50-1.20 (m, 94.5H, CH*Me*$_2$ terphenyl + imido + MoCHC*Me*$_3$).

General procedure for ROMP of DCMNBD MAP catalyst (3-10 mg) is dissolved in 0.50 ml of toluene while the monomer is dissolved in 0.70 ml of toluene and stirred in a separate vial. To the monomer vial the catalyst solution is added quickly and left stirring for 1 h until it forms a gel. The reaction is then quenched with 0.50 mL of benzaldehyde and some methylene chloride is added to solubilize the gel. This solution is stirred for another hour, at which point the solution is added to a 100 mL RBF containing 50-70 mL MeOH stirring vigorously. The polymer precipitates instantly and it is collected by filtration after 1 h of stirring. The dry polymer is examined by ^{1}H and ^{13}C NMR to determine the *tacticity* and *cis* content according to known literature reports.[5h]

X-ray Structure Determination Low-temperature diffraction data (φ-and ω-scans) were collected on a Siemens Platform three-circle diffractometer coupled to a Bruker-AXS Smart Apex CCD detector with graphite-monochromated Mo Kα radiation (λ = 0.71073 Å) for the

structure of compounds **2**, **3**, **16**, and **18** and on a Bruker-AXS X8 Kappa Duo diffractometer coupled to a Smart Apex2 CCD detector with Mo K_α radiation (λ = 0.71073 Å) from an $I\mu S$ micro-source for the structure of compounds **26**, and **28**. All structures were solved by direct methods using SHELXS[19] and refined against F^2 on all data by full-matrix least squares with SHELXL-97[20] using established refinement techniques.[21] All non-hydrogen atoms were refined anisotropically. All hydrogen atoms were included into the model at geometrically calculated positions and refined using a riding model unless otherwise noted. The isotropic displacement parameters of all hydrogen atoms were fixed to 1.2 times the U value of the atoms they are linked to (1.5 times for methyl groups). All disordered atoms were refined with the help of similarity restraints on the 1,2- and 1,3-distances and displacement parameters as well as rigid bond restraints for anisotropic displacement parameters.

Compound **2** crystallizes in the triclinic space group $P\bar{1}$ with one molecule in the asymmetric unit along with two molecules of THF. The THF molecules and imido ligands were refined with the help of similarity restraints on the 1,2- and 1,3-distances. Mild similar anisotropic displacement parameter as well as rigid bond restraints were applied to all atoms.

Compound **3** crystallizes in the monoclinic space group $C2/c$ with half a molecule in the asymmetric unit. The molybdenum atom is located on the crystallographic two-fold axis.

Compound **7** crystallizes in the monoclinic space group $P2_1/c$ with one molecule in the asymmetric unit. Coordinates for the methyl hydrogen atoms on C(1) and C(2) were taken from the difference Fourier synthesis. The hydrogen atoms in question were subsequently refined semi-freely with the help of distance restraints on C-H and H...H distances while constraining the U_{iso} values of the hydrogen atoms to 1.5 times the value of U_{eq} of the corresponding carbon atoms.

Compound **16** crystallizes in the monoclinic space group $P2_1/n$ with one molecule in the asymmetric unit. Coordinates for the hydrogen atom on C1 were taken from the difference Fourier synthesis and refined semi-freely with the help of a distance restraint while constraining the U_{iso} value of the hydrogen atom to 1.2 times the U_{eq} value of C1.

Compound **18** crystallizes in the monoclinic space group $P2_1/n$ with one molecule in the asymmetric unit along with one molecule of diethylether. Coordinates for the hydrogen atom on C1 were taken from the difference Fourier synthesis and refined semi-freely with the help of a distance restraint while constraining the U_{iso} value of the hydrogen atom to 1.2 times the U_{eq} value of C1. The diethylether was refined with the help of similarity restraints on the 1,2- and 1,3-distances and displacement parameters as well as rigid bond restraints for anisotropic displacement parameters.

Compound **26** crystallizes in the monoclinic space group $P2_1/n$ with one molecule in the asymmetric unit along with half a molecule of hexane. Coordinates for the hydrogen atom on C1

were taken from the difference Fourier synthesis and refined semi-freely with the help of a distance restraint while constraining the U_{iso} value of the hydrogen atom to 1.2 times the U_{eq} value of C1. The hexane molecule was found to be located near a crystallographic inversion center and is disordered accordingly.

Compound **28** crystallizes in the orthorhombic space group *Pbca* with one molecule in the asymmetric unit. Coordinates for the hydrogen atom on C1 were taken from the difference Fourier synthesis and refined semi-freely with the help of a distance restraint while constraining the U_{iso} value of the hydrogen atom to 1.2 times the U_{eq} value of C1.

Crystal information can be found in Tables 3 to 9 below.

Table 3. Crystal data and structure refinement for **2**.

Identification code	09217	
Empirical formula	C46 H62 Cl2 Mo N2 O4	
Formula weight	873.82	
Temperature	100(2) K	
Wavelength	0.71073 Å	
Crystal system	Triclinic	
Space group	$P\bar{1}$	
Unit cell dimensions	a = 12.8333(12) Å	α= 113.617(3)°
	b = 13.8685(14) Å	β= 107.683(3)°
	c = 14.858(2) Å	γ = 100.305(2)°
Volume	2167.3(5) $Å^3$	
Z	2	
Density (calculated)	1.339 Mg/m^3	
Absorption coefficient	0.470 mm^{-1}	
F(000)	920	
Crystal size	0.35 x 0.30 x 0.18 mm^3	
Theta range for data collection	1.65 to 30.55°	
Index ranges	-18<=h<=18, -13<=k<=19, -19<=l<=19	
Reflections collected	11907	
Independent reflections	8854 [R(int) = 0.0280]	
Completeness to theta = 30.55°	66.5 %	
Absorption correction	Semi-empirical from equivalents	
Max. and min. transmission	0.9202 and 0.8528	
Refinement method	Full-matrix least-squares on F^2	
Data / restraints / parameters	8854 / 638 / 502	
Goodness-of-fit on F^2	1.037	
Final R indices [I>2sigma(I)]	R1 = 0.0427, wR2 = 0.1067	
R indices (all data)	R1 = 0.0511, wR2 = 0.1140	
Largest diff. peak and hole	1.104 and -0.745 $e.Å^{-3}$	

Table 4. Crystal data and structure refinement for **3**.

Identification code	09419	
Empirical formula	C46 H64 Cl2 Mo N2 O2	
Formula weight	843.83	
Temperature	100(2) K	
Wavelength	0.71073 Å	
Crystal system	Monoclinic	
Space group	C2/c	
Unit cell dimensions	a = 26.538(3) Å	α= 90°
	b = 8.9534(10) Å	β= 111.058(2)°
	c = 20.104(2) Å	γ = 90°
Volume	4457.7(9) $Å^3$	
Z	4	
Density (calculated)	1.257 Mg/m^3	
Absorption coefficient	0.451 mm^{-1}	
F(000)	1784	
Crystal size	0.32 x 0.26 x 0.12 mm^3	
Theta range for data collection	1.64 to 29.57°	
Index ranges	-36<=h<=36, -12<=k<=12, -27<=l<=27	
Reflections collected	52820	
Independent reflections	6202 [R(int) = 0.0409]	
Completeness to theta = 29.57°	99.1 %	
Absorption correction	Semi-empirical from equivalents	
Max. and min. transmission	0.9478 and 0.8690	
Refinement method	Full-matrix least-squares on F^2	
Data / restraints / parameters	6202 / 0 / 247	
Goodness-of-fit on F^2	1.065	
Final R indices [I>2sigma(I)]	R1 = 0.0296, wR2 = 0.0748	
R indices (all data)	R1 = 0.0341, wR2 = 0.0780	
Largest diff. peak and hole	0.677 and -0.351 $e.Å^{-3}$	

Table 5. Crystal data and structure refinement for **7**.

Identification code	d09095	
Empirical formula	C44 H60 Mo N2	
Formula weight	712.88	
Temperature	100(2) K	
Wavelength	1.54178 Å	
Crystal system	Monoclinic	
Space group	$P2_1/c$	
Unit cell dimensions	a = 12.8086(3) Å	α= 90°
	b = 17.0410(3) Å	β= 98.5650(10)°
	c = 19.1969(4) Å	γ = 90°
Volume	4143.40(15) $Å^3$	
Z	4	
Density (calculated)	1.143 Mg/m^3	
Absorption coefficient	2.794 mm^{-1}	
F(000)	1520	
Crystal size	0.15 x 0.09 x 0.05 mm^3	
Theta range for data collection	3.49 to 68.24°	
Index ranges	-15<=h<=15, -20<=k<=20, -18<=l<=22	
Reflections collected	78263	
Independent reflections	7540 [R(int) = 0.0552]	
Completeness to theta = 68.24°	99.4 %	
Absorption correction	Semi-empirical from equivalents	
Max. and min. transmission	0.8729 and 0.6793	
Refinement method	Full-matrix least-squares on F^2	
Data / restraints / parameters	7540 / 21 / 454	
Goodness-of-fit on F^2	1.034	
Final R indices [I>2sigma(I)]	R1 = 0.0303, wR2 = 0.0733	
R indices (all data)	R1 = 0.0384, wR2 = 0.0775	
Largest diff. peak and hole	0.563 and -0.456 $e.Å^{-3}$	

Table 6. Crystal data and structure refinement for **16**.

Identification code	09274	
Empirical formula	C37 H43 Mo N3	
Formula weight	625.68	
Temperature	100(2) K	
Wavelength	0.71073 Å	
Crystal system	Monoclinic	
Space group	$P2_1/n$	
Unit cell dimensions	a = 13.524(2) Å	α= 90°
	b = 15.067(3) Å	β= 92.594(3)°
	c = 15.784(3) Å	γ = 90°
Volume	3213.1(10) $Å^3$	
Z	4	
Density (calculated)	1.293 Mg/m^3	
Absorption coefficient	0.437 mm^{-1}	
F(000)	1312	
Crystal size	0.25 x 0.20 x 0.10 mm^3	
Theta range for data collection	1.87 to 29.57°	
Index ranges	-18<=h<=18, 0<=k<=20, 0<=l<=21	
Reflections collected	8997	
Independent reflections	8997 [R(int) = 0.1168]	
Completeness to theta = 29.57°	100.0 %	
Absorption correction	Semi-empirical from equivalents	
Max. and min. transmission	0.9576 and 0.8986	
Refinement method	Full-matrix least-squares on F^2	
Data / restraints / parameters	8997 / 1 / 382	
Goodness-of-fit on F^2	1.096	
Final R indices [I>2sigma(I)]	R1 = 0.0385, wR2 = 0.0856	
R indices (all data)	R1 = 0.0545, wR2 = 0.0910	
Largest diff. peak and hole	1.220 and -0.511 $e.Å^{-3}$	

Table 7. Crystal data and structure refinement for **18**.

Identification code	09409	
Empirical formula	C89 H79 Mo N O3	
Formula weight	1306.47	
Temperature	100(2) K	
Wavelength	0.71073 Å	
Crystal system	Monoclinic	
Space group	$P2_1/n$	
Unit cell dimensions	a = 16.9320(16) Å	α= 90°
	b = 21.5492(19) Å	β= 103.902(2)°
	c = 19.4983(18) Å	γ = 90°
Volume	6906.0(11) $Å^3$	
Z	4	
Density (calculated)	1.257 Mg/m^3	
Absorption coefficient	0.243 mm^{-1}	
F(000)	2744	
Crystal size	0.25 x 0.15 x 0.10 mm^3	
Theta range for data collection	1.43 to 29.57°.	
Index ranges	-23<=h<=23, -29<=k<=29, -27<=l<=26	
Reflections collected	139120	
Independent reflections	19378 [R(int) = 0.1126]	
Completeness to theta = 29.57°	100.0 %	
Absorption correction	Semi-empirical from equivalents	
Max. and min. transmission	0.9761 and 0.9418	
Refinement method	Full-matrix least-squares on F^2	
Data / restraints / parameters	19378 / 33 / 855	
Goodness-of-fit on F^2	1.018	
Final R indices [I>2sigma(I)]	R1 = 0.0551, wR2 = 0.1145	
R indices (all data)	R1 = 0.0975, wR2 = 0.1354	
Largest diff. peak and hole	0.884 and -0.751 $e.Å^{-3}$	

Table 8. Crystal data and structure refinement for **26**.

Identification code	x10052	
Empirical formula	C57.50 H66 Mo N2 O	
Formula weight	897.06	
Temperature	100(2) K	
Wavelength	0.71073 Å	
Crystal system	Monoclinic	
Space group	$P2_1/n$	
Unit cell dimensions	a = 11.4726(7) Å	α= 90°
	b = 24.6541(15) Å	β= 99.7690(10)°
	c = 17.3141(10) Å	γ = 90°
Volume	4826.2(5) $Å^3$	
Z	4	
Density (calculated)	1.235 Mg/m^3	
Absorption coefficient	0.313 mm^{-1}	
F(000)	1900	
Crystal size	0.25 x 0.15 x 0.10 mm^3	
Theta range for data collection	1.45 to 31.30°	
Index ranges	-16<=h<=16, -36<=k<=35, -13<=l<=25	
Reflections collected	115720	
Independent reflections	15786 [R(int) = 0.0418]	
Completeness to theta = 31.30°	99.9 %	
Absorption correction	Semi-empirical from equivalents	
Max. and min. transmission	0.9694 and 0.9259	
Refinement method	Full-matrix least-squares on F^2	
Data / restraints / parameters	15786 / 41 / 593	
Goodness-of-fit on F^2	1.036	
Final R indices [I>2sigma(I)]	R1 = 0.0307, wR2 = 0.0734	
R indices (all data)	R1 = 0.0401, wR2 = 0.0782	
Largest diff. peak and hole	0.390 and -0.555 $e.Å^{-3}$	

Table 9. Crystal data and structure refinement for **28**.

Identification code	x11164	
Empirical formula	C56 H70 Mo N2 O	
Formula weight	883.08	
Temperature	100(2) K	
Wavelength	1.54178 Å	
Crystal system	Orthorhombic	
Space group	*Pbca*	
Unit cell dimensions	a = 9.9364(2) Å	α= 90°
	b = 20.6357(5) Å	β= 90°
	c = 47.6772(11) Å	γ = 90°
Volume	9775.9(4) $Å^3$	
Z	8	
Density (calculated)	1.200 Mg/m^3	
Absorption coefficient	2.482 mm^{-1}	
F(000)	3760	
Crystal size	0.05 x 0.02 x 0.02 mm^3	
Theta range for data collection	1.85 to 67.56°	
Index ranges	-11<=h<=11, -24<=k<=18, -51<=l<=56	
Reflections collected	67453	
Independent reflections	8813 [R(int) = 0.1004]	
Completeness to theta = 67.56°	99.9 %	
Absorption correction	Semi-empirical from equivalents	
Max. and min. transmission	0.9520 and 0.8859	
Refinement method	Full-matrix least-squares on F^2	
Data / restraints / parameters	8813 / 1 / 561	
Goodness-of-fit on F^2	1.012	
Final R indices [I>2sigma(I)]	R1 = 0.0403, wR2 = 0.0853	
R indices (all data)	R1 = 0.0701, wR2 = 0.0961	
Largest diff. peak and hole	0.542 and -0.437 $e.Å^{-3}$	

REFERENCES

(1) (a) Schrock, R. R. *Chem. Rev.* **2009**, *109*, 3211. (b) Schrock, R. R. *Chem. Rev.* **2002**, *102*, 145. (c) Schrock, R. R.; Hoveyda, A. H. *Angew. Chem. Int. Ed.* **2003**, *42*, 4592. (d) Schrock, R. R.; Czekelius, C. C. *Adv. Syn. Catal.* **2007**, *349*, 55.

(2) Schaverien, C. J.; Dewan, J. C.; Schrock, R. R. *J. Am. Chem. Soc.* **1986**, *108*, 2771.

(3) (a) Wengrovius, J. H.; Schrock, R. R.; Churchill, M. R.; Missert, J. R.; Youngs, W. J. *J. Am. Chem. Soc.* **1980**, *102*, 4515. (b) Schrock, R. R.; Rocklage, S. M.; Wengrovius, J. H.; Rupprecht, G.; Fellmann, J. *J. Molec. Catal.* **1980**, *8*, 73. (c) Wengrovius, J. H.; Schrock, R. R. *Organometallics* **1982**, *1*, 148.

(4) (a) Oskam, J. H.; Fox, H. H.; Yap, K. B.; McConville, D. H.; O'Dell, R.; Lichtenstein, B. J. Schrock, R. R. *J. Organomet. Chem.* **1993**, *459*, 185. (b) Fox, H. H.; Yap, K. B.; Robbins, J.; Cai, S.; Schrock, R. R. *Inorg. Chem.* **1992**, *31*, 2287. (c) Alexander, J. B.; Schrock, R. R.; Davis, W. M.; Hultzsch, K. C.; Hoveyda, A. H.; Houser, J. H. *Organometallics* **2000**, *19*, 3700. (d) Singh, R.; Czekelius, C.; Schrock, R. R.; Müller, P. Hoveyda, A. H. *Organometallics* **2007**, *26*, 2528.

(5) (a) Singh, R.; Schrock, R. R.; Müller, P.; Hoveyda, A. H. *J. Am. Chem. Soc.* **2007**, *129*, 12654. (b) Marinescu, S. C.; Schrock, R. R.; Li, B.; Hoveyda, A. H. *J. Am. Chem. Soc.* **2009**, *131*, 58. (c) Sattely, E. S.; Meek, S. J.; Malcolmson, S. J.; Schrock, R. R.; Hoveyda, A. H. *J. Am. Chem. Soc.* 2009, 131, 943. (d) Ibrahem, I; Yu, M.; Schrock, R. R.; Hoveyda, A. H. *J. Am. Chem. Soc.*, **2009**, *131*, 3844. (e) Jiang, A. J.; Simpson, J. H.; Müller, P.; Schrock, R. R. *J. Am. Chem. Soc.* **2009**, *131*, 7770. (f) Meek, S. J.; Malcolmson, S. J.; Li, B.; Schrock, R. R.; Hoveyda, A. H. *J. Am. Chem. Soc.* **2009**, *131*, 16407. (g) Jiang, A. J.; Zhao, Y.; Schrock, R. R.; Hoveyda, A. H. *J. Am. Chem. Soc.* **2009**, *131*, 16630. (h) Flook, M. M.; Jiang, A. J.; Schrock, R. R.; Müller, P.; Hoveyda, A. H. *J. Am. Chem. Soc.* **2009**, *131*, 7962. (i) Lee, Y.-J.; Schrock, R. R.; Hoveyda, A. H. *J. Am. Chem. Soc.* **2009**, *131*, 10652. (j) Marinescu, S. C.; Schrock, R. R.; Müller, P.; Hoveyda, A. H. *J. Am. Chem. Soc.* **2009**, *131*, 10840.

(6) (a) Malcolmson, S. J.; Meek, S. J.; Sattely, E. S.; Schrock, R. R.; Hoveyda, A. H. *Nature* **2008**, *456*, 933. (b) Meek, S. J.; O'Brien, R. V.; Llaveria, J.; Schrock, R. R.; Hoveyda, A. H. *Nature* **2011**, *471*, 461. (c) Yu, M.; Wang, C.; Kyle, A. F.; Jakubec, P.; Dixon, D. J.; Schrock, R. R.; Hoveyda, A. H. *Nature* **2011**, *479*, 88.

(7) Solans-Monfort, X.; Copéret, C.; Eisenstein, O. *J. Am. Chem. Soc.* **2010**, *132*, 7750.

(8) Gerber, L. C.; Schrock, R. R.; Müller, P.; Takase, M. K. *J. Am. Chem. Soc.* **2011**, *133*, 18142.

(9) (a) Gavenonis, J.; Tilley, T. D. *Organometallics* **2002**, *21*, 5549. (b) Gavenonis, J.; Tilley, T. D. *Organometallics* **2004**, *23*, 31.

(10) Huang, X.; Anderson, K. W.; Zim, D.; Jiang, L.; Klapars, A.; Buchwald, S. L. *J. Am. Chem. Soc.* **2003**, *125*, 6653.

(11) Hartmann, N.; Niemeyer, M. *Synth. Comm.* **2001**, *31*, 3839.

(12) Schrock, R. R.; Murdzek, J. S.; Bazan, G. C.; Robbins, J.; DiMare, M.; O'Regan, M. *J. Am. Chem. Soc.* **1990**, *112*, 3875.

(13) Marinescu, S. C.; Singh, R.; Hock, A. S.; Wampler, K. M.; Schrock, R. R.; Müller, P. *Organometallics* **2008**, *27*, 6570.

(14) Marinescu, S. C.; Schrock, R. R.; Müller, P.; Takase, M. K.; Hoveyda, A. H. *Organometallics* **2011**, *30*, 1780.

(15) Schrock, R. R. *Dalton Trans.* **2011**, *40*, 7484.

(16) (a) Sinnokrot, M. O.; Valeev, E. F.; Sherrill, C. D. *J. Am. Chem. Soc.* **2002**, *124*, 10887. (b) Hunter, C. A.; Sanders, J. K. M. *J. Am. Chem. Soc.* **1990**, *112*, 5525.

(17) Ruppel, J. V.; Jones, J. E.; Huff, C. A.; Kamble, R. M.; Chen, Y.; Zhang, X. P. *Org. Lett.* **2008**, *10*, 1995.

(18) Smolinsky, G. *J. Am. Chem. Soc.* **1960**, *82*, 4717.

(19) Sheldrick, G. M. *Acta Cryst.* **1990**, *A46*, 467-473.

(20) Sheldrick, G. M. *Acta Cryst.* **2008**, *A64*, 112-122.

(21) Müller, P. *Crystallography Reviews* **2009**, *15*, 57-83.

(22) Tabor, D. C.; White, F. H.; Collier, L. W.; Evans, S. A. *J. Org. Chem.* **1983**, *48*, 1638.

(23) Stanciu, C.; Olmstead, M. M.; Phillips, A. D.; Stender, M.; Power, P. P. *Eur. J. Inorg. Chem.* **2003**, 3495.

(24) Saeed, I.; Katao, S.; Nomura, K. *Organometallics* **2009**, *28*, 111.

(25) Schrock, R. R.; Sancho, J.; Pederson, S. F. *Inorganic Syntheses*, **1989**, *26*, 44.

(26) Yates, P.; Hyre, J. E. *J. Org. Chem.* **1962**, *27*, 4101.

CHAPTER 4

Bipyridine Adducts of Molybdenum Alkylidene and Molybdenum Alkylidyne Complexes: Their Use for Preparation of New Active Catalyst Species

INTRODUCTION

High oxidation state molybdenum and tungsten imido alkylidene complexes[1] with the generic formula M(NR)(CHR')(X)(Y) (where X and Y are monoanionic ligands) were discovered approximately 25 years ago.[2] In the last several years new types of Mo and W imido alkylidene complexes that have the formula M(NR)(CHR')(OR")(Pyr), where Pyr is a pyrrolide or substituted pyrrolide ligand and OR" usually is an aryloxide, have been prepared and explored; we refer to these monoaryloxide monopyrrolide complexes as MAP.[1a, 3] Preparation of such compounds was the result of the development of bispyrrolide complexes of the general formula M(NR)(CHR')$(Pyr)_2$,[4a-b] which serve as efficient catalyst precursors due to easy protonolysis and displacement of the pyrrolide ligand by alcohols and phenols. In addition, both unsubstituted and substituted pyrrole (byproduct of protonolysis) were shown to remain as innocent spectator molecules in the presence of active olefin metathesis catalysts. This inertness rendered bispyrrolide complexes most useful during screening of catalyst activity for various bisalkoxide and MAP species because they can be generated trivially *in situ* and used without purification.[3c-e, 3g, 3j]

A large variety of bispyrrolide complexes have been made in the past (where Pyr = pyrrolide;[4a] 2,5-Me_2-pyrrolide;[4b] 2,3,4,5-Me_4-pyrrolide; 2,5-*i*-Pr_2-pyrrolide; 2,5-Ph_2pyrrolide;[4c] 2-Mes-pyrrolide[4d]) and it has been shown that they can be protonated; however, when the alcohol or phenol, used for protonolysis, is bulky then only the smallest (pyrrolide and 2,5-Me_2-pyrrolide) can be easily protonated and substituted. As a result, the majority of MAP species that have been made contain the smallest pyrrolides from the aforementioned list, with mostly 2,5-Me_2-pyrrolide MAP's being made to date (see Chapter 3, Section 3.2.2 for a representive sample).[3] The low number of MAP compounds containing unsubstituted pyrrolide is due to the poor crystallinity and fast decomposition of Mo(NR)(CHR')$(pyrrolide)_2$ species. Two notable exceptions are the compounds where R = 2,6-*i*-$Pr_2C_6H_3$ and adamantyl, which are stable for many days at -35 °C.[4a] The latter has been used to synthesize Mo(NAd)$(CHCMe_2Ph)(NC_4H_4)$(OAr) catalysts, where Ar is a large hexa-substituted terphenyl, that are *Z*-selective in general.[3i, 5]

In this report we investigate the role of bipyridine as a base-adduct stabilizer for the synthesis of bispyrrolide complexes containing seven different imido groups and their use as catalyst precursors for the preparation of new Mo(NR)$(CHCMe_2Ph)(NC_4H_4)$(OAr) species, which reactivity is briefly studied. In addition, the preparation of Mo(NR)$(\equiv CCMe_2R')(Me_2Pyr)$(bipy) species from Mo(NR)$(CHCMe_2R')(Me_2Pyr)_2$ is presented, along with preliminary reactions.

RESULTS AND DISCUSSION

4.1 Preparation of bispyrrolide complexes

4.1.1 Attempts at preparing molybdenum alkylidene imido bispyrrolide complexes

As stated in the introduction, a small number of bispyrrolide complexes, $Mo(NR)(CHCMe_2Ph)(Pyr)_2$ (R = 2,6-*i*-$Pr_2C_6H_3$ (Ar), 2,6-Br_2-4-MeC_6H_2, or 1-adamantyl (Ad); Pyr = NC_4H_4) have been made and isolated successfully in the past[4a] (*hereafter, Pyr = pyrrolide and Me_2Pyr = 2,5-Me_2-pyrrolide*). Attempts to prepare analogous species containing other imido groups generally yielded non-crystalline samples that tended to decompose easily. For instance, when $Mo(NAr^{Ph})(CHCMe_3)(OTf)_2DME$ (Ar^{Ph} = 2-phenylC_6H_4) was treated with 2 equivalents of lithium pyrrolide, in Et_2O, $Mo(NAr^{Ph})(CHCMe_3)(Pyr)_2$, **1**, is obtained in low yield (10%) upon work-up and purification. On the other hand, when $Mo(NAr^{M})(CHCMe_2Ph)(OTf)_2DME$ (Ar^{M} = 2-mesitylC_6H_4) is treated with 2 equivalents of lithium pyrrolide no crystalline compound is obtained and decomposition is observed both in solution and upon solvent removal.

The ^1H NMR spectrum (in CD_2Cl_2) of compound **1** contains only broad resonances at RT, but upon cooling the solution down to – 30 °C the broad alkylidene peak decoalesces into two separate peaks. The same is observed with the *tert*-butyl resonance, while the pyrrolide resonance splits into various peaks (Figure 1). This behavior has also been observed for $Mo(NAr)(CHCMe_2Ph)(Pyr)_2$ in the past and it was shown that the complex exists as a unsymmetrical dimer in the solid state;[4a] therefore, complex **1** is suggested to also exist in solution as an equilibrium mixture of the monomeric and unsymmetrical dimer (Scheme 1).

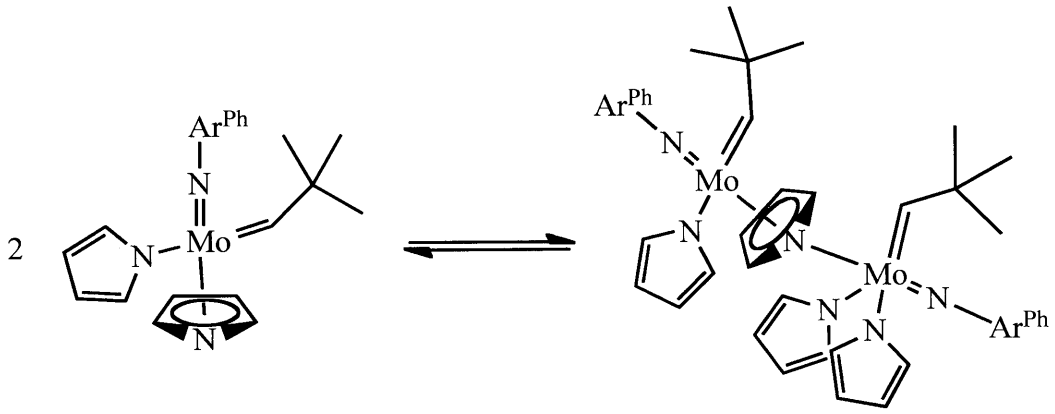

Scheme 1 – Solution equilibrium of **1** showing formation of an asymmetrical dimer.

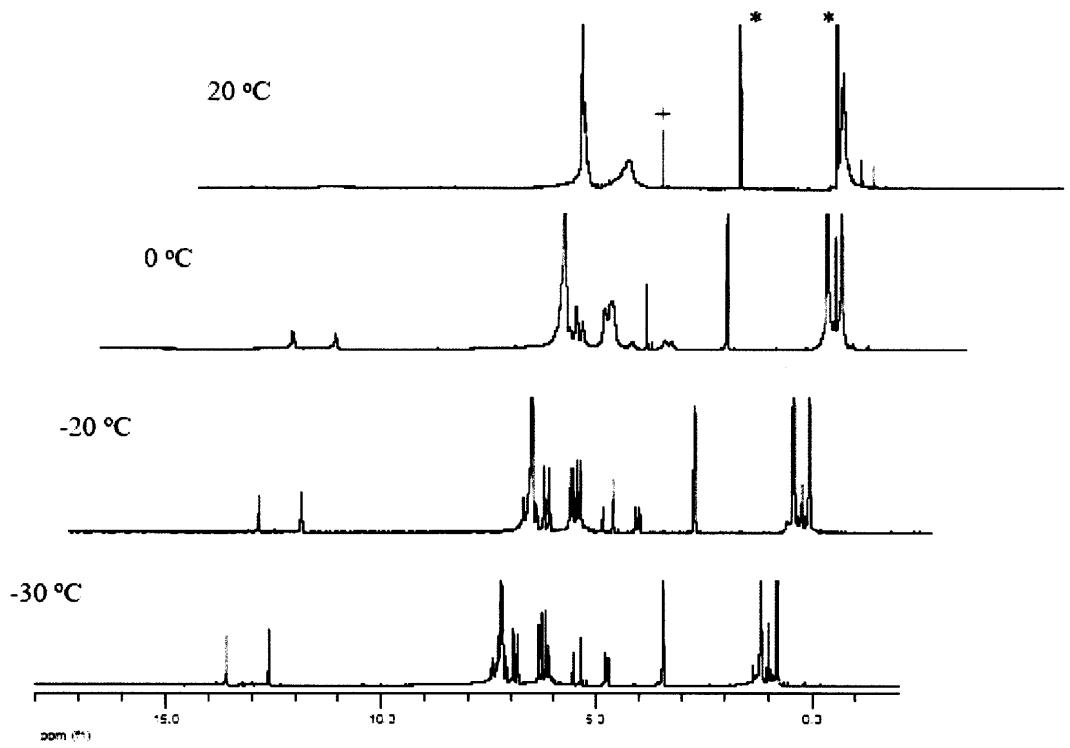

Figure 1 – VT ^{1}H NMR of **1** in CD_2Cl_2 from 20 °C (top) to – 30 °C (bottom). $^+CH_2Cl_2$; $^*Et_2O$.

Overall, formation of the asymmetrical dimer shows that when the pyrrolide has no substituents bimolecular decomposition can take place more readily, which explains the low stability of this type of complex. In the case of **1**, the low yield and the possibility of C-H activation of the *ortho*-phenyl group render the complex useless for subsequent studies. When the more robust *ortho*-mesityl group is used instead, no isolable bispyrrolide species can be obtained, but because it is substantially more stable than *ortho*-phenyl it will be discussed and studied in Sections 4.1.3-4.1.4. Since $Mo(NR)(CHCMe_2Ph)(Pyr)_2$ (R = Ar and Ad) can be obtained in good yield, they are used for subsequent studies mentioned in the next sections.

4.1.2 Preparation of stable bispyrrolide complexes containing bipy as a base adduct.

Recently, Fürstner reported the preparation of molybdenum alkylidene bisalkoxide catalysts containing bipyridine as a base-adduct and their enhanced air stability.[6] These complexes are shown in Figure 2. All were prepared by treatment of the corresponding bisalkoxides with one

equivalent of 2,2'-bipyridine (bipy). The most striking feature of these complexes is that they are stable in the solid state for weeks in the presence of air and that in solution they can liberate the active metathesis complex upon treatment with $ZnCl_2$ at high temperatures.

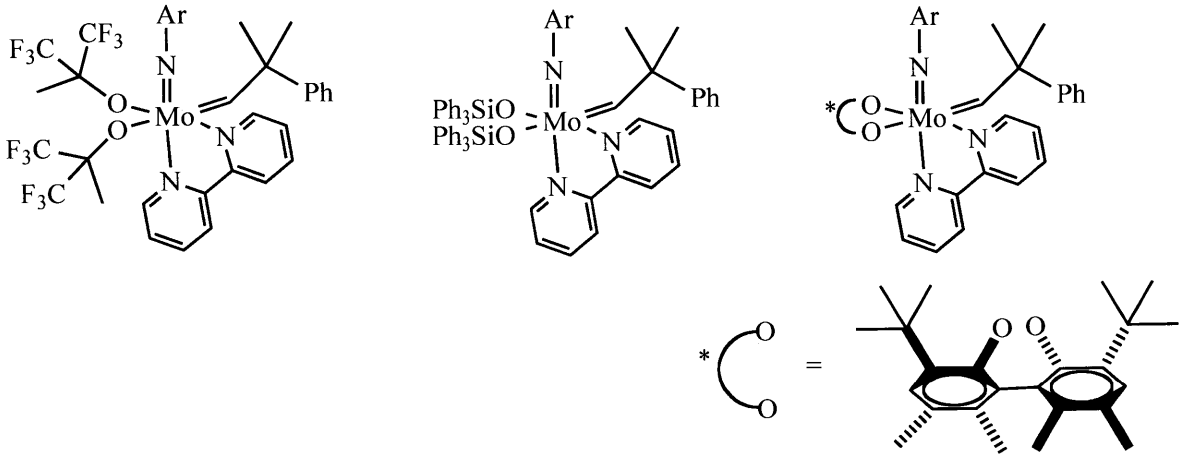

Figure 2 – Fürstner's molybdenum alkylidene bisalkoxide bipyridine adduct complexes.

Since $Mo(NR)(CHCMe_2Ph)(Pyr)_2$ complexes have small ligands, it was reasoned that bispyrrolide bipy adducts might be prepared, which would not only avoid formation of an asymmetric dimer in the solid state, but also improve the stability of the complexes overall. Thus, when $Mo(NR)(CHCMe_2Ph)(Pyr)_2$ was treated with one equivalent of bipy in Et_2O a precipitate resulted, which upon filtration gave complexes of general formula $Mo(NR)(CHCMe_2Ph)(Pyr)_2(bipy)$ (R = Ar, **9**; R = Ad, **10**) in good yields, equation 1. In the remainder of the chapter, this procedure will be referred as method A.

Compound **10** is not very soluble in common NMR solvents and as a result no ^{13}C NMR could be obtained; however, enough dissolves to obtain a proton NMR spectrum. This lack of solubility is a feature that is common for many of the bipy complexes to be presented in the next remaining sections of the chapter. The most striking feature in the ^1H NMR of **10** is the presence of three alkylidene peaks; which could arise from *cis* and *trans* isomerism of the pyrrolide ligands and possible *syn* (alkylidene pointing towards the imido group) to *anti* (alkylidene pointing away from the imido group) isomerism of one of the former geometric isomers.

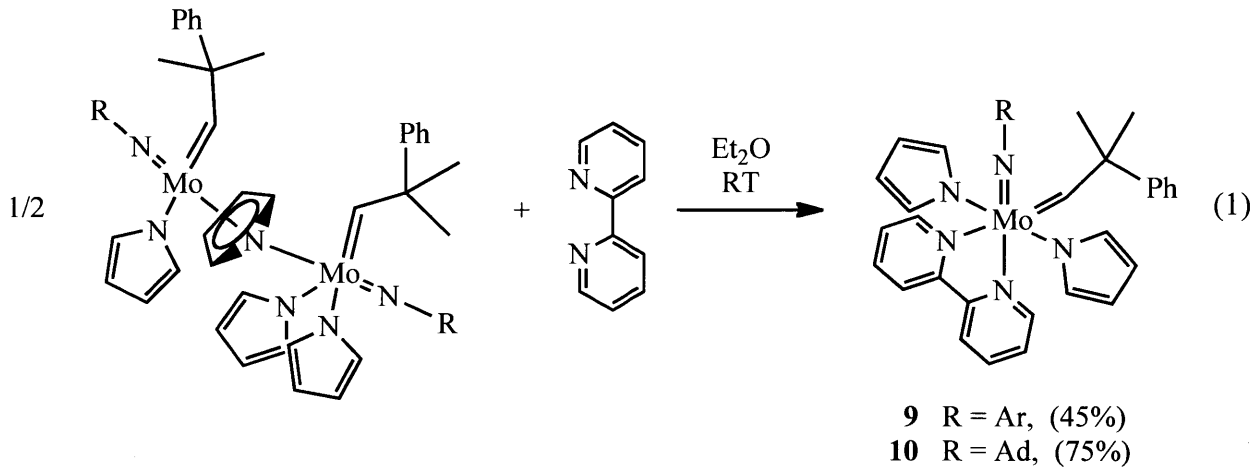

9 R = Ar, (45%)
10 R = Ad, (75%)

Unlike **10**, compound **9** dissolves more readily and both ^{1}H and ^{13}C NMR spectra can be obtained in CD_2Cl_2. There is only one alkylidene peak present in its ^{1}H NMR, implying that there is only one isomer in solution. In order to investigate the nature of the isomer, crystals of **9** were grown from CH_2Cl_2 at – 35 °C and analyzed by X-ray crystallography; the solved structure is shown in Figure 3 (provided generously by the Hoveyda Lab at Boston College). The complex has a pseudo octahedral structure with the pyrrolide ligands located *trans* to each other and bipyridine located *trans* to the imido and alkylidene groups. The *trans* influence of the pyrrolide ligands gives slightly longer Mo-N_{Pyr} bonds than those found in analogous compounds (2.135(3)° and 2.143(2)° in **9** vs. 2.082(4)°, 2.097(4)°, and 2.060(4)° in $[Mo(NAr)(CHCMe_2Ph)(Pyr)_2]_2$[4a] or 2.1134(17)° in $Mo(NAr^{M})(CHCMe_2Ph)(Me_2Pyr)$. Interestingly, Fürstner's $Mo(NAr)(CHCMe_2Ph)(OC(CF_3)_2CH_3)_2(bipy)$ compound adopts the *cis* configuration and bipyridine does not bind *trans* to the imido ligand. As a result, the Mo(1)-N(1) bond length in **9** (2.330(3)Å) is similar to the corresponding bond in Fürstner's compound (2.3503(11)Å) because they are both *trans* to the alkylidene group; however, the Mo(1)-N(2) bond length in **9** (2.354(3)Å), which is *trans* to the imido ligand, is substantially longer than in Fürstner's compound (2.2462(10)Å), which is *trans* to the alkoxide ligand. The Mo(1)-N(3)-C(21) and Mo(1)-C(11)-C(12) bond angles are similar to those observed in other bispyrrolide complexes[4a-b, 13b] and the N(4)-Mo(1)-N(5) bond angle is slightly bent (155.75(10)°), facing away from the imido group.

The stability of both **9** and **10** towards air is dramatically enhanced compared to their non-bipy adduct counterparts; however, preparation of similar complexes that contain other imido groups is the major drawback because it is required that $Mo(NR)(CHCMe_2Ph)(Pyr)_2$ be isolated

first. In Sections 4.1.3 and 4.1.4 different methods to circumvent this synthetic problem and a new variety of complexes will be presented.

4.1.3 Bispyrrolide bipyridine adduct complexes: preparation from bistriflate bipyridine adducts: Method B.

Attempts to prepare $Mo(NR)(CHCMe_2Ph)(OTf)_2(bipy)$ directly from $Mo(NR)_2(CH_2CMe_2Ph)_2$, by reacting the dialkyl species with acids in the presence of bipy, were not successful. Instead, the preparation of $Mo(NR)(CHCMe_2Ph)(OTf)_2(bipy)$ complexes from the $Mo(NR)(CHCMe_2Ph)(OTf)_2(dimethoxyethane)$ starting materials can be achieved simply by suspending the latter with one equivalent of bipyridine in benzene at RT (R = 2,6-$iPr_2C_6H_3$ (Ar), 1-adamantyl (Ad), 2,6-$Me_2C_6H_3$ (Ar'), and 2-$MesC_6H_4$ (Ar^M)), or in Et_2O at – 35 °C (R = 2-ClC_6H_4 (Ar^{Cl}), 2-*i*-PrC_6H_4 (Ar^{iPr}), 2-*t*-BuC_6H_4 (Ar^{tBu})) and stirring the mixture for 12 h at RT. In

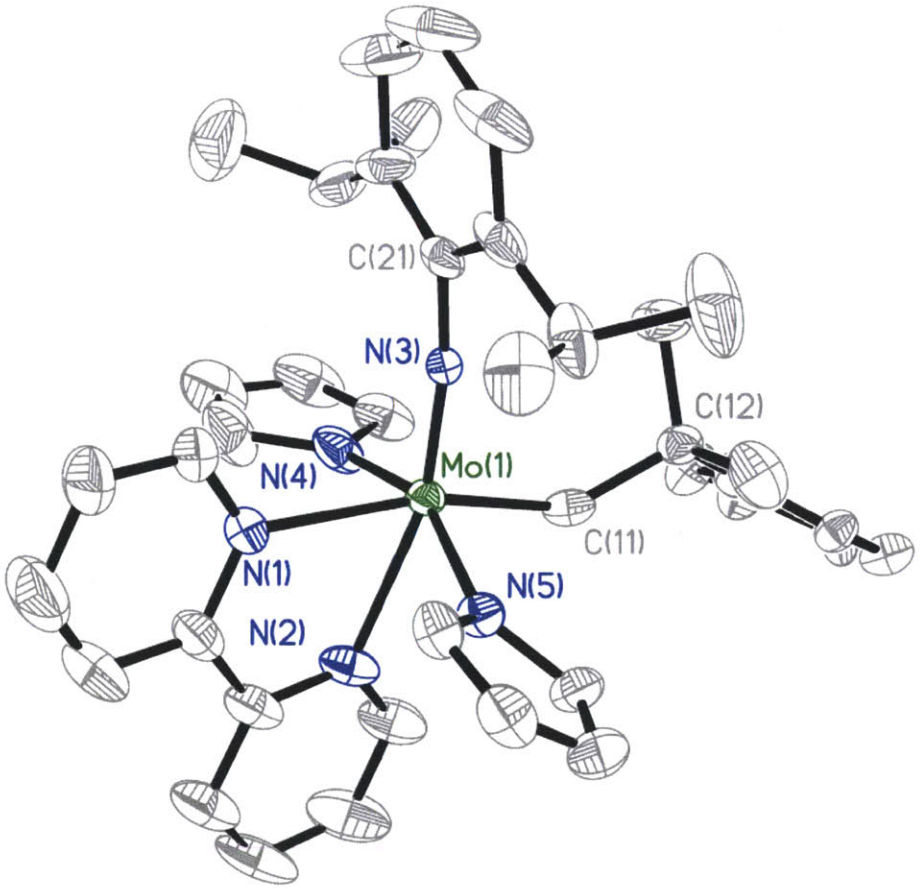

Figure 3 – Solid state structure of **9** (50% probability ellipsoids). Selected bond lengths (Å) and angles (°): Mo(1)-C(11) = 1.932(3), Mo(1)-N(1) = 2.330(3), Mo(1)-N(2) = 2.354(3), Mo(1)-N(3) = 1.730(2), Mo(1)-N(4) = 2.135(3), Mo(1)-N(5) = 2.143(2), C(12)-C(11)-Mo(1) = 138.3(2), C(21)-N(3)-Mo(1) = 171.0 (2), N(5)-Mo(1)-N(4) = 155.75(10).

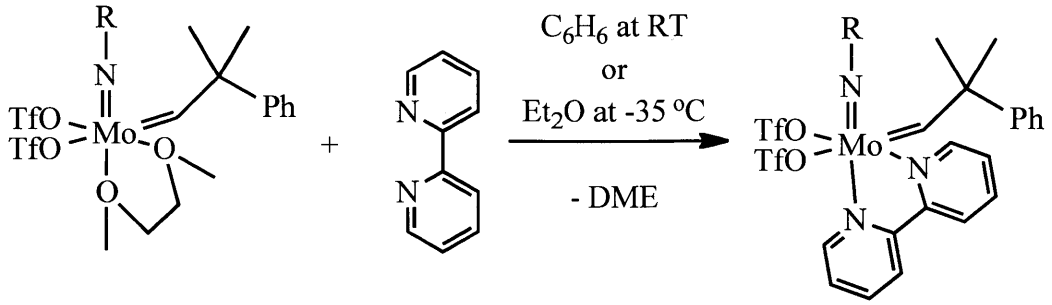

(2)

2 R = Ar, (84 %)
3 R = Ad, (91 %)
4 R = Ar', (67 %)
5 R = Ar^{Cl}, (66 %)
6 R = Ar^{iPr}, (76 %)
7 R = Ar^{tBu}, (76 %)
8 R = Ar^{M}, (73 %)

all cases, solid product precipitates out that can be collected by vacuum filtration in good yields (equation 2). In the case of complexes **5**, **6** and **7** the bistriflate solutions must be cooled down first to avoid major decomposition; also Et_2O helps remove the decomposed impurities better than other solvents. It is worth noting that decomposition is only a problem when the metal is bound to a relative small and unhindered aryl imido; whereas with larger, bulkier aryl imidos or alkyl imidos there is no need to take these precautions.

All complexes are very soluble in CH_2Cl_2 with the exception of **2** and **3**, which are only sparingly soluble and for which ^{13}C NMR could not be obtained. ^1H NMR of the complexes shows the presence of either 1 or 2 alkylidene peaks in CD_2Cl_2, which arise from *cis* and *trans* configurational isomerism, which is corroborated by the fluorine NMR of each compound. Interestingly, two isomers are observed only when the imido group has only one substituent, whereas 2,6-*i*-$Pr_2C_6H_3$, 2,6-$Me_2C_6H_3$, and 1-adamantyl complexes have only one isomer. Bistriflate complexes **2**, **4** and **6** react with 2 equivalents of $LiNC_4H_4$ to generate the analogous bispyrrolide species **9**, **11** and **13**. These molecules are even more insoluble than compounds **2-8** and can be isolated in moderate to good yields by running the reaction in Et_2O solutions for 12 h, collecting the precipitate product by filtration and washing the solids with Et_2O (equation 3). This method improves on the synthesis of **9**, via method A, where $Mo(NR)(CHCMe_2Ph)(Pyr)_2$ had to be isolated (Section 4.1.2).

^1H NMR in CD_2Cl_2 of **11** shows only one isomer in solution; while that of **13** shows 2 isomers, which could arise from *cis* and *trans* isomerism. ^{13}C NMR could not be obtained for either **11** or **13** because of their high insolubility in common organic solvents.

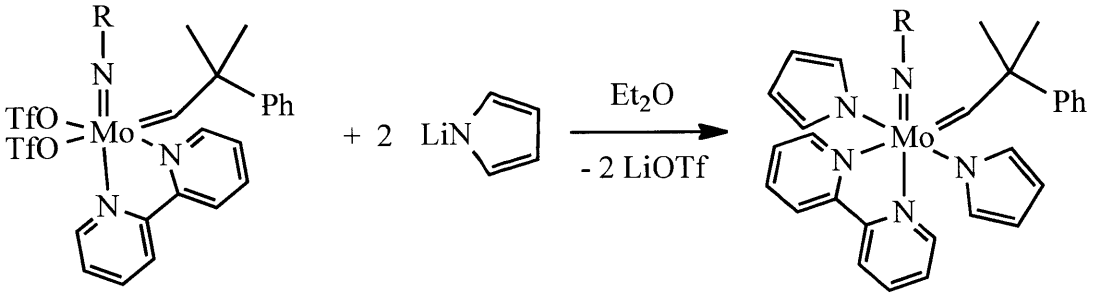

(3)

9 R = Ar, (61 %)
11 R = Ar', (77 %)
13 R = Ar^{iPr}, (85 %)

Unfortunately, when complexes **3**, **5**, and **7-8** are treated with 2 equivalents of $LiNC_4H_4$ impure product is obtained as a result of incomplete substitution; since all complexes are very insoluble, purification is not possible. The reaction is not driven to completion by letting the mixture react for longer times (1-2 days) and complications arise in subsequent reactions if these impure mixtures are used as starting materials.

Although method B allows access to two new bispyrrolide bipy adduct complexes, the procedure is not general and many other imido groups do not seem to give clean product. Because of these limitations, a different method of synthesis was sought. As it was mentioned earlier, $Mo(NR)(CHCMe_2Ph)(Pyr)_2$ complexes are very prone to decomposition upon work-up or removal of solvent, but if one can trap the species in solution before they decompose then it would be possible to access a variety of different imido groups. This idea is investigated in the next section.

4.1.4 Bispyrrolide bipyridine adduct complexes: preparation from bispyrrolide complexes formed *in situ*: Method C.

After the disappointing results presented in Section 4.1.3 it became clear that $Mo(NR)(CHMe_2Ph)(Pyr)_2$ species would need to be made first in order to access the corresponding bipy-bound complexes. The idea mentioned in the last section was to prepare the bispyrrolide species from the corresponding $Mo(NR)(CHCMe_2Ph)(OTf)_2DME$ complexes and to trap them by adding bipyridine to the solution mixture. Thus, $Mo(NR)(CHCMe_2Ph)(OTf)_2DME$ was dissolved in toluene at -35 °C and two equivalents of LiPyr were added. The mixture was allowed to react for no longer than 2 hours to avoid substantial decomposition, filtered to remove salts, and immediately treated with 0.8-0.9 equivalents of bipy to produce insoluble products (equation 4).

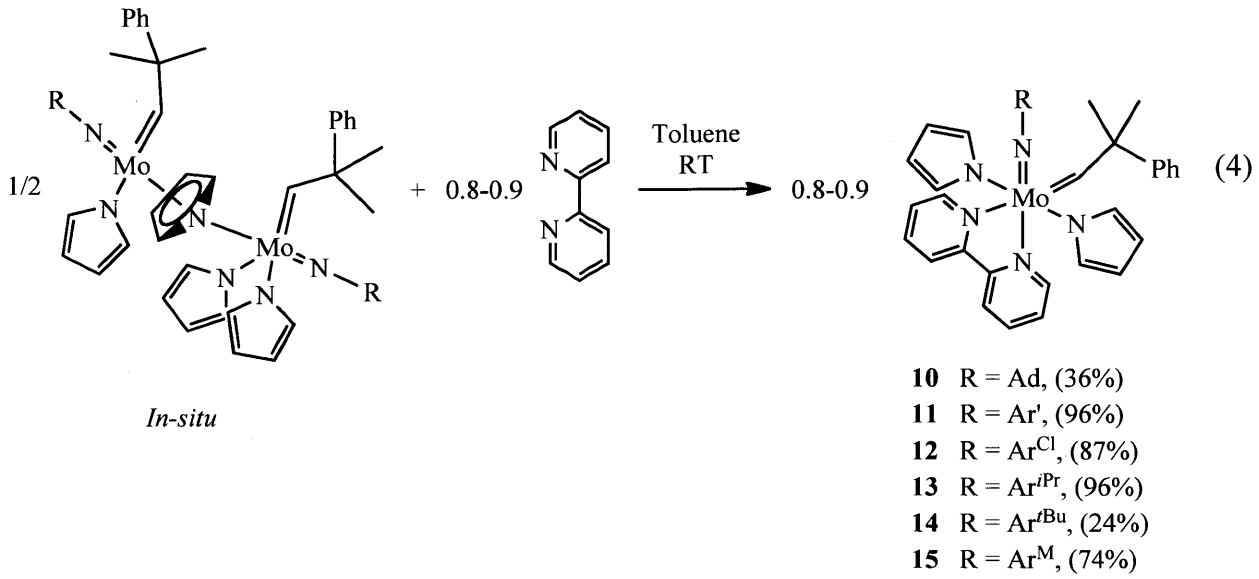

(4)

In-situ

10 R = Ad, (36%)
11 R = Ar', (96%)
12 R = Ar^{Cl}, (87%)
13 R = Ar^{iPr}, (96%)
14 R = Ar^{tBu}, (24%)
15 R = Ar^{M}, (74%)

Compounds **10-15** were obtained analytically pure upon collecting the precipitate product by filtration and drying under vacuum. The yields of most complexes (counting bipy as the limiting reactant) are high (74-96%) as a consequence of how insoluble all complexes are; however, complex **14** suffers in yield because it is slightly more soluble in toluene than the rest of the complexes. Likewise, complex **9**, which is soluble enough to get a ^{13}C NMR spectrum, is not efficiently made through this method; either method A or B is recommended.

The alkylidene region in the ^{1}H NMR (in CD_2Cl_2) of **11** and **14** shows only one isomer to be present in solution, while the spectra for **12** and **13** show two isomers and that of **15** shows up to three isomers. All isomers are presumed to arise from *cis* and *trans* isomerism of the pyrrolide ligands in the *syn* configuration. The third isomer of **15** can either arise from *anti* isomerism of the alkylidene, as suggested for **10**, or by restricted rotation of the NAr^{M} imido ligand. Unfortunately, due to the insolubility of samples **10-15** no J_{CH} coupling could be obtained to confirm our hypothesis. For the same reason, no high quality ^{13}C NMR spectra could be obtained for complexes **10-15**.

Method C works effectively for six out of seven imido ligands investigated and although not universal, it complements methods A and B. A moderately sized library of catalyst precursors can be prepared, which is more than double the number of previously known bispyrrolide complexes. The advantage of using bipy for isolation of these complexes is that it not only stabilizes the metal complex by completing the coordination sphere, but also enhances the crystallinity of the sample. The bipy complexes are easy to isolate, handle, and store without

decomposition problems that are usually experienced with $Mo(NR)(CHCMe_2Ph)(Pyr)_2$ complexes.

4.2 Preparation and reactivity studies of active MAP catalysts

4.2.1 Synthesis and structural studies of MAP complexes

It was mentioned in Section 4.1.2 that Fürstner was able to remove bipy from bisalkoxide complexes of the general formula $Mo(NAr)(CHR)(OR')_2(bipy)$ by heating the complexes at temperatures up to 100 °C in the presence of $ZnCl_2$ for 30 min.[6] In the case of complexes **9-15**, our goal is not only to produce bispyrrolide complexes in solution by removing bipy, but also to employ them as effective starting materials for the synthesis and isolation of active MAP catalysts. Thus, there are a few points that need to be taken into consideration: a) bipy must be removed under milder conditions in order to avoid decomposition of bipy-free bispyrrolide complexes, b) in order to keep the concentration of bipy-free bispyrrolide complexes low and to maximize the conversion to MAP catalysts, the desired alcohol/phenol must be present in solution while bipy is being removed; c) the solvent must dissolve the alcohol/phenol and the resulting MAP catalyst while all other byproducts or unreacted starting materials must remain insoluble. All of these points are addressed below.

The best way to avoid using high temperatures while encouraging insoluble materials to dissolve is to place them in an ultra-sonicator during the course of the reaction. The phenol that we chose to use was 2,6-bis(2',4',6'-trimethylphenyl)phenol (HMTOH) and the solvent was toluene, since HMTOH and the resulting MAP species dissolve in toluene and all bipy-containing compounds remain insoluble or very slightly soluble. $ZnCl_2$(dioxane) was employed because it is slightly more soluble than anhydrous $ZnCl_2$, which facilitates the use of relatively mild conditions. Sonication of complexes **9-15** at RT in the presence of one equivalent of HMTOH and one equivalent of $ZnCl_2$(dioxane) in toluene yields the desired MAP complexes in modest yields (equation 5). All catalysts are obtained in crystalline form by filtering off the insoluble salts over Celite and recrystallizing the solute from pentane at – 35 °C. Proton and carbon NMR spectra of complexes **16-22** are consistent with the presence of only one isomer in solution, which is similar to what was observed for $Mo(NAr^M)(CHCMe_2Ph)(Me_2Pyr)(OHMT)$ in Chapter 3.

The key features of the successful catalyst synthesis shown in equation 5 are a) removal of bipyridine by use of a bipy sponge such as $ZnCl_2$(dioxane); b) facile reaction between *in situ* generated $Mo(NR)(CHCMe_2Ph)(NC_4H_4)_2$ and HMTOH; and c) solubility differences between MAP catalysts and $ZnCl_2$(bipy), which simplifies purification and separation of byproducts.

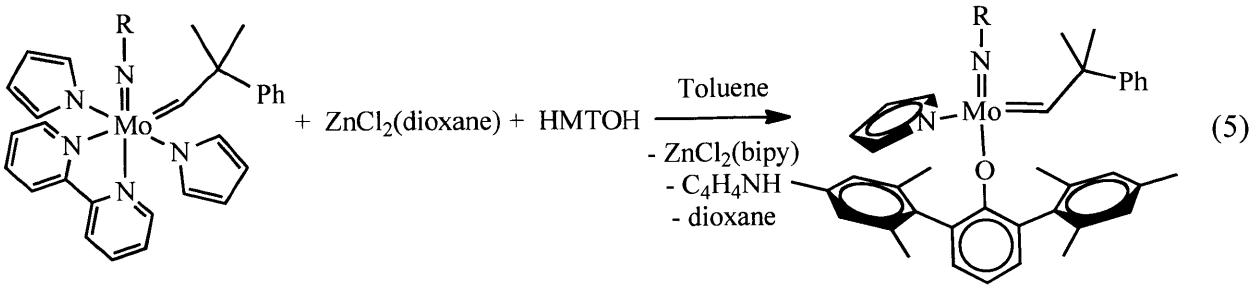

(5)

16 R = Ar, (46 %)
17 R = Ad, (64 %)
18 R = Ar', (79 %)
19 R = Ar^{Cl}, (47 %)
20 R = Ar^{iPr}, (42 %)
21 R = Ar^{tBu}, (36 %)
22 R = Ar^{M}, (37 %)

The synthesis of **17** directly from $Mo(NAd)(CHCMe_2Ph)(NC_4H_4)_2$ has already been reported[5] and this catalyst has been used effectively for numerous *cis*-selective olefin metathesis reactions; however, it is the only one that has been prepared directly from the isolated bispyrrolide.

The X-ray crystal structure of **20** was obtained. The complex crystallized out in the space group $P\bar{1}$ with both the *R* and *S* enantiomers present in the unit cell. For a clear view, *R*-**20** and *S*-**20** are shown in Figures 4a and 4b respectively. Both enantiomers have similar bond lengths and angles. The Mo=N(imido) angle is very close to linear (178.12(11)° and 177.45(11)°) while the Mo=CR" (145.61(11)° and 143.31(11)°) and Mo-O(HMT) (143.14(9)° and 150.15(9)°) angles are bent. The Mo(1)-C(1) and the Mo(2)-C(101) bond lengths (1.8769(15) Å and 1.8759(15) Å respectively), as well as the Mo(1)-N(1) and the Mo(2)-N(3) bond lengths (1.7300(12) Å and 1.7263(12) Å respectively) are reminiscent of Mo-C double bond and Mo-N triple bond character found in other molybdenum imido alkylidene complexes.[3] The isopropyl group on the imido ligand points away from where an incoming olefin is hypothesized to bind to the metal during the course of an olefin metathesis reaction. This is a structural feature that was also observed in Chapter 3 and that makes this type of imido ligand "small." In combination with the large HMTO ligand, these catalysts are best suited to perform *Z*-selective reactions because in the metallacyclobutane transition state there is little steric hindrance encountered by substituents located *syn* with respect to the imido group. Therefore, formation of *cis* bonds should be favored kinetically.

4.2.2 Reactivity studies of MAP catalysts

To test the reactivity of catalysts **16** and **18-22**, 50 equivalents of 2,3-dicarbomethoxynorbornadiene (DCMNBD) were treated with each catalyst at RT for 1-2 h. The polymer was subsequently quenched with benzaldehyde, isolated, purified, and examined by ^{1}H and ^{13}C NMR spectroscopy. The results are summarized in Table 1 and the representative ^{1}H NMR spectrum of isolated polyDCMNBD made with **16** is shown in Figure 5. All ROMP reactions are relatively fast and all cases yield polymer with > 98% *cis*-bonds, which can be clearly seen in the enlarged region of Figure 5.

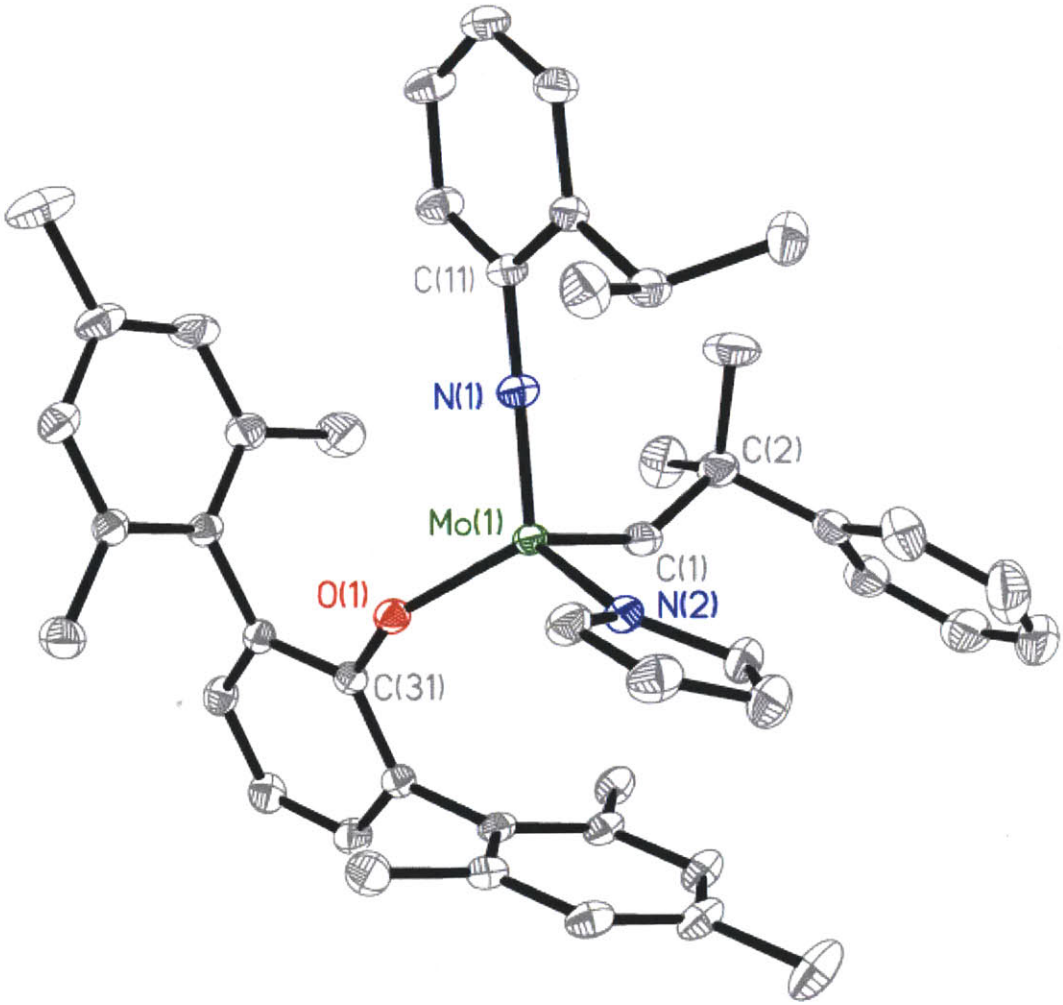

Figure 4a - The solid state structure of ***R*-20** (50% probability ellipsoids). Selected bond lengths (Å) and angles (°): Mo(1)-C(1) = 1.8769(15), Mo(1)-N(1) = 1.7300(12), Mo(1)-N(2) = 2.0198(13), Mo(1)-O(1) = 1.9186(10), C(2)-C(1)-Mo(1) = 145.61(11), C(11)-N(1)-Mo(1) = 178.12(11), C(31)-O(1)-Mo(1) = 143.14(9).

The high *Z*-selectivity of catalysts **19-22** was expected due to the analysis of the crystal structure of **20** and also from the known polymerization of DCMNDB with **17**,[5b] which gave polymer with > 98% *cis* bonds. However, since catalysts **16** and **18**, which have larger imido ligands also give the same selectivity upon polymerization of DCMNBD, other reasons are at play as well. The ^{13}C NMR spectra of all polymers show peaks (44.4 and 37.9 ppm) that match with the resonances for *cis-syndio*tactic polymer, formed with **17**.

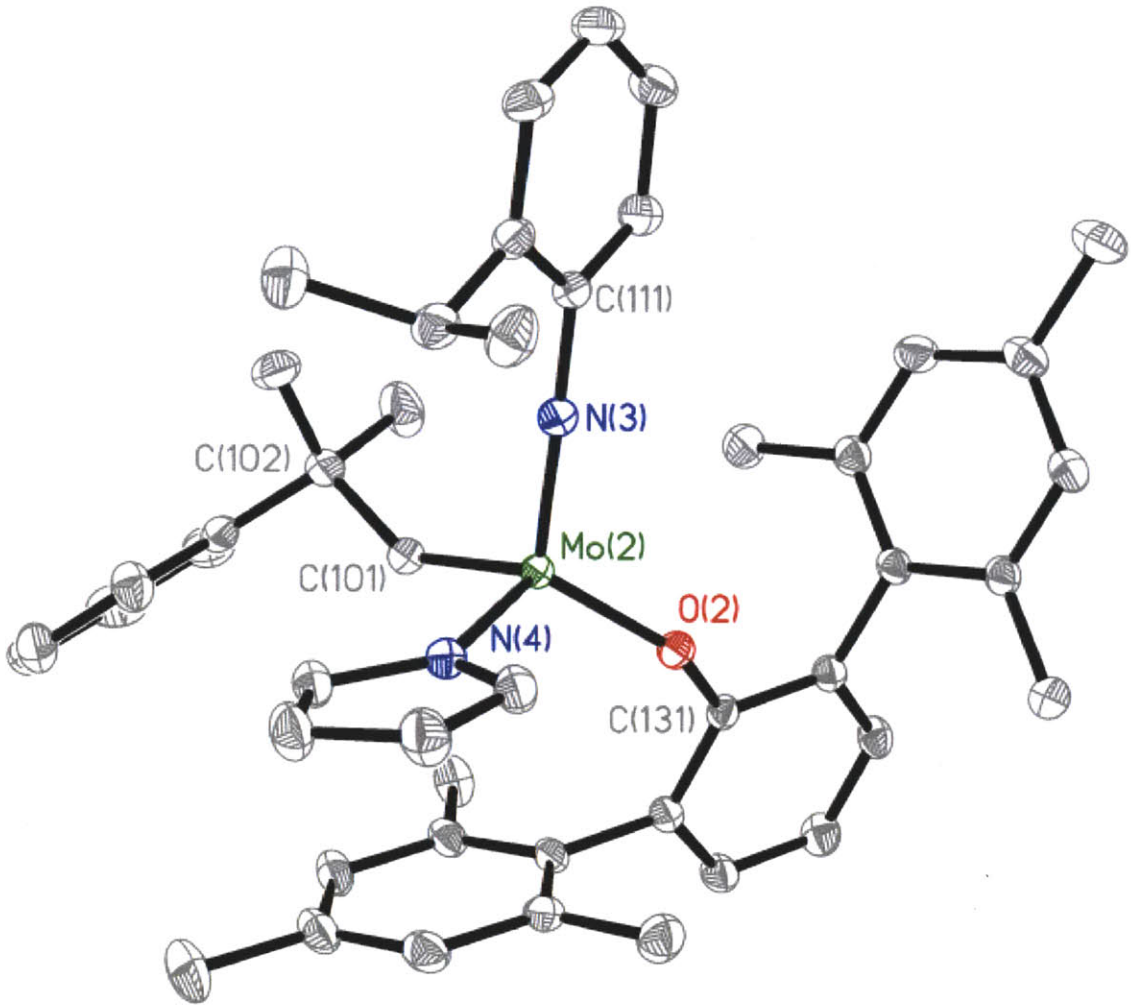

Figure 4b - The solid state structure of ***S*-20** (50% probability ellipsoids). Selected bond lengths (Å) and angles (°): Mo(2)-C(101) = 1.8759(15), Mo(2)-N(3) = 1.7263(12), Mo(2)-N(4) = 2.0294(13), Mo(2)-O(2) = 1.9168(10), C(102)-C(101)-Mo(2) = 143.31(11), C(111)-N(3)-Mo(2) = 177.45(11), C(131)-O(2)-Mo(2) = 150.15(9).

Table 1 – ROMP of DCMNBD with MAP catalysts **16-22**.				
Catalyst	**[Mo] (mM)**	**Monomer Equivalents**	**Time**	**Polymer Structure**
16	5.2	50	2 h	> 98% *cis*, syndiotactic
18	5.6	50	2 h	> 98% *cis*, syndiotactic
19	5.5	50	2 h	> 98% *cis*, syndiotactic
20	5.4	50	2 h	> 98% *cis*, syndiotactic
21	5.6	50	2 h	> 98% *cis*, syndiotactic
22	5.0	50	2 h	> 98% *cis*, syndiotactic

MAP complexes **16-22** are efficient *Z*-selective catalysts for the polymerization of DCMNBD, in contrast to the catalysts mentioned in Chapter 3. This difference in reactivity implies that the pyrrolide ligand plays a major role on the *Z*-selectivity of MAP catalysts and an unsubstituted pyrrolide facilitates olefin binding *syn* to the imido ligand.

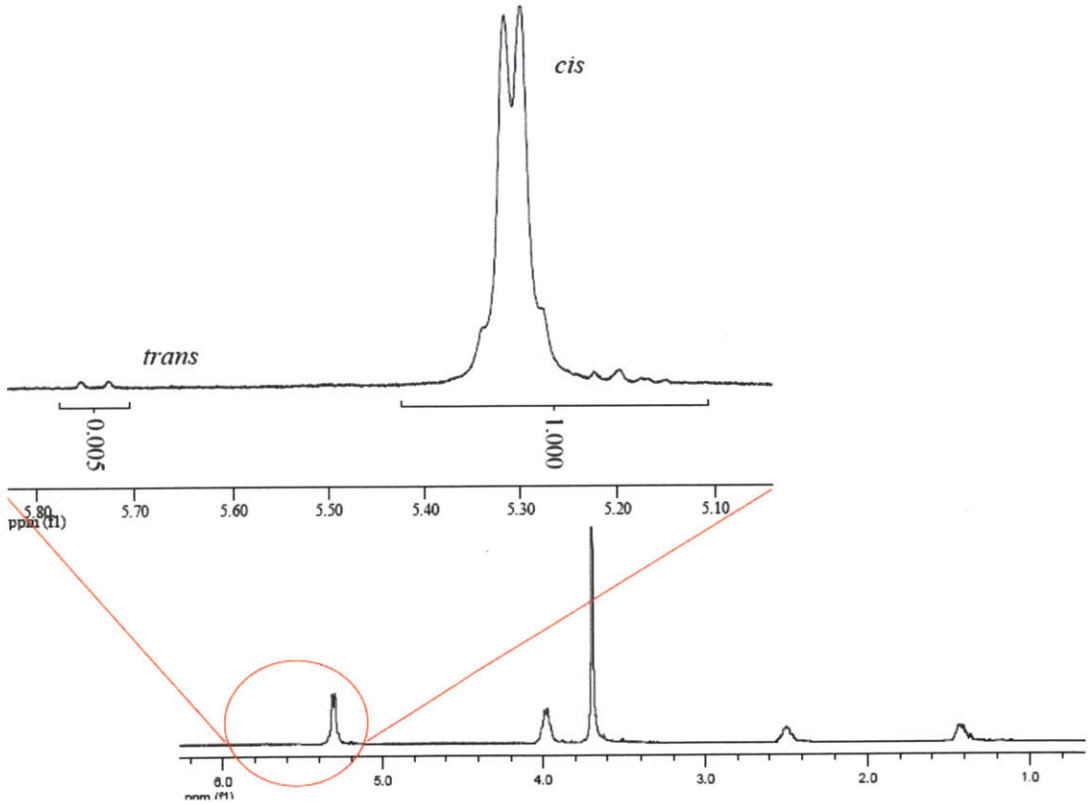

Figure 5 – ^{1}H NMR of isolated poly-DCMNBD in $CDCl_3$, prepared with **16**. The olefinic region is shown in greater detail and the integrations are shown for the corresponding *trans* and *cis* peaks.

4.3 Preparation and structural studies of molybdenum alkylidyne bipyridine adduct complexes

After the successful preparation of bipy adducts of bispyrrolide complexes and their use as catalyst precursors, we were interested in preparing analogous species with 2,5-dimethylpyrrolide (Me_2Pyr) instead of Pyr as the ligand. Therefore, one equivalent of bipy was added to six representative $Mo(NR)(CHCMe_2R')(Me_2Pyr)_2$ species (R = Ar, R' = Ph (**A**); R = Ar', R' = Ph (**B**); R = 2-$(CF_3)C_6H_4$ (Ar^{CF3}), R' = Me (**C**); R = Ar^{iPr}, R' = Ph (**D**); R = Ar^{M}, R' = Ph (**E**); and R = 2-(2',4',6'-$iPr_3C_6H_2$)C_6H_4 (Ar^{T}), R' = Me (**F**)). Only the reaction between **D** and one equivalent of bipy can be carried out to completion at RT in a 1:1 mixture of toluene and pentane. The reactions between **A**, **B**, and **C** and one equivalent of bipy must be carried out in toluene at 60 °C for 18 h, while those of **E** and **F** and bipy must be carried out in toluene at 60 °C for 2 d in order to reach completion. In all cases the color of the reaction mixture changes from orange-brown to red-purple.

Monitoring the reactions by ^1H NMR (in C_6D_6) shows that upon completion of the reaction, one equivalent of Me_2PyrH is present in solution, the alkylidene peak of the starting material (**A-F**) is gone and no new alkylidene peak is observed. The spectrum of the product has sharp peaks, consistent with formation of a new stable product containing bipy, no alkylidene ligand, and one less dimethylpyrrolide ligand. The best molecular candidate would be a complex with the general formula $Mo(NR)(\equiv CCMe_2R')(2,5\text{-}Me_2Pyr)(bipy)$. Upon solvent removal and washing with pentane, compounds **23-28** can be obtained as purple or red-purple solids in good to very good yields (equation 6).

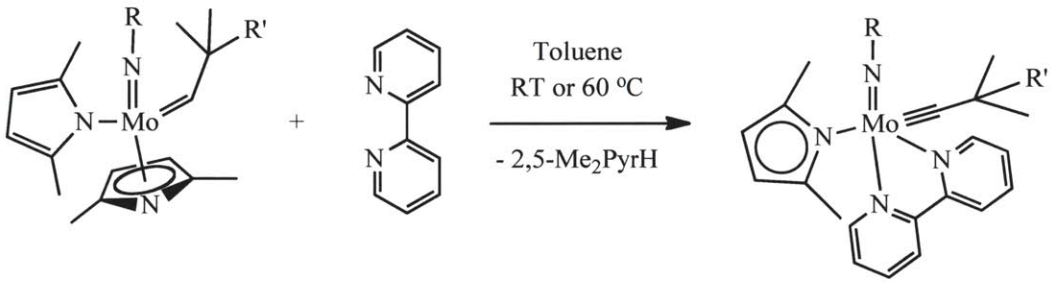

(6)

A
B
C
D
E
F

23 R = Ar, R' = Ph, T = 60 °C, (46%)
24 R = Ar', R' = Ph, T = 60 °C, (60%)
25 R = Ar^{CF3}, R' = Me, T = 60 °C, (69%)
26 R = Ar^{iPr}, R' = Ph, T = RT, (86%)
27 R = Ar^{M}, R' = Ph, T = 60 °C, (53%)
28 R = Ar^{T}, R' = Me, T = 60 °C, (69%)

X-ray studies of **23** and **24** (provided generously by the Hoveyda lab), as well as **28** were undertaken. Compounds **23** and **24** were grown from a CH_2Cl_2:pentane mixture at – 45 °C while **28** was grown from benzene at RT. Complex **23** crystallized in the monoclinic group $P2_1/n$, whereas **24** and **28** crystallized out in the monoclinic group $P2_1/c$. The structures are shown in Figures 6-8 respectively. In the case of **28** two independent molecules are present in the asymmetric unit along with six benzene molecules. The Mo-Mo distance between the two complexes is 17.144 Å. One of the molecules shows considerable disorder throughout the phenyl imido ligand (not shown) while the order does not. Compounds **23**, **24** and **28** can be best regarded as distorted square pyramids with the alkylidyne ligand located in the apical position. There is only one pyrrolide ligand bound to the metal, as well as a single bipy molecule, which is in agreement with the NMR data. The most striking features are the bond lengths Mo(1)-C(29) of **23** (1.764(3)Å), Mo(1)-C(1) of **24** (1.7643(17) Å) and **28** (1.780(5)Å), which are much shorter than a regular Mo-C double bond, but consistent with a Mo-C triple bond.[7] In addition, the Mo(1)-C(29)-C(30) bond angle of **23** (161.5(2)°), as well as the Mo(1)-C(1)-C(2) bond angles of **24** (159.05(14)°) and **28** (167.1(4)°) are large and close to linear, which is in agreement with an expected alkylidyne Mo-C triple bond. The Mo=NR bond lengths of **23** (1.804(3)Å), **24** (1.7958(14)Å) and **28** (1.823(4)Å) are longer than in analogous alkylidene complexes; likewise, the Mo(1)-N(3)-C(11) bond angle of **23** (159.6(2)°), the Mo(1)-N(1)-C(11) bond angle of **24** (162.64(12)°) and the Mo(1)-N(4)-C(31) bond angle of **28** (152.6(3)°) resemble a Mo-N double bond more than a triple bond. However, the imido ligand in {Mo(NAr)(C-t-Bu)[OCMe$(CF_3)_2]_2$}$^-$ is more bent[14] (Mo-N-C = 141.16(17)°) than any in **23**, **24**, or **28**. We propose that steric interactions between ligands in five-coordinate **23**, **24** and **28** prevent the imido ligands from being as bent as the imido ligand in four-coordinate {Mo(NAr)(C-t-Bu)[OCMe$(CF_3)_2]_2$}$^-$.

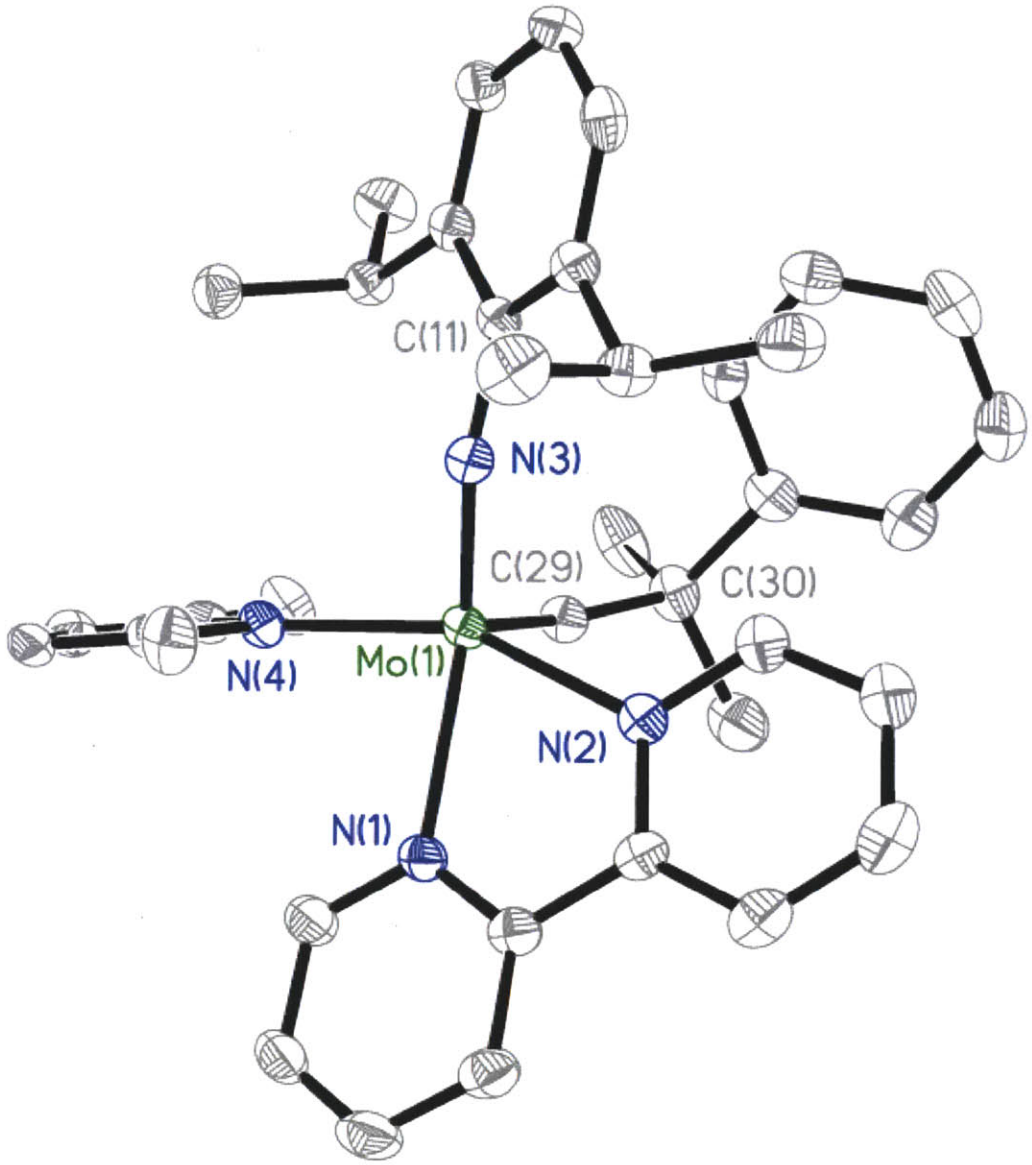

Figure 6 - The solid state structure of **23** (50 % probability ellipsoids). Selected bond lengths (Å) and angles (°): Mo(1)-C(29) = 1.764(3), Mo(1)-N(1) = 2.326(3), Mo(1)-N(2) = 2.209(3), Mo(1)-N(3) = 1.804(3), Mo(1)-N(4) = 2.098(3), C(30)-C(29)-Mo(1) = 161.5(2), C(11)-N(3)-Mo(1) = 159.6(2), N(1)-Mo(1)-N(3) = 144.12(10), N(2)-Mo(1)-N(4) = 153.05(10).

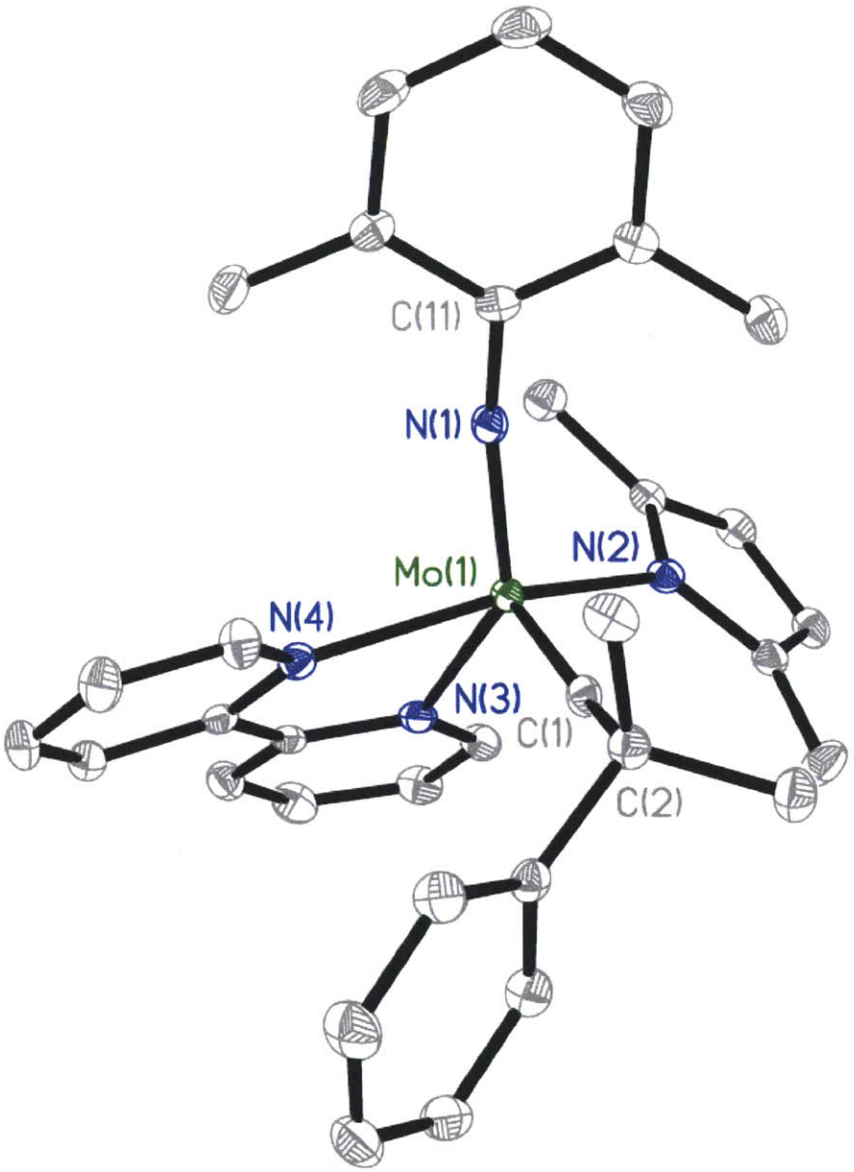

Figure 7 - The solid state structure of **24** (50 % probability ellipsoids). Selected bond lengths (Å) and angles (°): Mo(1)-C(1) = 1.7643(17), Mo(1)-N(1) = 1.7958(14), Mo(1)-N(2) = 2.1228(14), Mo(1)-N(3) = 2.3165(13), Mo(1)-N(4) = 2.2100(13), C(2)-C(1)-Mo(1) = 159.05(14), C(11)-N(1)-Mo(1) = 162.64(12), N(1)-Mo(1)-N(3) = 137.44(6), N(2)-Mo(1)-N(4) = 153.09(15).

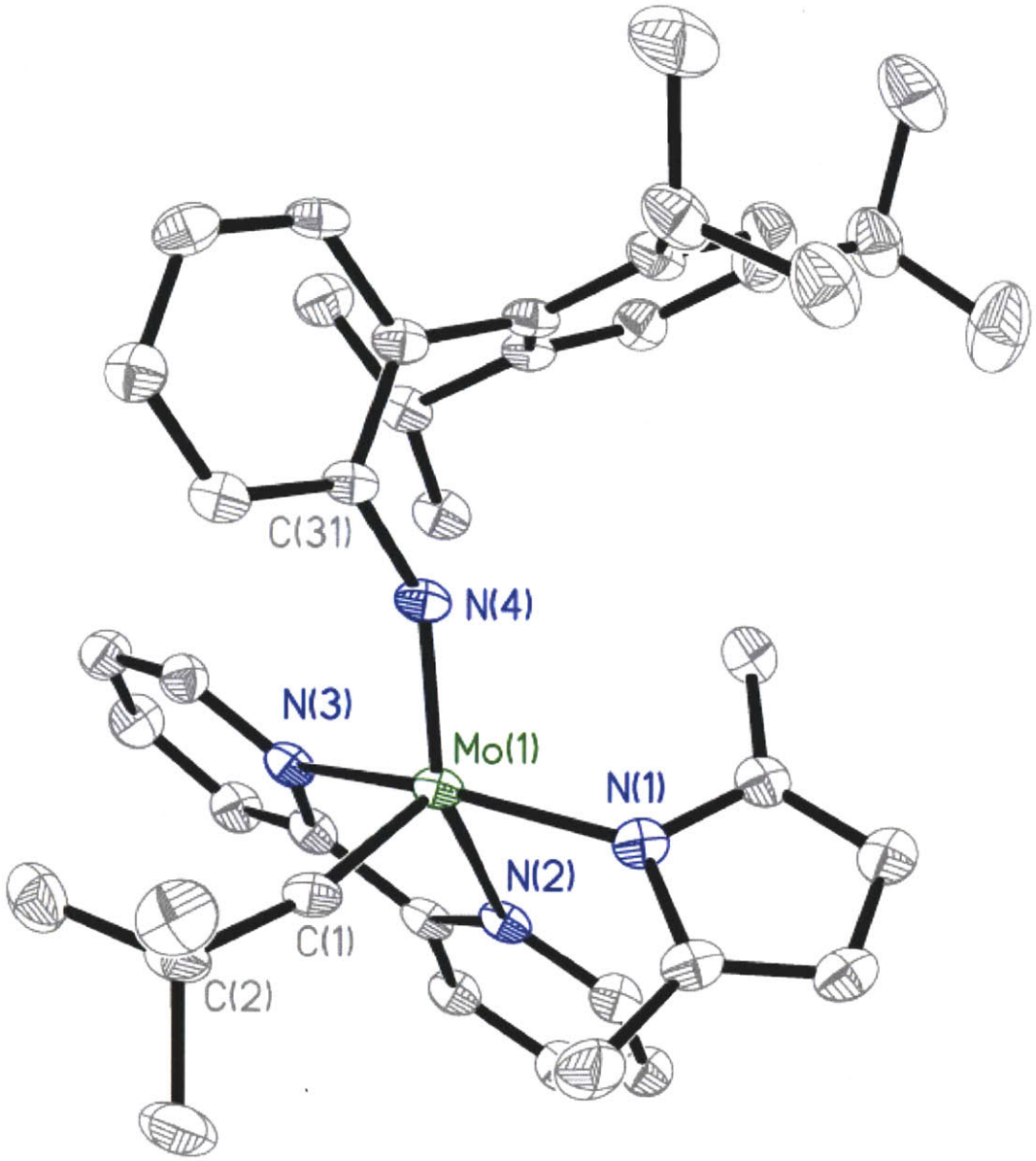

Figure 8 – The solid state structure of **28** (50 % probability ellipsoids). All solvent molecules and the disordered molecule are omitted for clarity. Selected bond lengths (Å) and angles (°): Mo(1)-C(1) = 1.780(5), Mo(1)-N(1) = 2.105(4), Mo(1)-N(2) = 2.306(3), Mo(1)-N(3) = 2.225(4), Mo(1)-N(4) = 1.823(4), C(2)-C(1)-Mo(1) = 167.1(4), C(31)-N(4)-Mo(1) = 152.6(3), N(1)-Mo(1)-N(3) = 153.28(14), N(2)-Mo(1)-N(4) = 140.98(15).

The lengthening and bending of the imido group in complexes **23**, **24**, and **28** is a direct result of electron-saturation of the metal orbitals to which the imido ligand would have to bind to form a triple bond. In molybdenum imido alkylidene complexes, where the alkylidene is not rotating, the imido group is linear because the π-bond responsible for triple-bond character is orthogonal to the alkylidene p-orbital (Figure 9). On the other hand, in molybdenum imido alkylidyne complexes, the π-bond responsible for triple-bond character of the imido ligand overlaps with one of the p-orbitals of the alkylidyne ligand. As a result, the Mo-N(imido) bond becomes more like a double bond in the presence of a Mo-C triple bond (Figure 9).

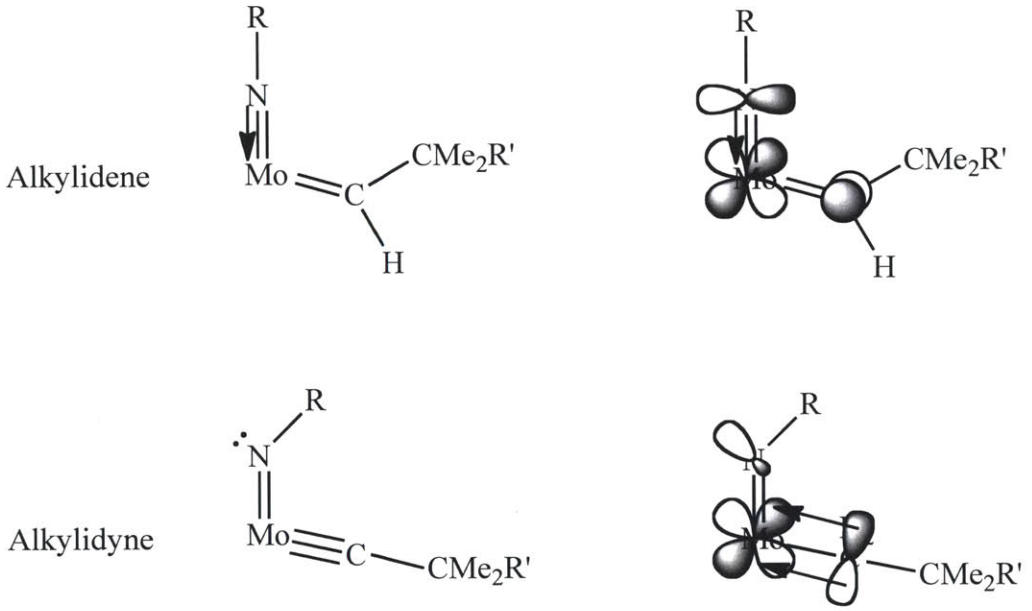

Figure 9 – Diagram depicting how the alkylidene (top) and alkylidyne (bottom) ligands affect the shape of the imido ligand as a result of metal-ligand orbital overlap.

The crystal structures of **23**, **24**, and **28** and the ^{1}H NMR data of **23-28** conclusively demonstrate that an alkylidyne complex is formed when $Mo(NR)(CHCMe_2R')(Me_2Pyr)_2$ reacts with bipy. It is hypothesized that complexes **A-F** initially form a bipy adduct just like species **9-15**. It is at this stage that the Me_2Pyr ligands experience a significant amount of steric crowding and α-abstraction of the alkylidene C-H bond by one of the dimethylpyrrolide ligands takes place forming Me_2PyrH and an alkylidyne complex (Scheme 2).

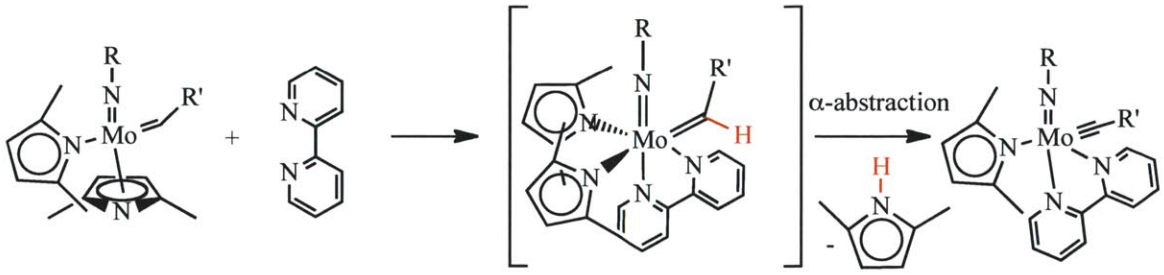

Scheme 2 – Proposed mechanism leading to formation of Mo(NR)(CCMe$_2$R')(Me$_2$Pyr)(bipy) complexes.

High oxidation state alkylidyne complexes of tantalum, tungsten, molybdenum and rhenium have been synthesized through several routes in the last thirty years.[7a-c] Formation of a neopentylidyne ligand through deprotonation of a neopentylidene ligand was first demonstrated in a reaction between Ta(CHCMe$_3$)(CH$_2$CMe$_3$)$_3$ and butyllithium to give a lithium salt of {Ta(CCMe$_3$)(CH$_2$CMe$_3$)$_3$}$^-$.[7d] A dehydrohalogenation of W(NPh)(CHCMe$_3$)(PEt$_3$)$_2$Cl$_2$ by Ph$_3$P=CH$_2$ led to W(NPh)(CCMe$_3$)(PEt$_3$)$_2$Cl,[7m] a compound that is most similar to **23-28**, although no X-ray structure of W(NPh)(CCMe$_3$)(PEt$_3$)$_2$Cl was determined. Deprotonation of Mo(NAr)(CHCMe$_3$)[OCMe(CF$_3$)$_2$]$_2$ by Ph$_3$P=CH$_2$ led to the alkylidyne complex, {Ph$_3$PMe}{Mo(NAr)(CCMe$_3$)[OCMe(CF$_3$)$_2$]$_2$},[14] as noted above. Attempts to prepare certain types of imido neopentylidene complexes have resulted in formation of amido neopentylidyne complexes as a consequence of migration of a proton from an alkylidene to an imido ligand, or to an actual deprotonation/readdition sequence.[7e] Neopentylidyne ligands have been generated from neopentyl ligands early in the development of high oxidation state organometallic chemistry of tungsten and molybdenum, a circumstance that has allowed tungsten and molybdenum alkylidyne complexes of the type M(C-t-Bu)$_3$(CH$_2$-t-Bu)$_3$ to be synthesized;[7f-g] α deprotonation of a neopentyl ligand to give an intermediate neopentylidene ligand is probably the rate limiting deprotonation in these reactions. Rhenium neopentylidyne complexes have been prepared through deprotonation of neopentylidene ligands, either by transfer of a proton to a neopentyl group or to an imido or amido group;[7h-l] reactions are complex and details are not known. A proton also has been added to an alkylidyne α carbon atom in several circumstances to give an alkylidene complex. For example, transfer of a proton from an amido ligand to a neopentylidyne α carbon atom was the first general method of preparing imido alkylidene complexes of tungsten.[7m-n] Intramolecular α proton migration has been known to be promoted in more sterically crowded circumstances, the first being ligand induced formation of tantalum neopentylidene complexes from tantalum dineopentyl complexes through addition of various

phosphines or even simply THF.[7o-p] On the basis of all of the above reports, it is fair to say that there is ample precedent for intramolecular migration of a proton from a neopentylidene ligand to a dimethylpyrrolide ligand, even though there is no specific example of this type to our knowledge in the literature. No details as to whether the proton migrates to the pyrrolide nitrogen directly or to a pyrrolide α or β carbon atom[1a] can be determined on the basis of data in hand.

Having established the structural features of complexes **23-28** we wanted to know whether these compounds could be used to generate MAP species in the same manner that **16-22** were synthesized. Preliminary work shows that reactions between complexes **23-28** with one equivalent of HMTOH and one equivalent of $ZnCl_2$(dioxane) do generate MAP species containing an alkylidene ligand as a result of proton-exchange from the phenol to the alkylidyne. However, the reactions are not clean and a significant amount of side products are also observed. It is believed that proton-exchange does not only take place between HMTOH and the alkylidyne ligand, but also with the pyrrolide itself. As a result, direct reaction with HMTOH or other phenols/alcohols is not an efficient or selective method to prepare active MAP species from Mo(NR)($CCMe_2R'$)(Me_2Pyr)(bipy) complexes. On the other hand, reactions of complexes **23-28** with small alcohols in the absence of $ZnCl_2$(dioxane) could generate bipy-bound MAP species of the general formula Mo(NR)($CHCMe_2R'$)(Me_2Pyr)(OR")(bipy), but this methodology has not yet been fully investigated, but it may be the topic of future studies.

CONCLUSION

The use of bipyridine as a base adduct was vital to the isolation of **9-15** as stable molybdenum complexes using three different methods with varying degree of success. All seven bispyrrolide complexes exhibit different number of isomers present in solution, which arise from *cis* and *trans* pyrrolide isomerism, as well as possible *syn* and *anti* alkylidene isomerism. The X-ray analysis of **9** shows that its only isomer corresponds to the *trans* isomer. Sonication of a mixture containing a Mo(NR)($CHCMe_2Ph$)($Pyr)_2$(bipy) complex (**9-15**), HMTOH, and $ZnCl_2$(dioxane) led to the formation of MAP species **16-22**, which can be isolated by filtration and purified by recrystallization. Both *R* and *S* enantiomers of **20** co-crystallized together and their structures have been determined; in both molecules the substituent on the imido ligand points away from the alkylidene ligand. Reactivity studies of **16-22** with DCMNBD suggest that all compounds are efficient *Z*-selective catalysts leading to formation of > 98% *cis* syndiotactic polymeric structures. Finally, preparation of complexes **23-28**, containing an alkylidyne ligand has been done by adding bipy to bispyrrolide complexes where the pyrrolide ligand is Me_2Pyr. The reaction is believed to occur via α-abstraction of the alkylidene proton by one of the Me_2Pyr ligands as a result of significant steric crowding at the metal. The X-ray structures of **23**, **24** and

28 were presented and showed characteristic bond lengths and angles corresponding to alkylidyne ligands and imido ligands with only double-bond character.

EXPERIMENTAL

General. All reactions and manipulations of air and moisture sensitive compounds were handled in oven-dried glassware (150 °C, 2 hr) under a N_2 atmosphere either in a dual Schlenk line or in vacuum atmosphere glove box. HPLC grade solvents (benzene, toluene, diethyl ether, tetrahydrofuran, pentane, and methylene chloride), were purge with N_2 and passed through activated alumina and stored over molecular sieves prior to use. 2,2'-bipyridine and benzaldehyde were purchased from Alfa-Aesar and used without further purification. $LiNC_4H_4$,[8] $ZnCl_2$(dioxane),[9] HMTOH,[10] and DCMNBD[11] were prepared according to literature reports. HMTOH was placed under high vacuum for 12 hours before use. All Mo(NR)($CHCMe_2Ph$)$(OTf)_2$DME,[12] Mo(NR)($CHCMe_2Ph$)$(Pyr)_2$ (R = 2,6-iPr$_2$C$_6$H$_3$, adamantyl),[4a] and Mo(NR)($CHCMe_2R'$)$(NC_4H_2Me_2)_2$[3a, 13] complexes were prepared according to literature procedures. All deuterated solvents (d_6-benzene, d_8-toluene, and d_2-dichloromethane) were stored over molecular sieves 12 hours prior to use. All the recorded NMR spectra were done with Bruker 400 MHz and Varian 500 MHz spectrometers. Sonications were performed on a Bransonic Ultrasonic Cleaner 1510R-MT purchased from Branson Ultrasonics Corporation. Elemental analyses were performed by Midwest Microlab, LLC.

Mo(NAr^{Ph})($CHCMe_3$)$(Pyr)_2$ (1) Mo(NAr^{Ph})($CHCMe_3$)$(OTf)_2$DME (1.50 g, 2.08 mmol) were dissolved in ether and subsequently cooled down to -35 °C for 1 h. Then, LiPyr (0.304 g, 4.16 mmol) was added in one portion and the mixture was allowed to stir at RT for 2 h. Removal of solvent, dissolution in CH_2Cl_2, and filtration through Celite was done to remove LiOTf salts. The salts were washed with more CH_2Cl_2 until colorless and all organic fractions collected and concentrated to dryness to yield crude brown solid. Finally, recrystallization from a concentrated ether-pentane solution at -35 °C after more than a week yielded 0.097 g of pure orange material upon filtration and vacuum drying (10%): ^{1}H NMR (400 MHz, CD_2Cl_2) δ 14.00-12.00 (s br, 1H, Mo=C*H*), 7.60-6.80 (m, 9H, aromatics), 6.70-5.30 (s br, 8H, NC_4H_4), 1.40-0.60 (s br, 9H, *t*-butyl). Anal. Calcd $C_{25}H_{27}F_6MoN_3$: C, 64.51; H, 5.85; N, 9.03. Found: C, 64.16; H, 5.83; N, 8.81. ^{13}C NMR could not be obtained at RT due to broadening of peaks.

Mo(NAr)($CHCMe_2Ph$)$(OTf)_2$(bipy) (2) Mo(NAr)($CHCMe_2Ph$)$(OTf)_2$(DME) (0.500 g, 0.632 mmol) was dissolved in benzene and bipyridine (0.099 g, 0.633 mmol) was added in one portion. After a few minutes a yellow precipitate began forming. The mixture was allowed to stir for 12 h and then it was filtered and dried under vacuo; yield 0.457 g (84%): ^{1}H NMR (400 MHz, CD_2Cl_2) δ 14.59 (s, 1H, Mo=C*H*, J_{CH} = 126.4 Hz), 8.85 (d, 1H, bipy), 8.25-8.18 (overlapping peaks, 2H, aromatic), 8.14 (m, 1H, aromatic), 8.08 (m, 1H, aromatic), 7.72 (m, 1H,

aromatic), 7.56 (d, 2H, aromatic), 7.47 (t, 2H, aromatic), 7.35 (t, 1H, aromatic), 7.24-7.13 (overlapping peaks, 3H, aromatic), 7.05-6.92 (overlapping peaks, 2H, aromatic), 3.94 (s br, 1H, C*H*Me$_2$), 2.70 (s br, 1H, C*H*Me$_2$), 2.10 (s, 3H, MoCHC*Me$_2$*Ph), 1.59 (s, 3H, MoCHC*Me$_2$*Ph), 1.34 (s br, 3H, CH*Me$_2$*), 1.14 (d, 6H, CH*Me$_2$*), - 0.05 (s br, 3H, CH*Me$_2$*). Anal. Calcd $C_{34}H_{37}F_6MoN_3O_6S_2$: C, 47.61; H, 4.35; N, 4.90. Found: C, 47.65; H, 4.40; N, 5.01. ^{13}C NMR could not be obtained due to insolubility of complex.

Mo(NAd)(CHCMe$_2$Ph)(OTf)$_2$(bipy) (3) The procedure is identical to the synthesis of **2**, employing Mo(NAd)(CHCMe$_2$Ph)(OTf)$_2$(DME) (0.500 g, 0.654 mmol) and bipyridine (0.102 g, 0.653 mmol); yield 0.496 g (91%): ^{1}H NMR (400 MHz, CD_2Cl_2) δ 14.29 (s, 1H, Mo=C*H*, J_{CH} = 123.6 Hz), 8.94 (d, 1H, bipy), 8.40-8.18 (overlapping peaks, 3H, aromatics), 8.06 (t, 1H, aromatic), 7.78 (m, 1H, aromatic), 7.65-7.10 (overlapping peaks, 5H, aromatics), 6.99 (m, 1H, aromatic), 6.59 (br, 1H, aromatic), 2.40 (s, 3H, Ad), 1.95 (s, 3H, C*Me$_2$*Ph), 1.78 (s, 6H, Ad), 1.65-1.40 (overlapping peaks, 9H, C*Me$_2$*Ph + Ad). Anal. Calcd $C_{32}H_{25}F_6MoN_3O_6S_2$: C, 46.21; H, 4.24; N, 5.05. Found: C, 45.82; H, 4.09; N, 5.19. ^{13}C NMR could not be obtained because sample is too insoluble.

Mo(NAr')(CHCMe$_2$Ph)(OTf)$_2$(bipy) (4) The procedure is identical to the synthesis of **2**, employing Mo(NAr')(CHCMe$_2$Ph)(OTf)$_2$(DME) (0.400 g, 0.544 mmol) and bipyridine (0.085 g, 0.544 mmol); yield 0.291 g (67%): ^{1}H NMR (400 MHz, CD_2Cl_2) δ 14.55 (s, 1H, Mo=C*H*, J_{CH} = 130.4 Hz), 8.83 (d, 1H, bipy), 8.23 (t, 2H, aromatic), 8.10 (m, 2H, aromatic), 7.68 (t, 1H, MoCHCMe$_2$*Ph*), 7.57 (m, 2H, MoCHCMe$_2$*Ph*), 7.44-7.32 (overlapping peaks, 3H, aromatics), 7.24 (t, 1H, aromatic), 7.02 (t,1H, aromatic), 6.96 (t, 1H, aromatic), 6.89 (s br, 2H, Ar'), 2.53 (s br, 3H, Ar' *Me*), 2.00 (s, 3H, MoCHC*Me$_2$*Ph), 1.57 (s, 3H, MoCHC*Me$_2$*Ph), 1.43 (s br, 3H, Ar' *Me*); ^{13}C NMR (100 MHz, CD_2Cl_2) δ 332.4 (Mo=*C*H), 160.3, 155.4, 152.5, 148.6, 147.1, 142.9, 141.7, 129.4, 129.0, 128.8, 127.9, 127.3, 127.2, 127.2, 123.9, 123.4, 58.0, 30.4, 28.8, 19.7 (br). Anal. Calcd $C_{30}H_{29}F_6MoN_3O_6S_2$: C, 44.95; H, 3.65; N, 5.24. Found: C, 44.57; H, 3.64; N, 5.32.

Mo(NAr^{Cl})(CHCMe$_2$Ph)(OTf)$_2$(bipy) (5) Mo(NAr^{Cl})(CHCMe$_2$Ph)(OTf)$_2$(DME) (0.166 g, 0.224 mmol) was dissolved in Et_2O and chilled to -35 °C for 1 hr. Then, bipyridine (0.035 g, 0.224 mmol) was added in one portion. After a few minutes a green precipitate began forming. The mixture was allowed to stir for 12 h and then it was filtered and dried under vacuo; yield 0.120 g (66%): ^{1}H NMR (400 MHz, CD_2Cl_2) δ 14.39 (s, 1H, Mo=C*H* major, J_{CH} = 127.1 Hz), 14.20 (s, 0.28H, Mo=C*H* minor, J_{CH} = 118.9 Hz), 8.86 (d, 0.28H, bipy minor), 8.81 (d, 1H, bipy major), 8.77 (d, 0.28H, aromatic minor), 8.73 (d, 0.28H, aromatic minor), 8.59 (m, 0.56H, aromatic minor), 8.53 (m, 0.56H, aromatic minor), 8.47 (m, 0.28H, aromatic minor), 8.30 (d, 1H,

aromatic major), 8.27 (d, 1H, aromatic major), 8.24 (m, 0.28H, aromatic minor), 8.18-8.06 (overlapping peaks, 2.56H, aromatic major + minor), 7.96 (d, 0.28H, aromatic minor), 7.90 (m, 0.28H, aromatic minor), 7.84 (m, 0.28H, aromatic minor), 7.80 (d, 1H, aromatic major), 7.71-7.63 (overlapping peaks, 1.56H, aromatic major + minor), 7.62-7.54 (overlapping peaks, 2.56H, aromatic major + minor), 7.50 (m, 0.56H, aromatic minor), 7.41 (overlapping peaks, 2.56H, aromatic major + minor), 7.36-7.22 (overlapping peaks, 4H, aromatic major), 7.20-7.10 (overlapping peaks, 4.28H, aromatic major + minor), 7.01 (m, 1H, aromatic major), 2.15 (s, 3H, MoCHC*Me*$_2$Ph major), 1.89 (s, 0.84H, MoCHC*Me*$_2$Ph minor), 1.76 (s, 0.84H, MoCHC*Me*$_2$Ph minor), 1.59 (s, 3H, MoCHC*Me*$_2$Ph major); ^{13}C NMR (100 MHz, CD_2Cl_2) δ 332.7 (Mo=*C*H), 161.3, 159.8, 155.4, 155.3, 153.6, 153.4, 152.6, 152.0, 151.7, 151.3, 150.5, 148.6, 148.4, 147.1, 145.9, 145.8, 143.7, 143.3, 142.8, 141.9, 133.8, 131.9, 131.7, 131.6, 131.3, 131.2, 130.3, 130.2, 129.6, 129.5, 128.9, 128.7, 128.2, 127.8, 127.7, 127.3, 127.3, 126.9, 126.7, 126.5, 125.4, 125.3, 123.9, 123.3, 121.7. 118.5, 58.9, 58.4, 30.7, 30.2, 29.6, 29.5; ^{19}F NMR (376 MHz, CD_2Cl_2) δ –77.1 (s, 1F, *cis*), -78.7 to -79.7 (overlapping peaks, 1.28F, *cis* + *trans*). Anal. Calcd $C_{28}H_{24}ClF_6MoN_3O_6S_2$: C, 41.62; H, 2.99; N, 5.20. Found: C, 41.50; H, 3.10; N, 5.31.

Mo(NAr^{iPr})(CHCMe$_2$Ph)(OTf)$_2$(bipy) (6) The procedure is identical to the synthesis of **5**, employing Mo(NAr^{iPr})(CHCMe$_2$Ph)(OTf)$_2$(DME) (0.247 g, 0.330 mmol) and bipyridine (0.051 g, 0.327 mmol); yield 0.205 g of a yellow solid (76%): ^{1}H NMR (400 MHz, CD_2Cl_2) δ 14.46 (s, 1H, Mo=C*H*, J_{CH} = 125.7 Hz, major), 14.23 (s, 0.12H, Mo=C*H*, minor), 8.85 (d, 1H, bipy major), 8.80 (d, 0.12H, bipy minor), 8.74 (d, 0.12H, aromatic minor), 8.60 (d, 0.12H, aromatic minor), 8.55 (m, 0.24H, aromatic minor), 8.48 (m, 0.12H, aromatic minor), 8.44 (m, 0.12H, aromatic minor), 8.29 (d, 1H, aromatic major), 8.24 (d, 1H, aromatic major), 8.12 (m, 2.24H, aromatic major + minor), 7.95 (m, 0.12H, aromatic minor), 7.85 (m, 0.12H, aromatic minor), 7.82 (m, 0.12H, aromatic minor), 7.68 (m, 1H, aromatic major), 7.65 (m, 0.12H, aromatic minor), 7.57 (m, 2.12H, aromatic major + minor), 7.45 (t, 2H, aromatic major), 7.34 (t, 1H, aromatic major), 7.30-7.08 (overlapping peaks, 5.36H, aromatic major + minor), 7.02 (t, 1H, aromatic major), 3.13 (m, 1H, C*H*Me$_2$ major), 2.98 (m, 0.12H, C*H*Me$_2$ minor), 2.18 (s, 3H, MoCHC*Me*$_2$Ph major), 1.83 (s, 0.72H, C*Me*$_2$Ph minor), 1.58 (s, 3H, C*Me*$_2$Ph major), 1.03 (d, 3H, CH*Me*$_2$ major), 0.96 (d, 0.36H, CH*Me*$_2$ minor), 0.74 (d, 3H, CH*Me*$_2$ major), 0.44 (d, 0.36H, CH*Me*$_2$ minor); ^{13}C NMR (100 MHz, CD_2Cl_2) δ 331.9 (*syn* Mo*C*H), 160.9, 159.2, 155.5, 155.4, 153.5, 152.9, 152.8, 152.3, 151.6, 151.3, 149.3, 148.6, 148.5, 148.4, 147.3, 146.0, 145.9, 143.7, 143.3, 142.8, 141.9, 131.7, 130.9, 130.2, 130.0, 129.7, 129.5, 128.7, 128.0, 127.9, 127.8, 127.4, 127.3, 127.0, 126.9, 126.7, 126.6, 126.6, 126.4, 125.5, 125.4, 124.1, 123.3, 121.7, 118.6, 155.4, 58.6, 58.3, 30.8, 30.4, 29.7, 29.5, 29.3, 23.7, 23.6, 23.5, 22.8; ^{19}F NMR (376 MHz, CD_2Cl_2) δ -

77.3 (s, 0.5F, *cis*), - 79.1 (s br, 0.12F, *trans*), - 79.4 (s, 0.5F, *cis*). Anal. Calcd $C_{31}H_{31}F_6MoN_3O_6S_2$: C, 45.65; H, 3.83; N, 5.15. Found: C, 45.89; H, 3.90; N, 4.92.

Mo(NAr^{tBu})(CHCMe$_2$Ph)(OTf)$_2$(bipy) (7) The procedure is identical to the synthesis of **5**, employing Mo(NAr^{tBu})(CHCMe$_2$Ph)(OTf)$_2$(DME) (0.543 g, 0.711 mmol) and bipyridine (0.111 g, 0.711 mmol); yield 0.450 g of a red solid (76%): ^{1}H NMR (400 MHz, CD_2Cl_2) δ 14.52 (s, 1H, Mo=C*H*, J_{CH} = 125.1 Hz, major), 13.94 (s, 0.13H, Mo=C*H*, minor), 9.55 (dd, 0.13H, bipy minor), 8.97 (dd, 0.28H, aromatic minor), 8.84 (dd, 1H, bipy major), 8.50-6.80 (overlapping peaks, 18H, aromatics), 2.18 (s, 3H, C*Me*$_2$Ph major), 1.91 (s, 0.42H, C*Me*$_2$Ph minor), 1.64 (s, 0.42H, C*Me*$_2$Ph minor), 1.57 (s, 3H, C*Me*$_2$Ph major), 1.15 (s, 9H, *t*-Bu major), 0.98 (s, 1.26H, *t*-Bu minor); ^{13}C NMR (100 MHz, CD_2Cl_2) δ 331.6 (*syn* MoCH), 159.9, 159.5, 155.5, 155.4, 153.7, 153.6, 152.5, 150.5, 148.7, 147.4, 147.3, 147.2, 147.1, 143.7, 143.5, 142.8, 142.5, 141.9, 141.3, 134.0, 133.0, 130.1, 129.8, 129.5, 129.1, 128.7, 128.2, 127.8, 127.7, 127.4, 127.3, 126.9, 126.8, 124.0, 123.6, 123.2, 122.8, 121.6, 118.5, 58.8, 58.1, 35.7, 35.1, 31.2, 30.8, 30.6, 29.2. Anal. Calcd $C_{32}H_{33}F_6MoN_3O_6S_2$: C, 46.32; H, 4.01; N, 5.06. Found: C, 46.42; H, 4.21; N, 5.01.

Mo(NAr^M)(CHCMe$_2$Ph)(OTf)$_2$(bipy) (8). The procedure is identical to the synthesis of **2**, employing Mo(NAr^M)(CHCMe$_2$Ph)(OTf)$_2$DME (0.215 g, 0.260 mmol) and bipy (0.041 g, 0.263 mmol); yield 0.170 g of a green solid (73%): ^{1}H NMR (400 MHz, CD_2Cl_2) δ 14.3 (s, 1H, MoC*H* J_{CH} = 128 Hz major), 13.9 (s, 0.03H, MoC*H* minor), 8.64 (d, 1H, aromatic), 8.29 (d, 1H, aromatic), 8.11 (t, 1H, aromatic), 8.00 (d, 1H, aromatic), 7.88 (d, 2H, aromatic), 7.59, (t, 1H, aromatic), 7.49 (d, 2H, aromatic), 7.46 (t, 1H, aromatic), 7.41 (t, 2H, aromatic), 7.31 (dd, 2H, aromatic), 6.77 (d, 2H, aromatic), 6.69 (dd, 1H, aromatic), 6.153 (s, 1H, Mes), 5.901 (s, 1H, Mes), 2.38 (s, 3H, MoCHC*Me*$_2$Ph), 1.97 (s, 3H, MoCHC*Me*$_2$Ph), 1.78 (s, 3.27H, Mes), 1.57 (s, 3H, Mes), 0.99 (s, 3H, Mes); ^{13}C NMR (100 MHz, C_6D_6) δ 329.7 (*syn*, MoCH), 329.3 (MoCH), 158.1, 154.3, 153.1, 152.2, 148.0, 146.5, 141.2, 140.8, 138.3, 136.7, 135.7, 135.3, 134.1, 132.1, 130.4, 129.4, 129.2, 129.0, 128.7, 128.2, 128.0, 127.9, 127.2, 126.9, 126.8, 126.6, 126.0, 125.8, 125.6, 123.5, 123.5, 122.9, 120.9, 118.4, 58.4, 30.3, 29.6, 20.8, 20.6, 19.6; ^{19}F NMR (376 MHz, CD_2Cl_2) δ -77.1 (s, 1F, *cis*), - 78.6 (s, 0.06, *trans*), - 79.5 (s br, 1F, *cis*). Anal. Calcd $C_{37}H_{35}F_6MoN_3O_6S_2$: C, 49.83; H, 3.96; N, 4.71. Found: C, 50.01; H, 3.96; N, 4.56.

Mo(NAr)(CHCMe$_2$Ph)(Pyr)$_2$(bipy) (9) *Method A:* [Mo(NAr)(CHCMe$_2$Ph)(Pyr)$_2$]$_2$ (0.100 g, 0.187 mmol) was dissolved in Et_2O and bipy (0.029 g, 0.186 mmol) was added. The solution was stirred for 2 h. The precipitate was collected and dried by vacuum filtration to yield 0.058 g of an orange solid (45%) *Method B:* **2** (1.11 g, 1.29 mmol) was suspended in Et_2O and $LiNC_4H_4$ (0.189 g, 2.59 mmol) was added in one portion. The solution was left stirring for 12 hours at RT

and the orange precipitate was collected and dried by vacuum filtration to yield 0.549 g (61%). X-ray quality crystals were obtained by crystallization from 1:1 CH_2Cl_2:*n*-pentane at -35 °C for 48 hours: ^{1}H NMR (400 MHz, CD_2Cl_2) δ 13.87 (s, 1H, MoC*H*, J_{CH} = 116.3 Hz), 9.26 (d, 1H, aromatic), 9.00 (d, 1H, aromatic), 8.20-8.08 (overlapping peaks, 2H, aromatics), 7.83 (d, 1H, aromatics), 7.75-.7.57 (overlapping peaks, 4H, aromatics), 7.44-7.32 (overlapping peaks, 3H, aromatics), 7.30-7.20 (overlapping peaks, 2H, aromatics), 7.20-7.14 (overlapping peaks, 2H, aromatics), 5.89 (s, 4H, NC_4H_4), 5.61 (s, 4H, NC_4H_4), 3.48 (m, 2H, C*H*Me$_2$), 1.94 (s, 6H, MoCHC*Me*$_2$Ph), 0.98 (d, 6H, CH*Me*$_2$), 0.90 (d, 6H, CH*Me*$_2$); ^{13}C NMR (100 MHz, CD_2Cl_2) δ 316.9 (Mo=*C*H), 153.5, 151.9, 151.5, 151.4, 150.7, 148.4, 141.2, 139.4, 134.3, 128.9, 128.3, 126.9, 126.8 126.4, 124.1, 123.5, 122.9, 106.8, 57.2, 31.9, 27.7, 26.2, 24.0. Anal. Calcd $C_{40}H_{45}MoN_5$: C, 69.45; H, 6.56; N, 10.12. Found: C, 69.45; H, 6.41; N, 10.02.

Mo(NAd)(CHCMe$_2$Ph)(Pyr)$_2$(bipy) (10) *Method A*: The procedure is the same as the synthesis of **9**, employing [Mo(NAd)(CHCMe$_2$Ph)(Pyr)$_2$]$_2$ (0.488 g, 0.958 mmol) and bipy (0.150 g, 0.960 mmol) to yield a yellow solid (0.478 g, 75%). *Method C*: Mo(NAd)(CHCMe$_2$Ph)(OTf)$_2$(DME) (0.353 g, 0.462 mmol) was dissolved in toluene (15.0 ml) and cooled down to – 35 °C for 1 h. Then, $LiNC_4H_4$ (0.067 g, 0.918 mmol) was added in one portion and the mixture was allowed to stir at RT for 2 h, during which time salts precipitated out. The salts were removed by filtering the solution through celite and washing with toluene until colorless. Finally, bipy (0.067 g, 0.429 mmol) was added to the solution and the mixture was allowed to stir at RT overnight. Collection and drying of the resulting precipitate by vacuum filtration yielded a yellow solid (0.101 g, 36%): ^{1}H NMR (400 MHz, CD_2Cl_2) δ 13.99 (s, 1H, MoC*H*), 13.40 (s, 1H, MoC*H*), 12.97 (s, 0.9H, MoC*H*), 9.53 (dd, 1H, bipy), 9.00 (dd, 0.9H, bipy), 8.69 (dd, 1H, bipy), 8.61 (dd, 0.9H, bipy), 8.10-7.85 (overlapping peaks, 11.9H, aromatics), 7.65-6.70 (overlapping peaks, 22.1H, aromatics), 6.24 (t, 4H, NC_4H_4), 6.20 (t, 4H, NC_4H_4), 6.15 (t, 4H, NC_4H_4), 6.06 (t, 1.6H, NC_4H_4), 6.04 (t, 1.6H, NC_4H_4), 5.67 (t, 4H, NC_4H_4), 5.55 (t, 1.6H, NC_4H_4), 5.54 (t, 1.6H, NC_4H_4), 2.40-1.30 (overlapping peaks, 61H, aliphatics). Anal. Calcd $C_{38}H_{43}MoN_5$: C, 68.56; H, 6.51; N, 10.52. Found: C, 68.33; H, 6.61; N, 10.62. ^{13}C NMR could not be obtained due to the insolubility of complex.

Mo(NAr')(CHCMe$_2$Ph)(Pyr)$_2$(bipy) (11) *Method B*: The procedure is the same as the synthesis of **9** employing **4** (0.108 g, 0.135 mmol) and $LiNC_4H_4$ (0.020 g, 0.274 mmol) to yield 0.066 g of a yellow solid (77%). *Method C*: The procedure is the same as the synthesis of **10** employing Mo(NAr')(CHCMe$_2$Ph)(OTf)$_2$(DME) (0.307 g, 0.418 mmol), $LiNC_4H_4$ (0.061 g, 0.835 mmol) and bipy (0.052 g, 0.333 mmol) to get a yellow solid (0.205 g, 96%): ^{1}H NMR (400 MHz, CD_2Cl_2) δ 13.78 (s, 1H, MoC*H*), 9.39 (d, 1H, bipy), 8.90 (d, 1H, bipy), 8.18-8.10

(overlapping peaks, 2H, aromatic), 7.96 (d, 1H, aromatic), 7.87 (m, 1H, aromatic), 7.63-7.55 (overlapping peaks, 3H, aromatic), 7.50 (m, 1H, aromatic), 7.24 (t, 2H, aromatic), 7.10-6.93 (overlapping peaks, 5H, aromatic), 5.93 (s, 4H, NC_4H_4), 5.58 (s, 4H, NC_4H_4), 2.03 (s, 6H, Ar' *Me*), 1.85 (s, 6H, $MoCHCMe_2Ph$). Anal. Calcd $C_{36}H_{37}MoN_5$: C, 68.02; H, 5.87; N, 11.02. Found: C, 67.86; H, 5.66; N, 11.04. ^{13}C NMR could not be obtained due to insolubility of the complex.

$Mo(NAr^{Cl})(CHCMe_3)(Pyr)_2(bipy)$ (12) *Method C*: The procedure is the same as the synthesis of **10**, employing $Mo(NAr^{Cl})(CHCMe_2Ph)(OTf)_2(DME)$ (0.304 g, 0.410 mmol), $LiNC_4H_4$ (0.060 g, 0.822 mmol) and bipy (0.051 g, 0.327 mmol) to yield 0.184 g of orange-yellow **12** (87%): ^1H NMR (400 MHz, CD_2Cl_2) δ 13.57 (s, 1H, MoC*H*), 12.66 (s, 0.2H, MoC*H*), 9.50 (dd, 1H, bipy), 8.97 (dd, 1H, bipy), 8.18-7.86 (overlapping peaks, 5H, aromatics), 7.58 (m, 2H, CMe_2Ph), 7.46 (dd, 2H, CMe_2Ph), 7.40-7.35 (overlapping peaks, 1H, CMe_2Ph minor isomer), 7.28-6.90 (overlapping peaks, 8H, aromatics), 6.39 (t, 0.2H, NC_4H_4), 6.17 (t, 4H, NC_4H_4), 6.06 (t, 0.2H, NC_4H_4), 5.93 (t, 0.2H, NC_4H_4), 5.73 (t, 0.2H, NC_4H_4), 5.67 (t, 4H, NC_4H_4), 2.34 (s, 1.2H, CMe_2Ph minor isomer), 1.76 (s, 6H, CMe_2Ph minor isomer). Anal. Calcd $C_{34}H_{32}ClMoN_5$: C, 63.60; H, 5.02; N, 10.91. Found: C, 63.39; H 5.05; N 10.67. ^{13}C NMR could not be obtained due to insolubility of complex.

$Mo(NAr^{iPr})(CHCMe_2Ph)(Pyr)_2(bipy)$ (13) *Method B*: The procedure is the same as the synthesis of **9**, employing **6** (1.100 g, 1.35 mmol) and $LiNC_4H_4$ (0.197 g, 2.70 mmol) to yield 0.680 g of a yellow solid (85%). *Method C*: The procedure is the same as the synthesis of **10**, employing $Mo(NAr^{iPr})(CHCMe_2Ph)(OTf)_2(DME)$ (0.323 g, 0.431 mmol), $LiNC_4H_4$ (0.063 g, 0.863 mmol), and bipy (0.054 g, 0.346 mmol) to get 0.215 g of yellow **13** (96%): ^1H NMR (400 MHz, CD_2Cl_2) δ 13.61 (s, 1H, MoC*H* major isomer), 12.75 (s, 0.1H, MoC*H* minor isomer), 9.47 (dd, 1H, bipy), 8.93 (dd, 1H, bipy), 8.85 (d, 0.1H, bipy), 8.66 (d, 0.2H, CMe_2Ph), 8.42 (d, 0.2H, CMe_2Ph), 8.12 (m, 0.2H, aromatic), 8.60-7.94 (overlapping peaks, 2H, aromatic), 7.86-7.76 (overlapping peaks, 2H, aromatic), 7.58-7.44 (overlapping peaks, 4H, aromatic), 7.38-7.10 (overlapping peaks, 8H, aromatic), 7.00-6.88 (overlapping peaks, 1H, aromatic), 6.18 (t, 0.2H, NC_4H_4), 6.09 (t, 4H, NC_4H_4), 6.01 (t, 0.2H, NC_4H_4), 5.93 (t, 0.2H, NC_4H_4), 5.76 (t, 0.2H, NC_4H_4), 5.68 (t, 4H, NC_4H_4), 3.69 (m, 0.1H, $CHMe_2$), 3.55 (m, 1H, $CHMe_2$), 1.87 (s, 0.3H, CMe_2Ph), 1.79 (s, 6H, CMe_2Ph), 1.47 (s, 0.3H, CMe_2Ph), 1.07 (d, 6H, $CHMe_2$), 0.95 (d, 6H, $CHMe_2$), 0.85 (d, 6H, $CHMe_2$). Anal. Calcd $C_{37}H_{39}MoN_5$: C, 68.40; H, 6.05; N, 10.78. Found: C, 68.30; H, 6.04; N, 10.56. ^{13}C NMR could not be obtained due to insolubility of complex.

Mo(NAr^{tBu})(CHCMe$_2$Ph)(Pyr)$_2$(bipy) (14) *Method C*: The procedure is the same as the synthesis of **10**, employing Mo(NAr^{tBu})(CHCMe$_2$Ph)(OTf)$_2$(DME) (0.150 g, 0.196 mmol), LiNC$_4$H$_4$ (0.029 g, 0.397 mmol), and bipy (0.024 g, 0.154 mmol) to get 0.025 g of yellow **14** (24%): ^{1}H NMR (400 MHz, CD_2Cl_2) δ 13.72 (s, 1H, MoC*H*), 9.33 (dd, 1H, bipy), 9.04 (dd, 1H, bipy), 8.12-8.08 (overlapping peaks, 2H, aromatic), 7.96 (d, 1H, aromatic), 7.88 (td, 1H, aromatic), 7.60-7.56 (overlapping peaks, 3H, aromatic), 7.50 (m, 1H, aromatic), 7.40 (dd, 1H, aromatic), 7.36-7.30 (overlapping peaks, 2H, aromatic), 7.24-7.15 (overlapping peaks, 4H, aromatic), 7.10 (td, 1H, aromatic), 5.96 (d, 4H, NC$_4$*H*$_4$), 5.62 (d, 4H, NC$_4$*H*$_4$), 1.84 (s, 6H, C*Me*$_2$Ph), 1.34 (s, 9H, *t*-Bu). Anal. Calcd $C_{38}H_{41}MoN_5$: C, 68.77; H, 6.23; N, 10.55. Found: C, 68.82; H, 6.24; N, 10.37. ^{13}C NMR could not be obtained due to insolubility of complex.

Mo(NAr^M)(CHCMe$_2$Ph)(Pyr)$_2$(bipy) (15) *Method C*: The procedure is the same as the synthesis of **10**, employing Mo(NAr^M)(CHCMe$_2$Ph)(OTf)$_2$(DME) (0.320 g, 0.388 mmol), LiNC$_4$H$_4$ (0.057 g, 0.781 mmol), and bipy (0.048 g, 0.307 mmol) to get 0.167 g of orange **15** (74%): ^{1}H NMR (400 MHz, CD_2Cl_2) δ 13.97 (s, 1H, MoC*H* major isomer), 13.39 (s, 0.7H, MoC*H*), 12.54 (s, 0.4H, MoC*H* minor isomer), 9.38 (dd, 0.7H, bipy), 8.94 (dd, 0.7H, bipy), 8.71 (dd, 0.7H, aromatic), 8.10-6.70 (overlapping peaks, 37.8H, aromatic), 6.35 (m, 0.8H, NC$_4$*H*$_4$ minor isomer), 6.15 (t, 2H, NC$_4$*H*$_4$ major isomer), 6.08 (m, 0.8H, NC$_4$*H*$_4$ minor isomer), 5.94 (m, 0.8H, NC$_4$*H*$_4$ minor isomer), 5.90 (t, 2H, NC$_4$*H*$_4$ major isomer), 5.77 (t, 2.8H, NC$_4$*H*$_4$), 5.70 (m, 0.8H, NC$_4$*H*$_4$ minor isomer), 5.56 (t, 2.8H, NC$_4$*H*$_4$), 5.39 (m, 2H, NC$_4$*H*$_4$ major isomer), 5.33-5.31 (m, 2H, NC$_4$*H*$_4$ major isomer), 2.46 (s, 1.2H, aliphatic minor isomer), 2.34 (s, 1.2H, aliphatic minor isomer), 2.27 (s, 2.1H, aliphatic), 2.16-2.12 (overlapping peaks, 4.2H, aliphatic major + minor isomers), 2.07 (s, 1.2H, aliphatic minor isomer), 2.03 (s, 2.1H, aliphatic), 2.01 (s, 2.1H, aliphatic), 1.80 (s, 6H, aliphatic major isomer), 1.79 (s, 3H, aliphatic major isomer), 1.71 (s, 1.2H, aliphatic minor isomer), 1.54 (s, 3H, aliphatic major isomer), 1.17 (s, 4.2H, aliphatic) Anal. Calcd $C_{43}H_{43}MoN_5$: C, 71.16; H, 5.97; N, 9.65. Found: C, 70.84; H, 5.86; N, 9.41. ^{13}C NMR could not be obtained due to insolubility of complex.

Mo(NAr)(CHCMe$_2$Ph)(Pyr)(OHMT) (16) **9** (0.156 g, 0.226 mmol), HMTOH (0.074 g, 0.224 mmol), and $ZnCl_2$(dioxane) (0.055 g, 0.245 mmol) were placed in a 25 mL Schlenk flask (Teflon-sealed cap) and toluene was added until all solids were at the bottom of the flask (10.0 mL). The flask was sealed and sonicated at RT for 4 h. Then, the solution was filtered through Celite and the salts rinsed with toluene. The solvent was removed from the filtrate and the crude was redissolved in pentane and passed through a second plug of Celite, and the salts were washed with pentane. The solvent was removed and the crude dissolved in a minimal amount of pentane before placing at -35 °C for 2 days. **16** was obtained as red crystals upon filtration; yield

0.083 g (46%): ^{1}H NMR (400 MHz, C_6D_6) δ 11.72 (s, 1, MoC*H* J_{CH} = 125.5 Hz), 7.20-7.12 (overlapping peaks, 5H, aromatic), 7.50-6.90 (overlapping peaks, 10H, aromatic), 6.83 (t, 2H, NC_4H_4), 6.78 (t, 2H, NC_4H_4), 3.30 (m, 2H, C*H*Me$_2$), 2.16 (s, 6H, Mes), 2.10 (s, 6H, Mes), 2.04 (s, 6H, Mes), 1.51 (s, 3, C*Me*$_2$Ph), 1.46 (s, 3, C*Me*$_2$Ph), 1.11 (d, 6H, CH*Me*$_2$), 1.03 (d, 6H, CH*Me*$_2$); ^{13}C NMR (100 MHz, C_6D_6) δ 293.3 (Mo*C*H), 158.2, 153.7, 148.5, 145.9, 136.8, 136.7, 136.6, 135.9, 132.6, 132.2, 130.0, 129.0, 128.9, 128.4, 127.3, 126.4, 126.2, 123.0, 110.2, 55.7, 31.1, 30.5, 28.6, 24.3, 23.4, 21.1, 20.9, 20.5. Anal. Calcd $C_{50}H_{58}MoN_2O$: C, 75.17; H, 7.32; N, 3.51. Found: C, 75.16; H, 7.21; N, 3.66.

Mo(NAd)(CHCMe$_2$Ph)(Pyr)(OHMT) (17) The procedure is the same as the synthesis of **16**, employing **10** (0.113 g, 0.170 mmol), HMTOH (0.056 g, 0.169 mmol), and $ZnCl_2$(dioxane) (0.038 g, 0.169 mmol) to yield 0.084 g of yellow crystalline solid (64%). Characterization of this compound has appeared before in the literature and here we give only proton NMR as a reference: ^{1}H NMR (500 MHz, C_6D_6) δ 11.04 (s, 1H, MoC*H*, J_{CH} = 121.8 Hz), 7.28-6.75 (overlapping peaks, 12 H, aromatics), 6.73 (t, 2H, NC_4H_4), 6.50 (t, 2H, NC_4H_4), 2.20 (s, 6H, Mes), 2.04 (s, 6H, Mes), 2.02 (s, 6H, Mes), 1.78 (br t, 3H NAd), 1.66 (s, 3H, CHC*Me*$_2$Ph), 1.62 (br, 3H, NAd), 1.53 (br, 3H, NAd), 1.48 (s 3H, CHC*Me*$_2$Ph), 1.38 (brs, 6H, NAd).

Mo(NAr')(CHCMe$_2$Ph)(Pyr)(OHMT) (18) The procedure is the same as the synthesis of **16**, employing **11** (0.200 g, 0.315 mmol), HMTOH (0.115 g, 0.348 mmol), and $ZnCl_2$(dioxane) (0.080 g, 0.356 mmol) to yield 0.185 g of yellow solid (79%): ^{1}H NMR (500 MHz, C_6D_6) δ 11.53 (s, 1H, MoC*H* J_{CH} = 123.0 Hz), 7.15 (d, 2H, MoCHCMe$_2$*Ph*), 7.07 (t, 2H, MoCHCMe$_2$*Ph*), 7.00-6.92 (overlapping peaks, 4H, aromatic), 6.75-6.68 (overlapping peaks, 9H, aromatic), 6.47 (m, 2H, NC_4H_4), 2.11 (s, 6H, HMTO), 2.05 (s, 6H, HMTO), 2.00 (s, 6H, HMTO), 1.94 (s, 6H, Mo=N*Ar'*), 1.44 (s, 3H, MoCHC*Me*$_2$Ph), 1.36 (s, 3H, MoCHC*Me*$_2$Ph); ^{13}C NMR (125 MHz, C_6D_6) δ 291.3 (*syn*, Mo*C*H), 158.1, 155.9, 148.4, 136.9, 136.8, 136.7, 135.8, 135.4, 132.2, 132.0, 128.7, 129.2, 128.6, 127.2, 126.5, 126.3, 122.8, 110.3, 30.7, 29.8, 21.1, 21.0, 20.8, 20.5, 18.9, 18.2. Anal. Calcd $C_{46}H_{50}MoN_2O$: C, 74.37; H, 6.78; N, 3.77. Found: C, 74.53; H, 6.85; N, 3.74.

Mo(NAr^{Cl})(CHCMe$_2$Ph)(Pyr)(OHMT) (19) The procedure is the same as the synthesis of **16**, employing **12** (0.100 g, 0.156 mmol), HMTOH (0.052 g, 0.157 mmol), and $ZnCl_2$(dioxane) (0.035 g, 0.156 mmol) to yield 0.055 g of yellow solid (47%): ^{1}H NMR (400 MHz, C_6D_6) δ 11.53 (s, 1H, MoC*H* J_{CH} = 126.3 Hz), 7.19 (dd, 2H, CMe$_2$*Ph*), 7.08 (td, 2H CMe$_2$*Ph*), 7.00-6.78 (overlapping peaks, 6H, aromatic), 6.76 (t, 2H, NC_4H_4), 6.72 (s, 2H, Mes), 6.69 (s, 2H, Mes), 6.63 (td, 1H, aromatic), 6.51 (td, 1H, aromatic), 6.46 (t, 2H, NC_4H_4), 2.06-1.97 (overlapping

peaks, 18H, Mes), 1.53 (s, 3H, C*Me*$_2$Ph), 1.42 (s, 3H, C*Me*$_2$Ph); ^{13}C NMR (100 MHz, C_6D_6) δ 291.7 (*syn*, Mo*C*H), 157.9, 153.6, 148.4, 137.3, 137.1, 136.8, 136.6, 136.4, 135.3, 132.2, 132.1, 129.9, 129.5, 129.4, 129.3, 129.0, 128.8, 128.6, 128.4, 126.7, 126.3, 123.2, 110.3, 54.6, 34.4, 30.9, 29.5, 22.7, 21.9, 20.8, 20.5, 14.3. Anal. Calcd $C_{44}H_{45}ClMoN_2O$: C, 70.53; H, 6.05; N, 3.74. Found: C, 70.29; H, 5.91; N, 3.83.

Mo(NAr^{iPr})(CHCMe$_2$Ph)(Pyr)(OHMT) (20) The procedure is the same as the synthesis of **16**, employing **13** (0.157 g, 0.242 mmol), HMTOH (0.080 g, 0.242 mmol), and $ZnCl_2$(dioxane) (0.054 g, 0.242 mmol) to yield 0.077 g of yellow crystalline solid (42%). This crystalline material was used to get the X-ray structure of **20**: ^{1}H NMR (400 MHz, C_6D_6) δ 11.46 (s, 1H, Mo*CH* J_{CH} = 123.9 Hz), 7.25-6.65 (overlapping peaks, 16H, aromatic), 6.58 (t, 2H, NC$_4$*H*$_4$), 6.39 (t, 2H, NC$_4$*H*$_4$), 3.18 (m, 1H, C*H*Me$_2$), 2.09-2.02 (overlapping peaks, 18H, Mes), 1.53 (s, 3H, C*Me*$_2$Ph), 1.45 (s, 3H, C*Me*$_2$Ph), 0.93 (d, 6H, CHC*Me*$_2$).); ^{13}C NMR (100 MHz, C_6D_6) δ 289.0 (*syn*, Mo*C*H), 158.1, 155.1, 148.5, 146.1, 137.2, 137.1, 136.8, 136.5, 135.4, 133.8, 131.9, 131.9, 129.9, 129.6, 129.2, 128.8, 128.6, 128.5, 127.4, 126.3, 125.7, 125.5, 122.8, 110.0, 54.9, 31.5, 30.2, 28.1, 24.3, 22.5, 21.2, 20.9, 20.5, 20.4. Anal. Calcd $C_{47}H_{52}MoN_2O$: C, 74.58; H, 6.92; N, 3.70. Found: C, 74.16; H, 6.86; N, 3.35.

Mo(NAr^{tBu})(CHCMe$_2$Ph)(Pyr)(OHMT) (21) The procedure is the same as the synthesis of **16**, employing **14** (0.119 g, 0.179 mmol), HMTOH (0.059 g, 0.179 mmol), and $ZnCl_2$(dioxane) (0.040 g, 0.178 mmol) to yield 0.050 g of yellow crystalline solid (36%): ^{1}H NMR (400 MHz, C_6D_6) δ 11.30 (s, 1H, Mo*CH*, J_{CH} = 122.8 Hz), 7.19 (dd, 2H, CMe$_2$*Ph*), 7.12 (dd, 2H, CMe$_2$*Ph*), 7.06 (dd, 1H, CMe$_2$*Ph*), 7.30-6.80 (overlapping peaks, 7H, aromatic), 6.69 (s, 4, Mes), 6.66 (td, 2H, NC$_4$*H*$_4$), 6.44 (td, 2H, NC$_4$*H*$_4$), 2.07 (s, 6H, Mes), 2.02 (s, 6H, Mes), 2.01 (s, 6H, Mes), 1.58 (s, 3H, C*Me*$_2$Ph), 1.44 (s, 3H, C*Me*$_2$Ph), 1.19 (s, 9H, *t*-Bu); ^{13}C NMR (100 MHz, C_6D_6) δ 288.9 (*syn*, Mo*C*H), 158.0, 156.0, 148.6, 144.4, 136.7, 136.3, 135.3, 133.3, 132.0, 132.0, 129.6, 129.4, 128.5, 126.8, 126.4, 126.3, 126.2, 125.9, 122.9, 110.0, 55.5, 35.3, 34.4, 31.6, 30.4, 30.2, 22.7, 21.2, 20.9, 20.3. Anal. Calcd $C_{48}H_{54}MoN_2O$: C, 74.78; H, 7.06; N, 3.63. Found: C, 74.63; H, 6.91; N, 3.42.

Mo(NAr^{M})(CHCMe$_2$Ph)(Pyr)(OHMT) (22) The procedure is the same as the synthesis of **16**, employing **15** (0.100 g, 0.138 mmol), HMTOH (0.046 g, 0.139 mmol), and $ZnCl_2$(dioxane) (0.031 g, 0.138 mmol) to yield 0.037 g of yellow crystalline solid (33%): ^{1}H NMR (400 MHz, C_6D_6) δ 11.00 (s, 1H, Mo*CH*, J_{CH} = 121.7 Hz), 7.20-7.10 (overlapping peaks, 3H, aromatic), 7.06-6.84 (overlapping peaks, 8H, aromatic), 6.78-6.56 (overlapping peaks, 7H, aromatic), 6.19 (t, 2H, NC$_4$*H*$_4$), 5.97 (t, 2H, NC$_4$*H*$_4$), 2.18 (s, 3H, NAr^M Mes), 2.04 (s, 6H, OHMT Mes), 2.01 (s,

6H, OHMT Mes), 1.99 (s, 6H, OHMT Mes), 1.90 (s, 3H, NAr^M Mes), 1.85 (s, 3H, NAr^M Mes), 1.55 (s, 3H, C*Me*$_2$Ph), 1.45 (s, 3H, C*Me*$_2$Ph); ^{13}C NMR (100 MHz, C_6D_6) δ 286.1 (*syn*, Mo*C*H), 158.1, 155.5, 148.3, 137.0, 136.6, 136.5, 136.4, 135.9, 135.5, 135.3, 135.2, 131.7, 131.3, 130.6, 129.8, 129.6, 128.9, 128.8, 128.5, 127.2, 126.5, 126.4, 126.4, 109.0, 54.3, 31.2, 30.2, 21.2, 21.2, 21.0, 20.7, 20.6, 20.3. Anal. Calcd $C_{53}H_{56}MoN_2O$: C, 76.42; H, 6.78; N, 3.36. Found: C, 76.41; H, 6.81; N, 3.32.

Mo(NAr)(≡CCMe$_2$Ph)(NC$_4$H$_2$Me$_2$)(bipy) (23) Mo(NAr)(CHCMe$_2$Ph)(NC$_4$H$_2$Me$_2$)$_2$ (0.500 g, 0.840 mmol), bipy (0.131 g, 0.839 mmol) and benzene (5.00 mL) were placed in a 25.0 mL Schlenk flask and sealed with a Teflon-seal cap. The mixture was heated at 60 °C for 18 h and then cooled down to RT. The solvent was removed under vacuum and the crude was triturated with pentane and filtered-off to yield 0.252 g of purple solid (46%). X-ray quality crystals were obtained by crystallization from 1:7 CH_2Cl_2:*n*-pentane at -35 °C for 48 hours: ^{1}H NMR (600 MHz, C_6D_6) δ 8.11 (dd, 1H, bipy), 7.34 (dd, 2H, CMe$_2$*Ph*), 7.13 (t, 1H, aromatic), 7.08 (m, 1H, aromatic), 6.99 (dd, 2H, CMe$_2$*Ph*), 6.78-6.64 (overlapping peaks, 8H, aromatic), 6.47 (dd, 1H, aromatic), 6.44 (td, 1H, NC$_4$*H*$_2$Me$_2$), 6.18 (td, 1H, NC$_4$*H*$_2$Me$_2$), 4.35 (m, 2H, C*H*Me$_2$), 3.17 (s, 3H, NC$_4$H$_2$*Me*$_2$), 2.59 (s, 3H, NC$_4$H$_2$*Me*$_2$), 1.74 (s, 3H, C*Me*$_2$Ph), 1.39 (d, 6H, CH*Me*$_2$), 1.32 (s, 3H, C*Me*$_2$Ph), 1.14 (d, 6H, CH*Me*$_2$). Anal. Calcd $C_{38}H_{44}MoN_4$: C, 69.92; H, 6.79; N, 8.58. Found: C, 69.63; H, 6.59; N, 8.36. ^{13}C NMR could not be obtained due to insolubility of complex.

Mo(NAr')(≡CCMe$_2$Ph)(NC$_4$H$_2$Me$_2$)(bipy) (24) The procedure is the same as the synthesis of **23**, employing Mo(NAr')(CHCMe$_2$Ph)(NC$_4$H$_2$Me$_2$)$_2$ (0.221 g, 0.413 mmol) and bipy (0.065 g, 0.416 mmol) to yield 0.147 g of purple solid (60%). X-ray quality crystals were obtained by crystallization from 1:7 CH_2Cl_2:*n*-pentane at -35 °C for 48 hours: ^{1}H NMR (600 MHz, C_6D_6) δ 8.16 (dd, 1H, bipy), 7.22 (d, 2H, CMe$_2$*Ph*), 7.05 (d, 1H, aromatic), 6.99 (d, 2H, aromatic), 6.93 (td, 1H, aromatic), 6.80 (dd, 1H, aromatic), 6.77-6.64 (overlapping peaks, 7H, aromatic), 6.46 (d, 2H, NC$_4$*H*$_2$Me$_2$), 6.01 (td, 1H, aromatic), 3.16 (s, 3H, NC$_4$H$_2$*Me*$_2$), 2.52 (s, 3H, NC$_4$H$_2$*Me*$_2$), 1.93 (s, 6H, NAr' Me), 1.78 (s, 3H, C*Me*$_2$Ph), 1.33 (s, 3H, C*Me*$_2$Ph). Anal. Calcd $C_{34}H_{36}MoN_4$: C, 6845; H, 6.08; N, 9.39. Found: C, 68.35; H, 6.07; N, 9.38. ^{13}C NMR could not be obtained due to insolubility of complex.

Mo(NAr^{CF3})(≡CCMe$_3$)(NC$_4$H$_2$Me$_2$)(bipy) (25) The procedure is the same as the synthesis of **23**, employing Mo(NAr^{CF3})(CHCMe$_3$)(NC$_4$H$_2$Me$_2$)$_2$ (0.374 g, 0.728 mmol) and bipy (0.114 g, 0.730 mmol) to yield 0.290 g of purple solid (69%): ^{1}H NMR (600 MHz, C_6D_6) δ 8.95 (dd, 1H, bipy), 8.16 (dd, 1H, aromatic), 7.63 (m, 1H, aromatic), 7.21 (td, 1H, aromatic), 6.90-6.60

(overlapping peaks, 7H, aromatic), 6.43 (t, 2H, $NC_4H_2Me_2$), 6.39 (dd, 1H, aromatic), 6.25 (d, 2H, $NC_4H_2Me_2$), 3.11 (s, 3H, $NC_4H_2Me_2$), 2.62 (s, 3H, $NC_4H_2Me_2$), 1.12 (s, 9H, *t*-Bu). Anal. Calcd $C_{28}H_{29}F_3MoN_4$: C, 58.54; H, 5.09; N, 9.75. Found: C, 58.38; H, 5.11; N, 9.63. ^{13}C NMR could not be obtained due to insolubility of complex.

Mo(NAr^{iPr})(≡CCMe$_2$Ph)(NC$_4$H$_2$Me$_2$)(bipy) (26) (NAr^{iPr})(CHCMe$_2$Ph)(NC$_4$H$_2$Me$_2$)$_2$ (0.255 g, 0.464 mmoles) and bipy (0.073 g, 0.467 mmoles) in a 1:1 toluene/pentane mixture (7.00 ml) were stirred at RT for 12 h, during which time a red precipitate formed. Filtration yielded 0.244 g of red-purple solid (86%): ^1H NMR (600 MHz, CD_2Cl_2) δ 8.45 (dd, 1H, bipy), 8.14 (dd, 1H, aromatic), 8.09 (dd, 1H, aromatic), 8.02 (td, 1H, aromatic), 7.87 (td, 1H, aromatic), 7.44 (dd, 1H, aromatic), 7.40 (m, 1H, aromatic), 7.18 (dd, 1H, aromatic), 7.14 (m, 1H, aromatic), 7.01 (m, 1H, aromatic), 6.93 (dd, 2H, CMe_2Ph), 6.90-6.88 (overlapping peaks, 5H, aromatic), 5.91 (dd, 1H, $NC_4H_2Me_2$), 5.75 (t, 2H, $NC_4H_2Me_2$), 3.50 (m, 1H, $CHMe_2$), 2.49 (s, 3H, $NC_4H_2Me_2$), 2.15 (s, 3H, $NC_4H_2Me_2$), 1.56 (s, 3H, CMe_2Ph), 1.34 (s, 3H, CMe_2Ph), 1.06 (d, 3H, $CHMe_2$), 0.85 (d, 3H, $CHMe_2$). Anal. Calcd $C_{35}H_{38}MoN_4$: C, 68.84; H, 6.27; N, 9.18. Found: C, 68.46; H, 6.18; N, 9.03. ^{13}C NMR could not be obtained due to insolubility of complex.

Mo(NAr^{M})(≡CCMe$_2$Ph)(NC$_4$H$_2$Me$_2$)(bipy) (27) Mo(NAr^{M})(CHCMe$_2$Ph)(NC$_4$H$_2$Me$_2$)$_2$ (0.052 g, 0.083 mmol) and bipy (0.013 g, 0.083 mmol) were dissolved in C_6H_6, placed in a 25.0 mL Schlenk flask, and sealed with a teflon cap. The mixture was left heating at 60 °C for 2 days and then it was cooled down to RT, the solvent was removed under vacuo and the product recrystallized from Et_2O at – 35 °C to yield 0.030 g of dark purple solid product (53%): ^1H NMR (400 MHz, C_6D_6) δ 8.1 (d, 1H, aromatic), 7.7 (d, 1H, aromatic), 7.50-6.00 (m, 17H, aromatics), 5.90 (s, 2H, $Me_2C_4H_2N$), 2.50-1.20 (br singlets, 21H, aliphatics). Anal. Calcd $C_{39}H_{37}MoN_3$: C, 71.71; H, 6.16; N, 8.16. Found: C, 71.61; H, 6.15; N, 8.18. ^{13}C NMR could not be obtained due to insolubility of complex.

Mo(NAr^{T})(≡CCMe$_3$)(NC$_4$H$_2$Me$_2$)(bipy) (28) The procedure is the same as the synthesis of **27**, employing Mo(NAr^{T})(CHCMe$_3$)(NC$_4$H$_2$Me$_2$)$_2$ (0.053 g, 0.082 mmol) and bipy (0.013 g, 0.082 mmol) to yield 0.040 g of crystalline purple solid (69%). A small portion of these crystals were used for X-ray chemical structure determination: ^1H NMR (400 MHz, C_6D_6) δ 8.4 (m, 1H, aromatic), 8.1 (m, 2H, aromatic), 7.80 (m, 3H, aromatic), 7.50 (m, 1H, aromatic), 7.25 (m, 3H, aromatic), 7.05 (m, 1H, aromatic), 6.95 (m, 3H, aromatic), 6.88 (m, 1H, aromatic), 6.82 (m, 2H, aromatic), 6.60 (m, 2H, aromatic), 5.65 (s, 2H, $Me_2C_4H_2N$), 2.90 (m, 3H, $CHMe_2$), 2.28 (s, 3H, $Me_2C_4H_2N$), 2.20 (s, 3H, $Me_2C_4H_2N$), 1.2 (d, 3H, *i*-Pr), 0.94 (s, 9H, *t*-Bu), 0.87 (d, 3H, *i*-Pr), 0.75

(d, 3H, *i*-Pr). Anal. Calcd $C_{39}H_{37}MoN_3$: C, 71.17; H, 7.39; N, 7.90. Found: C, 70.81; H, 7.47; N, 7.91. ^{13}C NMR could not be obtained due to insolubility of complex.

General procedure for ROMP of DCMNBD MAP catalyst (0.005 g) is dissolved in 0.500 ml of toluene while 50 equivalents of the monomer are dissolved in 0.700 ml of toluene and stirred in a separate vial. To the monomer vial the catalyst solution is added quickly and left stirring for 2 h until it forms a gel. The reaction is then quenched with 0.500 mL of benzaldehyde and some methylene chloride is added to solubilize the gel. This solution is stirred for another hour, at which point the solution is added to a 100 mL RBF containing 50.0-70.0 mL MeOH stirring vigorously. The polymer precipitates instantly and it is collected by filtration after 1 h of stirring. The dry polymer is examined by ^1H and ^{13}C NMR to determine the *tacticity* and *cis* content according to known literature reports.

X-ray Crystallographic Procedures

Low-temperature diffraction data (*ø*- and *ω*-scans) were collected on a Bruker-AXS X8 Kappa Duo diffractometer coupled to a Smart Apex2 CCD detector with Mo K_α radiation (λ = 0.71073 Å) from a Si-monochromated sealed tube for compounds **9**, **23**, and **24**, on a Bruker D8 three circle diffractometer coupled to a Bruker-AXS Smart Apex CCD detector with graphite-monochromated Cu K_α radiation (λ = 1.54178 Å) for the structure of compound **28**, and on a Bruker-AXS X8 Kappa Duo diffractometer coupled to a Smart Apex2 CCD detector with Mo K_α radiation (λ = 0.71073 Å) from a *IμS* micro-source for the structure of compound **20**.

For all structures, data reduction was performed with the program SAINT,[15] absorption correction and scaling were performed with the program SADABS.[16] The structures were solved by direct methods using SHELXS[17] and refined against F^2 on all data by full-matrix least squares with SHELXL-97,[18] following established refinement strategies.[19] All non-hydrogen atoms were refined anisotropically. Unless noted otherwise below, all hydrogen atoms were included into the model at geometrically calculated positions and refined using a riding model. The isotropic displacement parameters of all hydrogen atoms were constrained to 1.2 times the U_{eq} value of the atoms they are linked to (1.5 times for methyl groups). Crystal and structural refinement results are listed in Tables 2-6.

Description of Structure of **9**

Compound **1a** crystallizes in the monoclinic space group *C*2/c with one molecule of **1a** and one molecule of dichloromethane in the asymmetric unit. Coordinates for the hydrogen atom on C11 which binds directly to Mo, were taken from the difference Fourier synthesis. This hydrogen atom was subsequently refined semi-freely with the help of distance restraints

while constraining their U_{iso} to 1.2 times the U_{eq} value of the atoms they are linked to. Phenyl ring on one of the ligands and the solvent dichloromethane were modeled as a two part disorder. The disorder was refined with the help of similarity restraints on 1-2 and 1-3 distances and displacements parameters as well as rigid bond restraints for anisotropic displacement parameters. The ratio between the two components was refined freely and converged at 0.498(10) and 0.447(10), respectively.

Description of Structure of **20**

Compound **20** crystallizes in the triclinic space group $P\bar{1}$ with two molecules of **20** in the asymmetric unit. Coordinates for the hydrogen atoms on carbon binding directly to Mo, C1 and C101, respectively, were taken from the difference Fourier synthesis. Those hydrogen atoms were subsequently refined semi-freely with the help of distance restraints while constraining their U_{iso} to 1.2 times the U_{eq} value of the atoms they are linked to. The structure contains two independent molecules (Z=4); bond lengths are identical within one to three standard uncertainties and for discussion parameters from the first independent molecule were used.

Description of Structure of **23**

Compound **23** crystallizes in the monoclinic space group $P2_1/n$ with one molecule of **23** in the asymmetric unit.

Description of Structure of **24**

Compound **24** crystallizes in the monoclinic space group $P2_1/c$ with one molecule of **24** in the asymmetric unit.

Description of Structure of **28**

Compound **28** crystallizes in the monoclinic space group $P2_1/c$ with two molecules of **28** and six molecules of benzene in the asymmetric unit (Z=8). One of the ligands on the second molecule was modeled as a two part disorder and all structural parameters discussed in the paper refer to the un-distorted molecule. The disorder was refined with the help of similarity restraints on 1-2 and 1-3 distances and displacements parameters as well as rigid bond restraints for anisotropic displacement parameters. The ratio between the two components was refined freely and converged at 0.647(10).

Table 2. Crystal data and structure refinement for **9**.

Identification code	(C40H45MoN5)(CH2Cl2)	
Empirical formula	C41 H47 Cl2 Mo N5	
Formula weight	776.68	
Temperature	130(2) K	
Wavelength	0.71073 Å	
Crystal system	Monoclinic	
Space group	C2/c	
Unit cell dimensions	a = 15.8436(8) Å	α= 90°
	b = 14.1814(7) Å	β= 94.318(3)°
	c = 34.0620(16) Å	γ= 90°
Volume	7631.5(6) $Å^3$	
Z	8	
Density (calculated)	1.352 Mg/m^3	
Absorption coefficient	0.519 mm^{-1}	
F(000)	3232	
Crystal size	0.04 x 0.03 x 0.02 mm^3	
Theta range for data collection	1.93 to 26.00°	
Index ranges	-19<=h<=19, -17<=k<=17, -41<=l<=40	
Reflections collected	71876	
Independent reflections	7486 [R(int) = 0.1135]	
Completeness to theta = 26.00°	99.9 %	
Absorption correction	Semi-empirical from equivalents	
Max. and min. transmission	0.9897 and 0.9795	
Refinement method	Full-matrix least-squares on F^2	
Data / restraints / parameters	7486 / 67 / 489	
Goodness-of-fit on F^2	1.007	
Final R indices [I>2sigma(I)]	R1 = 0.0416, wR2 = 0.0775	
R indices (all data)	R1 = 0.0759, wR2 = 0.0888	
Extinction coefficient	na	
Largest diff. peak and hole	0.410 and -0.496 $e.Å^{-3}$	

Table 3. Crystal data and structure refinement for **20**.

Identification code	x11172	
Empirical formula	C47 H52 Mo N2 O	
Formula weight	756.85	
Temperature	100(2) K	
Wavelength	0.71073 Å	
Crystal system	Triclinic	
Space group	$P\bar{1}$	
Unit cell dimensions	a = 10.6943(6) Å	α= 94.8550(10)°
	b = 11.4798(6) Å	β= 91.9520(10)°
	c = 34.8506(19) Å	γ= 111.2780(10)°
Volume	3962.9(4) $Å^3$	
Z	4	
Density (calculated)	1.269 Mg/m^3	
Absorption coefficient	0.368 mm^{-1}	
F(000)	1592	
Crystal size	0.20 x 0.20 x 0.15 mm^3	
Theta range for data collection	1.18 to 30.32°	
Index ranges	-15<=h<=15, -16<=k<=16, -49<=l<=49	
Reflections collected	181235	
Independent reflections	23780 [R(int) = 0.0322]	
Completeness to theta = 30.32°	99.9 %	
Absorption correction	Semi-empirical from equivalents	
Max. and min. transmission	0.9469 and 0.9301	
Refinement method	Full-matrix least-squares on F^2	
Data / restraints / parameters	23780 / 2 / 945	
Goodness-of-fit on F^2	1.114	
Final R indices [I>2sigma(I)]	R1 = 0.0328, wR2 = 0.0758	
R indices (all data)	R1 = 0.0374, wR2 = 0.0783	
Largest diff. peak and hole	0.959 and -0.838 $e.Å^{-3}$	

Table 4. Crystal data and structure refinement for **23**.

Identification code	C38H44MoN4	
Empirical formula	C38 H44 Mo N4	
Formula weight	652.71	
Temperature	100(2) K	
Wavelength	0.71073 Å	
Crystal system	Monoclinic	
Space group	$P2_1/n$	
Unit cell dimensions	a = 11.2310(10) Å	α= 90°
	b = 18.7037(18) Å	β= 97.074(6)°
	c = 15.8997(15) Å	γ= 90°
Volume	3314.5(5) $Å^3$	
Z	4	
Density (calculated)	1.308 Mg/m^3	
Absorption coefficient	0.428 mm^{-1}	
F(000)	1368	
Crystal size	0.13 x 0.10 x 0.07 mm^3	
Theta range for data collection	1.69 to 28.00°	
Index ranges	-14<=h<=14, -24<=k<=22, -21<=l<=20	
Reflections collected	58456	
Independent reflections	8003 [R(int) = 0.0972]	
Completeness to theta = 28.00°	100.0 %	
Absorption correction	Semi-empirical from equivalents	
Max. and min. transmission	0.9707 and 0.9465	
Refinement method	Full-matrix least-squares on F^2	
Data / restraints / parameters	8003 / 0 / 390	
Goodness-of-fit on F^2	1.018	
Final R indices [I>2sigma(I)]	R1 = 0.0475, wR2 = 0.1082	
R indices (all data)	R1 = 0.0858, wR2 = 0.1274	
Extinction coefficient	na	
Largest diff. peak and hole	1.474 and -1.162 $e.Å^{-3}$	

Table 5. Crystal data and structure refinement for **24**.

Identification code	C34H36MoN4	
Empirical formula	C34 H36 Mo N4	
Formula weight	596.61	
Temperature	100(2) K	
Wavelength	0.71073 Å	
Crystal system	Monoclinic	
Space group	$P2_1/c$	
Unit cell dimensions	a = 14.9819(3) Å	α= 90°
	b = 11.6518(3) Å	β= 107.7250(10)°
	c = 17.4969(4) Å	γ = 90°
Volume	2909.37(12) $Å^3$	
Z	4	
Density (calculated)	1.362 Mg/m^3	
Absorption coefficient	0.480 mm^{-1}	
F(000)	1240	
Crystal size	0.12 x 0.04 x 0.03 mm^3	
Theta range for data collection	1.43 to 27.49°	
Index ranges	-18<=h<=19, -14<=k<=15, -22<=l<=22	
Reflections collected	63038	
Independent reflections	6668 [R(int) = 0.0434]	
Completeness to theta = 27.49°	99.8 %	
Absorption correction	Semi-empirical from equivalents	
Max. and min. transmission	0.9857 and 0.9446	
Refinement method	Full-matrix least-squares on F^2	
Data / restraints / parameters	6668 / 0 / 356	
Goodness-of-fit on F^2	1.034	
Final R indices [I>2sigma(I)]	R1 = 0.0242, wR2 = 0.0549	
R indices (all data)	R1 = 0.0339, wR2 = 0.0587	
Extinction coefficient	na	
Largest diff. peak and hole	0.386 and -0.323 $e.Å^{-3}$	

Table 6. Crystal data and structure refinement for **28**.

Identification code	d10116	
Empirical formula	C60 H70 Mo N4	
Formula weight	943.14	
Temperature	100(2) K	
Wavelength	1.54178 Å	
Crystal system	Monoclinic	
Space group	$P2_1/c$	
Unit cell dimensions	a = 25.0928(4) Å	α= 90°
	b = 25.8149(4) Å	β= 108.0810(10)°
	c = 17.2021(3) Å	γ= 90°
Volume	10592.7(3) $Å^3$	
Z	8	
Density (calculated)	1.183 Mg/m^3	
Absorption coefficient	2.321 mm^{-1}	
F(000)	4000	
Crystal size	0.30 x 0.20 x 0.10 mm^3	
Theta range for data collection	1.85 to 69.31°	
Index ranges	-30<=h<=30, -31<=k<=31, -20<=l<=19	
Reflections collected	200905	
Independent reflections	19616 [R(int) = 0.0398]	
Completeness to theta = 69.31°	99.0 %	
Absorption correction	Semi-empirical from equivalents	
Max. and min. transmission	0.8011 and 0.5427	
Refinement method	Full-matrix least-squares on F^2	
Data / restraints / parameters	19616 / 2996 / 1398	
Goodness-of-fit on F^2	1.223	
Final R indices [I>2sigma(I)]	R1 = 0.0652, wR2 = 0.1714	
R indices (all data)	R1 = 0.0708, wR2 = 0.1744	
Largest diff. peak and hole	3.266 and -1.408 $e.Å^{-3}$	

REFERENCES

1. (a) Schrock, R. R. *Chem. Rev.* **2009**, *109*, 3211. (b) Schrock, R. R. *Chem. Rev.* **2002**, *102*, 145. (c) Schrock, R. R.; Hoveyda, A. H. *Agnew. Chem. Int. Ed.* **2003**, *42*, 4592. (d) Schrock, R. R.; Czekelius, C. C. *Adv. Syn. Catal.* **2007**, *349*, 55.
2. Schaverien, C. J.; Dewan, J. C.; Schrock, R. R. *J. Am. Chem. Soc.* **1986**, *108*, 2771.
3. (a) Singh, R.; Schrock, R. R.; Müller, P.; Hoveyda, A. H. *J. Am. Chem. Soc.* **2007**, *129*, 12654. (b) Marinescu, S. C.; Schrock, R. R.; Li, B.; Hoveyda, A. H. *J. Am. Chem. Soc.* **2009**, *131*, 58. (c) Malcomson, S. J.; Meek, S. J.; Sattely, E. S.; Schrock, R. R.; Hoveyda, A. H. *Nature* **2008**, *456*, 933. (d) Sattely, E. S.; Meek, S. J.; Malcolmson, S. J.; Schrock, R. R.; Hoveyda, A. H. *J. Am. Chem. Soc.* **2009**, *131*, 943. (e) Ibrahem, I; Yu, M.: Schrock, R. R.; Hoveyda, A. H. *J. Am. Chem. Soc.* **2009**, *131*, 3844. (f) Jiang, A. J.; Simpson, J. H.; Müller, P.; Schrock, R. R. *J. Am. Chem. Soc.* **2009**, *131*, 7770. (g) Meek, S. J.; Malcomson, S. J.; Li, R.; Schrock, R. R.; Hoveyda, A. H. *J. Am. Chem. Soc.* **2009**, *131*, 16407. (h) Jiang, A. J.; Zhao, Y.; Schrock, R. R.; Hoveyda, A. H. *J. Am. Chem. Soc.* **2009**, *131*, 16630. (i) Flook, M. M.; Jiang, A. J.; Schrock, R. R.; Müller, P.; Hoveyda, A. H. *J. Am. Chem. Soc.* **2009**, *131*, 7962. (j) Lee, Y.-J.; Schrock, R. R.; Hoveyda, A. H. *J. Am. Chem. Soc.* **2009**, *131*, 10652. (k) Marinescu, S. C.; Schrock, R. R.; Müller, P.; Hoveyda, A. H. *J. Am. Chem. Soc.* **2009**, *131*, 10840. (l) Gerber, L. C.; Schrock, R. R.; Müller, P.; Takase, K. M. *J. Am. Chem. Soc.* **2011**, *133*, 18142.
4. (a) Hock, A. S.; Schrock, R. R.; Hoveyda, A. H. *J. Am. Chem. Soc.* **2006**, *128*, 16373. (b) Singh, R; Czekelius, C.; Schrock, R. R.; Müller, P. *Organometallics*, **2007**, *26*, 2528. (c) Marinescu, S. C.; Singh, R.; Hock, A. S.; Wampler, K. M.; Schrock, R. R.; Müller, P. *Organometallics* **2008**, *27*, 6570. (d) King, A. J. H. Ph.D. Thesis, 2010, Massachusetts Institute of Technology.
5. (a) Flook, M. M.; Ng, V. W. L.; Schrock, R. R. *J. Am. Chem. Soc.* **2011**, *133*, 1784. (b) Flook, M. M. Ph.D. Thesis, 2011, Massachusetts Institute of Technology.
6. Heppekausen, J.; Fürstner, A. *Angew. Chem. Int. Ed.* **2011**, *50*, 1.
7. (a) Schrock, R. R. *Acc. Chem. Res.* **1986**, *19*, 342. (b) Murdzek, J. S.; Schrock, R. R. in *Carbyne Complexes* VCH Publishers: Weinheim, New York, 1988, p. 147. (c) Schrock, R. R. in *Handbook of Metathesis*, Grubbs, R. H., Ed., Wiley-VCH, Weinheim, 2003, p. 173. (d) Guggenberger, L. J.; Schrock, R. R.; Churchill, M. R.; Wasserman, H. J. *Organometallics* **1982**, *1*, 1332. (e) Schrock, R. R.; Jamieson, J. Y.; Araujo, J. P.; Bonitatebus, P. J., Jr.; Sinha, A.; Lopez, L. P. H. *Jour. Organomet. Chem.* **2003**, *684*, 56. (f) Clark, D. N.; Schrock, R. R. *J. Am. Chem. Soc.* **1978**, *100*, 6774. (g) Schrock, R. R.; Clark, D. N.; Sancho, J.; Wengrovius, J. H.; Rocklage, S. M.; Pedersen, S. F. *Organometallics* **1982**, *1*, 1645. (h) Edwards, D. S.; Biondi, L. V.; Ziller, J. W.; Churchill, M. R.; Schrock, R. R.

Organometallics **1983**, *2*, 1505. (i) Schrock R. R.; Weinstock, I. A.; Horton, A. D.; Liu, A. H.; Schofield, M. H. *J. Am. Chem. Soc.* **1988**, *110*, 2686. (j) Weinstock, I. A.; Schrock, R. R.; Davis, W. M. *J. Am. Chem. Soc.* **1991**, *113*, 135. (k) Toreki, R.; Schrock, R. R. *J. Am. Chem. Soc.* **1990**, *112*, 2448. (l) Toreki, R.; Schrock, R. R.; Davis, W. M. *J. Am. Chem. Soc.* **1992**, *114*, 3367. (m) Rocklage, S. M.; Schrock, R. R.; Churchill, M. R.; Wasserman, H. J. *Organometallics* **1982**, *1*, 1332. (n) Schaverien, C. J.; Dewan, J. C.; Schrock, R. R. *J. Am. Chem. Soc.* **1986**, *108*, 2771. (o) Schrock, R. R.; Fellmann, J. D. *J. Am. Chem. Soc.* **1978**, *100*, 3359. (p) Rupprecht, G. A.; Messerle, L. W.; Fellmann, J. D.; Schrock, R. R. *J. Am. Chem. Soc.* **1980**, *102*, 6236.

8. Deiter, T. *Z. Anorg. Allgem. Chem.* **1971**, *384*, 136.
9. Hatch, L. F.; Everett, G. D. *J. Org. Chem.* **1968**, *33*, 2551.
10. Stanciu, C.; Olmstead, M. M.; Phillips, A. D.; Stender, M.; Power, P. P. *Eur. J. Inorg. Chem.* **2003**, 3495.
11. Tabor, D. C.; White, F. H.; Collier, L. W.; Evans, S. A. *J. Org. Chem.* **1983**, *48*, 1638-1643.
12. (a) Schrock, R. R.; Murdzek, J. S.; Bazan, G. C.; Robbins, J.; DiMare, M.; O'Regan, M. *J. Am. Chem. Soc.* **1990**, *112*, 3875. (b) Oskam, J. H.; Fox, H. H.; Yap, K. B.; McConville, D. H.; O'Dell, R.; Lichtenstein, B. J.; Schrock, R. R. *J. Organomet. Chem.* **1993**, *459*, 185.
13. (a) Singh, R. Ph.D. Thesis , 2008, Massachusetts Institute of Technology. (b) Lichtscheidl, A. G.; Ng, V. W. L.; Müller, P.; Takase, M. K.; Schrock, R. R. *Organometallics* **2012**, *31*, 2388.
14. Tonzetich, Z. J.; Schrock, R. R.; Müller, P. *Organometallics* **2006**, *25*, 4301.
15. Chambers, J. L. (2005). SAINT 7.23, Bruker-AXS, Inc., Madison, Wisconsin, USA.
16. Sheldrick, G. M. (2006a). SADABS, Bruker AXS, Inc. Madison, Wisconsin, USA.
17. Sheldrick, G. M. (1990). *Acta Cryst.* **A46**, 467-473.
18. Sheldrick, G. M. (2008). *Acta Cryst.* **A64**, 112-122.
19. Müller, P. *Crystallography Reviews* **2009**, *15*, 57-83.

CHAPTER 5

Preparation of Mo(NR)($CHCMe_2Ph$)(X)(Y) Complexes:
Examining the Effect of Sigma and Pi Donor Ligands on Reactivity and Selectivity

INTRODUCTION

DFT calculations performed by Odile Eisenstein provided a picture of the transition states that high-oxidation molybdenum, tungsten, and rhenium catalysts undergo during the course of an olefin-metathesis reaction.[1] It was pointed-out that catalysts of the type M(NR)(CHR')(X)(Y), where X is a good sigma-donor ligand and Y is a poor one, are better catalysts in general than either bisalkoxide or dialkyl analogs. In addition, the study found that catalysts composed of group VI metals (M = Mo, W) were better catalysts than M = Re. According to the calculations the lower activation barriers for olefin coordination and olefin dissociation of M(NR)(CHR')(X)(Y) than for either M(NR)(CHR')$(X)_2$ or M(NR)(CHR')$(Y)_2$ is the key reason for the enhanced reactivity of the X/Y catalysts.

More recently, Eisenstein discussed another DFT result where M(NR)(CHR')(X)$(OSiH_3)$ catalysts containing X = pyrrolide or alkyl were compared.[7] In this case, it was found that the transition states are similar for both complexes. The main differences concern intercoversion of the TBP metallacyclobutane structure and the SP metallacyclobutane structures. When X = alkyl the barrier of interconversion is much higher (~ 20 kcal/mol) than when X = pyr (~ 12 kcal/mol). Nevertheless, if conversion to the SP metallacyclobutane does take place, then the reaction coordinate towards β-H elimination can take place more easily when X = alkyl (Ea ~ 23 kcal/mol) than when X = pyr (Ea ~ 29 kcal/mol). Many other decomposition pathways can follow, but since β-H elimination has the highest activation energy, it is the rate-determining step of decomposition of a metallacyclobutane.

Catalysts investigated in the Schrock and Hoveyda laboratories that contained four different ligands were the monoalkoxidemonopyrrolide (MAP) species, where X = pyrrolide and Y = alkoxide, phenoxide.[2] This type of high-oxidation state molybdenum alkylidene catalyst opened the door to olefin metathesis reactions that were not achievable in the past. These reactions include, but are not limited to, the stereoselective synthesis of natural alkaloids,[3] β-selective enyne RCM,[2,4] *Z*-selective coupling reactions such as ROMP of dicarbomethoxynorbornadiene[5] and cross-coupling of vinylic and allylic substrates. Synthetic access to the first MAP species was possible after it was discovered that Mo(NR)(CHR')$(R"_2Pyr)_2$ precursors[6] can exchange a pyrrolide ligand for an alkoxide/phenoxide through protonolysis of the pyrrolide with one equivalent of a(n) alcohol/phenol[2] or more recently with Mo(NR)(CHR')$(Pyr)_2$(bipy) in the presence of $ZnCl_2$(dioxane) and one equivalent of a bulky phenol (see Chapter 4, Section 4.2).

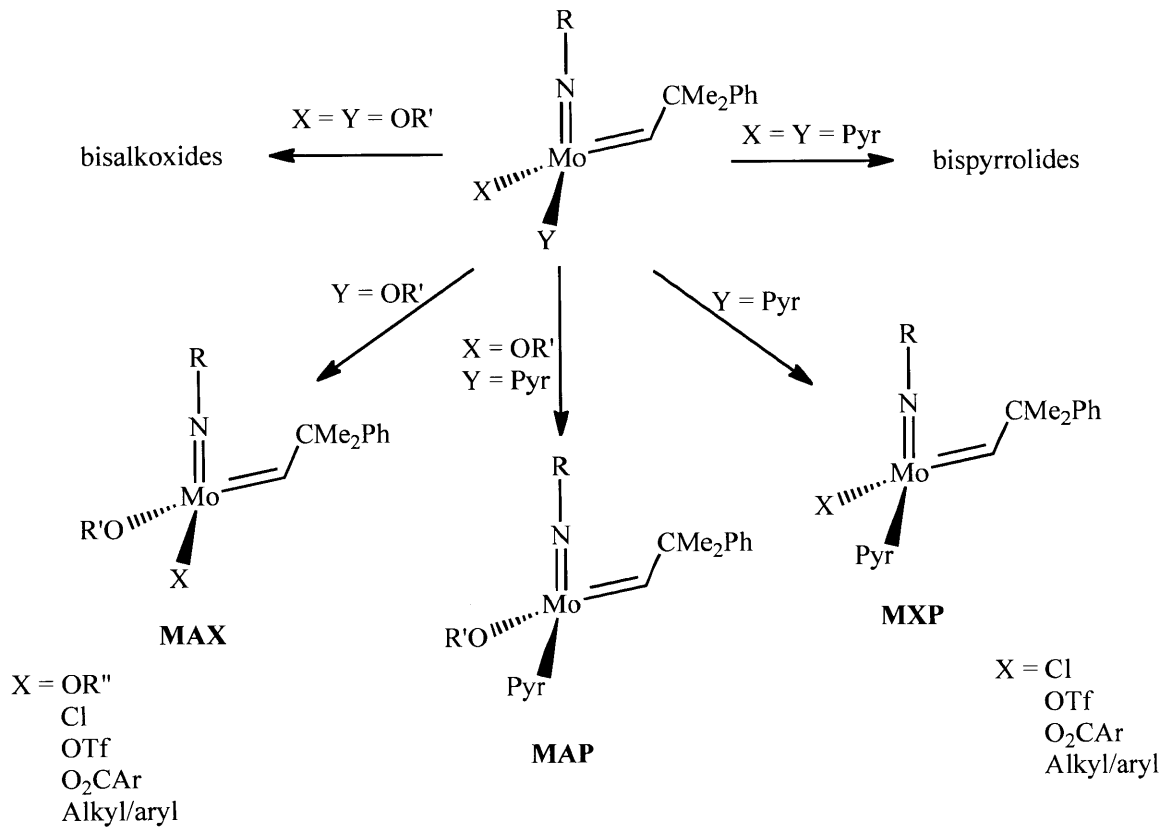

Figure 1 - Possible ligand combinations and their denominations.

Figure 1 depicts the corresponding high-oxidation state molybdenum catalysts that can be generated by changing the X and Y ligands in $Mo(NR)(CHCMe_2Ph)(X)(Y)$. When $X \neq Y$ two broad classes of compounds are those where the common ligand is an alkoxide/phenoxide (MAX) and those where the common ligand is a pyrrolide (MXP). MAP complexes can then be considered to be a shared subunit of all possible MAX and MXP complexes and for clarity we will continue referring to them as MAPs.

Excluding MAPs, many MAX and MXP complexes can be prepared by varying the X ligand. Some of the combinations are given in Figure 1. The only MAX compounds that have been made in the past contain alkyl, chloride, triflate, or alkoxide ligands; while the only MXP class of compounds made contain carboxylate (see Chapter 2, Section 2.2) or triflate ligands.[19] Few MAX and MXP complexes have been prepared, in comparison, to MAP species.

The first MAX catalysts produced by the Schrock group were synthesized from $Mo(NR)(CH_2\text{-}t\text{-}Bu)_3Cl$ complexes by substituting the chloro group with phenoxides and heating the resulting complex to generate $Mo(NR)(CH\text{-}t\text{-}Bu)(CH_2\text{-}t\text{-}Bu)(OAr)$ MAX species where X =

alkyl.[8,9] Similar catalysts with smaller alkoxides or with chloride instead of OAr could not be isolated due to their fast bimolecular decomposition. However, MAX compounds containing a chloro ligand are now known for molybdenum catalysts that contain the very bulky 2,6-dimesitylphenylimido ligand, which is capable of stabilizing the metal complex and which also allows the alkylidene group to be present in the *anti* form (with relation to the imido group) both in solution and the solid state[14].

The first MAX species made which contained a triflate group was achieved by Dr. Marinescu by treating Mo(NAd)(CHCMe$_2$Ph)(OTf)$_2$(DME) with one equivalent of lithium 2,2',4,4',6,6'-hexa*iso*propylterphenoxide (LiOHIPT), which generated Mo(NAd)(CHCMe$_2$Ph)(OTf)(OHIPT) as the final complex[15]. This MAX complex could be used to generate mixed-alkoxide MAX species or new MAP complexes via salt-metathesis of the triflate group with alkoxides or substituted-pyrrolides respectively (Scheme 1).

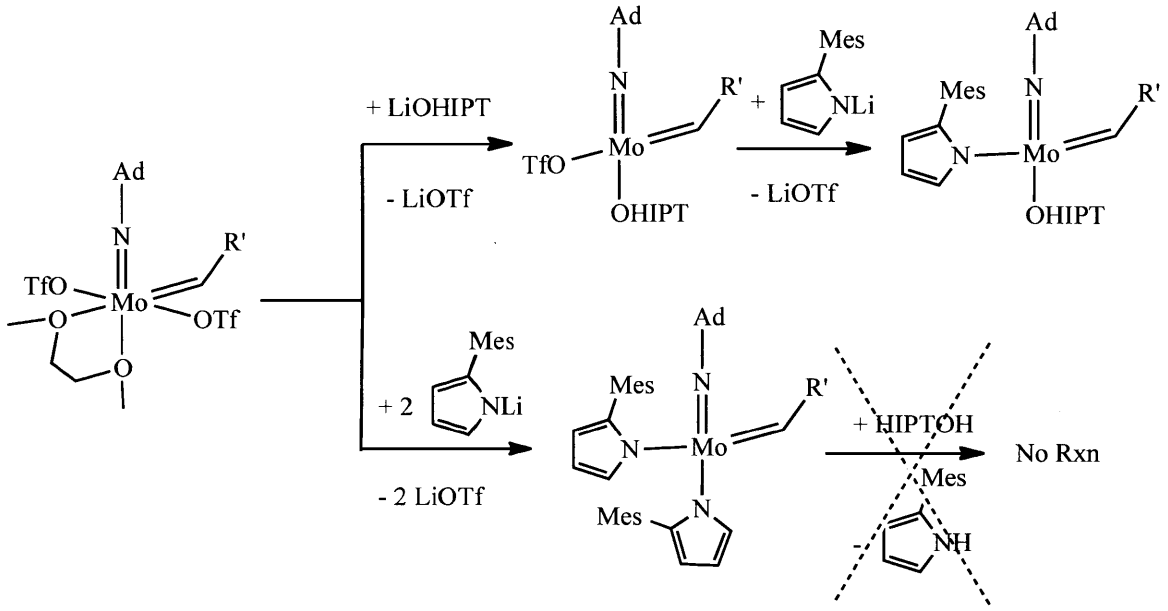

Scheme 1 – Pathways to synthesize Mo(NAd)(CHCMe$_2$Ph)(2-MesC$_4$H$_3$N)(OHIPT).

In this chapter the synthesis and reactivity of new MAX species that contain carboxylate, phenoxide, amide, and aryl ligands will be discussed. Catalytic reactions of all MAX complexes along with their MAP and MXP counterparts will be presented and a few conclusions will be drawn from these data.

RESULTS AND DISCUSSION

5.1 Synthesis, characterization and structural studies of MAX complexes

5.1.1 Reaction between Mo(NR)(CHR')(OTf)$_2$(DME) and lithium salts.

Syntheses of the Mo(NR)(CHR')(OTf)(OHIPT) specie shown in Scheme 1, does not appear to be successful as R is varied. For instance, when Mo(NAr^M)(CHCMe$_2$Ph)(OTf)$_2$DME (Ar^M = 2-mesitylphenyl) and Mo(NAr^T)(CHCMe$_3$)(OTf)$_2$DME (Ar^T = 2-(2',4',6'-triisopropylphenyl) were each treated with one equivalent of LiOHIPT the alkylidene peaks corresponding to the starting materials disappeared over time, but no new alkylidene species was formed. In addition, HIPTOH was formed during the course of the reaction. Similarly, reaction of LiOHIPT with bistriflate complexes containing commercially-available aromatic imido groups render isolation of monotriflate species impractical. It is hypothesized that the presence of the less basic aromatic imido groups could lower the pKa of the alkylidene proton to the point where it is susceptible to deprotonation by a strong base (e.g. HIPTO-) forming an alkylidyne complex. Equation 1 depicts this proposed reaction.

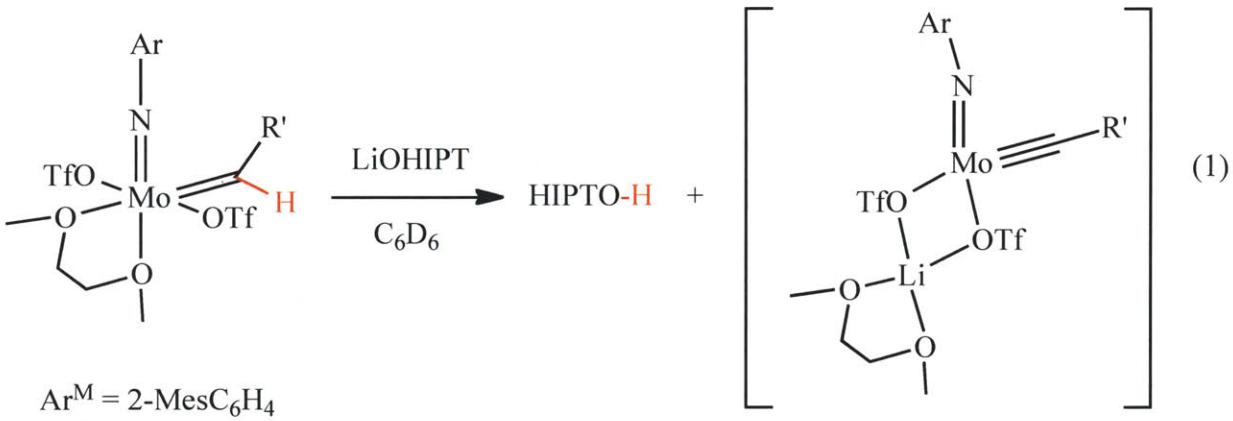

(1)

Ar^M = 2-MesC$_6$H$_4$
Ar^T = 2-TRIPC$_6$H$_4$

Since Mo(NAd)(CHCMe$_2$Ph)(OTf)(OHIPT) can be prepared, analogs that contain the same aliphatic imido ligand were sought. Lithium aryls were chosen mainly because they are intermediates in the synthesis of terphenols like HMTOH (hexamethylterphenol), TIPTOH (tetraisopropylterphenol), and HIPTOH (hexaisopropylterphenol)[10] and can be readily synthesized from the corresponding aryl iodides as shown in equation 2.

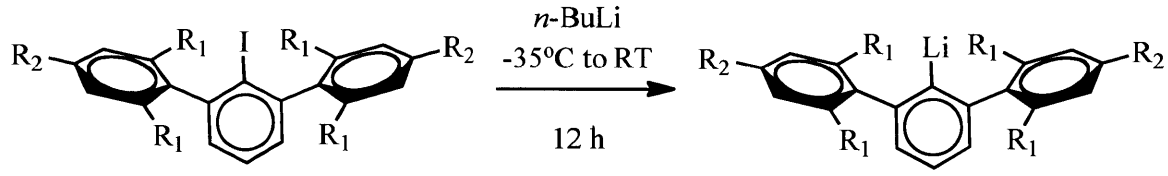

(2)

HMT: $R_1 = R_2 = Me$ (85%)
TIPT: $R_1 = i\text{-Pr}$, $R_2 = H$ (74%)
HIPT: $R_1 = R_2 = i\text{-Pr}$ (74%)

When Mo(NAd)(CHCMe$_2$Ph)(OTf)$_2$DME is treated with one equivalent of HMT-Li, TIPT-Li, or HIPT-Li the alkylidene peak corresponding to the starting material disappears completely, but no new alkylidene is formed. Apparent decomposition is reminiscent of past attempts to make bisamide species with the general formula Mo(NR)(CHR')(NR"$_2$)$_2$ starting from the bistriflate precursor;[12] all were plagued by decomposition reactions which made isolation of the desired species not possible. However, it was later shown that bisamides could be prepared if the triflate groups were replaced with OCMe(CF$_3$)$_2$ groups first.

5.1.2 Reaction between Mo(NAr)(CHCMe$_2$Ph)(OC(CF$_3$)$_2$(CH$_3$))$_2$ and carboxylic acids.

Exchanging triflates with hexafluoro-*t*-butoxides (OR$_{F6}$) via salt-metathesis of the bistriflate affords the classical high-oxidation molybdenum bisalkoxide alkylidene complexes Mo(NR)(CHR')(OR$_{F6}$)$_2$, which when treated with 2 equivalents of LiNPh$_2$ form the corresponding Mo(NR)(CHR')(NPh$_2$)$_2$ complexes without byproduct formation or decomposition. Therefore, Mo(NR)(CHR')(OR$_{F6}$)$_2$ was chosen as the starting point for synthesis of MAX species. It is worth pointing out that it is also possible to protonate the alkoxides with carboxylic acids, something that could not be done with bistriflate complexes.

The reaction between bisalkoxide Mo(NAr)(CHCMe$_2$Ph)(OR$_{F6}$)$_2$ and one equivalent of 2,6-bis(4'-methylphenyl)benzoic acid (Ter$_{Me}$CO$_2$H) yielded the MAX species

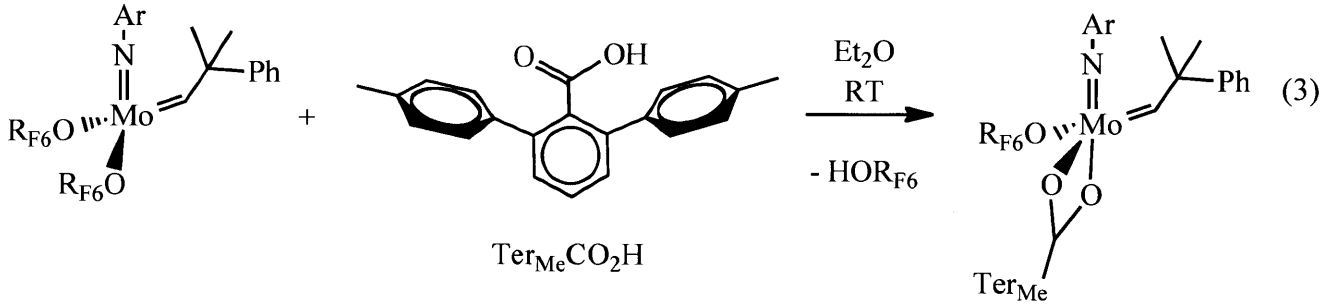

(3)

1 (45 %)

$Mo(NAr)(CHCMe_2Ph)(OR_{F6})(O_2CTer_{Me})$, **1**, in moderate yield as orange crystals (equation 3). The main reason for the low yield is due to formation of biscarboxylate complex. In fact, if the reaction is too concentrated or if the solution containing the carboxylic acid is added too quickly, the yield can be even lower and, in the most extreme case, insufficient to isolate.

The proton NMR spectrum of **1** shows one alkylidene peak at 13.07 ppm and a set of quartets in its ^{19}F NMR spectrum, which is consistent with C_1 symmetry at the metal center. The ^{19}F NMR feature is very characteristic of MAX species that contain only one OR_{F6} ligand and serves as the indicative spectroscopic signature that such species have been made (Figure 2). In particular, ^{19}F NMR is a useful probe during test reactions.

As with the monocarboxylate complexes presented in Chapter 2, MAX complexes that contain carboxylate ligands can only be made when the imido group is 2,6-iPr$_2$C$_6$H$_3$ (Ar). Attempts to make analogous MAX species with smaller imido ligands only yield biscarboxylates as the major products. Reactions with 2,6-bis(2',4',6'-trimethylphenyl)benzoic acid ($HMTCO_2H$) and $Mo(NR)(CHCMe_2Ph)(OR_{F6})_2$ (R = 2,6-dimethylphenyl; 1-adamantyl; 2-isopropyl) also did not yield MAX species. However, although substitution of one OR_{F6} ligand by carboxyates has limited scope the next section reports that a wider variety of complexes can be made through salt-metathesis with phenoxides, amides, and even aryls.

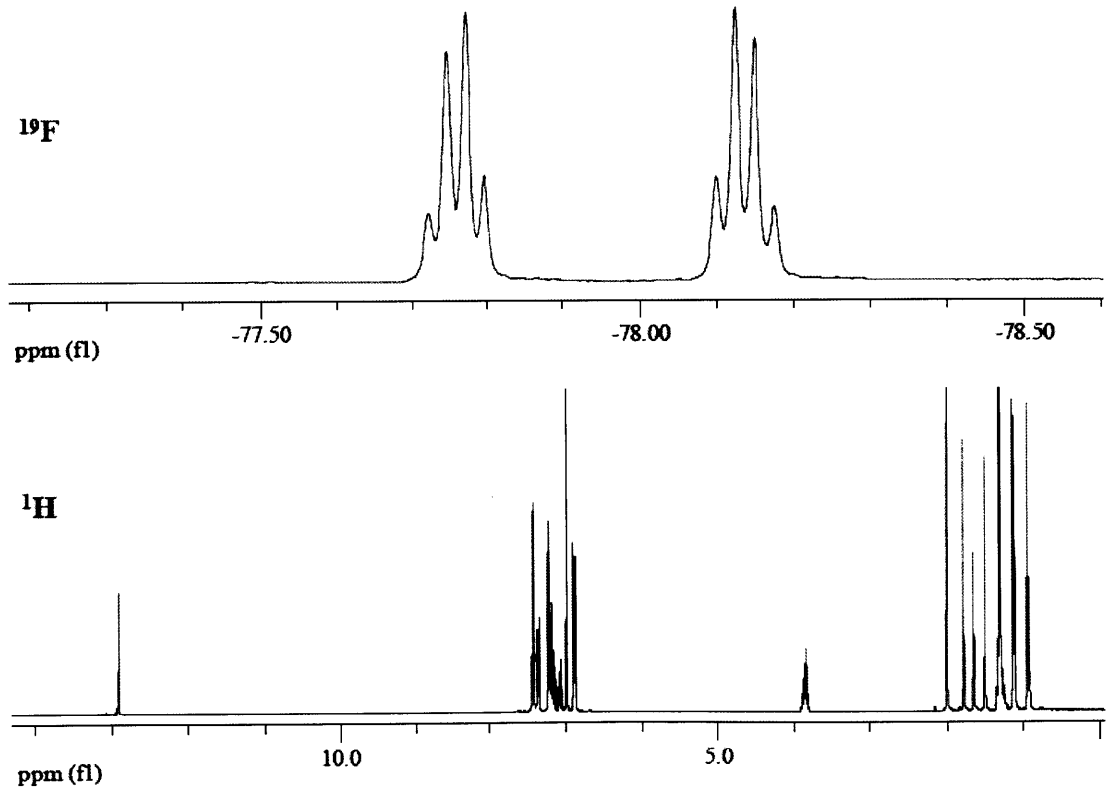

Figure 2 – ^1H NMR (bottom) and ^{19}F NMR (top) spectra of compound **1**.

5.1.3 Reaction between $Mo(NR)(CHCMe_2Ph)(OC(CF_3)_2(CH_3))_2$ and lithium salts.

It was mentioned in Section 5.1.1 that preparation of terphenyl lithium compounds can be prepared easily from the terphenyl iodides by treatment of the latter with *n*-butyl lithium at – 35 °C. In turn, terphenyl lithium derivatives can be turned into terphenols and terphenyl amines. Both terphenols and terphenyl amines have been used in the past in our group (see Chapters 3 and 4, and reference 14). Examples are those that contain a HMT (2,6-dimesityl phenyl) group. LiOHMT, LiN(H)HMT, and LiHMT can all be prepared readily, as shown in Scheme 2.

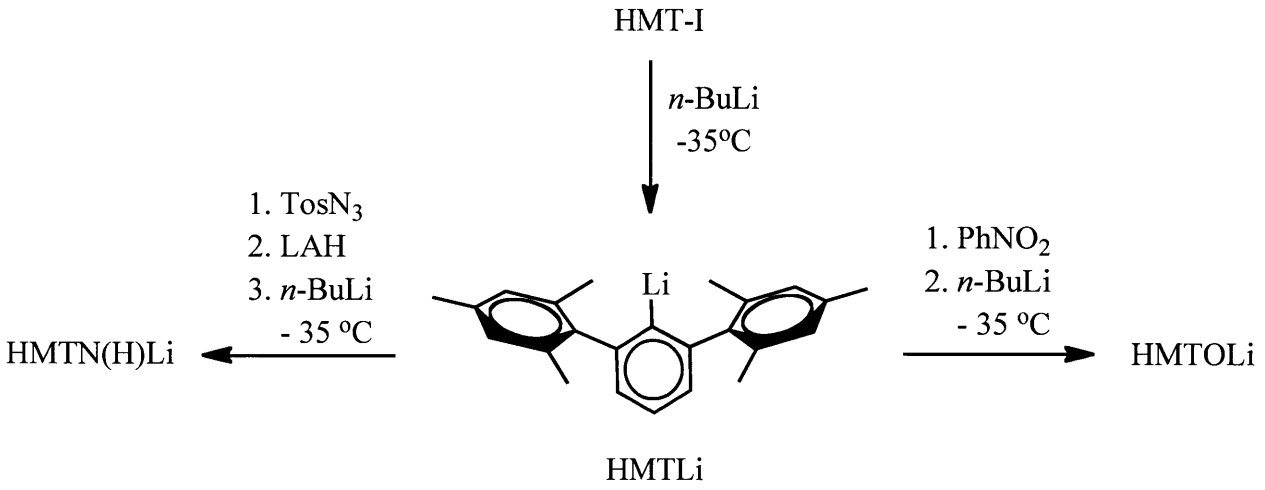

Scheme 2 – Synthesis of HMTLi, HMTOLi and HMTN(H)Li starting from HMT-I.

When bisalkoxide complexes of the general formula $Mo(NR)(CHCMe_2Ph)(OR_{F6})_2$ are treated with one equivalent of HMTOLi, MAX species of the kind $Mo(NR)(CHCMe_2Ph)(OR_{F6})$(OHMT) can be formed for R = Ar (**2**); R = 2,6-$Me_2C_6H_3$ (Ar', **3**); R = 2-*i*PrC_6H_4 (Ar^{iPr}, **4**); and R = 1-adamantyl (Ad, **5**) in moderate to good yields (43-80%, equation 4). Complexes **3-4** can be made without any byproduct formation, but syntheses of complex **2**, which contains the bigger (Ar) imido group is not free from byproducts, as suggested by formation of HMTOH, which is hypothesized to arise through deprotonation of the alkylidene C-H bond. As a result, multiple recrystallizations must be performed to obtain pure **2**, which explains its lower yield compared to the rest of the complexes. Elemental analysis for complex **2** has not been obtained.

The ^{1}H NMR of complexes **2-5** shows a single alkylidene peak present between 11.70 and 11.40 ppm. In addition, a singlet that integrates to three protons and corresponds to one of the methyl resonances appears at around 0.80 ppm (complexes **2-4**) and 1.20 (complex **5**). The ^{19}F NMR of each complex shows a set of quartets, confirming the formation of the desired MAX

species. This synthetic method for preparation of MAX species is a vast improvement over the reaction between bistriflates complexes $Mo(NR)(CHCMe_2Ph)(OTf)_2(DME)$ and LiOHIPT. The analogous reaction between $Mo(NR)(CHCMe_2Ph)(OTf)_2(DME)$ and LiOHMT does not yield OTf/OHMT species for any combination of imido groups.

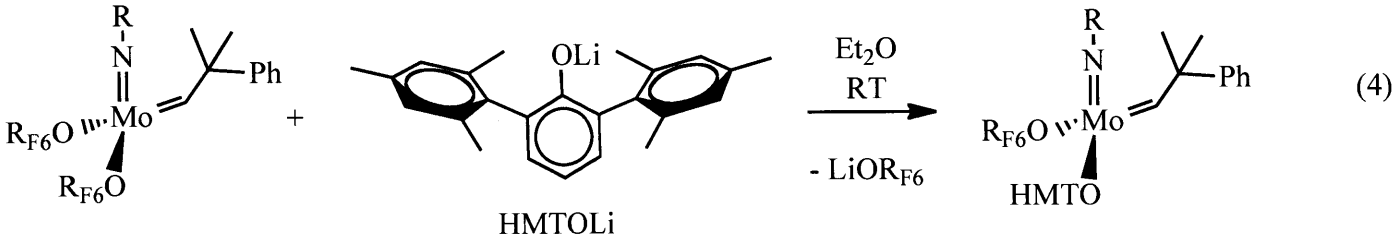

(4)

2 R = Ar; (43 %)
3 R = Ar'; (80 %)
4 R = Ar^{iPr}; (71%)
5 R = Ad; (59 %)

All MAX species (except **3**) are highly crystalline and can be recrystallized from pentane at – 35 °C. The structure of complex **5** is shown in Figure 3. Complex **5** crystallizes out in the triclinic space group $P\bar{1}$ with only one molecule present in the asymmetric unit. One of the mesityl groups in the HMTO ligand faces parallel to the imido group while the other is positioned in the empty COO face of the tetrahedron. The Mo(1)-C(1), Mo(1)-N(1), Mo(1)-O(1), and Mo(1)-O(2) bond lengths are typical of those found in MAP species. The Mo(1)-C(1)-C(2) bond angle is also typical of MAP species in the *syn* configuration. The Mo(1)-N(1)-C(11) bond angle is close to linear, which is common for high-oxidation state molybdenum alkylidene imido complexes. The Mo(1)-O(1)-C(21) bond angle is slightly less than the Mo(1)-O(2)-C(31) bond angle (145.23(12)° and 154.38(10)° respectively) and it is attributed to the greater sterics of the HMTO ligand compared to OR_{F6}.

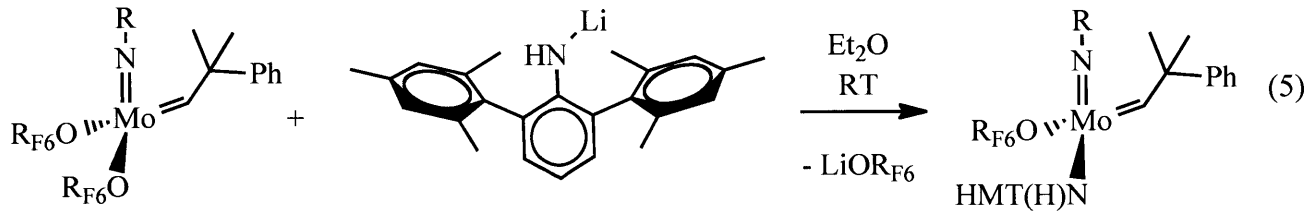

(5)

6 R = Ar', (48 %)
7 R = Ar^{iPr}, (92 %)

When $Mo(NR)(CHCMe_2Ph)(OR_{F6})_2$ is treated with one equivalent of LiN(H)HMT at RT in Et_2O, only complexes **6** (R = Ar') and **7** (R = Ar^{iPr}) can be obtained (equation 5). Complex **7** is highly crystalline, while **6** is not as crystalline and elemental analysis has not passed successfully. Proton NMR spectra of both complexes show only one alkylidene peak at 11.86 ppm for **6** and at 11.72 ppm for **7** and one NH resonance at 7.82 ppm for **6** and 7.99 ppm for **7**. Similarly to complexes **2-5**, both **6** and **7** do have a methyl peak resonance at 1.00 and 0.80 ppm respectively. The ^{19}F NMR of both complexes shows a set of quartets indicating a complex with C_1 symmetry.

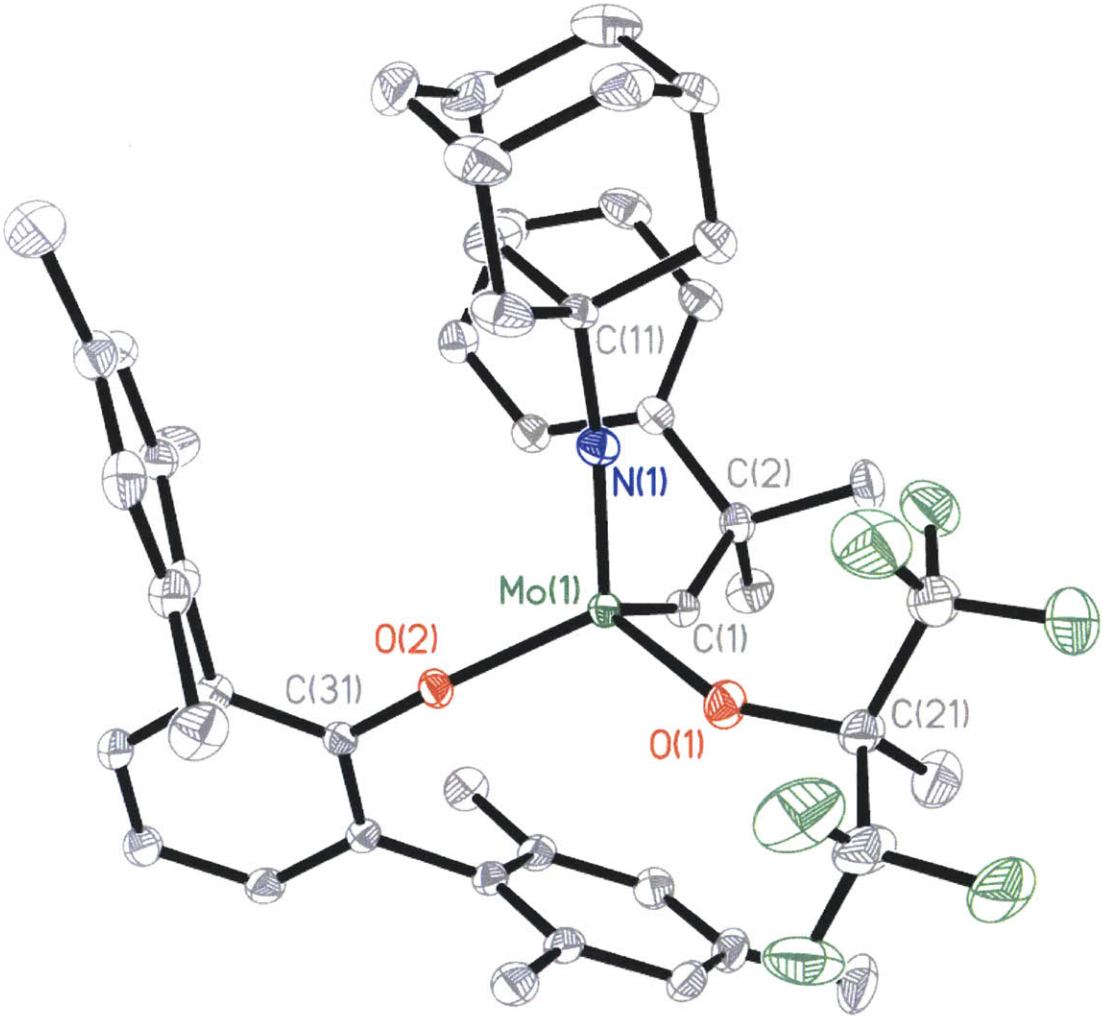

Figure 3 - The solid state structure of **5** (50% probability ellipsoids). Selected bond lengths (Å) and bond angles (°): Mo(1)-C(1) = 1.8821(16), Mo(1)-N(1) = 1.7028(14), Mo(1)-O(1) = 1.9444(12), Mo(1)-O(2) = 1.9230(11), Mo(1)-C(1)-C(2) = 141.90(12), Mo(1)-N(1)-C(11) = 169.14(12) Mo(1)-O(1)-C(21) = 145.23(12), Mo(1)-O(2)-C(31) = 154.38(10).

As it was observed above, during the salt metathesis reaction between $Mo(NAr)(CHCMe_2Ph)(OR_{F6})_2$ and LiN(H)HMT, substantial side products are produced due to the higher basicity of lithium amide compared to that of LiOHMT. It is worth noting that the same reaction carried out with smaller amides (e.g. $LiNPh_2$) yields salt-metathesis products with no side products.[12] Byproduct formation during salt-metathesis reactions with LiOHMT or LiN(H)HMT is attributed to the higher steric demands of the terphenyl ligands. In the case of the $Mo(NAd)(CHCMe_2Ph)(OR_{F6})_2$, substitution takes place but the product is not crystalline and could not be purified.

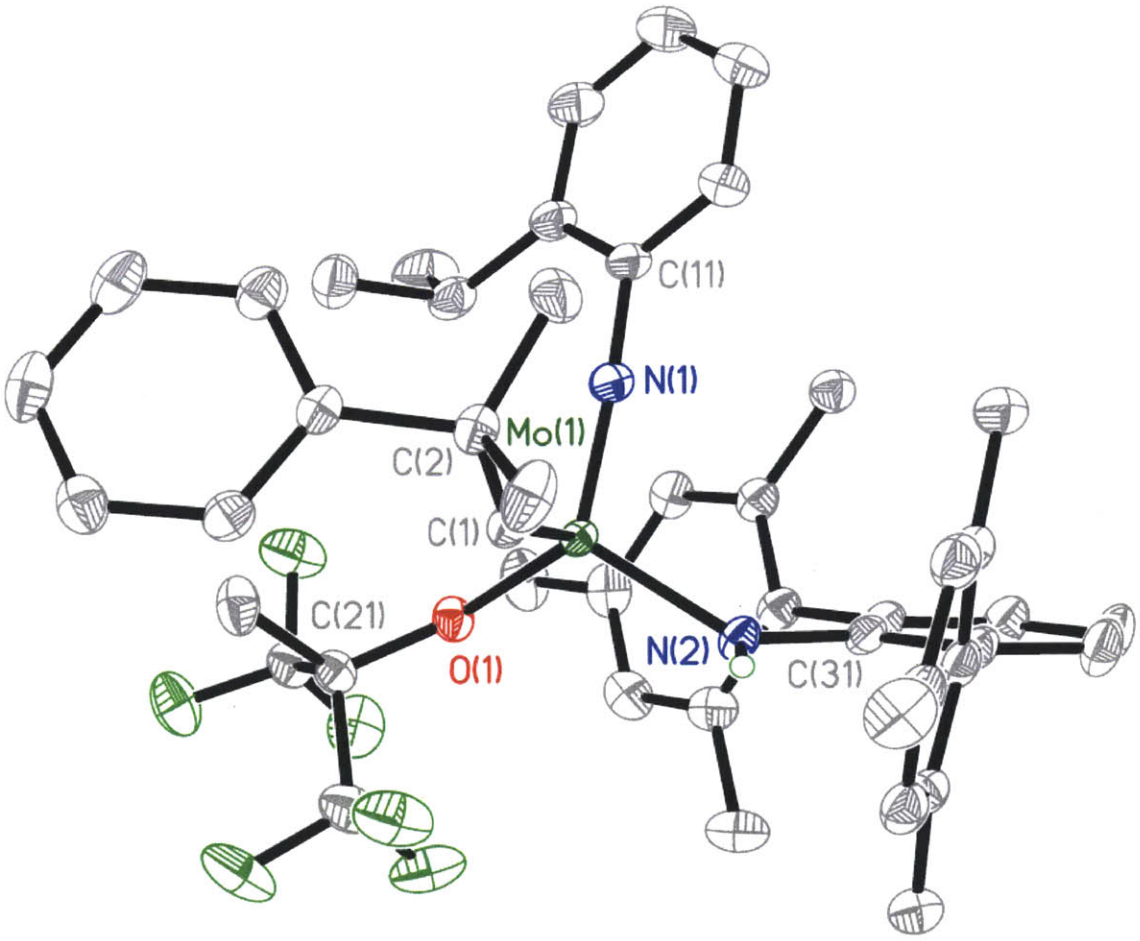

Figure 4 – The solid state structure of **7** (50% probability ellipsoids). Selected bond lengths (Å) and bond angles (°): Mo(1)-C(1) = 1.8833(16), Mo(1)-N(1) = 1.7261(13), Mo(1)-N(2) = 1.9950(13), Mo(1)-O(1) = 1.9518(11), Mo, Mo(1)-C(1)-C(2) = 144.78(12), Mo(1)-N(1)-C(11) = 173.09(12), Mo(1)-N(2)-C(31) = 133.32(11), Mo(1)-O(1)-C(21) = 140.93(10).

The crystal structure of **7** is shown in Figure 4. Complex **7** crystallizes in the monoclinic space group $P2_1/c$ and its structure is best described as a distorted tetrahedron. The HMTN(H) group points its mesityl arms towards the NNO and the CNN faces of the tetrahedron, leaving the CON(amide) face exposed. The Mo(1)-N(1) and Mo(1)-O(1) bond distances of **7** (1.7261(13) Å and 1.9518(11) Å respectively) are slightly longer than those of **5** (1.7028(14) Å and 1.9444(12) Å respectively), but the Mo(1)-C(1) bond lengths of **7** (1.8833(16) Å) and **5** (1.8821(16) Å) are very similar. In addition, the Mo(1)-N(1)-C(11) bond angle of **7** (173.09(12)°) is larger than that of **5** (169.14(12)°) while the Mo(1)-O(1)-C(21) of **7** (140.93(12)°) is shorter than that of **5** (145.23(12)°). The differences in the bond lengths and angles of the imido ligands are reflected by the different steric interactions encountered by each imido group. In the case of **7** Ar^{iPr} is slightly larger than Ad, which explains the slight elongation of the bond. On the other hand, the Mo(1)-N(1)-C(11) bond angle in **5** is shorter than **7** because the mesityl arm of the HMTO ligand (complex **5**) points directly towards the imido ligand, whereas, the analogous interaction in **7** is absent, thus creating a larger and more linear bond.

The differences in the Mo(1)-O(1) bond lengths and the Mo(1)-O(1)-C(21) bond angles of **5** and **7** can be rationalized by comparison of the σ-donating and π-donating abilities of the HMTO and HMTN(H) ligands respectively. Since HMTO is less effective both as a σ-donor and a π-donor, compared to HMTN(H), it has a lesser *trans*-influence on the OR_{F6}, which explains why the Mo(1)-O(1) bond length is longer and the Mo(1)-O(1)-C(21) bond angle is shorter for **7** than for **5**. Finally, the Mo(1)-N(2) bond distance (1.9950(13) Å) of **7** is similar to the analogous distances in $Mo(NAr)(CHCMe_2Ph)(NPh_2)_2$ species[12] (2.007(3) and 2.009(3) Å), but the Mo(1)-N(2)-C(31) bond angle (133.32(11)°) of **7** is significantly larger than those of the bisamide complex (118.61(19)° and 117.6(3)°). This difference could be attributed to the difference in sterics of both amide ligands; however, a possible N-H agostic interaction is not discounted and could, in part, be responsible for the discrepancy in bond angles.

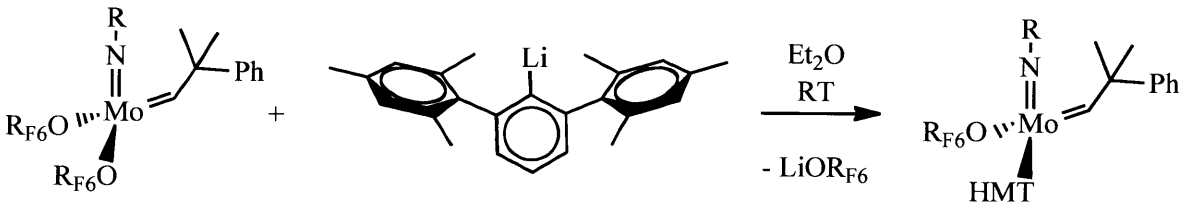

(6)

8 R = Ad, RT; (95 %)
9 R = Ar^m, RT; (oil)
10 R = Ar', 80 °C; (90 % conv)
11 R = Ar, 80 °C; (18 % conv)

When $Mo(NR)(CHCMe_2Ph)(OR_{F6})_2$ was treated with one equivalent of LiHMT, at RT overnight, $Mo(NR)(CHCMe_2Ph)(OR_{F6})(HMT)$ species (R = Ad, **8**; R = 3,5-$Me_2C_6H_3$ (Ar^m), **9**) could be generated in solution. Unfortunately, **9** is not a crystalline complex and could not be purified by recrystallization even from TMS at – 35 °C. On the other hand, **8** is obtained as a yellow crystalline compound (equation 6). ^1H NMR of **8** reveals the presence of only one alkylidene product at 10.99 ppm and ^{19}F NMR reveals the characteristic set of quartets.

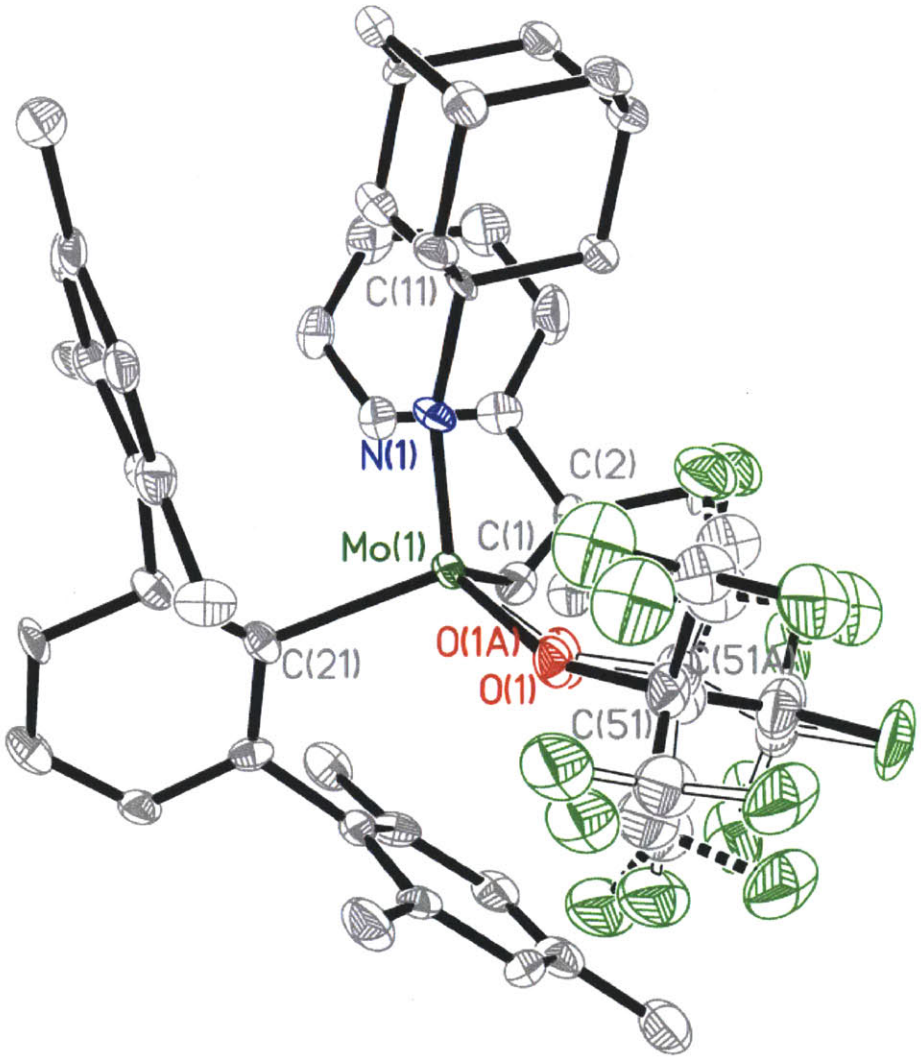

Figure 5a – The solid state structure of **8** (50% probability ellipsoids).. Selected bond lengths (Å) and bond angles (°): Mo(1)-C(1) = 1.891(8), Mo(1)-N(1) = 1.701(6), Mo(1)-C(21) = 2.193(7), Mo(1)-O(1) = 1.940(6), Mo(1)-O(1A) = 1.933(14), Mo(1)-O(1B) = 1.928(15), Mo(1)-C(1)-C(2) = 144.2(6), Mo(1)-N(1)-C(11) = 162.0(5), Mo(1)-O(1)-C(51) = 155.6(9), Mo(1)-O(1A)-C(51A) = 153(3), Mo(1)-O(1B)-C(51B) = 158(7).

In the case where R = Ar' (**10**) the reaction reaches 90 % completion after 5 days at 80 °C and two new alkylidene resonances at 11.7 ppm (78%) and 11.0 ppm (12 %) are observed in its proton NMR spectrum. Unfortunately isolation of either species was not possible by recrystallization. In the case where R = Ar (**11**) only 18% of a new species is formed after 5 days at 80 °C.

Complex **8** was recrystallized from pentane at -35 °C to yield X-ray quality crystals and its structure is shown in Figure 5a. Complex **8** crystallizes in the triclinic group $P\bar{1}$ and its structure is described as a distorted tetrahedron. A three-part disorder is observed for the $(CF_3)_2CH_3CO$ group and a front view picture is shown in Figure 5b. The Mo(1)-N(1)-C(11) angle of 162.0(5)° is a bit shorter than that of complex **5** (169.14(12)°) and it is due to the closer proximity of the mesityl ring in **8**. However, the Mo(1)-N(1) bond length of **8** (1.701(6) Å) is similar to that of **5** (1.7028(14) Å) and to analogous MAX species[8-9]. The Mo(1)-O(1)-C(51) angle (155.6(9)°) of **8** is larger than the Mo(1)-O(1)-C(21) angle (145.23(12)°) of **5**. On the other hand, the Mo(1)-O(1) bond length of **8** (1.940(6) Å) is very similar to the Mo(1)-O(1) bond length (1.9444(12) Å). The differences in bond angles of the OR_{F6} fragments are due to the presence (HMTO) or absence (HMT) of a good π-donor ligand. Thus, in complex **8**, the OR_{F6} ligand does not compete for π-bonding and has a more linear bond angle.

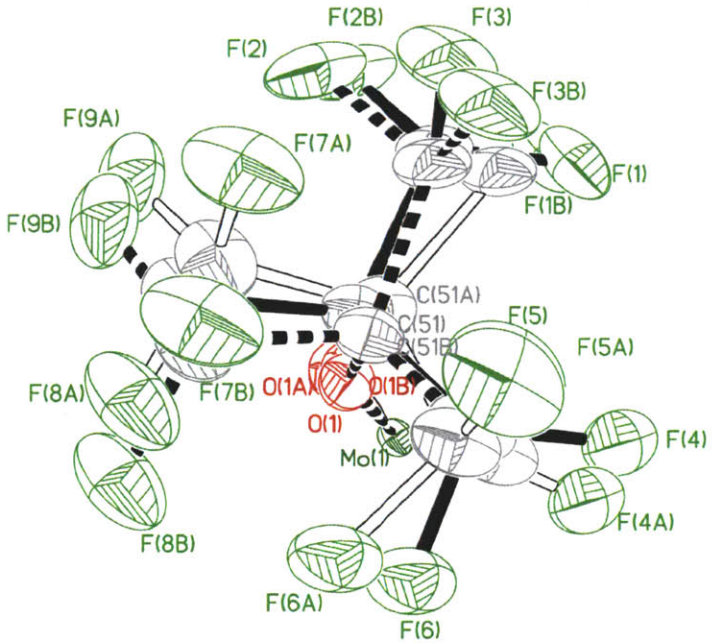

Figure 5b – Front view of the three-part disorder of the alkoxide group of compound **8** (50% probability ellipsoids). Selected bond lengths (Å) and angles (°) are shown. Mo(1)-O(1) = 1.940(6), Mo(1)-O(1A) = 1.933(14), Mo(1)-O(1B) = 1.928(15), Mo(1)-O(1)-C(51) = 155.6(9), Mo(1)-O(1A)-C(51A) = 153(3), Mo(1)-O(1B)-C(51B) = 158(7).

The Mo(1)-C(21) bond length (2.193(7) Å) is similar to metal-alkyl lengths like those of $Mo(NAr^T)_2(CH_3)_2$ (Ar^T = 2-(2',4',6'-triisopropylphenyl)phenyl; 2.127(2) Å and 2.121(2)Å, Chapter 3) and as a result, the distance between the metal center and the HMT group is about 1 Å shorter than the distance found in $Mo(NAr^M)(CHCMe_2Ph)(2,5\text{-}Me_2Pyr)(OHMT)$ (3.199 Å, Chapter 3), $Mo(NAr^{iPr})(CHCMe_2Ph)(Pyr)(OHMT)$ (3.166 Å, Chapter 4), **5** (3.193 Å), and **7** (3.130 Å). Moreover, the Mo-HMT distance in **8** is about 2 Å shorter than in $Mo(NAr)(CHCMe_2Ph)(Me_2Pyr)(O_2CTer_{Me})$. Figure 6, shows the Mo-O_2CTer_{Me}, Mo-OHMT, Mo-N(H)HMT, and Mo-HMT fragments of $Mo(NAr)(CHCMe_2Ph)(Me_2Pyr)(O_2CTer_{Me})$, **5**, **7**, and **8** respectively for comparison.

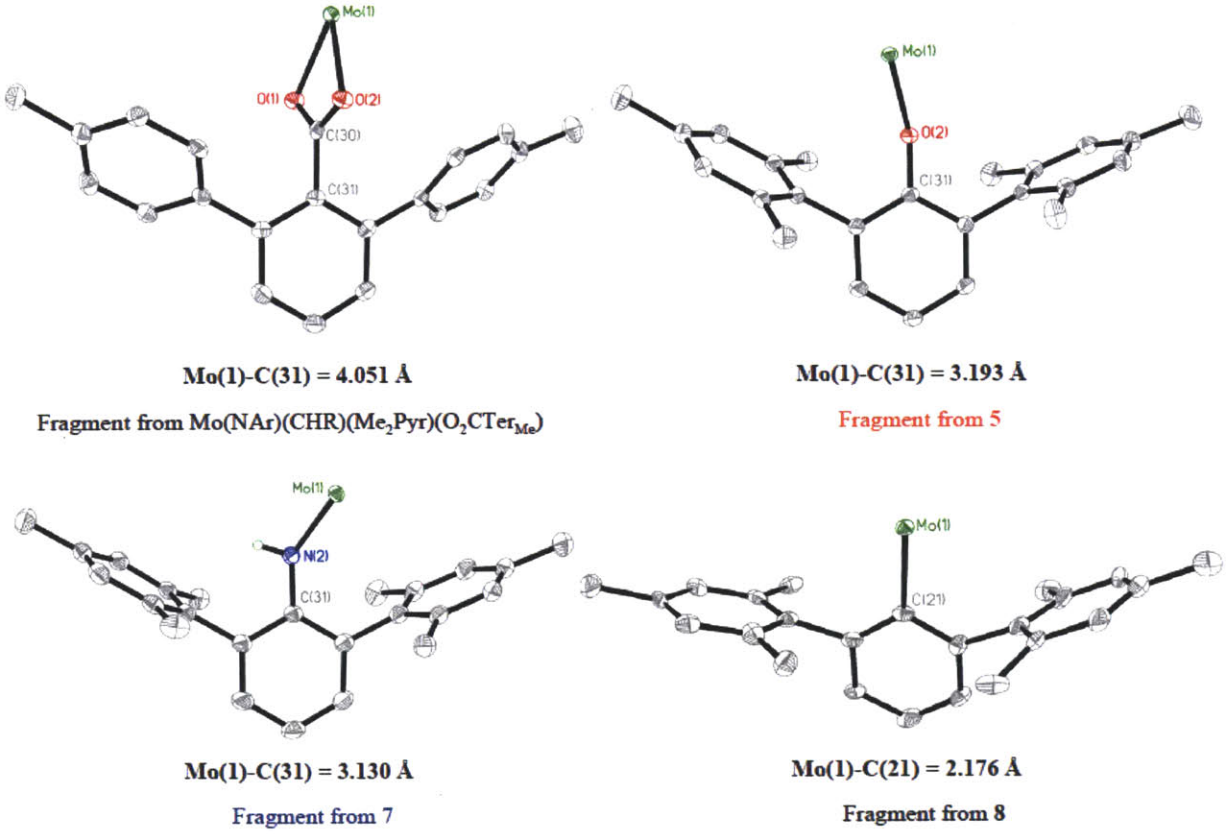

Figure 6 – The solid state structures (50 % probability ellipsoids) of the carboxylate fragment of $Mo(NAr)(CHCMe_2Ph)(Me_2Pyr)(O_2CTer_{Me})$ (top left), the phenoxide fragment of **5** (top right), the amido fragment of **7** (bottom left), and the phenyl fragment of **8** (bottom right). Selected distances and bond lengths (Å) shown below each fragment.

When the Mo-Aryl distances of each of the fragments are considered, the results observed during the preparation of MAX complexes from $(NAr)(CHCMe_2Ph)(OR_{F6})_2$ can be easily rationalized. For instance, the long distance between the terphenyl group of the O_2CTer_{Me} ligand and the metal center is long enough that MAX species containing this ligand can only be made when the imido group is NAr because it provides enough steric crowding to favor monosubstitution slightly more over disubstitution. Decreasing the size of the imido ligand to any extent leads to disubstitution. If the distance between the metal center and the terphenyl is decreased to about 3 Å then synthesis of MAX species containing both big (Ar) and small (Ar', Ar^{iPr}, Ad) imido groups is possible. However, decreasing the distance between the metal center and the aryl group to 2 Å makes the resulting MAX complexes very crowded and only the complex with the smallest imido (Ad) can be produced.

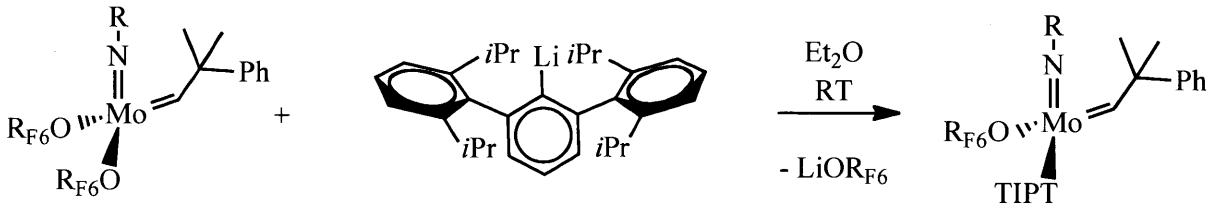

(7)

12 R = Ad, 80 °C; (100 % conv)
13 R = Ar', 80 °C; (28 % conv)
14 R = Ar, 80 °C; (7 % conv)

Finally, increasing the size of the aryl group from hexamethylterphenyl (HMT) to tetraisopropylterphenyl (TIPT) has only detrimental effects (equation 7). For example heating a mixture of $Mo(NR)(CHCMe_2Ph)(OR_{F6})_2$ and LiTIPT at 80 °C for 2 weeks only generates 7% of **14** (R = Ar) and 28% of **13** (R = Ar'). Moreover, 82% of **12** (R = Ad) can be obtained as a mixture of products after heating at 80 °C for 17 h. However, after 5 days at 80 °C only one product resonance remains (Figure 7). Attemps to isolate the pure product have been unsuccessful.

5.1.4 Reaction between $Mo(NAd)(CHCMe_2Ph)(OR)_2$ complexes and LiHMT

With the synthetic success of **8**, other MAX species containing the adamantyl imido group were pursued. Two bisalkoxide complexes of interest were used as potential starting materials: $Mo(NAd)(CHCMe_2Ph)(OR_{F9})_2$ (OR_{F9} = $OC(CF_3)_3$) and $Li[Mo(NAd)(CHCMe_2Ph)(OiPr^{F6})_3]$[11] ($OiPr^{F6}$ = $OCH(CF_3)_2$). $Mo(NAd)(CHCMe_2Ph)(OiPr^{F6})_2$ cannot be used as the starting material because it is not stable towards disproportionation. When $Li[Mo(NAd)(CHCMe_2Ph)(OiPr^{F6})_3]$ is

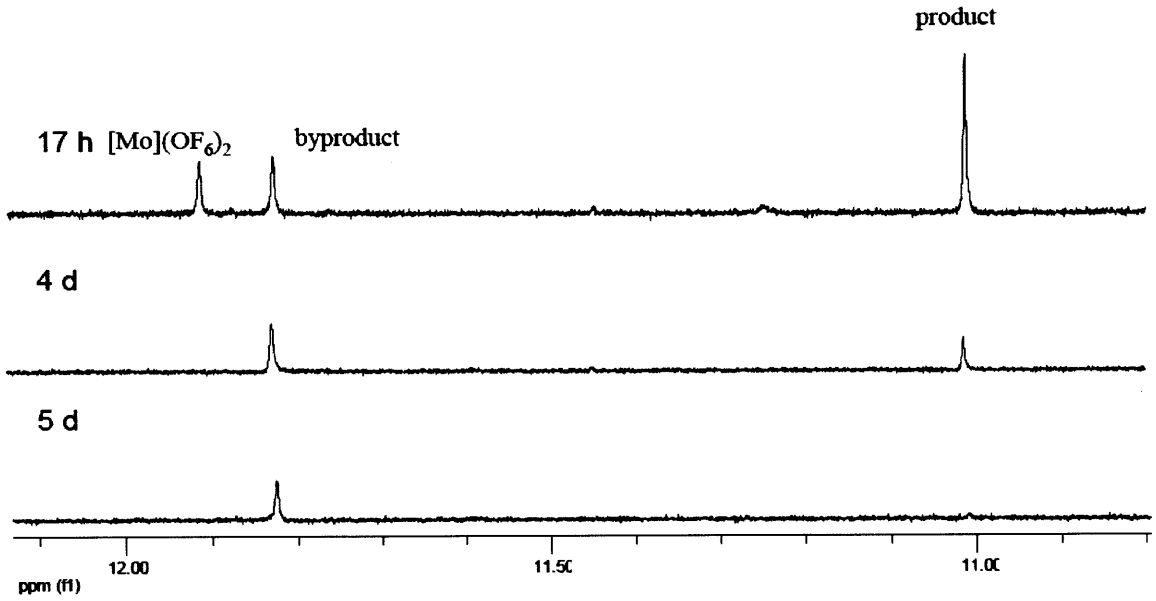

Figure 7 – ^{1}H NMR spectra of the reaction between Mo(NAd)(CHR)(OR_{F6})$_2$ and LiTIPT at 80 °C over a period of 5 d.

treated with one equivalent of LiHMT at 80 °C for 3 d less than 2% of a new alkylidene species is made (equation 8). It is believed that slow conversion is due to the negative charge of the ate complex, but the sterics around the metal center may also detriment the progress of this reaction. At this point, this molecule is no longer being pursued.

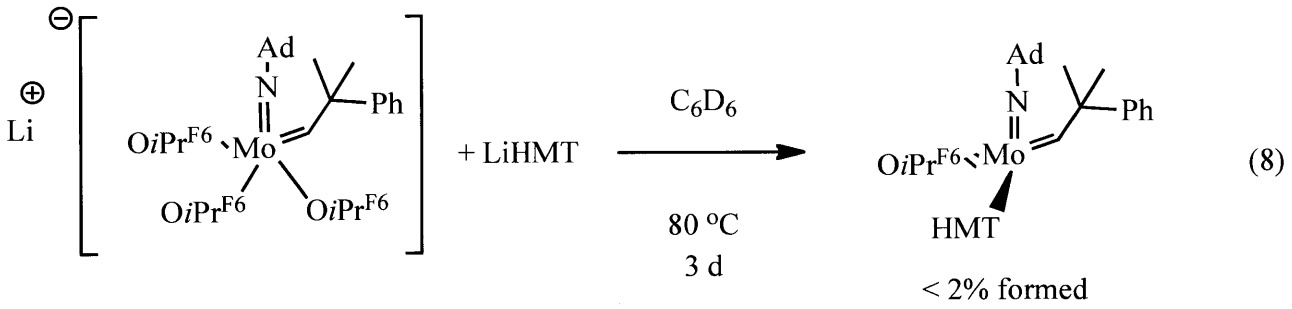

(8)

On the other hand, Mo(NAd)(CHCMe$_2$Ph)(OR_{F9})$_2$, **15**, can be synthesized from Mo(NAd)(CHCMe$_2$Ph)(OTf)$_2$DME resulting in 66% of a yellow solid (equation 9). This is the first reported synthesis of complex **15**. In the ^{1}H NMR spectrum of **15**, both the *anti* (J_{CH} =

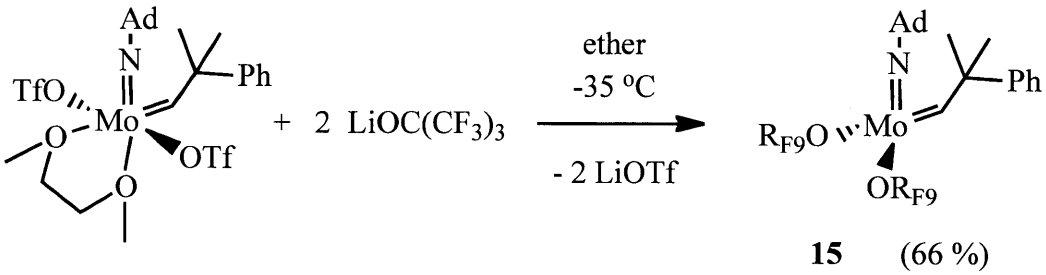

15 (66 %) (9)

151.9 Hz) and *syn* (J_{CH} = 121.9 Hz) isomers are observed in 25% and 75% respectively (Figure 8). Similarly, the ^{19}F NMR spectrum of **15**, has two resonances that integrate 1:3 in relation to each other. It is known that alkylidene rotation at the metal slows down considerably with the electron-withdrawing ability of the alkoxide ligands[13] and observation of both isomers in solution is in accordance with that.

Preliminary work suggests that reaction between Mo(NAd)(CHCMe$_2$Ph)(OR$_{F9}$)$_2$ and one equivalent of LiHMT takes place in the same manner as **8** and after 12 h at RT the isomeric resonances of the starting material completely disappear while a new one appears at 11.3 ppm corresponding to the desired MAX species Mo(NAd)(CHR)(OR$_{F9}$)(HMT), **16**, (Figure 8).

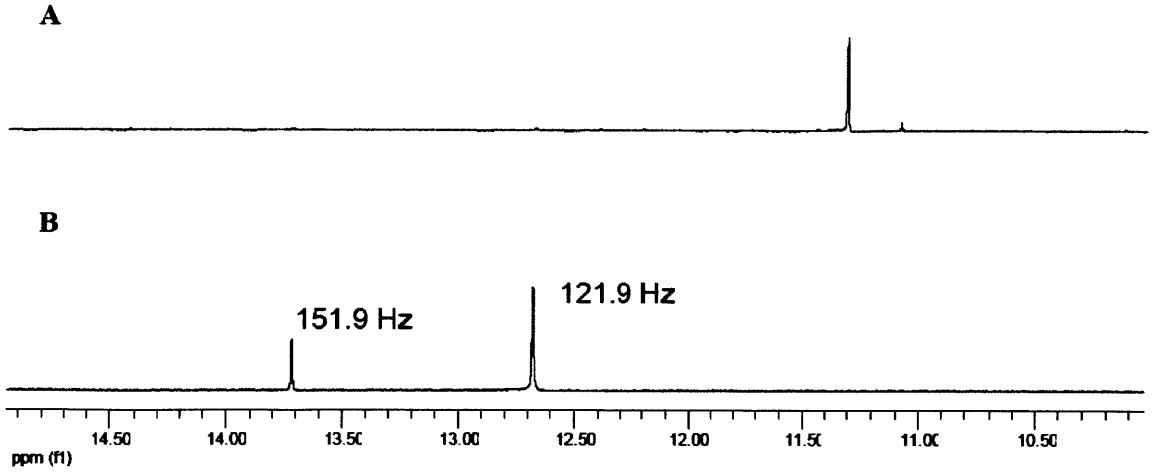

Figure 8 – Alkylidene region in the ^1H NMR of Mo(NAd)(CHR)(OR$_{F9}$)(HMT), **A**, and Mo(NAd)(CHR)(OR$_{F9}$)$_2$, **B**.

5.2 Reactivity Studies

In this section the reactivity of MAX species **1-8** will be compared to the analgous MXP (Mo(NAr)(CHCMe$_2$Ph)(Me$_2$Pyr)(O$_2$CTer$_{Me}$), **1a**, Me$_2$Pyr = 2,5-Me$_2$C$_4$H$_2$N)) and MAX (Mo(NR)(CHCMe$_2$Ph)(Pyr)(OHMT) (R = Ar, **2a**; R = Ar', **3a**; R = Ar^{iPr}, **4a**; R = Ad, **5a**; Pyr = pyrrolide)) complexes. The reactions screened are the ring closing metathesis (RCM) of diallyl ether, the homocouplings of 1-hexene and 1-octene, and the ring opening metathesis polymerization (ROMP) of 2,3-dicarbomethoxynorbonadiene (DCMNBD). All reactions are discussed below.

5.2.1 RCM of diallyl ether

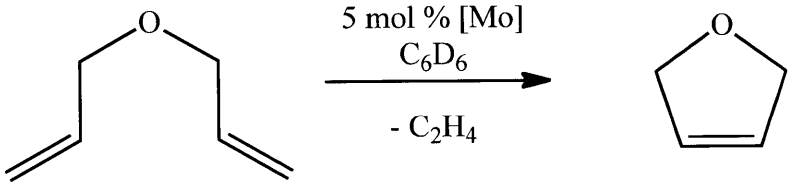

DAE (10)

The RCM of diallyl ether (DAE) is one of the most basic test reactions for the catalylic activity and stability of new alkylidene complexes in the presence of ethylene. MAX species of the type Mo(NR)(CHCMe$_3$)(Np)(OR') (R = Ar or CPh$_3$; R' = Ad, OCMe$_3$, OC$_6$F$_5$, or OAr), where the X ligand is an alkyl have been evaluated in the past with DAE[8,9] and it was found that the catalysts were inefficient when the imido and/or the alkoxide ligands were electron-rich ligands. Therefore, complexes **1-8** are good choices as catalysts because they all have an electron-poor alkoxide (OR$_{F6}$).

MAX species **1-8**, MAP species **2a-5a**, and MXP species **1a** were evaluated by reacting 11 μmoles of each catalyst with 20 equivalents of DAE in 0.7 mL of C$_6$D$_6$ within a Teflon-sealed J-Young tube. The reactions were monitored during a period of 20-60 min and 15 h after mixing and the results are shown in Table 1. To arrive at meaningful conclusions, Table 2 will be analyzed in two sections: a) catalysts that have the same imido ligand and b) catalysts that have all common ligands, except for the imido ligand.

Table 1 – RCM of DAE with MAP, MAX, and MXP catalysts						
Catalyst	**R**	**X**	**Y**	**[Mo], mM**	**Eq. Subs.**	**Conversion, Time**
1	Ar	OR_{F6}	O_2CTer_{Me}	15	20	91%, 20 m
						98%, 2 h
						98%, 15 h
1a	Ar	Me_2Pyr	O_2CTer_{Me}	17	20	33%, 30 m
						94%, 2 h
						96%, 22 h
2	Ar	OR_{F6}	OHMT	15	20	91%, 40 m
						91%, 2.5 h
						91%, 15 h
2a	Ar	Pyr	OHMT	17	20	97%, 30 m
						97%, 2.3 h
						97%, 15 h
3	Ar'	OR_{F6}	OHMT	15	20	95%, 40 m
						95%, 2.5 h
						95%, 15 h
3a	Ar'	Pyr	OHMT	18	20	95%, 40 m
						95%, 2.3 h
						96%, 15 h
4	Ar^{iPr}	OR_{F6}	OHMT	15	20	96%, 40 m
						96%, 2.5 h
						96%, 15 h
4a	Ar^{iPr}	Pyr	OHMT	18	20	93%, 40 m
						93%, 2.3 h
						93%, 15 h
5	Ad	OR_{F6}	OHMT	15	20	2%, 50 m
						4%, 2.6 h
						12%, 15 h
5a	Ad	Pyr	OHMT	17	20	94%, 1 h
						94%, 2.5 h
						94%, 15 h
6	Ar'	OR_{F6}	N(H)HMT	16	20	35%, 30 m
						50%, 2.5 h
						69%, 12 h
7	Ar^{iPr}	OR_{F6}	N(H)HMT	15	20	57%, 30 m
						64%, 2.5 h
						65%, 12 h
8	Ad	OR_{F6}	HMT	15	20	26%, 50 m
						87%, 15 h
						93%, 22 h

Catalysts **1**, **1a**, **2**, and **2a** share the Ar imido group. All catalysts are competent, with **2a** being the most reactive, which reaches 97% completion within 20 min. Catalyst **2** reaches 91% completion after 40 min and stays steady even after 15 h, which could mean it is no longer active

due to decomposition. On the other hand, catalyst **1** reaches 91% conversion within 20 min, continues up to 98% conversion after 2 h, and remains steady thereafter. Catalyst **1a** reacts slowly in comparison with only 33% conversion after 30 min, but reaches up to 96% conversion after 22 h. The fact that the presence of a κ^2-bound carboxylate ligand diminishes the activity of the catalyst when a pyrrolide ligand is present instead of OR_{F6} suggests that having a more electron-deficient metal center is better for this reaction; however, this is the opposite trend observed when instead of a carboxylate, HMTO is present.

Catalysts **3**, **3a**, and **6** share the Ar' imido ligand and both **3** and **3a** are very active catalysts with virtually the same activity. On the other hand, catalyst **6** is very slow, reaching only 35% completion after 30 min and reaching only 69% completion after 12 h. In this case the presence of the better π-donating HMTN(H) ligand makes the metal center more electron rich than those of either **3** or **3a** and diminishes its activity in comparison. Similarly, catalysts **4** and **4a**, which bear the Ar^{iPr} imido ligand, are very active reaching 96% and 93% completion respectively, after 40 min, but catalyst **7** is slow reaching only 57% completion after 30 min and 65% after 12 h.

Catalysts **5**, **5a**, and **8** share the Ad imido ligand and their reactivity suggests that the ligand combination of **5** is not ideal for catalysis since the conversion of DAE only reaches 12% after 15 h. On the other hand, catalyst **5a** reaches 94% completion within 1 h. and remains steady. Catalyst **8** reacts slowly, reaching only 26% conversion after 50 min, but reaching 93% completion after 22 h. In both **5a** and **8** the ligand combination involves a poor sigma donor (OR_{F6}) and a good sigma donor (Pyr and HMT).

Comparison of all MAX catalysts shows that catalysts **1**, that contains two poor sigma donor ligands, **3** and **4**, which have one poor sigma donor and a better one, are the most competent of them all. They are followed closely in activity by **2**, which contains the bigger Ar imido ligand (in comparison to **3** and **4**). Catalysts **6-8** are all slow, but **8** is slightly more active because the bulky HMT ligand is not a good π-donor. Finally, **5** has the worst activity among all the MAX catalysts and its poor reactivity may arise from fast degenerate metathesis reactions taking place at similar rates than the productive reaction.

Comparison of MXP and MAP complexes **1a-5a** shows that catalysts **2a** and **3a** are slightly better than **4a** and **5a**, but all perform very well nonetheless. On the other hand, catalyst **1a** performs poorly in comparison mainly due to the κ^2-binding of the carboxylate ligand, which makes the metal center less electron-poor. Overall, MAX species **2-5** are just as competent as MAP complexes **2a-5a**. MAX complex **1** is better than MXP complex **1a** and MAX complexes **6-8** are slow in comparison to **2a-5a**.

5.2.2 Homocoupling of 1-hexene

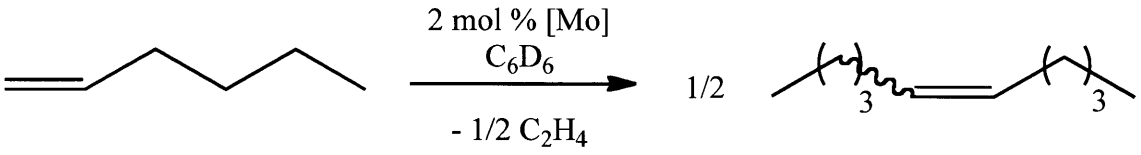

(11)

The second reaction that was used to evaluate the usefulness of MAX species **1-8**, MAP species **2a-5a**, and MXP species **1a** was the homocoupling of 1-hexene by reacting 11 μmoles of each catalyst with 50 equivalents of 1-hexene in 1.5 mL of C_6D_6 in an open vial under inert-gas atmosphere. The vial was kept open to allow removal of ethylene gas (a byproduct of the reaction) and to reach complete conversion. The reactions were stirred at RT for 1 h, with the exception of 2 cases. The reaction was evaluated by ^1H and ^{13}C NMR and the results are shown in Table 2. The same analysis used for the interpretation of Table 2 will be used here.

Catalysts **1-2** and **2a** are 98-99% complete after 1 h of mixing; whereas, catalyst **1b** reaches only 82% conversion after the same period of time. In the case of **1-2** and **2a** the product is 82-84% *trans*-5-decene, but with **1a** the product is only 53% *trans*-5-decene. This result shows that although **1a** is slow in comparison, it is more selective for formation of *cis* bonds.

Catalysts **3**, **3a**, and **6** attain high conversion (96-99%) after 1 h and give 83-86% *trans*-5-decene as the product. Similarly, catalysts **4**, **4a**, and **7** attain high conversion (94-99%) after 1 h and give product that is 87%, 81%, and 85% *trans*-5-decene respectively.

Catalysts that contain the Ad imido ligand vary in their results drastically. Complex **5a** reaches 92% conversion after 1 h and yields 89% *trans*-5-decene as the product; whereas, catalyst **5** reaches only 71% conversion and levels off at 74% conversion after 5 h, which is only 54% *trans* product. Finally, catalyst **8** is the slowest, reaching only 10% conversion after 5 h. These results are similar to the findings of RCM of DAE, where **5** and **8** are slow and **5a** performs best.

Comparison of all MAX species shows that species **1-4**, **6-7** are very efficient catalysts for homocoupling of 1-hexene yielding 5-decene product that is 84-87% *trans* in content. **5** is slow in comparison and gives 5-decene product with significant lower *trans* content (54%), while **8** is very slow. Similarly, MAP catalysts **2a-5a** are also very efficient catalysts and yield 5-decene product that is 81-89% *trans* in content. MXP catalyst **1a** is slow in comparison and yields 5-decene that is only 53% *trans* in content.

Table 2 – Homocoupling of 1-hexene with MAP, MAX, and MXP catalysts						
Catalyst	**R**	**X**	**Y**	**[Mo], mM**	**Eq. Subs.**	**Conversion, Time**
1	Ar	OR_{F6}	O_2CTer_{Me}	8	50	98%, 84% *trans*, 1 h
1a	Ar	Me_2Pyr	O_2CTer_{Me}	9	50	82%, 53% *trans*, 1 h
2	Ar	OR_{F6}	OHMT	8	50	99%, 84% *trans*, 1 h
2a	Ar	Pyr	OHMT	9	50	99%, 82% *trans*, 1 h
3	Ar'	OR_{F6}	OHMT	8	50	99%, 86% *trans*, 1 h
3a	Ar'	Pyr	OHMT	9	50	99%, 86% *trans*, 1 h
4	Ar^{iPr}	OR_{F6}	OHMT	8	50	99%, 87% *trans*, 1 h
4a	Ar^{iPr}	Pyr	OHMT	9	50	99%, 81% *trans*, 1 h
5	Ad	OR_{F6}	OHMT	8	50	71%, 3 h 74%, 54% *trans*, 5 h ----------
5a	Ad	Pyr	OHMT	9	50	92%, 89% *trans*, 1 h
6	Ar'	OR_{F6}	N(H)HMT	8	50	96%, 83% *trans*, 1 h
7	Ar^{iPr}	OR_{F6}	N(H)HMT	7	50	94%, 85% *trans*, 1 h
8	Ad	OR_{F6}	HMT	8	50	10%, 5 h

5.2.3 Homocoupling of 1-octene

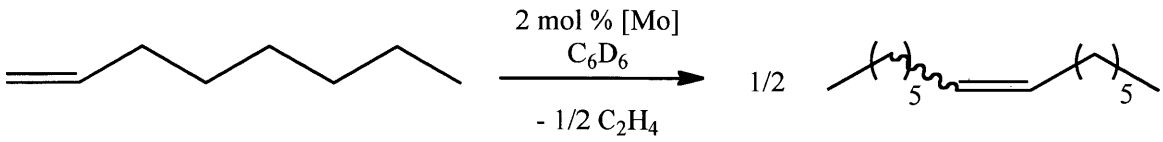

(12)

Since the homocoupling reactions with 1-hexene yielded almost primarily product containing *trans* bonds, we looked at the homocoupling reaction of a slightly larger olefin, 1-octene. The reactions were carried out with 6 μmoles of each catalyst and 50 equivalents of 1-octene in 0.75 mL of C_6D_6 in an open vial under inert-gas atmosphere and the reaction was evaluated by ^1H NMR in $CDCl_3$. The results are shown in Table 3.

Comparison of the homocoupling reactions of 1-octene with catalysts **1-2** and **1a-2a** shows that **1**, **2**, and **2a** are all very efficient at catalyzing the reaction under 1 h, but the product, in all cases, is primarily *trans* (81-83%). On the other hand, **1a** takes 4 h to reach 16% completion; however, the product is only 57% *trans*. These results are very similar to those obtained with 1-hexene.

Catalysts **3**, **3a**, and **6** catalyzed the conversion to completion within 1 h and the product is 80-85% *trans*. Similarly, catalysts **4**, **4a**, and **7** convert 1-octene completely to product with 81%, 73%, and 83% *trans* bonds respectively.

Catalyst **5** is slow, giving only 26% conversion after 1 h, but reaching 75% conversion after 5 h. During the course of the reaction it is observed that the content of *cis* versus *trans* bonds changes. For instance, after 1 h the product is composed of 62% *cis* bonds, but after 4 h the product is only 55% *cis*. After 5 h the product is only 52% *cis*. This data suggests that catalyst **5** is not slow, but very reactive. In other words, **5** reacts with not only the starting material, but also the product leading to isomerism of the internal olefin bond. For comparison, catalyst **5a** catalyzes the reaction within 1 h, but the product is 82% *trans*. In the case of **8** the reaction is too slow to get conclusive results.

Comparison of MAX complexes **1-8** shows that among catalysts **1-4** and **6-7** there is no discernable difference with all catalyzing the reaction to completion within 1 h and yielding 80-83% *trans*-7-tetradecene. Complex **5**; however, yields initially product with 62% *cis* bonds, but as the reaction continues **5** isomerizes the product to yield 7-tetradecene with lower *cis* content. Complex **8** is too bulky to carried out the reaction efficiently within a reasonable period of time. On the other hand, MAP complexes **2a-5a** are all fast and yield product that has mostly *trans* bonds. In the case of **4a**, which has the smallest aromatic imido ligand, the amount of *trans* bonds is the lowest (73%) even in comparison with **5a**, which contains the adamantyl imido

ligand (82%). Similarly to the results with 1-hexene, **1a** is a slow catalyst for this reaction and yields product that has higher *cis* content than any of the MAP species.

Table 3 – Homocoupling of 1-octene with MAP, MAX, and MXP catalysts

Catalyst	R	X	Y	[Mo], mM	Eq. Subs.	Conversion, Time
1	Ar	OR_{F6}	O_2CTer_{Me}	7.5	50	99% conv, 83% *trans*, 1 h
1a	Ar	Me_2Pyr	O_2CTer_{Me}	8.3	50	16% conv, 57% *trans*, 4 h
2	Ar	OR_{F6}	OHMT	7.4	50	99% conv, 81% *trans*, 1 h
2a	Ar	Pyr	OHMT	8.3	50	99% conv, 82% *trans*, 1 h
3	Ar'	OR_{F6}	OHMT	7.8	50	99% conv, 80% *trans*, 1 h
3a	Ar'	Pyr	OHMT	9.0	50	99% conv, 85% *trans*, 1 h
4	Ar^{iPr}	OR_{F6}	OHMT	7.7	50	99% conv, 81% *trans*, 1 h
4a	Ar^{iPr}	Pyr	OHMT	8.6	50	99% conv, 73% *trans*, 1 h
5	Ad	OR_{F6}	OHMT	7.5	50	26% conv, 62% *cis*, 1 h 59% conv, 55% *cis*, 4 h 75% conv, 52% *cis*, 5 h
5a	Ad	Pyr	OHMT	13.8	50	99% conv, 82% *trans*, 1 h
6	Ar'	OR_{F6}	N(H)HMT	7.8	50	99% conv, 83% *trans*, 1 h
7	Ar^{iPr}	OR_{F6}	N(H)HMT	7.7	50	99% conv, 82% *trans*, 1 h
8	Ad	OR_{F6}	HMT	7.7	50	Slow

5.2.4 ROMP of DCMNBD

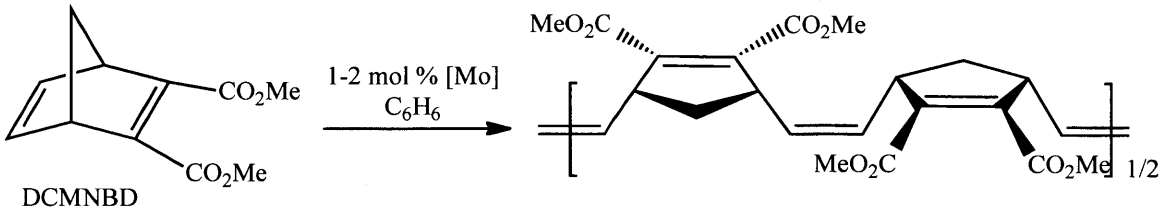

(13)

Since substrates 1-hexene and 1-octene proved too small for complexes **1-7** and **1a-5a** to be effective *Z*-selective catalysts, ROMP of 2,3-dicarbomethoxynorbornadiene (DCMNBD) was investigated because it is considerably more bulky and because it has served as a reliable means of studying the overall reactivity and selectivity of catalysts in the past (see Chapters 3 and 4). The reactions were carried out using 6 μmoles of catalyst and 50 equivalents of DCMNBD in 1.2 mL of toluene at RT. The resulting polymer was analyzed by ^{1}H and ^{13}C NMR methods and the results are shown in Table 4.

Comparison of catalysts **1-2** and **1a-2a** shows that **1** and **1a** are not effective catalysts for this reaction, whereas **2** and **2a** polymerize DCMNBD within 2 h to form polymer that is > 98% *cis*. Presence of a 5-coordinate complex (**1** and **1a**) coupled with the bulkiness of DCMNBD make the polymerization inefficient, even for **1**, which can homocouple 1-hexene and 1-octene. In the case of **2** the polymer is 78% isotactic; whereas **2a** is all syndiotactic. This result shows the crucial difference between using the OR_{F6} ligand instead of pyrrolide and suggests that the required inversion at the metal, which is known for MAP complexes, may not take place readily for MAX complexes.

Complexes **3**, **3a**, and **6** are fast and efficient catalysts for the polymerization of DCMNBD. All are high *Z*-selective catalysts, with **3a** giving > 98% *cis*-syndiotactic polymer. Similarly, **3** yields polymer that is 95% *cis*, but only 73% syndiotactic. Compared to **2**, complex **3** shows major improvement towards syndiotactic selectivity and this is attributed to the smaller size of the imido ligand. Finally, **6** yields polymer that is also 95% *cis*, but 71% isotactic. From these results it can be said that MAP complexes are most efficient for yielding all-syndiotactic polymer; whereas MAX complexes tend to yield a considerable amount of isotactic polymer. In the case of **6**, which has a good π-donor ligand, the amount of isotacticity is very similar to that obtained with **2** and shows that electronics are the main influence on the regioselectivity of the catalysts.

Complexes **4**, **4a**, and **7** show a similar trend of results as those of **3**, **3a**, and **6**. MAP catalyst **3a** yields polymer that is > 98% *cis-syndiotactic* and MAX catalyst **3** yields polymer that is

>98% *cis* and 95% syndiotactic. Thus, decreasing the size of the imido ligand in MAX species (**2** vs **3** vs **4**) tends to give higher content of syndiotactic polymer; however, this only applies when discussing aryl imidos (see discussion of **5** below). Complex **7** yields polymer that is 90% *cis* and 54% isotactic. In comparison to **6**, complex **7** gives lower content of isotactic polymer

Table 4 – ROMP of DCMNBD with MAP, MAX, and MXP catalysts

Catalyst	R	X	Y	[Mo], mM	Eq. Subs.	Polymer Structure
1	Ar	OR_{F6}	O_2CTer_{Me}	4.7	50	Slow
1a	Ar	Me_2Pyr	O_2CTer_{Me}	5.2	50	Slow
2	Ar	OR_{F6}	OHMT	4.6	50	> 98% *cis*; 78% isotactic
2a	Ar	Pyr	OHMT	5.2	50	> 98% *cis*, syndiotactic
3	Ar'	OR_{F6}	OHMT	4.9	50	95% *cis*, 73% syndiotactic
3a	Ar'	Pyr	OHMT	5.6	50	> 98% *cis*, syndiotactic
4	Ar^{iPr}	OR_{F6}	OHMT	4.8	50	98% *cis*, 95% syndiotactic
4a	Ar^{iPr}	Pyr	OHMT	5.4	50	> 98% *cis*, syndiotactic
5	Ad	OR_{F6}	OHMT	4.7	50	90% *cis*, 76% syndiotactic
5a	Ad	Pyr	OHMT	8.6	100	> 98% *cis*, syndiotactic
6	Ar'	OR_{F6}	N(H)HMT	4.9	50	95% *cis*, 71% isotactic
7	Ar^{iPr}	OR_{F6}	N(H)HMT	4.8	50	90% *cis*, 54% isotactic
8	Ad	OR_{F6}	HMT	4.8	100	83 % *cis*, 91% syndiotactic (5 d)

but the difference is not as pronounced as that between complexes **2** and **3**. This difference is also attributed to the better π-donating effect of N(H)HMT, compared to OHMT.

Complexes **5** and **5a** polymerize DCMNBD within 2 h and yield polymer that is 90% *cis*-76% syndiotactic and > 98% *cis*-syndiotactic respectively. The lower syndiotactic content of **5**, compared to **4**, suggests that using electron-rich imidos (alkyl instead of phenyl) decreases the overall selectivity of syndiotactic polymer; moreover, it also gives another example that electronic tuning is a major contributor of how selective MAX catalysts can be. Complex **8** is a very slow catalyst for this reaction, which takes 5 d to polymerize 50 equivalents of DCMNBD. The polymer formed is 83% *cis* and 91% syndiotactic, which makes it more regioselective than **5** with respect to tacticity but less selective with respect to *Z*-selectivity.

CONCLUSION

The synthesis of seven MAX complexes via salt metathesis of $Mo(NR)(CHCMe_2Ph)(OR_{F6})_2$ with LiOHMT, LiN(H)HMT, and LiHMT was presented here. In addition, the preparation of a MAX complex containing a carboxylate ligand was effected by protonolysis of $Mo(NAr)(CHCMe_2Ph)(OR_{F6})_2$ with $Ter_{Me}CO_2H$. Synthesis of these molecules from bistriflate precursors is not possible, which shows that the use of good leaving groups that are weakly basic are required for efficient preparation. The size of the imido ligand affects the outcome of the synthesis. Preparation of MAX complexes that contain a carboxylate ligand are only possible when R = Ar, but MAX species that contain HMTO can be made for imidos of varying sizes. On the other hand, MAX complexes that contain N(H)HMT can only be made for intermediate-sized imido ligands; while MAX complexes that contain HMT can only be made with the smallest imido ligands. The structures of **5**, **7**, and **8** were investigated by X-ray studies and they show that **7** differs significantly from **5** and **8**. Finally, the catalytic activity of MAX and analogous MAP and MXP species were studied by the RCM reaction of DAE, the homocoupling reaction of 1-hexene and 1-octene, and ROMP of DCMNBD. In reactions where only *cis* and *trans* bonds are involved MAX species behave similarly to MAP species, but **1** and **5** behave considerably different from **1a** and **5a**, which are rather slow catalysts and tend to homocouple olefins to make bonds with more *cis* content. Complex **8** is slow but stable in the presence of ethylene. On the other hand, polymerization of DCMNBD has drastic results which show that MAX species are prone to forming highly isotactic polymer if large imido ligands and/or good π-donor ligands are present. Whether or not formation of isotactic polymer is due to retention of configuration at the metal is not known from these studies, but investigation of MAX complexes using chiral phenoxides or amides may yield the answer.

EXPERIMENTAL

General. All reactions and manipulations of air and moisture sensitive compounds were handled in oven-dried glassware (150 °C, 2 h) under a N_2 atmosphere either in a dual Schlenk line or in vacuum atmosphere glove box. HPLC grade solvents (benzene, toluene, diethyl ether, tetrahydrofuran, pentane, and methylene chloride), were purge with N_2 and passed through activated alumina and stored over molecular sieves 12 hours prior to use. 1,2-dimethoxyethane was dried in an oven-dried Schlenk flask with sodium and benzophenone ketal, vacuumed transferred into another oven-dried Schlenk flask and stored over molecular sieves 12 hours prior to use. *n*-BuLi, F_9OH were bought from VWR and used as received. Diallyl ether, 1-hexene, and 1-octene were bought from Sigma-Aldrich and dried over activated 3 Å molecular sieves overnight before use. DCMNBD,[20] Mo(NAd)(CHCMe$_2$Ph)(OTf)$_2$(DME) and Mo(NR)(CHCMe$_2$Ph)(OR$_{F6}$)$_2$ complexes,[13] LiOHMT, LiN(H)HMT, LiHMT, LiTIPT and LiHIPT[10] were prepared according to literature procedures. Benzene-d_6 was stored over molecular sieves 12 hours prior to use. All NMR spectra were recorded with a Bruker 400 MHz spectrometer. Elemental analyses were performed by Midwest Microlab, LLC.

Mo(NAr)(CHCMe$_2$Ph)(OR$_{F6}$)(O$_2$CTer$_{Me}$) (1). Mo(NAr)(CHCMe$_2$Ph)(OR$_{F6}$)$_2$ (0.207 g, 0.270 mmol) was dissolved in Et_2O (5.00 mL) and cooled down to – 35 °C for 1 h. In a separate vial, Ter$_{Me}$CO$_2$H (0.082 g, 0.270 mmol) was dissolved in Et_2O (5.00 mL) and also cooled down to – 35 °C for 1 h. Then, the carboxylic acid solution was added dropwise to the bisalkoxide solution and left stirring at RT for 1 h. The volatiles were removed under reduced pressure and the crude was dissolved in a minimal amount of pentane and place at – 35 °C for a few days to generate orange crystals of pure **1** (0.109 g, 45 %): ^{1}H NMR (400 MHz, C_6D_6) δ 13.07 (s, 1H, Mo=C*H*, J_{CH} = 125.8 Hz), 7.59 (d, 4H, *p*-tolyl), 7.52 (dd, 2H, aromatic), 7.42-7.28 (overlapping peaks, 7H, aromatic), 7.23 (td, 1H, aromatic), 7.17-7.14 (t, 1H, aromatic), 4.02 (sept, 2H, C*H*Me$_2$), 2.17 (s, 6H, *p*-*Me*C$_6$H$_4$), 1.95 (s, 3H, C*H*$_3$), 1.82 (s, 3H, C*H*$_3$), 1.67 (s, 3H, C*H*$_3$), 1.48 (d, 6H, CH*Me*$_2$), 1.29 (d, 6H, CH*Me*$_2$); ^{13}C NMR (100 MHz, C_6D_6) δ 289.3 (Mo=*C*HCMe$_2$Ph), 189.3 (Ter$_{Me}$*C*O$_2$Mo), 152.4, 149.2, 149.2, 140.9, 138.0, 137.6, 134.0, 130.2, 129.5, 128.8, 128.7, 128.6, 128.6, 126.6, 126.3, 123.2, 55.3, 32.4, 29.3, 28.5, 24.4, 23.5, 20.9, 18.3; ^{19}F NMR (376 MHz, C_6D_6) δ – 77.7 (q, 3F, C*F*$_3$), - 78.1 (q, 3F, C*F*$_3$). Anal. Calcd for $C_{47}H_{49}F_6MoNO_3$: C, 63.72; H, 5.58, N, 1.58. Found: C, 63.54; H, 5.31; N, 1.47.

Mo(NAr)(CHCMe$_2$Ph)(OR$_{F6}$)(OHMT) (2). Mo(NAr)(CHCMe$_2$Ph)(OR$_{F6}$)$_2$ (0.312 g, 0.408 mmol) was dissolved in Et_2O and LiOHMT (0.137 g, 0.407 mmol) was added in one portion. The reaction mixture was left stirring at RT overnight. The volatiles were removed and the crude was dissolved in minimal pentane and placed at – 35 °C overnight to yield orange

crystalline solid (0.160 g, 43%): ^{1}H NMR (400 MHz, C_6D_6) δ 11.59 (s, 1H, Mo=C*H*CMe$_2$Ph, J_{CH} = 124.2 Hz), 7.25-6.85 (overlapping peaks, 15H, aromatics), 3.45 (sept, 2H, C*H*Me$_2$), 2.30 (s, 12H, HMTO), 2.20 (s, 6H, HMTO), 1.79 (s, 3H, C*H$_3$*), 1.31 (d, 6H, CH*Me$_2$*), 1.25 (s, 3H, C*H$_3$*), 1.18 (d, 6H, CH*Me$_2$*), 0.78 (s, 3H, C*H$_3$*); ^{13}C NMR (100 MHz, C_6D_6) δ 281.3 (Mo=*C*HCMe$_2$Ph), 158.4, 153.4, 148.7, 143.0, 136.6, 132.3, 130.0, 129.2, 128.4, 128.4, 126.4, 125.6, 123.3, 123.1, 122.9, 54.3, 31.6, 29.8, 28.3, 24.3, 23.8, 20.9, 20.8, 19.2; ^{19}F NMR (376 MHz, C_6D_6) δ – 77.2 (q, 3F, C*F$_3$*), - 77.7 (q, 3F, C*F$_3$*). Anal. Calcd for $C_{50}H_{57}F_6MoNO_2$: C, 65.71; H, 6.29, N, 1.53.

Mo(NAr')(CHCMe$_2$Ph)(OR$_{F6}$)(OHMT) (3). The procedure is the same as that of **2**, employing Mo(NAr')(CHCMe$_2$Ph)(OR$_{F6}$)$_2$ (0.306 g, 0.431 mmol) and LiOHMT (0.145 g, 0.431 mmol) to yield yellow solid (0.298 g, 80%): ^{1}H NMR (400 MHz, C_6D_6) δ 11.40 (s, 1H, Mo=C*H*CMe$_2$Ph, J_{CH} = 123.8 Hz), 7.05-6.55 (overlapping peaks, 15H, aromatics), 2.19 (s, 6H, HMTO), 2.15 (s, 6H, HMTO), 2.06 (s, 6H, Ar' C*H$_3$*), 2.03 (s, 6H, HMTO), 1.45 (s, 3H, C*H$_3$*), 1.22 (s, 3H, C*H$_3$*), 0.80 (s, 3H, C*H$_3$*); ^{13}C NMR (100 MHz, C_6D_6) δ 281.7 (Mo=*C*HCMe$_2$Ph), 158.0, 156.0, 148.6, 136.6, 136.4, 136.2, 135.7, 135.3, 132.0, 129.6, 129.1, 128.4, 128.1, 128.0, 126.9, 126.5, 126.2, 126.0, 125.9, 122.6, 53.6, 40.3, 31.1, 29.6, 29.1, 20.8, 20.6, 19.5, 19.2; ^{19}F NMR (376 MHz, C_6D_6) δ – 77.4 (q, 3F, C*F$_3$*), - 77.6 (q, 3F, C*F$_3$*). Anal. Calcd for $C_{46}H_{44}F_6MoNO_2$: C, 64.41; H, 5.76, N, 1.63. Found: C, 64.83; H, 5.86; N, 1.30.

Mo(NAr^{iPr})(CHCMe$_2$Ph)(OR$_{F6}$)(OHMT) (4). The procedure is the same as that of **2**, employing Mo(NAr^{iPr})(CHCMe$_2$Ph)(OR$_{F6}$)$_2$ (0.360 g, 0.498 mmol) and LiOHMT (0.168 g, 0.499 mmol) to yield orange crystalline solid (0.367 g, 71%). ^{1}H NMR (400 MHz, C_6D_6) δ 11.20 (s, 1H, Mo=C*H*CMe$_2$Ph, J_{CH} = 124.5 Hz), 7.14 (dd, 2H, aromatic), 7.08 (td, 2H, Ar^{iPr}), 7.02-6.78 (overlapping peaks, 8H, aromatics), 6.76 (s, 2H, HMTO), 6.67 (s, 2H, HMTO), 3.31 (sept, 1H, C*H*Me$_2$), 2.14 (s, 6H, HMTO), 2.08 (s, 6H, HMTO), 2.04 (s, 6H, HMTO), 1.49 (s, 3H, C*H$_3$*), 1.43 (s, 3H, C*H$_3$*), 1.15 (d, 3H, CH(Me)C*H$_3$*), 1.13 (d, 3H, CH(C*H$_3$*)Me), 0.94 (s, 3H, C*H$_3$*); ^{13}C NMR (100 MHz, C_6D_6) δ 281.7 (Mo=*C*HCMe$_2$Ph), 157.9, 155.3, 149.0, 146.7, 136.5, 136.4, 136.0, 135.4, 132.1, 129.7, 128.7, 128.4, 127.9, 127.9, 126.2, 125.5, 122.9, 54.3, 32.4, 30.5, 28.2, 23.6, 21.1, 20.9, 20.5, 18.6; ^{19}F NMR (375 MHz, C_6D_6) δ – 77.7 (q, 3F, C*F$_3$*), - 78.1 (1, 3F, C*F$_3$*). Anal. Calcd for $C_{47}H_{51}F_6MoNO_2$: C, 64.75; H, 5.90, N, 1.61. Found: C, 64.60; H, 6.01; N, 1.41.

Mo(NAd)(CHCMe$_2$Ph)(OR$_{F6}$)(OHMT) (5). The procedure is the same as that of **2**, employing Mo(NAd)(CHCMe$_2$Ph)(OR$_{F6}$)$_2$ (0.190 g, 0.257 mmol) and LiOHMT (0.086 g, 0.256 mmol) to yield yellow crystalline solid (0.135 g, 59%): ^{1}H NMR (400 MHz, C_6D_6) δ 10.64 (s,

1H, Mo=C*H*CMe$_2$Ph, J_{CH} = 122.7 Hz), 7.25-7.08 (overlapping peaks, 4H, aromatics), 7.05-6.93 (overlapping peaks 3H, aromatics), 6.92-6.53 (overlapping peaks 3H, aromatics), 6.72 (s, 2H, HMTO), 2.26 (s, 6H, HMTO), 2.20 (s, 6H, HMTO), 1.97 (s, 6H, HMTO), 1.80 (s, 3H, Ad), 1.70-1.50 (overlapping peaks, 9H, MoCHC*Me$_2$*Ph + Ad), 1.47-1.30 (overlapping peaks, 9H, MoCHC*Me$_2$*Ph + Ad), 1.16 (s, 3H, C*H$_3$*); ^{13}C NMR (100 MHz, C_6D_6) δ 276.0 (Mo=*C*HCMe$_2$Ph), 158.7, 150.3, 137.5, 136.6, 136.4, 136.3, 131.9, 130.5, 129.2, 128.7, 126.7, 126.1, 122.2, 76.9, 50.5, 43.7, 35.6, 33.2, 31.0, 29.9, 21.1, 20.7, 20.6; ^{19}F NMR (376 MHz, C_6D_6) δ – 77.4 (q, 3F, C*F$_3$*), - 78.1 (q, 3F, C*F$_3$*). Anal. Calcd for $C_{48}H_{55}F_6MoNO_2$: C, 64.93; H, 6.24, N, 1.58. Found: C, 64.95; H, 6.12; N, 1.56.

Mo(NAr')(CHCMe$_2$Ph)(OR$_{F6}$)(N(H)HMT) (6). The procedure is the same as that of **2**, employing Mo(NAr')(CHCMe$_2$Ph)(OR$_{F6}$)$_2$ (0.209 g, 0.295 mmol) and LiN(H)HMT (0.099 g, 0.295 mmol) to yield yellow solid (0.120 g, 48%): ^{1}H NMR (400 MHz, C_6D_6) δ 11.86 (s, 1H, Mo=C*H*CMe$_2$Ph, J_{CH} = 121.2 Hz), 7.82 (s, 1H, MoN(*H*)HMT), 7.25-7.10 (overlapping peaks, 3H, aromatics), 7.00-6.55 (overlapping peaks, 11H, aromatics), 6.40 (s br, 1H, aromatic), 2.38 (s, 3H, C*H$_3$*), 2.23 (s, 6H, C*H$_3$*), 2.19 (s, 3H, C*H$_3$*), 2.10 (s, 3H, C*H$_3$*), 2.03 (s, 6H, C*H$_3$*), 1.67 (s, 3H, C*H$_3$*), 1.19 (s, 3H, C*H$_3$*), 1.16 (s, 3H, C*H$_3$*), 1.00 (s, 3H, C*H$_3$*); ^{13}C NMR (100 MHz, C_6D_6) δ 287.3 (Mo=*C*HCMe$_2$Ph), 156.1, 149.5, 148.2, 135.6, 131.3, 130.7, 130.2, 129.2, 129.2, 128.9, 128.6, 127.1, 126.1, 125.8, 121.1, 54.5, 30.5, 28.8, 21.2, 20.6, 20.5, 20.3, 20.0, 19.4, 19.3; ^{19}F NMR (376 MHz, C_6D_6) δ – 76.7 (q, 3F, C*F$_3$*), - 77.2 (q, 3F, C*H$_3$*). Anal. Calcd for $C_{46}H_{50}F_6MoN_2O$: C, 64.48; H, 5.88, N, 3.27.

Mo(NAr^{iPr})(CHCMe$_2$Ph)(OR$_{F6}$)(N(H)HMT) (7). The procedure is the same as that of **2**, employing Mo(NAr^{iPr})(CHCMe$_2$Ph)(OR$_{F6}$)$_2$ (0.296 g, 0.409 mmol) and LiN(H)HMT (0.137 g, 0.408 mmol) to yield orange crystalline solid (0.326 g, 92%): ^{1}H NMR (400 MHz, C_6D_6) δ; 11.72 (s, 1H, Mo=C*H*CMe$_2$Ph, J_{CH} = 117.9 Hz), 7.99 (s, 1H, MoN(*H*)HMT), 7.23 (dd, 1H, aromatic), 7.08 (dd, 1H, aromatic), 7.05-6.70 (overlapping peaks, 12H, aromatics), 6.72 (s br, 2H, aromatic), 3.22 (sept, 1H, C*H*Me$_2$), 2.31 (s, 6H, C*H$_3$*), 2.24 (s, 6H, C*H$_3$*), 1.94 (s br, 6H, C*H$_3$*), 1.53 (s, 3H, C*H$_3$*), 1.25 (d, 3H, CH(Me)C*H$_3$*), 1.19 (s, 3H, C*H$_3$*), 1.12 (d, 3H, CH(C*H$_3$*)Me), 0.82 (s, 3H, C*H$_3$*); ^{13}C NMR (100 MHz, C_6D_6) δ 286.5 (Mo=*C*HCMe$_2$Ph), 155.5, 149.4, 148.0, 146.1, 137.9, 137.4, 137.4, 135.5, 130.3, 129.0, 128.5, 128.2, 126.3, 125.7, 125.6, 125.5, 121.5, 55.6, 30.4, 30.1, 27.8, 24.4, 22.6, 21.2, 20.5, 19.4; ^{19}F NMR (376 MHz, C_6D_6) δ – 77.1 (q, 3F, C*F$_3$*), - 77.7 (q, 3F, C*H$_3$*). Anal. Calcd for $C_{47}H_{52}F_6MoN_2O$: C, 64.82; H, 6.02, N, 3.22. Found: C, 64.43; H, 5.89; N, 3.15.

Mo(NAd)(CHCMe$_2$Ph)(OR$_{F6}$)(HMT) (8) Mo(NAd)(CHCMe$_2$Ph)(OR$_{F6}$)$_2$DME (0.300 g, 0.362 mmol) and LiHMT (0.116 g, 0.362 mmol) were mixed together in 3.00 mL of toluene at RT and left stirring for 12 h. Then, the solution was placed at -35 °C overnight and then passed through Celite. The Celite was washed with cold toluene until the color was gone and the solvent was removed from the filtrate under reduced pressure. The crude was triturated with pentane 3 times and twice with TMS to induce precipitation of the product, which was collected by filtration (0.308 g, 95%). X-ray quality crystals were grown by dissolving **8** (0.060 g) in a minimal amount of pentane and placing the solution at – 35 °C a few days: ^{1}H NMR (400 MHz, C_6D_6) δ 10.99 (s, 1H, MoC*H*, J_{CH} = 120.2 Hz), 7.40 (d, 2H, HMT), 7.20-7.10 (m, 3H, Ph), 7.03 (t, 1H, HMT), 6.90 (s, 2H, Mes), 6.84 (m, 2H, Ph), 6.79 (s, 2H, Mes), 2.23 (s, 6H, *o*-Mes), 2.21 (s, 6H, *o*-Mes), 2.16 (s, 6H, *p*-Mes), 1.71 (s, 3H, Ad), 1.44 (s, 6H, C*Me*$_2$Ph), 1.36 (s, 6H, C*Me*$_2$Ph *syn*), 1.33 (s, 6H, Ad), 1.13 (s, 3H, (CF$_3$)$_2$C*H*$_3$C); ^{13}C NMR (100 MHz, C_6D_6) δ 279.4 (Mo*C*H, J_{CH} = 120.23 Hz), 173.7 (*C*F$_3$), 150.9, 150.5, 145.6, 136.7, 136.2, 136.0, 135.7, 129.7, 129.5, 129.3, 128.1, 125.9, 77.6, 53.5, 42.5, 35.6, 35.2, 30.4, 30.0, 22.1, 21.8, 21.1; ^{19}F NMR (375 MHz, C_6D_6) δ -77.2 (q, 1F), -77.9 (q, 1F). Anal. Calcd for $C_{48}H_{55}F_6MoNO$: C, 66.12; H, 6.36, N, 1.61. Found: C, 66.37; H, 6.30; N, 1.74.

Mo(NAd)(CHCMe$_2$Ph)(OR$_{F9}$)$_2$ (15) Mo(NAd)(CHCMe$_2$Ph)(OTf)$_2$DME (0.503 g, 0.658 mmol) was suspended in Et$_2$O and stored at -35 °C for 1 h. Then, LiOR$_{F9}$ (0.319 g, 1.32 mmol) was added in one portion and the mixture was allowed to warm-up to RT and stir for 12 h. The solvent was removed under vacuo; the crude solid redissolved in CH_2Cl_2 and passed through Celite to remove LiOTf. Solvent was removed from the filtrate under reduced pressure and the crude was triturated with pentane to precipitate a yellow solid, which was collected by filtration (0.370 g, 66%): ^{1}H NMR (400 MHz, C_6D_6) δ 13.65 (s, 0.35H, MoC*H*, J_{CH} = 151.9 Hz), 12.61 (s, 1H, MoC*H*, J_{CH} = 121.9 Hz), 7.30 (d, 1H, Ar *syn*), 7.24-7.14 (m, 4H, Ar *anti* + *syn*), 7.06-6.98 (m, 1.5H, Ar *anti* + *syn*), 3.20-2.90 (overlapping peaks, 3.5H, DME *anti*), 2.05 (s, 2H, C*Me*$_2$Ph *anti*), 1.82 (m, 8H, Ad *anti* + *syn*), 1.73 (s br, 4H, Ad *anti* + *syn*), 1.47 (s, 6H, C*Me*$_2$Ph *syn*), 1.28 (m, 8H, Ad *anti* + *syn*); ^{13}C NMR (100 MHz, C_6D_6) δ 307.7 (Mo*C*H, J_{CH} = 151.9 Hz), 292.6 (Mo*C*H, J_{CH} = 121.9 Hz), 149.9 (*C*F$_3$ *anti*), 149.0 (*C*F$_3$ *syn*), 128.8, 128.7, 127.1, 126.8, 126.7, 125.7, 122.9, 120.0, 84.0 (*C*(CF$_3$)$_3$ *anti*), 81.8 (*C*(CF$_3$)$_3$ *syn*), 53.7 (*C*Me$_2$Ph *anti*), 50.6 (*C*Me$_2$Ph *syn*), 43.8, 43.1, 35.4, 31.1, 29.8, 29.6, 26.7; ^{19}F NMR (376 MHz, C_6D_6) δ -74.5 (s, 1F, *syn*), -74.7 (s, 0.35F, *anti*). Anal. Calcd for $C_{116}H_{118}F_{72}Mo_4N_4O_{10}$: C, 40.04; H, 3.42, N, 1.61. Found: C, 40.00; H, 3.50; N, 1.50.

Mo(NAr^m)(CHCMe$_2$Ph)(OR$_{F6}$)(HMT) (9) Mo(NAr^m)(CHCMe$_2$Ph)(OR$_{F6}$)$_2$(DME) (0.258 g, 0.323 mmol) and LiHMT (0.103 g, 0.321 mmol) were mixed in benzene (2.00 mL) at RT in a vial, capped and left stirring at 12 h to get 100% of product: ^{1}H NMR (400 MHz, C_6D_6) δ 10.90 (s, 1H, Mo=C*H*CMe$_2$Ph, J_{CH} = 122.0 Hz), 7.34 (dd, 2H, aromatic), 7.24 (td, 1H, aromatic), 7.15-7.02 (overlapping peaks, 3H, aromatic), 6.98 (dd, 2H, aromatic), 6.86 (s, 4H, HMT), 6.74 (s, 1H, Ar^m), 6.68 (s, 1H, Ar^m), 6.61 (s, 1H, Ar^m), 2.21 (s, 6H, C*H*$_3$), 2.18 (s, 3H, C*H*$_3$), 2.11 (s, 3H, C*H*$_3$), 2.06 (s, 12H, C*H*$_3$), 2.03 (s, 3H, C*H*$_3$), 1.32 (s, 3H, C*H*$_3$); ^{13}C NMR (100 MHz, C_6D_6) δ 282.8 (Mo*C*HCMe$_2$Ph); ^{19}F NMR (376 MHz, C_6D_6) δ -77.4 (q, 3F, C*F*$_3$), - 78.6 (q, 3F, C*F*$_3$).

Mo(NAr')(CHCMe$_2$Ph)(OR$_{F6}$)(HMT) (10) Mo(NAr')(CHCMe$_2$Ph)(OR$_{F6}$)$_2$ (0.010 g, 0.014 mmol) and LiHMT (0.005 g, 0.014 mmol) were mixed together and heated at 80 °C for 5 d to get 90% of products: ^{1}H NMR (400 MHz, C_6D_6) δ 10.93 (s, 1H, Mo=C*H*CMe$_2$Ph, 90%).

Mo(NAr)(CHCMe$_2$Ph)(OR$_{F6}$)(HMT) (11) Mo(NAr)(CHCMe$_2$Ph)(OR$_{F6}$)$_2$ (0.010 g, 0.013 mmol) and LiHMT (0.004 g, 0.013 mmol) were mixed and heated at 80 °C for 5 d to get 18% of products: ^{1}H NMR (400 MHz, C_6D_6) δ 10.90 (s, 1H, Mo=C*H*CMe$_2$Ph).

Mo(NAd)(CHCMe$_2$Ph)(OR$_{F6}$)(TIPT) (12) Mo(NAd)(CHCMe$_2$Ph)(OR$_{F6}$)$_2$DME (0.300 g, 0.362 mmol) and LiTIPT (0.146 g, 361 mmol) were mixed together and heated at 80 °C for 5 d to get full conversion to a single product: ^{1}H NMR (400 MHz, C_6D_6) δ 11.75 (s, 1H, Mo=C*H*CMe$_2$Ph).

Mo(NAr')(CHCMe$_2$Ph)(OR$_{F6}$)(TIPT) (13) Mo(NAr')(CHCMe$_2$Ph)(OR$_{F6}$)$_2$ (0.010 g, 0.014 mmol) and LiTIPT (0.006 g, 0.014 mmol) were mixed together and heated at 80 °C for 2 wk to get 28% of products: ^{1}H NMR (400 MHz, C_6D_6) δ 12.14 (s, 1H, Mo=C*H*CMe$_2$Ph), 11.26 (s, 0.6H, Mo=CHCMe$_2$Ph), 10.95 (s, 1H, Mo=CHCMe$_2$Ph).

Mo(NAr)(CHCMe$_2$Ph)(OR$_{F6}$)(TIPT) (14) Mo(NAr)(CHCMe$_2$Ph)(OR$_{F6}$)$_2$ (0.010 g, 0.013 mmol) and LiTIPT (0.005 g, 0.013 mmol) were mixed and heated at 80 °C for 5 d to get 7% of products: ^{1}H NMR (400 MHz, C_6D_6) δ 12.24 (s, 1H, Mo=C*H*CMe$_2$Ph), 11.35 (s, 0.75H, Mo=C*H*CMe$_2$Ph).

Mo(NAd)(CHCMe$_2$Ph)(OR$_{F9}$)(HMT) (16) Mo(NAd)(CHCMe$_2$Ph)(OR$_{F9}$)$_2$ (0.300 g, 0.354 mmol) and LiHMT (0.113 g, 0.354 mmol) were mixed together in toluene (3.00 mL) at RT for 12 h to get a single product: ^{1}H NMR (400 MHz, C_6D_6) δ 11.24 (s, 1H, Mo=C*H*CMe$_2$Ph, J_{CH} =

119.2 Hz), 7.40-6.70 (overlapping peaks, 12H, aromatics), 2.22 (s, 6H, C*H*$_3$), 2.21 (s, 3H, C*H*$_3$), 2.19 (s, 6H, C*H*$_3$), 2.07 (s, 6H, C*H*$_3$), 1.68 (s, 3H, Ad), 1.50-1.40 (overlapping peaks, 6H, Ad + C*H*$_3$), 1.30 (s, 6H, Ad), 0.96 (s, 3H, Ad); ^{13}C NMR (100 MHz, C_6D_6) δ 285.3 (Mo*CH*CMe$_2$Ph), 174.4, 150.8, 150.4, 145.7, 141.9, 139.4, 136.5, 136.4, 135.7, 130.7, 130.3, 129.6, 129.4, 128.5, 128.3, 127.7, 126.5, 126.0, 79.2 (O*C*(CF$_3$)$_3$), 54.4, 41.9, 35.4, 29.9, 22.0, 21.7, 21.1, 21.1, 20.0; ^{19}F NMR (376 MHz, C_6D_6) δ -73.4 (s, 9F, C*F*$_3$).

RCM of DAE Complexes **1-8** and **1a-5a** (0.010 g, 0.011 mmol) were dissolved in 0.70 mL of C_6D_6 and place inside a J-Young tube. Then, DAE (0.022 g, 0.230 mmol) was added to it and the NMR tube was sealed and monitored over the course of 1 day.

Homocoupling of 1-hexene Complexes **1-8** and **1a-5a** (0.010 g, 0.011 mmol) were dissolved in 1.50 mL of C_6D_6 in a vial. Then, 1-hexene (0.075-0.080 mL, 0.570 mmol) was added to it and the solution was stirred in an open vial, under a nitrogen-filled atmosphere, for the indicated time. The solutions were placed in a J-Young tube to monitor its progress by ^{1}H and ^{13}C NMR, based on the spectra of pure *cis*- and *trans*-5-decene obtained from Sigma-Aldrich.

Homocoupling of 1-octene Complexes **1-8** and **1a-5a** (0.005 g, 0.006 mmol) were dissolved in 0.75 mL of C_6D_6 in a vial. Then, 1-octene (0.043-0.050 mL, 0.300 mmol) was added to it and the solution was stirred in an open vial, under a nitrogen-filled atmosphere, for the indicated time. An aliquot was then dissolved in $CDCl_3$ to monitor its progress by ^{1}H NMR.

ROMP of DCMNBD Complexes **1-8** and **1a** (0.005 g, 0.006 mmol) were dissolved in 0.50 ml of toluene and added to a stirring toluene solution of DCMNBD (0.70 mL, 50 eq, 0.300 mmol). The solution was left stirring for 2 h until it formed a gel. Then, the gel was redissolved in CH_2Cl_2 (7.00 mL) and quenched with benzaldehyde (0.100 mL) before precipitation from methanol (60.0 mL) and isolation by vacuum filtration. The dry polymer was examined by ^{1}H and ^{13}C NMR to determine the *tacticity* and *cis* content according to known literature reports.

X-ray Structure Determination Low-temperature diffraction data (ϕ-and ω-scans) were collected on a Bruker-AXS X8 Kappa Duo diffractometer coupled to a Smart Apex2 CCD detector with Mo K_α radiation (λ = 0.71073 Å) from an *IμS* micro-source for the structure of compounds **5**, **7**, and **8**. All structures were solved by direct methods using SHELXS[16] and refined against F^2 on all data by full-matrix least squares with SHELXL-97[17] using established refinement techniques.[18] All non-hydrogen atoms were refined anisotropically. All hydrogen atoms were included into the model at geometrically calculated positions and refined using a riding model

unless otherwise noted. The isotropic displacement parameters of all hydrogen atoms were fixed to 1.2 times the *U* value of the atoms they are linked to (1.5 times for methyl groups). All disordered atoms were refined with the help of similarity restraints on the 1,2- and 1,3-distances and displacement parameters as well as rigid bond restraints for anisotropic displacement parameters.

Compound **5** crystallizes in the triclinic space group $P\bar{1}$. The analyzed crystal was a non-merohedral twin and it was refined using cell_now/SAINT/TWINABS against the HKLF5 format file. Coordinates for the hydrogen atom of C(1) were taken from the difference Fourier synthesis.

Compound **7** crystallizes in the monoclinic space group $P2_1/c$ and was refined as stated above.

Compound **8** crystallized in the triclinic space group $P\bar{1}$. The crystal used for analysis was a nonmerohedral twin and the diffraction data was treated with cell now, followed by SAINT, TWINABS, SHELXL refinement against the HKLF5 format file. The value for R(int) in the CIF file is taken from the output of TWINABS. There is a three part disorder for the alkoxide ligand due to rotation. The anisotropic displacement parameters of the F and C atoms of the CF_3 groups were constrained to be equivalent pairwise. As a result of merohedral twin treatment, there are three more observations than unique reflections. In order to correctly estimate the standard uncertainties, the third parameter of the L. S. card was set to 238, above the difference between observed and unique reflections.

Crystal data are shown in Tables 5-7.

Table 5. Crystal data and structure refinement for **5**.

Identification code	x12044	
Empirical formula	C48 H55 F6 Mo N O2	
Formula weight	887.87	
Temperature	100(2) K	
Wavelength	0.71073 Å	
Crystal system	Triclinic	
Space group	$P\bar{1}$	
Unit cell dimensions	a = 11.3519(5) Å	α =102.7680(10)°
	b = 11.6306(6) Å	β=95.3350(10)°
	c = 18.6057(9) Å	γ =112.9690(10)°
Volume	2161.43(18) $Å^3$	
Z	2	
Density (calculated)	1.364 Mg/m^3	
Absorption coefficient	0.368 mm^{-1}	
F(000)	924	
Crystal size	0.23 x 0.22 x 0.10 mm^3	
Theta range for data collection	1.98 to 31.15°	
Index ranges	-16<=h<=16, -16<=k<=16, 0<=l<=27	
Reflections collected	13841	
Independent reflections	13841 [R(int) = 0.0495]	
Completeness to theta = 31.15°	99.2 %	
Absorption correction	Semi-empirical from equivalents	
Max. and min. transmission	0.9641 and 0.9201	
Refinement method	Full-matrix least-squares on F^2	
Data / restraints / parameters	13841 / 49 / 536	
Goodness-of-fit on F^2	1.043	
Final R indices [I>2sigma(I)]	R1 = 0.0354, wR2 = 0.0943	
R indices (all data)	R1 = 0.0374, wR2 = 0.0958	
Largest diff. peak and hole	0.894 and -1.196 $e.Å^{-3}$	

Table 6. Crystal data and structure refinement for **7**.

Identification code	x12055	
Empirical formula	C47 H52 F6 Mo N2 O	
Formula weight	870.85	
Temperature	100(2) K	
Wavelength	0.71073 Å	
Crystal system	Monoclinic	
Space group	$P2_1/c$	
Unit cell dimensions	a = 20.7835(19) Å	α= 90°
	b = 10.8355(10) Å	β= 104.390(2)°
	c = 19.7836(18) Å	γ = 90°
Volume	4315.5(7) $Å^3$	
Z	4	
Density (calculated)	1.340 Mg/m^3	
Absorption coefficient	0.366 mm^{-1}	
F(000)	1808	
Crystal size	0.06 x 0.05 x 0.02 mm^3	
Theta range for data collection	2.02 to 31.00°	
Index ranges	-30<=h<=30, -15<=k<=15, -28<=l<=28	
Reflections collected	205294	
Independent reflections	13705 [R(int) = 0.0537]	
Completeness to theta = 31.00°	99.6 %	
Absorption correction	Semi-empirical from equivalents	
Max. and min. transmission	0.9927 and 0.9783	
Refinement method	Full-matrix least-squares on F^2	
Data / restraints / parameters	13705 / 2 / 531	
Goodness-of-fit on F^2	1.061	
Final R indices [I>2sigma(I)]	R1 = 0.0327, wR2 = 0.0786	
R indices (all data)	R1 = 0.0432, wR2 = 0.0836	
Largest diff. peak and hole	1.422 and -0.642 $e.Å^{-3}$	

Table 7. Crystal data and structure refinement for **8**.

Identification code	x11109_t5	
Empirical formula	C48 H54 F6 Mo N O	
Formula weight	870.86	
Temperature	100(2) K	
Wavelength	0.71073 Å	
Crystal system	Triclinic	
Space group	$P\bar{1}$	
Unit cell dimensions	a = 10.6178(9) Å	α= 109.268(2)°
	b = 18.8500(16) Å	β= 96.928(2)°
	c = 22.2527(19) Å	γ = 90.162(2)°
Volume	4169.3(6) $Å^3$	
Z	4	
Density (calculated)	1.387 Mg/m^3	
Absorption coefficient	0.379 mm^{-1}	
F(000)	1812	
Crystal size	0.20 x 0.15 x 0.05 mm^3	
Theta range for data collection	1.15 to 30.62°	
Index ranges	-15<=h<=15, -26<=k<=25, 0<=l<=31	
Reflections collected	23776	
Independent reflections	23776 [R(int) = 0.0958]	
Completeness to theta = 25.00°	98.0 %	
Absorption correction	Semi-empirical from equivalents	
Max. and min. transmission	0.9813 and 0.9281	
Refinement method	Full-matrix least-squares on F^2	
Data / restraints / parameters	23538 / 3839 / 1265	
Goodness-of-fit on F^2	1.031	
Final R indices [I>2sigma(I)]	R1 = 0.0989, wR2 = 0.2536	
R indices (all data)	R1 = 0.1250, wR2 = 0.2788	
Largest diff. peak and hole	5.229 and -7.881 $e.Å^{-3}$	

REFERENCES

(1) Poater, A.; Solans-Monfort, X.; Clot, E.; Coperet, C. ; Eisenstein, O. *J. Am. Chem. Soc.* **2007**, *129*, 8207.

(2) Singh, R.; Schrock, R. R.; Muller, P.; Hoveyda, A. H. *J. Am. Chem. Soc.* **2007**, *129*, 12654.

(3) Malcolmson, S. J.; Meek, S. J.; Satterly, E. S.; Schrock, R. R.; Hoveyda, A. H. *Nature*, **2008**, *456*, 933.

(4) Marinescu, S. C.; Singh, R.; Hock, A. S.; Wampler, K. M.; Schrock, R. R.; Muller, P. *Organometallics* **2008**, *27*, 6570.

(5) Flook, M. M.; Jiang, A. J.; Schrock, R. R.; Muller, P.; Hoveyda, A. H. *J. Am. Chem. Soc.* **2009**, *131*, 7962.

(6) Hock, A. S.; *J. Am. Chem. Soc.* **2006**, *128*, 16373.

(7) Solans-Monfort, X.; Coperet, C.; Eisenstein, O. *J. Am. Chem. Soc.* **2010**, *132*, 7750.

(8) Pilyugina, T. S.; Schrock, R. R.; Hock, A. S.; Muller, P. *Organometallics* **2005**, *24*, 1929.

(9) Sinha, A.; Lopez, L. P. H.; Schrock, R. R.; Hock, A. S.; Muller, P. *Organometallics* **2006**, *25*, 1412.

(10) Schiemenz, B.; Power, P. P. *Organometallics* **1996**, *15*, 958.

(11) Schrock, R. R.; Luo, S.; Lee, J. C., Jr.; Zanetti, N. C.; Davis, W. M. *J. Am. Chem. Soc.* **1996**, *118*, 3883.

(12) Sinha, A.; Schrock, R. R.; Muller, P.; Hoveyda, A. H. *Organometallics* **2006**, *25*, 4621.

(13) Oskam, J. H.; Fox, H. H.; Yap, K. B.; McConville, D. H.; O'Dell, R.; Lichtenstein, B. J.; Schrock, R. R. *Jour. Organomet. Chem.* **1993**, *459*, 185.

(14) Gerber, L. C. H.; Schrock, R. R.; Müller, P. Takase, M. K. *J. Am. Chem. Soc.* **2011**, *133*, 18142.

(15) Dr. Smaranda C. Marinescu, Ph.D. Thesis (MIT, 2011).

(16) Sheldrick, G. M. (1990). *Acta Cryst.* **A46**, 467-473.

(17) Sheldrick, G. M. (2008). *Acta Cryst.* **A64**, 112-122.

(18) Müller, P. *Crystallography Reviews* **2009**, *15*, 57-83.

(19) Dr. Annie Jinying Hannah King, Ph.D. Thesis (MIT 2010).

(20) Tabor, D. C.; White, F. H.; Collier, L. W.; Evans, S. A. *J. Org. Chem.* **1983**, *48*, 1638.

APPENDIX

Survey of the Catalytic Selectivity of Molybdenum Alkylidene Imido Bisalkoxide and Molybdenum Alkylidene Imido Alkoxide Pyrrolide Complexes

INTRODUCTION

The synthesis of long unsaturated polymers containing conjugated double bonds throughout the chain is of interest to the scientific community due to their important applications in photophysics.[1,2] For instance, they can be used as third-order nonlinear optical materials, such as optical switches.[1] In addition, these polymers could display interesting electrical, photoconductive, and photorefractive properties.[2] A main challenge, however, has been the synthesis of conjugated polymers that are relatively stable to air oxidation, are soluble in common solvents, and retain planarity along their structure.[3,4] Ring closing metathesis polymerization (RCMP) of substituted 1,6-heptadiynes produces polymers that meet all these criteria.[5] The polymers resulting from RCMP contain 5- and/or 6-membered rings, which are hypothesized to be formed by α- and β-addition of the alkyne to the metal center, respectively (Scheme 1).[6]

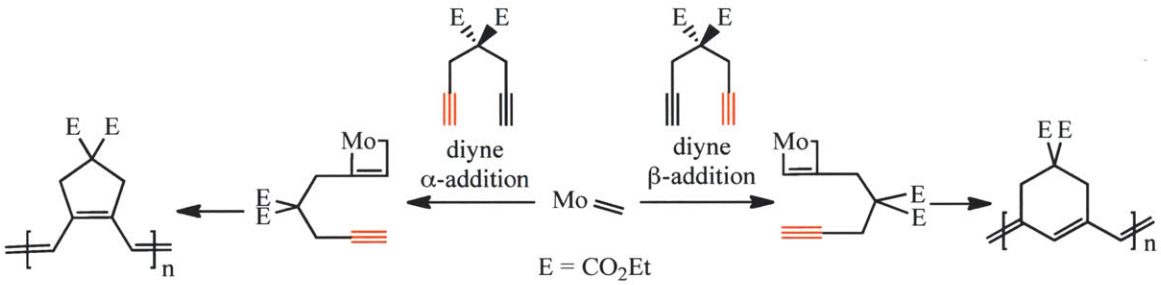

Scheme 1 – Polymeric structural units that arise during RCMP of DEDPM by molybdenum alkylidene catalysts as a result of α-addition (left) and β-addition (right) of the monomer.

Previous studies showed that with molybdenum imido alkylidene bisalkoxide catalysts, α-addition of the substrate is preferred, yielding polymer containing 5-membered rings.[7-10] Ru catalysts that accomplish the same task are also known.[11-14] On the other hand, when the catalyst is supported by carboxylate ligands, β-addition prevails and polymers containing mostly 6-membered rings are obtained.[15-16] The most selective catalysts towards β-addition are $Mo(NAr^{tBu})(CH\text{-}t\text{-}Bu)(O_2CCPh_3)_2$ (Ar^{tBu} = 2-*t*-BuC_6H_4) and $Mo(NAr)(CHCMe_2Ph)(Me_2Pyr)(O_2CTRIP)$ (Ar = 2,6-*i*-$Pr_2C_6H_3$; Me_2Pyr = 2,5-$Me_2C_4H_2N$; TRIP = 2,4,6-*i*-$Pr_3C_6H_2$; see Chapter 2).

Although molybdenum imido alkylidene catalysts bearing two alkoxide or two carboxylate ligands produce regioselective α or β product during diyne polymerizations, the similar ring closing enyne metathesis (RCEM) of disubstituted 2-allyl-2-propargylmalonate, such as diethyl-2-allyl-2-propargylmalonate (DEAPM), is not catalyzed by either type of catalyst.[17] With the

initial preparation of molybdenum imido alkylidene bispyrrolide catalyst precursors,[18] the group has begun synthesizing molybdenum imido alkylidene monopyrrolide monoalkoxide catalysts (see Chapters 3-4) that have been shown to exhibit catalytic activity for the RCEM of this kind of substrates.[19] As with the diyne pathway, the enyne reaction can form either α or β products (Scheme 2). Mo(NAr)(CHCMe$_2$Ph)(Me$_2$Pyr)(OC(CF$_3$)$_2$Me) catalysts favor the formation of the β product only, which complements ruthenium catalysts that only favor α-product formation for the same substrates. [20-21]

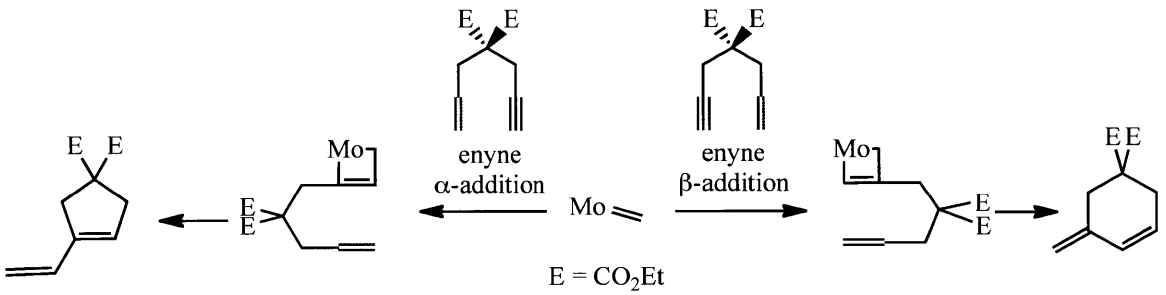

Scheme 2 – Cyclic dienes that can be produced by RCM of DEAPM by molybdenum alkylidene catalysts as a result of α-addition (left) and β-addition (right) of the substrate.

In Section A.2 we survey the reactivity of a variety of MAP and bisalkoxide species towards the polymerization of DEDPM to the effect of learning what combination of ligands can yield polymer containing a high number of 5-membered ring structures. The synthesis of two such complexes is detailed in Section A.1, along with some other reactions of interest. Preparation of polymer with only 5-membered rings can open opportunities for detailed spectroscopic studies as learning tools for biological systems where polyconjugation is known to exist, as well as in the preparation of new electronic devices.

RESULTS AND DISCUSSION

A.1 Synthesis and characterization of catalysts containing chiral alkoxides or phenoxides.

A.1.1 Preparation, structural studies, and reactivity of diastereomerically pure (*R*)-Mo(NAr)(CHCMe$_2$Ph)(Me$_2$Pyr)(OR*).

The synthesis of the first monoalkoxide monopyrrolide (MAP) molybdenum alkylidene complexes established a facile route for the preparation of molybdenum catalysts containing four different ligands. The preparation of MAP species containing chiral alkoxides or phenoxides produces diastereomers that can be separated and isolated in certain cases. The use of diastereomeric MAP complexes in metathesis reactions has vastly improved the reactivity and selectivity of many previously known molybdenum alkylidene catalysts.[33]

The first chiral alcohol that was studied in the Schrock group was (2*R*)-R*OH, which can be prepared stereospecifically in good yields from camphor using *p*-chlorophenyl magnesium iodide in the presence of the Lewis acid $LaCl_3$*2LiCl, according to literature reports (equation 1).[32] Treatment of Mo(NAr)(CHCMe$_2$Ph)(Me$_2$Pyr)$_2$ with one equivalent of the pure alcohol was found to give a mixture of diastereomers in an initial ratio of 3:1, but was not further investigated due to the high solubility of the complex in common organic solvents.[19b]

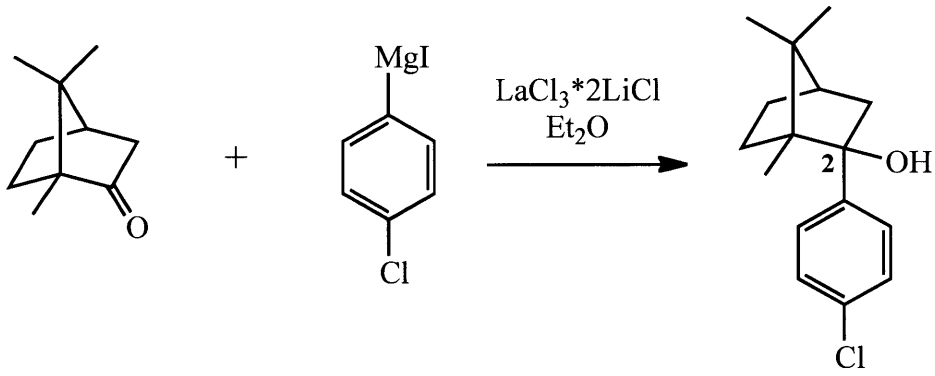

(1)

(2*R*)-R*OH

Our goal was to isolate at least one of the diastereomers formed. In order to accomplish this, a 1.50 g scale reaction between Mo(NAr)(CHCMe$_2$Ph)(Me$_2$Pyr)$_2$ and one equivalent of (2*R*)-R*OH was prepared and the crude product (containing 75% of the *R*, *R* diasteromer) was recrystallized from pentane at -35 °C over a period of days to yield a mixture containing 88% of the *R* diastereomer in an overall yield of 28%. Recrystallization of this mixture once more yielded the pure *R*-diastereomer in low overall yield (7%). The ^{1}H NMR spectra of the mixture at all three purification steps is shown in Figure 1, while equation 2 summarizes the purification procedure.

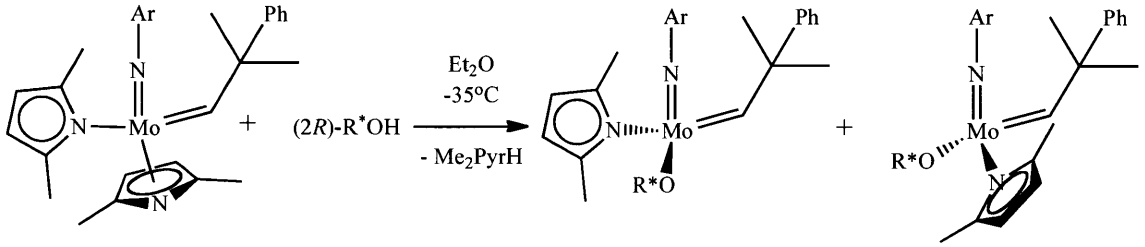

(2)

Crude product: *S*-**1** (25%) and *R*-**1** (75%)
1st recrystallization: *S*-**1** (12%) and *R*-**1** (88%); yield = 28%
2nd recrystallization: *S*-**1** (< 0.1%) and *R*-**1** (> 99.9%); yield = 7%

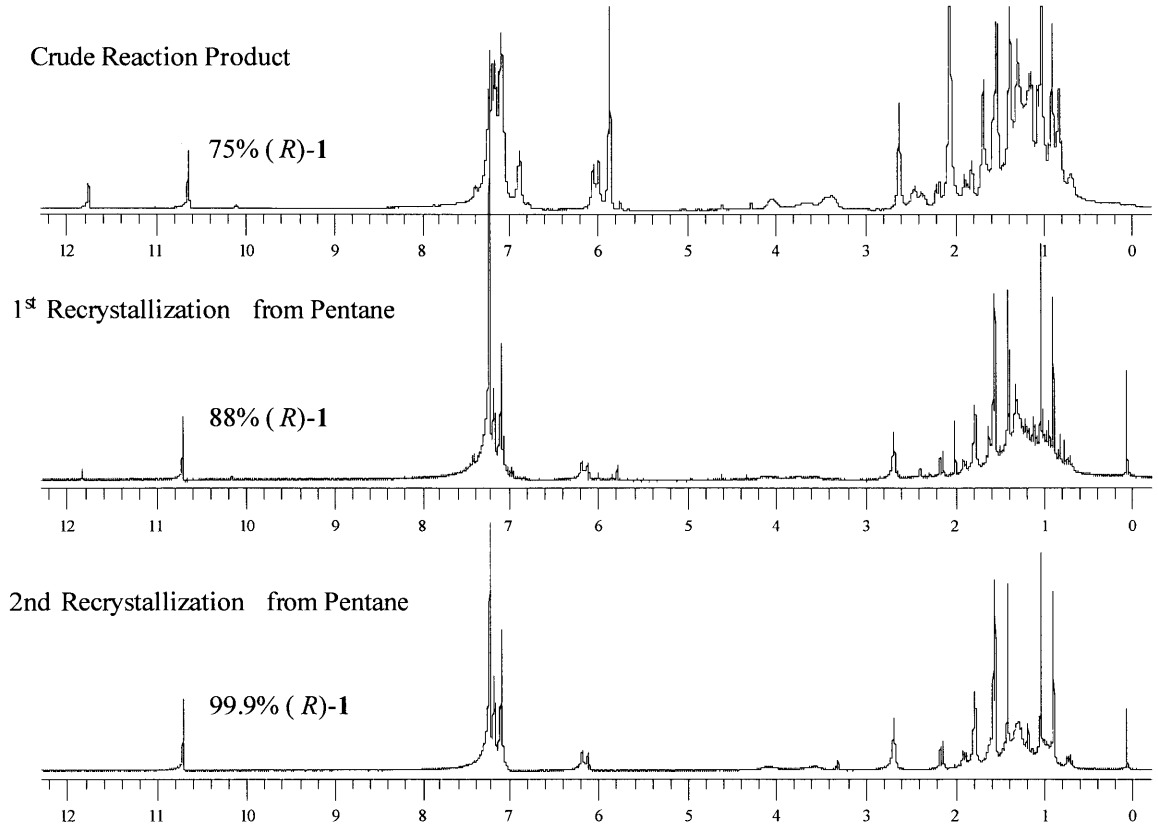

Figure 1 – ^{1}H NMR, in C_6D_6, of the diastereomeric mixture of **1** from the crude (above), first recrystallized product (middle) and second recrystallized product (below). Overall enrichment of *R*-**1** is 99.9%.

It can be seen from Figure 1 that the resonances corresponding to the pyrrolide and imido ligand are broad, which could be a result of restricted rotation of the ligands. To gain better insight of the environment around the metal of the pure diastereomer, crystals of (*R*)-**1** were grown from a 1:1 ether/pentane solution and analyzed by X-ray crystallography; the structure of the complex is shown in Figure 2. The diastereomer (*R*)-**1** crystallized in the orthorhombic space group $P2_12_12_1$ and it is described as a pseudo-tetrahedral complex. All bond lengths, as well as the Mo(1)-C(1)-C(2) (147.60(16)°) and the Mo(1)-N(1)-C(11) (171.77(16)°) bond angles are similar to those observed in other MAP species. The configuration of the alkylidene ligand is *syn* (directed towards the imido group) and the *p*-chlorophenyl group of the alkoxide protects the CON(pyr) face of the molecule.

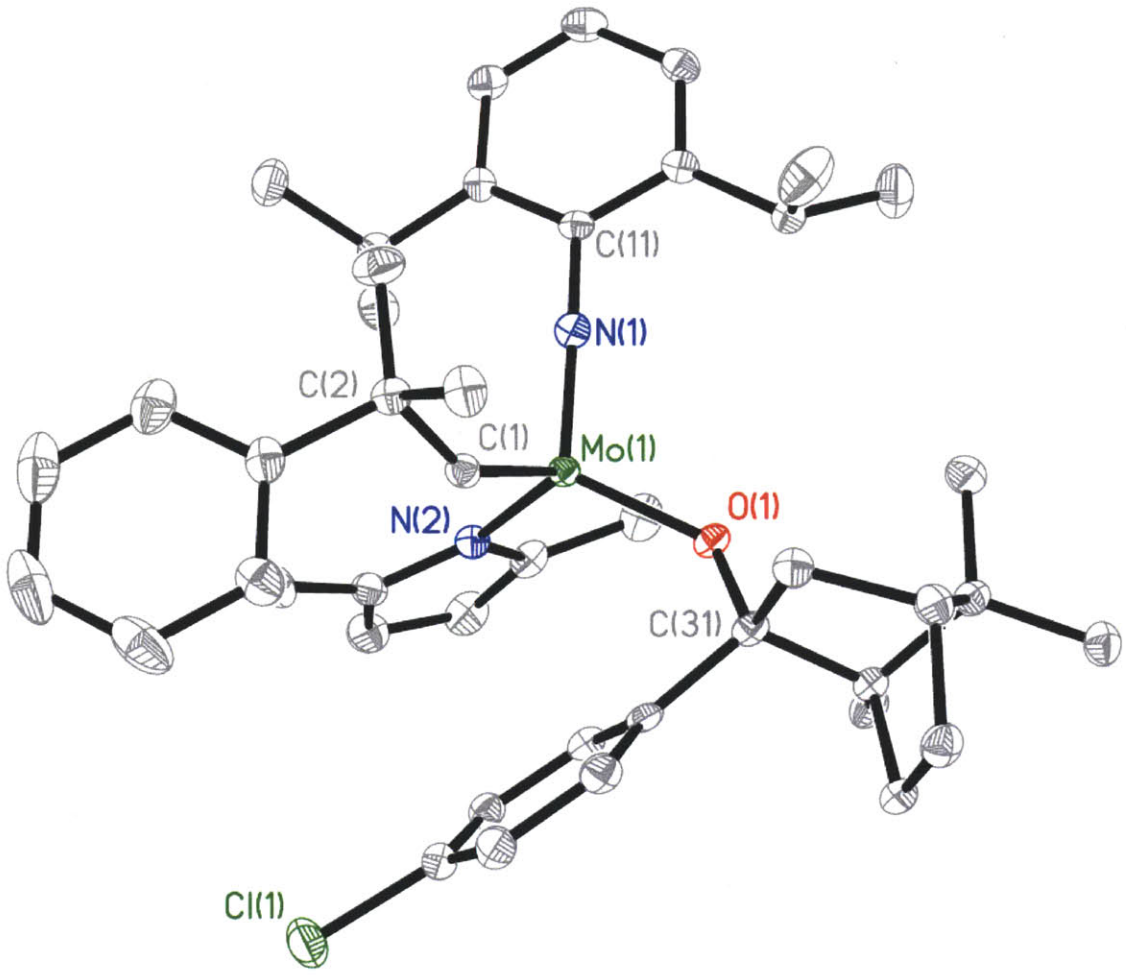

Figure 2 - The solid state structure of (*R*)-**1** (50% probability ellipsoids). Selected bond distances (Å) and angles (°): Mo(1)-N(1) = 1.7285(18), Mo(1)-C(1) = 1.8731(22), Mo(1)-O(1) = 1.9143(15), Mo(1)-N(2) = 2.0367(19), Mo(1)-N(1)-C(11) = 171.77(16), Mo(1)-C(1)-C(2) = 147.60(16), Mo(1)-O(1)-C(31) = 132.35(12).

Pure MAP diastereomers have been shown in the past to be excellent enantioselective catalysts, specially in the enantioselective ring closing metathesis of an N,N-disubstituted aniline (**A**; equation 3) and various natural products.[33] When **A** is treated with 5 mole % of (*R*)-**1**, product **B** is obtained as a mixture with only 4% ee, which is virtually racemic. On the other hand, when **A** is treated with 5 mole % racemic **1** or with 5 mole % 75% (*R*)-**1**, product **B** is obtained as a mixture containing 10% ee and 15% ee respectively. A rough extrapolation shows that if 5 mole % (*S*)-**1** were used as the catalyst then product **B** will be obtained in no more than 20% ee. The difference in reactivity between **1** and other known diastereomerically pure MAP catalysts shows that the chiral alkoxide (R*O) of **1** is a poor choice of ligand for this type of reaction. On the other hand, reaction between DEAPM and 5 mole % (*R*)-**1** gives > 99% β-ring

product (Scheme 2), which is the same result obtained with Mo(NAr)(CHCMe$_2$Ph)(Me$_2$Pyr)(OR) (R = C(CF$_3$)$_2$Me, CH(CF$_3$)$_2$) species.[19b] It should be pointed out that the RCM of DEAPM with Mo(NAr)(CHCMe$_2$Ph)(Me$_2$Pyr)(OR) (R = C(CH$_3$)$_3$, CH(CH$_3$)$_2$, or Ar) polymerize the sample and < 5% ring closed product is observed;[19b] therefore, R*O is a better ligand than either *t*-butoxide or isopropoxide for this type of reaction.

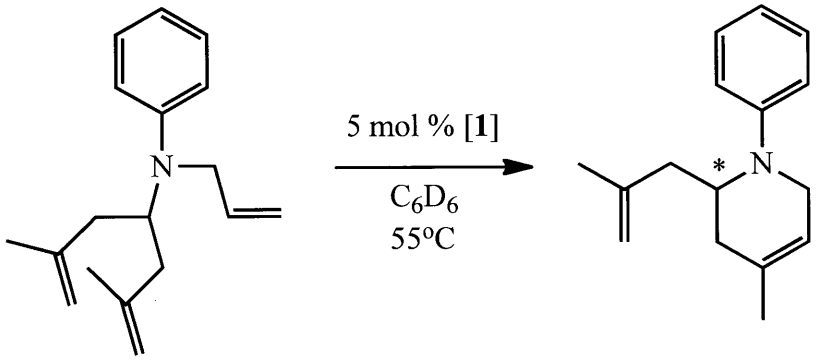

A B (3)

A.1.2 Preparation and structural study of Mo(NAd)(CHCMe$_2$Ph)(OR$^+$)$_2$.

Preparation of the first diastereomerically pure MAP catalyst containing a chiral phenoxide was accomplished with Mo(NAr)(CHCMe$_2$Ph)(Me$_2$Pyr)(OR$^+$) (R$^+$ = (*R*)-3,3-dibromo-5,5',6,6',7,7',8,8'-octahydro-1,1'-bi-2'-(*tert*-butyldimethylsiloxide)naphtha-2-ol; Scheme 3).[33] Catalysts of this kind have been used successfully for ring closing reactions, and it was desired to isolate other derivatives where the imido group was smaller than Ar in order to make them more *Z*-selective.[19g] The imido ligand that was chosen for this task was 1-adamantyl (Ad) because it allows groups on the molybdenacyclobutane to point freely towards it without encountering steric crowding, thus yielding *cis* olefin bonds (see Chapter 1). Unfortunately, when Mo(NAd)(CHCMe$_2$Ph)(Me$_2$Pyr)$_2$ is treated with one equivalent of R$^+$OH a mixture of MAP diastereomers, bisphenoxide, and bispyrrolide complexes is observed in solution, but only the bisphenoxide is isolated by recrystallization (32% accounting for R$^+$OH being the limiting reagent). Mo(NAd)(CHCMe$_2$Ph)(OR$^+$)$_2$, **21**, can be generated in better yields by using two equivalents of R$^+$OH (equation 4). In contrast, Mo(NAr)(CHCMe$_2$Ph)(Me$_2$Pyr)(OR$^+$) does not form any bisphenoxide during the course of the reaction. In fact, the only known route for preparing Mo(NAr)(CHCMe$_2$Ph)(OR$^+$)$_2$, **9**, is via salt-metathesis of the bistriflate complex (Scheme 3).[19f]

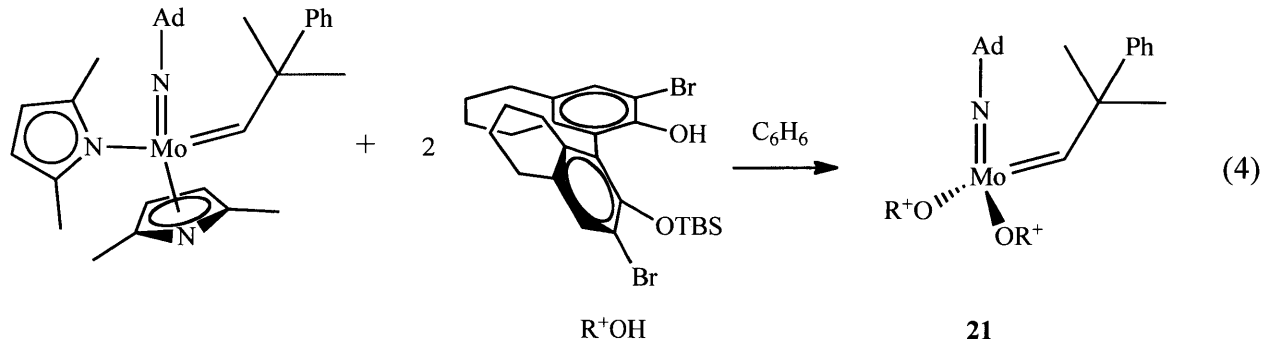

X-ray quality crystals of **21** can be grown from a pentane : TMS solution and the X-ray crystal structure of this complex is shown in Figure 3. The complex crystallizes out in the orthorhombic space group $P2_12_12_1$ with only one molecule of **21** and a disordered molecule of pentane in the asymmetric unit. The structure of **21** is best described as pseudo tetrahedral with the metal located in the tetrahedral hole. The R^+O ligands bind perpendicular with relation to each other

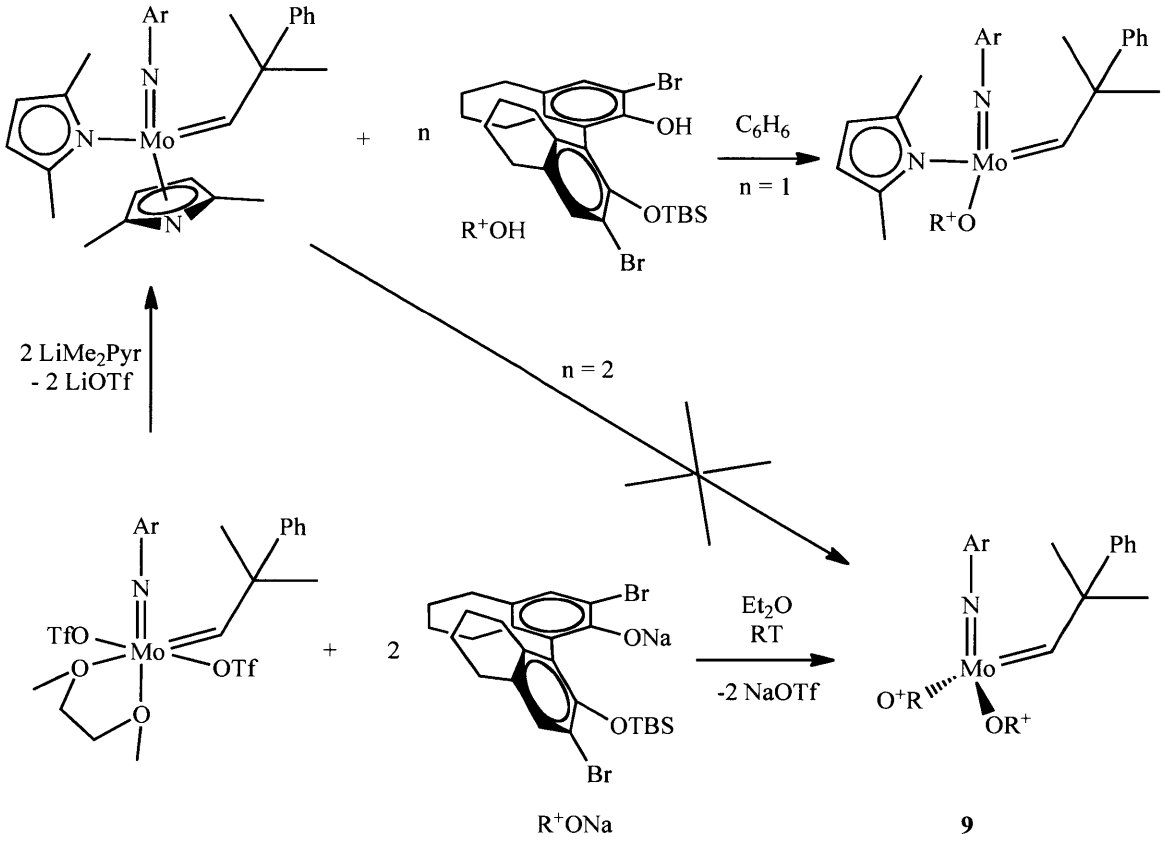

Scheme 3 – Synthetic scheme for making Mo(NAr)($CHCMe_2Ph$)(Me_2Pyr)(OR^+) and **9**.

and the alkylidene ligand binds *syn* in relation to the imido group. The Mo(1)-C(1) (1.917(11) Å), the Mo(1)-N(1) (1.709(7) Å), and the Mo-O (1.967(5) and 1.949(6) Å) bond lengths of **21** are similar to those found for **9**. However, the alkylidene ligand remains *syn* in **21**; while the major isomer of **9** is the *anti*-alkylidene. As a result, the major differences are found in the Mo=C-C (**21** = 149.1(9)°; **9** = 123.9(4)°) and the Mo=N-R (**21** = 159.8(7)°, **9** = 174.0(3)°) bond angles of the two molecules. The larger Mo=C-C bond angle in **21**, in comparison to **9**, is attributed to the C-H agostic interaction of the *syn* alkylidene ligand, which is absent in the *anti* species. Another feature that is worth pointing out is the very weak interaction between two of the bromine atoms and the metal center (Mo(1)-Br(1) = 3.248 Å, Mo(1)-Br(3) = 3.367 Å); however, due to the long Mo-Br distances their influence may not be consequential to metathesis reactions.

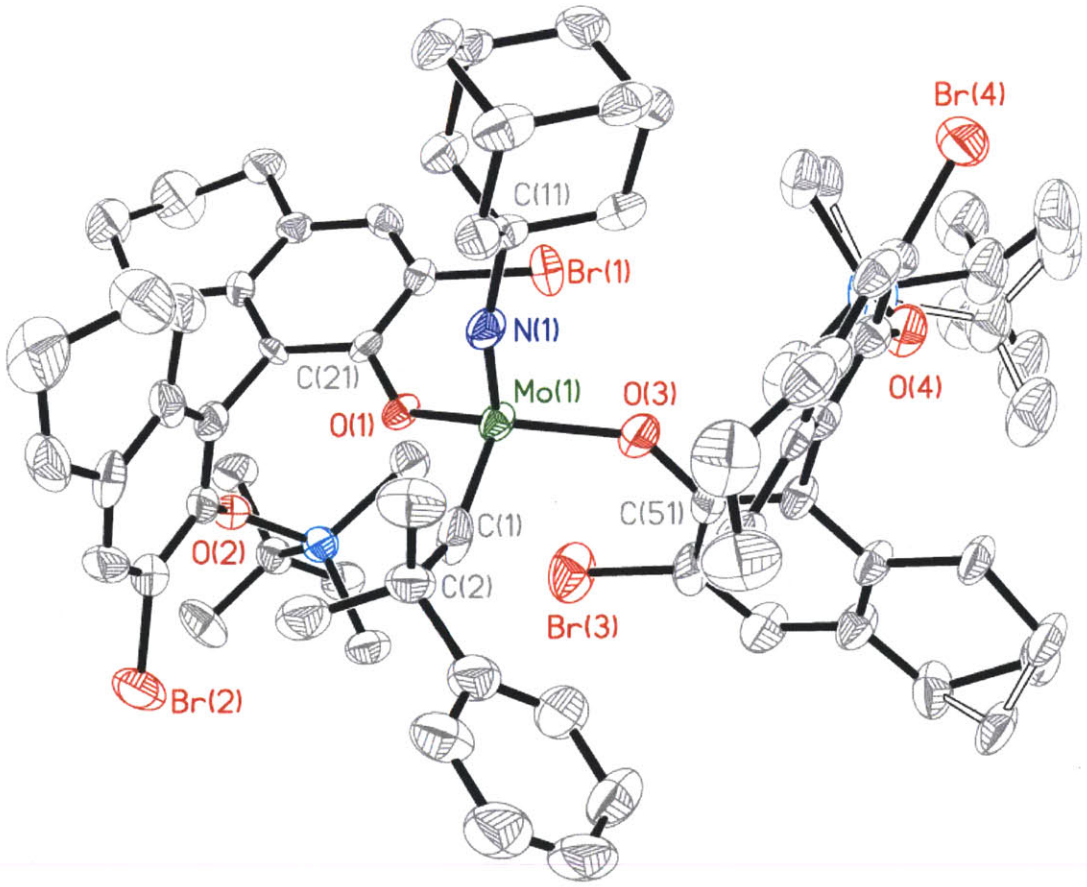

Figure 3 - The solid state structure of **21** (50% probability ellipsoids) with solvent molecules omitted for clarity. Selected bond lengths (Å) and angles (°): Mo(1)-C(1) = 1.917(11), Mo(1)-N(1) = 1.709(7), Mo(1)-O(1) = 1.967(5), Mo(1)-O(3) = 1.949(6), Mo(1)-C(1)-C(2) = 149.1(9), Mo(1)-N(1)-C(11) = 159.8(7), Mo(1)-O(1)-C(21) = 137.1(5), Mo(1)-O(3)-C(51) = 142.2(6).

In the next section compounds **1**, **9**, **21**, and some compounds that were characterized in the past will be screened for RCMP of DEDPM to investigate their overall selectivity.

A.2 Catalyst screening for the selective polymerization of ^{13}C-labeled DEDPM

A.2.1 Screening with MAP catalysts

A total of 13 MAP catalysts (Figures 4 and 5) were tested for the regioselective polymerization of dipropargyl malonates by using ^{13}C-labeled DEDPM and the resulting purple polymer was analyzed by ^{13}C NMR methods. The results are summarized in Tables 1 and 2.

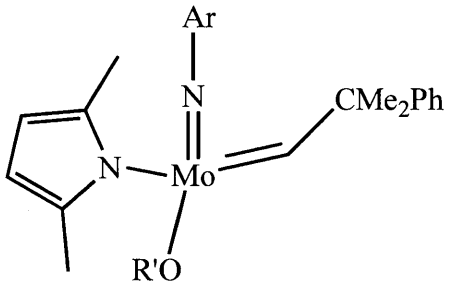

Figure 4 – Molecular structure of MAP complexes used for polymerization of ^{13}C-labeled DEDPM in Table 1.

Table 1 shows the polymerization results for 8 MAP species. The catalyst concentrations range from as low as 8.5 mM to as high as 17 mM in $CDCl_3$ and either 20 or 25 equivalents of DEDPM monomer were used. Among all catalysts used, none is particularly selective for either α or β addition, with most of the catalysts producing polymer containing ~ 50% of each ring in the organic chain. For instance, catalyst **1**, which gives excellent β-selectivity for RCM of DEAPM, the enyne derivative of DEDPM, is not selective for RCMP of DEDPM and does produce polymer with equal amounts of 5-membered and 6-membered rings. The same is true of catalyst **3**, which is known to give 100% β product for the RCM of DEAPM, but produces polymer with barely 61% of 6-membered rings.

Although, most of the results discussed so far do not follow a particular trend, one of the best results is observed when catalyst **4**, which contains the smaller and more electron-donating *iso*propoxide ligand, is used. In this case the polymer formed contains 80% 5-membered rings. Interestingly, this MAP complex is not a good catalyst for the RCM of DEAPM due to fast oligomerization of DEDPM into intractable products. On the other hand, when the slightly bulky 2,4-di-*tert*-butyl-6-bromophenoxide ligand of catalyst **8** is used the polymer produced contains

77% 6-membered rings. Thus the general trend with MAP compounds is that in order to get 5-membered rings small, electron-rich, alkoxides are needed, but to get 6-membered rings semi-bulky ligands need to be used, which is similar to the results observed and discussed in Chapter 2.

Table 1 - Polymerization of ^{13}C-DEDPM using MAP catalysts				
Catalyst	**R'**	**[Mo], mM**	**Eq. DEDPM**	**% α**
1	R*	17	20	50
2	R^+	15	20	43
3	$(CF_3)_2MeC$	9.8	20	39
4	*i*-Pr	17	20	80
5	Ar	9.9	25	45
6	$(t\text{-BuO})_3Si$	8.8	25	44
7	Ph_3Si	11	25	50
8	$2,4\text{-}(t\text{-bu})_2\text{-}6\text{-}BrC_6H_2$	8.5	25	23

To investigate whether the pyrrolide in MAP species can have a drastic effect on the polymerization of DEDPM, $Mo(NAr)(CHCMe_2Ph)((R_1)_2(R_2)_2C_4N)(OC(CF_3)_2CH_3)$ complexes (Figure 5) were used to polymerize ^{13}C-labeled DEDPM and the results are shown in Table 2. When the substituents in the pyrrolide ligand are changed from R_1 = Me, **3** , to R_1 = Ph, **3b**, there is a slight increase in the amount of 5-membered rings formed (39% vs 44%). Moreover, increasing the sterics of the pyrrolide ligand by changing R_1 = Ph to R_1 = *i*-Pr, **3d**, we see a further increase in the amount of 5-membered rings produced (44% to 53%).

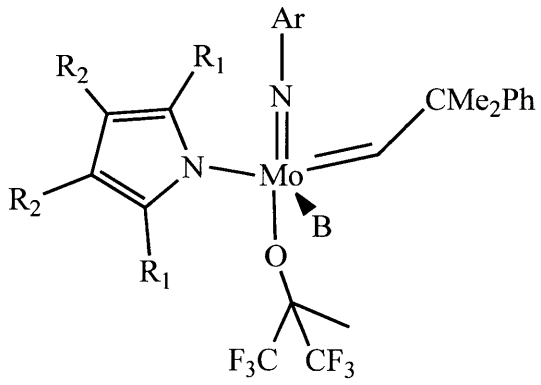

Figure 5 - Molecular structure of MAP complexes that either contain PMe_3 or not and that are used for polymerization of ^{13}C-labeled DEDPM in Table 2.

Table 2 - Polymerization of ^{13}C-DEDPM using MAP and PMe_3-bound MAP catalysts.						
Catalyst	**R_1**	**R_2**	**B**	**[Mo], mM**	**Eq. DEDPM**	**% α**
3	Me	H	------	9.8	20	39
3a	Me	Me	PMe_3	8.5	20	39
3b	Ph	H	------	8.3	20	44
3c	Ph	H	PMe_3	7.6	25	29
3d	*i*-Pr	H	------	9.1	20	53
3e	*i*-Pr	H	PMe_3	8.2	25	36

PMe_3 bound to each of the MAP species has a detrimental effect on the amount of 5-membered rings produced. For instance, the polymers produced with **3c** (R_1 = Ph) have only 29% 5-membered rings, in contrast to 44% 5-membered rings when **3b** is used instead. Likewise, when **3e** (R_1 = *i*-Pr) is used instead of **3d** there is a decrease from 53% down to 36% 5-membered ring. Unfortunately, a direct correlation between **3** and **3a** cannot be made because the sterics of the pyrrolide are not quite the same; however, it is known that in solution PMe_3 dissociates almost completely and the results hint that **3** and **3a** are not very different sterically.

Overall, the results discussed above suggest that increasing the size of the pyrrolide ligand favors the number of 5-membered rings produced during polymerization of DEDPM, but ligation of PMe_3 inhibits α-binding of DEDPM more efficiently, decreasing the content of 5-membered rings formed along the polymeric chain. It is possible that using a small alkoxide in combination with a big pyrrolide could yield even better results.

A.2.2 Screening with bisalkoxide and bisphenoxide catalysts

In order to obtain a better understanding of how alkoxides and imido groups (Ar' = 2,6-$Me_2C_6H_3$, Ar^{CF3} = 2-$(CF_3)C_6H_4$, Ar^{tBu} = 2-*t*-BuC_6H_4, Ar^{Ph} = 2-PhC_6H_4) affect regioselectivity, a variety of bisalkoxide complexes, of the type shown in Figure 6, were tested with ^{13}C-labeled DEDPM. The results are shown in Table 3.

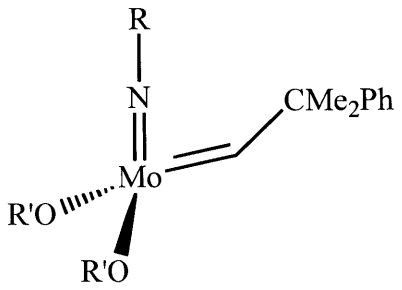

Figure 6 - Molecular structure of bisalkoxide and bisphenoxide complexes used for polymerization of ^{13}C-labeled DEDPM in Table 3.

Table 3 - Polymerization of ^{13}C-DEDPM using bisalkoxide catalysts.					
Catalyst	**R**	**R'**	**[Mo], mM**	**Eq. DEDPM**	**% α**
9	Ar	R^+	5.5	25	22
10	Ar	$(CF_3)Me_2C$	10	25	78
11	Ar	$(CF_3)_3C$	7.6	25	48
12	Ar	$(C_6F_5)_2MeC$	5.6	25	74
13	Ar	$(t\text{-bu})Me_2Si$	10	25	69
14	Ar	Ar	8.8	25	33
15	Ar'	$(CF_3)_2MeC$	9.4	25	60
16	Ar'	Ar	9.5	25	54
17	Ar^{CF3}	$(CF_3)_2MeC$	8.9	25	52
18	Ar^{tBu}	$(CF_3)_2MeC$	9.0	20	54
19	Ar^{Ph}	$(CF_3)_2MeC$	8.8	20	51
20	Ad	$(CF_3)_2MeC$	8.0	25	22
21	Ad	R^+	2.2	50	33

Comparing the results of catalysts **9-14** the overall number of 5-membered ring formation in the polymer chain is higher when catalysts containing alkoxide ligands (**10-13**), rather than phenoxide ligands (**9** and **14**), are used. The same trend is also observed with catalysts that have the Ar' imido group (**15-16**), but not with catalysts that have the Ad imido ligand (**20-21**). Catalyst **21** gives polymer with 33% 5-membered rings, whereas catalyst **20** gives polymer with only 22% 5-membered rings. For comparison, catalyst **9** gives polymer with 22% 5-membered rings, while catalysts **10** and **11** give polymer with 78% and 48% 5-membered rings,

respectively. The discrepancy between the reactivity of **9** and **21** could be attributed to the fact that **9** exists mainly as the *anti* isomer, whereas **21** does not.

Comparing all catalysts that contain the OR_{F6} group ($OC(CF_3)_2CH_3$; **15**, **17-20**) we can see that decreasing the size of the imido ligand has a detrimental effect on the overall amount of 5-membered rings formed. For instance, catalyst **15** produces polymer with 60% 5-membered rings, but catalysts **17-19**, which have an *ortho*-substituted phenyl imido ligand, produce polymer with only 50% 5-membered rings. Decreasing the size of the imido to Ad lowers the amount of 5-membered rings to only 22%. On the other hand, catalysts with the ArO ligand (**14** and **16**) have the opposite results. Since no other catalysts were made that contain this ligand, a precise trend cannot be drawn at this time, but the results suggest that in combination with the adamantyl imido group, phenoxide ligands are a better choice to make more 5-membered rings.

CONCLUSION

Synthesis of compounds **1** and **21** were presented and both compounds were analyzed by X-ray studies. Compound **1** is isolated a single diastereomer with the *R*-configuration at the metal. Initial reactions show that this catalyst is competent for RCM of DEAPM, but not for other olefin metathesis reactions. Compound **21** is obtained as the *syn* isomer and attains a pseudo octahedral arrangement if the weak bromide interactions are included.

Polymerization of DEDPM with 8 MAP complexes, 9 bisalkoxide complexes, and 4 bisphenoxide complexes were presented. Three trends were found: a) among MAP complexes, small electron-rich alkoxides or pyrrolides with bulkier substituents on the 2 and 5 positions produce polymer with higher amount of 5-membered rings; b) among bisalkoxide complexes, smaller imido ligands increase the content of 5-membered rings and, c) among bisalkoxide/bisphenoxide complexes, bisalkoxides tend to give polymer containing higher percentages of 5-membered rings.

EXPERIMENTAL

General. All reactions and manipulations of air and moisture sensitive compounds were handled in oven-dried glassware (150°C, 2 hr) under a N_2 atmosphere either in a dual Schlenk line or in vacuum atmosphere glove box. All complexes used for polymerization screening were synthesized according to published methods[10-11] or according to other group semiannuals[12]. HPLC grade solvents (toluene, diethyl ether, tetrahydrofuran, pentane, and methylene chloride), were purged with N_2 and passed through activated alumina and stored over molecular sieves 12 hours prior to use. 1,2-dimethoxyethane was dried in an oven-dried Schlenk flask with sodium and benzophenone ketal, vacuumed transferred into another oven-dried Schlenk flask and stored over molecular sieves 12 hours prior to use. R*OH[32], R^+OH[33], Mo(NR)(CHCMe$_2$Ph)(Me$_2$Pyr)$_2$ species[19a], MAP complexes[19b-c, 31, 33] and bisalkoxide/bisphenoxide complexes[19d-f, 31] were prepared according to literature reports. All deuterated solvents (d_6-benzene and d_1-chloroform) were stored over molecular sieves 12 hours prior to use. All the recorded NMR spectra were obtained with a Bruker 400 MHz spectrometer.

(*R*)-Mo(NAr)(CHCMe$_2$Ph)(Me$_2$Pyr)(OR*) (1) Mo(NAr)(CHCMe$_2$Ph)(Me$_2$Pyr)$_2$ (1.13 g, 1.90 mmol) was dissolved in a minimal amount of ether and placed at -35 °C for 1 h. R*OH (0.503 g, 1.90 mmol) was dissolved in a minimal amount of ether and placed at -35 °C for 1 h. At the end of the cooling period, the solution containing R*OH was added to the precatalyst solution dropwise and the mixture was stirred at RT for 45 min. Then, the volatiles were removed to yield a crude product containing the *R* and *S* diastereomers in a ratio of 3:1. Then, the sample was redissolved in minimal amount of $SiMe_4$ and placed at -35 °C for 2 days to generate a yellow-green solid, which was enriched up to 88% with the *R* isomer (0.405 g, 28%). This diastereomeric mixture was re-dissolved in a minimal amount of a 4:1 mixture of $SiMe_4$:Et_2O and recrystallized at -35 °C over a period of a few days to give a yellow green solid 99.9% enriched with the *R* diastereomer (0.100 g, 7%). Enriched **1** (99.9%; 0.030 g) was dissolved in a pentane:Et_2O 1:1 pentane/diethyl ether solution and placed at -35 °C for a couple of days to produce orange crystals suitable for X-ray diffraction: ^{1}H NMR (400 MHz, CD_2Cl_2) δ 10.46 (s, 1H, MoC*H*, J_{CH} = 120.25 Hz), 7.60-7.10 (m, 12H, aromatics), 5.85 (s br, 2H, Me$_2$C$_4$*H*$_2$N), 4.20-3.00 (d br, 2H, C*H*Me$_2$), 2.68 (s br, 3H, *Me*$_2$C$_4$H$_2$N), 2.32 (d, 1H, O*R* C3*), 2.00-1.70 (m, 4H, O*R* C3-C5*), 1.58 (d, 6H, CHC*Me*$_2$Ph), 1.35 (s, 3H, O*R* C1*), 1.26 (s br, 12H, CH*Me*$_2$), 1.06 (s, 3H, O*R* C8*), 0.99 (s, 3H, O*R* C9*), 0.72 (m, 2H, O*R* C6*); ^{13}C NMR (100 MHz, CD_2Cl_2) δ 284.14 (MoCHR), 153.3, 148.1, 145.5, 133.1, 129.0 (br, Me$_2$*C*$_2$C$_2$H$_4$N), 128.2, 127.6, 126.1, 125.9, 123 (br Me$_2$C$_2$*C*$_2$H$_4$N), 108.2 (br, *Me*$_2$C$_4$H$_2$N), 95.4, 55.4, 54.5, 54.2, 53.9, 50.2, 47.2, 45.8, 31.7, 31.4, 29.2, 28.5 (br, *C*HMe$_2$), 26.3, 23.8 (br, CH*Me*$_2$), 21.5, 21.4, 17.4 (br, CH*Me*$_2$), 15.6, 14.0, 10.4.

Mo(NAd)(CHCMe$_2$Ph)(OR$^+$)$_2$ (21) Mo(NAd)(CHCMe$_2$Ph)(OTf)$_2$(DME) (0.227 g, 0.297 mmol) was dissolved in Et_2O (7.0 mL) and NaOR$^+$ (0.350 g, 0.595 mmol) was added in one portion and the mixture was left reacting at RT for 2 h. Then, the volatiles were removed and the crude was redissolved in pentane and filtered through celite to remove salts. The solvent was removed under reduced pressure and the orange solid was collected by filtration (0.264 g, 59%). **21** (0.030 g) was dissolved in a 1:1 pentane:Et_2O solution and placed at -35 °C for a couple of days to produce orange crystals suitable for X-ray diffraction: ^{1}H NMR (400 MHz, CD_2Cl_2) δ 12.63 (s, 1H, MoC*H*, J_{CH} = 129.0 Hz), 7.40-6.70 (overlapping peaks, 9H, aromatics), 2.70-1.10 (overlapping peaks, 31H, aliphatics), 1.04 (s, 18H, SiC(C*H*$_3$)$_3$), 0.94 (s, 6H, aliphatic), 0.48 (s, 3H, SiC*H*$_3$), 0.21 (s, 3H, SiC*H*$_3$), 1.00 (s, 3H, SiC*H*$_3$), - 0.02 (s, 3H, SiC*H*$_3$); ^{13}C NMR (100 MHz, C_6D_6) δ 281.5 (Mo=CHCMe$_2$Ph), 161.4, 159.8, 150.3, 148.2, 148.1, 137.8, 136.2, 135.9, 134.3, 133.3, 133.0, 132.1, 132.0, 131.8, 131.6, 131.4, 131.1, 130.6, 130.5, 130.4, 125.8, 125.3, 113.8, 113.6, 112.9, 112.3, 106.5, 77.9, 50.9, 44.1, 36.0, 34.4, 32.6, 31.8, 30.0, 29.7, 29.2, 28.3, 27.7, 27.6, 27.4, 26.8, 26.7, 23.5, 22.7, 21.4, 19.2, 14.3, 13.1, - 2.5, - 2.6, - 2.9, - 3.3.

General procedure for the polymerization of ^{13}C-labeled DEDPM. The catalyst (0.010 g) was measured, placed in a vial, and dissolved in about 0.50 mL of $CDCl_3$; likewise, 20-25 equivalents of ^{13}C-labeled DEDPM were dissolved in 0.50 mL of $CDCl_3$ separately. The solution containing the catalyst was added to the solution containing the substrate to yield a purple solution within 2 min. The mixture was monitored by ^{13}C NMR in the 54-58 ppm region to determine the amounts of α and β products in solution.

X-ray Structure Determination Low-temperature diffraction data (ϕ-and ω-scans) were collected on a Siemens Platform three-circle diffractometer coupled to a Bruker-AXS Smart Apex CCD detector with graphite-monochromated Mo Kα radiation (λ = 0.71073 Å) for the structure of compound **1** and on a Bruker-AXS X8 Kappa Duo diffractometer coupled to a Smart Apex2 CCD detector with Mo K_α radiation (λ = 0.71073 Å) from an *IμS* micro-source for the structure of compound **21**. All structures were solved by direct methods using SHELXS[34] and refined against F^2 on all data by full-matrix least squares with SHELXL-97[35] using established refinement techniques.[36] All non-hydrogen atoms were refined anisotropically. All hydrogen atoms were included into the model at geometrically calculated positions and refined using a riding model unless otherwise noted. The isotropic displacement parameters of all hydrogen atoms were fixed to 1.2 times the *U* value of the atoms they are linked to (1.5 times for methyl groups). All disordered atoms were refined with the help of similarity restraints on the 1,2- and 1,3-distances and displacement parameters as well as rigid bond restraints for anisotropic displacement parameters.

Compounds **1** and **21** crystallize in the orthorhombic space group $P2_12_12_1$. Compound **21** crystallizes with a molecule of pentane that is treated as a two-part disorder. One of the TBS groups, corresponding to Si(2) is also disordered and treated as a two-part disorder, as well as C(56) on the one of the BITET rings.
Crystal information can be found in Tables 4 and 5.

Table 4 - Crystal Data and Structure Refinement Details for **1**.

Empirical formula	C44 H57 Cl Mo N2 O	
Formula weight	761.31	
Temperature	100(2) K	
Wavelength	0.71073 Å	
Crystal system	Orthorhombic	
Space group	$P2_12_12_1$	
Unit cell dimensions	a = 9.756(4) Å	α = 90°
	b = 19.892(8) Å	β = 90°
	c = 20.649(8) Å	γ = 90°
Volume	4007(3) $Å^3$	
Z	4	
Density (calculated)	1.262 Mg/m^3	
Absorption coefficient	0.428 mm^{-1}	
F(000)	1608	
Crystal size	0.25 x 0.20 x 0.10 mm^3	
Theta range for data collection	1.97 to 29.57°	
Index ranges	-13<=h<=13, -27<=k<=27, -28<=l<=28	
Reflections collected	88176	
Independent reflections	11246 [R(int) = 0.0723]	
Completeness to theta = 29.57°	100.0 %	
Absorption correction	Semi-empirical from equivalents	
Max. and min. transmission	0.9584 and 0.9005	
Refinement method	Full-matrix least-squares on F^2	
Data / restraints / parameters	11246 / 1 / 456	
Goodness-of-fit on F^2	1.046	
Final R indices [I>2sigma(I)]	R1 = 0.0321, wR2 = 0.0589	
R indices (all data)	R1 = 0.0401, wR2 = 0.0625	
Absolute structure parameter	-0.039(19)	
Largest diff. peak and hole	0.489 and -0.436 $e.Å^{-3}$	

Table 5 - Crystal data and structure refinement for **21**.

Identification code	x11003	
Empirical formula	C77 H105 Br4 Mo N O4 Si2	
Formula weight	1580.38	
Temperature	100(2) K	
Wavelength	0.71073 Å	
Crystal system	Orthorhombic	
Space group	$P2_12_12_1$	
Unit cell dimensions	a = 16.0937(12) Å	α= 90°
	b = 16.4303(12) Å	β= 90°
	c = 28.536(2) Å	γ = 90°
Volume	7545.5(10) $Å^3$	
Z	4	
Density (calculated)	1.391 Mg/m^3	
Absorption coefficient	2.371 mm^{-1}	
F(000)	3264	
Crystal size	0.15 x 0.10 x 0.05 mm^3	
Theta range for data collection	1.43 to 26.02°	
Index ranges	-19<=h<=19, -20<=k<=20, -35<=l<=35	
Reflections collected	94170	
Independent reflections	14859 [R(int) = 0.0815]	
Completeness to theta = 26.02°	99.9 %	
Absorption correction	Semi-empirical from equivalents	
Max. and min. transmission	0.8907 and 0.7175	
Refinement method	Full-matrix least-squares on F^2	
Data / restraints / parameters	14859 / 563 / 887	
Goodness-of-fit on F^2	1.037	
Final R indices [I>2sigma(I)]	R1 = 0.0752, wR2 = 0.1930	
R indices (all data)	R1 = 0.0979, wR2 = 0.2119	
Absolute structure parameter	0.011(12)	
Largest diff. peak and hole	4.049 and -1.376 $e.Å^{-3}$	

REFERENCES

(1) Nalwa, H. S.; Miyata, S. *Nonlinear Optics of Organic Molecules and Polymers*; CRC Press: Boca Raton, FL, 1997.

(2) Choi, S. *Chem. Rev.* **2000**, *100*, 1645.

(3) Knoll, K.; Krouse, S. A.; Schrock, R. R. *J. Am. Chem. Soc.* **1988**, *110*, 4424.

(4) Masuda, T.; Abdul Karim, S. M.; Nombra, R. J. *Molec. Catal. A* **2000**, *160*, 125.

(5) Chirstensen, R. L.; Faksh, A.; Meyers, J. A.; Samuel, I. D. W.; Wood, P.; Schrock, R. R.; Hultzsch, K. C. *J. Phys. Chem. A* **2004**, *108*, 8229.

(6) Fox, H. H.; Wolf, M. O.; O'Dell, R.; Lin, B. L.; Schrock, R. R.; Wrighton, M. S. *J. Am. Chem. Soc.* **1994**, *116*, 2827.

(7) Fox, H. H.; Schrock, R. R. *Organometallics* **1992**, *11*, 2763.

(8) Anders, U.; Nuyken, O.; Buchmeiser, M. R.; Wurst, K. *Angew. Chem., Int. Ed. Engl.* **2002**, *41*, 4044.

(9) Anders, U.; Nuyken, O.; Buchmeiser, M. R.; Wurst, K. *Macromolecules* **2002**, *35*, 9029.

(10) Adamchuk, J.; Schrock, R. R.; Tonzetich, Z. J.; Muller, P. *Organometallics* **2006**, *25*, 2364.

(11) Krause, J. O.; Nuyken, O.; Buchmeiser, M. R. *Chem. Eur. J.* **2004**, *10*, 2029.

(12) Yang, L.; Mayr, M.; Wurst, K.; Buchmeiser Michael, R. *Chem. Eur. J.* **2004**, *10*, 5761.

(13) Halbach, T. S.; Krause, J. O.; Nuyken, O.; Buchmeiser, M. R. *Macromol. Rapid. Commun.* **2005**, *26*, 784.

(14) Halbach, T. S.; Mix, S.; Fischer, D.; Maechling, S.; Krause, J. O.; Sievers, C.; Blechert, S.; Nuyken, O.; Buchmeiser, M. R. *J. Org. Chem.* **2005**, *70*, 4687.

(15) Schattenmann, F. J.; Schrock, R. R.; Davis, W. M. *J. Am. Chem. Soc.* **1996**, *118*, 3295.

(16) Schattenmann, F. J.; Schrock, R. R. *Macromolecules* **1996**, *29*, 8990.

(17) Diver, S. T.; Giessert, J. A. *Chem. Rev.* **2004**, *104*, 1317.

(18) Hock, A. S.; Schrock, R. R.; Hoveyda, A. H. *J. Am. Chem. Soc.* **2006**, *128*, 16373.

(19) (a) Singh, R.; Czekelius, C.; Schrock, R. R.; Müller, P. *Organometallics* **2007**, *26*, 2528. (b) Singh, R.; Schrock, R. R.; Muller, P.; Hoveyda, A. H. *J. Am. Chem. Soc.* **2007**, *129*, 16278. (c) Marinescu, S. C.; Singh, R. S.; Hock, A. S.; Wampler, K. M.; Schrock, R. R.; Müller, P. *Organometallics* **2008**, *27*, 6570. (d) Schrock, R. R.; Murdzek, J. S.; Bazan, G. C.; Robbins, J.; DiMare, M.; O'Regan, M. *J. Am. Chem. Soc.* **1990**, *112*, 3875. (e) Oskam, J. H.; Fox, H. H.; Yap, K. B.; McConville, D. H.; O'Dell, R.; Lichtenstein, B. J.; Schrock, R. R. *Jour. Organomet. Chem.* **1993**, *459*, 185. (f) Marinescu, S. C. Ph.D. Thesis, 2010, Massachusetts Institute of Technology. (g) Flook, M. M.; Jiang, A. J.; Schrock, R. R.; Müller, P.; Hoveyda, A. H. *J. Am. Chem. Soc.* **2009**, *131*, 7962.

(20) Kinoshita, A.; Mori, M. *Synlett.* **1994**, 1024.

(21) Mori, M.; Sakakibara, N.; Kinoshita, A. *J. Org. Chem.* **1998**, *63*, 6082.

(22) Du, C.-J. F.; Hart, H.; Ng, K.-K. D. *J. Org. Chem.* **1986**, *51*, 3162.

(23) Saednya, A.; Hart, H. *Synthesis* **1996**, 1455.

(24) *Organometallics* **2002**, *21*, 409.

(25) Czekelius, C.; Hafer, J.; Tonzetich, Z. J.; Schrock, R. R.; Christensen, R. L.; Muller, P. *J. Am. Chem. Soc.* **2006**, 16664.

(26) Singh, R.; Czekelius, C.; Schrock, R. R. *Macromolecules* **2006**, *39*, 1316.

(27) Sinha, A.; Lopez, L. P. H.; Schrock, R. R.; Hock, A. S.; Muller, P. *Organometallics*, **2006**, *25*, 1402.

(28) Kajzar, F.; Messier, J. *Phys. Rev.* **1985**, *A32*, 2352.

(29) Oskam, J. H.; Fox, H. H.; McConville, D. H.; O'Dell, R.; Lichtenstein, B. J.; Schrock, R. R. *Jour. Organometallic Chem.* **1993**, *459*, 185.

(30) Marinescu, S.; Schrock, R. R.; *Organometallics* **2008**, *27*, 6570.

(31) Bailey, B. C.; Schrock, R. R.; Kundu, S.; Goldman, A. S.; Huang, Z.; Brookhart, M. *Organometallics* **2009**, *28*, 355.

(32) Krasovskiy, A.; Kopp, F.; Knochel, P. *Angew. Chem. Int. Ed.* **2006**, *45*, 497.

(33) Meek, S. J.; O'Brien, R. V.; Llaveria, J.; Schrock, R. R.; Hoveyda, A. H. *Nature* **2008**, *456*, 933.

(34) Sheldrick, G. M. (1990). *Acta Cryst.* **A46**, 467-473.

(35) Sheldrick, G. M. (2008). *Acta Cryst.* **A64**, 112-122.

(36) Müller, P. *Crystallography Reviews* **2009**, *15*, 57-83.

ALEJANDRO G. LICHTSCHEIDL

Graduate Research Assistant
MIT, Room 6-428
77 Massachusetts Avenue
Cambridge, MA 02139

phone: 617-253-1795
email: alichtsc@mit.edu

Education

2006-2012	Ph.D. Candidate in Inorganic Chemistry; Massachusetts Institute of Technology
2003-2006	B.S. Chemistry; University of California Irvine
2004-2006	B.S. Biochemistry and Molecular Biology; University of California Irvine
2001-2003	A.S. Biological and Physical Sciences; College of the Canyons

Research Experience

2006-2012	Graduate Research Assistant, MIT – Advisor: Prof. Richard R. Schrock Molybdenum species for the polymerization of diyne and strained-dienes substrates.
2005-2006	Research Assistant, UCI – Advisor: Prof. Patrick J. Farmer Synthesis of mercury-based cumertilin drugs for treatment of cancerous melanoma cells.
06-08 2005	Summer Intern, NIST – Mentor: Dr. Jeffrey W. Hudgens Implementations of Hadamard Transforms on ToF mass spectrometry.
2004-2005	Research Assistant, UCI – Advisor: Prof. Patrick J. Farmer Preparation of mutated myoglobin for mechanistic studies of HNO.

Publications

3. Lichtscheidl, A. G.; Ng, V. W. L.; Müller, P.; Takase, M. K.; Schrock, R. R.; Malcomson, S. J.; Meek, S. J; Li, B.; Kiesewetter, E. T.; Hoveyda, A. H. "Bipyridine Adducts of Molybdenum Alkylidene and Molybdenum Alkylidyne Complexes: Their Use for Preparation of New Active Catalyst Species" *Organometallics* **2012**, *31*, ASAP.

2. Lichtscheidl, A. G.; Ng, V. W. L.; Müller, P.; Takase, M. K.; Schrock, R. R. "Molybdenum Monoaryloxide Pyrrolide Alkylidene Complexes that Contain Mono-*ortho*-substituted Phenyl Imido Ligands" *Organometallics* **2012**, *31*, 2388-2394.

1. Schrock, R. R.; Tonzetich, Z. J.; Lichtscheidl, A. G.; Müller, P.; Schattenmann, F. J. "Carboxylate-Based Molybdenum Alkylidene Catalysts: Synthesis, Characterization, and Use as Initiators for 1,6-Heptdiyne Cyclopolymerizations" *Organometallics* **2008**, *27*, 3986-3995.

Posters and Presentations

Lichtscheidl, A. G.; Schrock, R. R. "Probing the Good-Sigma Bad-Sigma Donor Effect of Ligands on the Efficiency of High-Oxidation Molybdenum Alkylidene Olefin-Metathesis Catalysts" ACS National Conference, San Diego-CA, March 2012.

Lichtscheidl, A. G.; Schrock, R. R. "Enhanced Stability of High-Oxidation Molybdenum Alkylidene Complexes Containing Bipyridine and Their Use as Catalyst Precursors" ACS National Conference, San Diego-CA, March 2012.

Lichtscheidl, A. G. "Preparation of Molybdenum Alkylidene Complexes and Their Use as Polymerization Catalysts: Extending the Scope of the Imido and Pyrrolide Ligands" CSS Seminar, MIT, November 2011.

Lichtscheidl, A. G.; Schrock, R. R. "Enhanced Stability of High-Oxidation Molybdenum Alkylidene Complexes Containing Bipyridine and Their Use as Catalyst Precursors" Poster, BRIC Symposium, Clark University, Worcester-MA, September 2011.

Lichtscheidl, A. G. "Preparation of Molybdenum Alkylidene Complexes and Their Use as Polymerization Catalysts: Extending the Scope of the Imido, Carboxylate, and Alkoxide Ligands" MIT Seminar, February 2011.

Lichtscheidl, A. G.; Schrock, R. R.; Müller, P. "Investigation of New Imido Ligands and Their Application to Olefin Metathesis" Poster, ACS National Meeting, Boston-MA, 2010.

Lichtscheidl, A. G.; Schrock, R. R."Molybdenum monocarboxylate and biscarboxlate catalysts for the cyclopolymerization of 1,6-heptadiynes" SACNAS National Meeting, Salt Lake City-UT, October 2008.

Lichtscheidl, A. G. "Synthesis of Cumertilin Derivatives for the Treatment of Melanoma Cancerous Cells" Poster, AAAS National Meeting, St. Louis-MO, February 2006.

Lichtscheidl, A. G. "Synthesis of Cumertilin Derivatives for the Treatment of Melanoma Cancerous Cells" Poster, ACS Regional Meeting, Anaheim-CA, January 2006.

Lichtscheidl, A. G. "Myoglobin Mutants for Studies on the Reactivity of HNO" Poster, SACNAS National Meeting, Denver-CO, September 2005.

Lichtscheidl, A. G.; Hudgens, J. W. "Hadamard Transform Time of Flight Mass Spectrometry" SURF program, NIST, July 2005.

Lichtscheidl, A. G. "Nitric Oxide Studies of Myoglobin Mutants" Poster, AAAS National Meeting, Washington D. C., February 2005.

Lichtscheidl, A. G. "Structure and Crystallization of Calretinin" Poster, SACNAS National Meeting, Austin-TX, October 2004.

Teaching Experience

2011	Graduate Student Teaching Certificate Program
2008-2009	Chemistry Outreach Program, MIT
Fall 2006	Teaching Assistant for Introductory Chemical Experimentation (5.311), MIT; instructors: Dr. Janet Schrenk and Prof. Joseph Sadighi
Jan 2007	Teaching Assistant for Chemistry Laboratory Techniques (5.301), MIT; instructor: Dr. Kimberly L. Berkowski
2005-2006	Chemistry Tutor for the Minority Science Programs (MSP), UCI
2003	Chemistry Tutor, COC
2002-2003	General Chemistry Workshop Facilitator for the MESA program, COC

Honors and Awards

Outstanding Senior in Chemistry	2006
Hypercube Scholar Award	2005
Excellence in Biological Science Alumni Scholarship	2005
Minority Access Research Careers Grant	2005-2006
Hispanic Scholarship Foundation Scholarship	2005-2006
Chancellor's Achievement Scholarship	2003-2005
Edison Scholarship	2003-2005
H.R. Textron Math and Science Transfer Student Scholarship	2003
PFE Mathematics and Sciences Continuing Student Scholarship	2002
Golf Classic Mathematics and Sciences General Motors Scholarship	2002

Collaborators

Prof. Amir H. Hoveyda (Boston College), Dr. Peter Müller (X-ray Facility, MIT), Michael K. Takase (X-ray Facility, MIT), Dr. Bo Li (Boston College).

References

Prof. Richard R. Schrock
MIT, Room 6-331
77 Massachusetts Ave.
Cambridge, MA 02139
Phone: 617-253-1596
rrs@mit.edu

Prof. Patrick J. Farmer
Baylor Sciences Building D.208
1 Bear Place
Waco, TX 76706
Phone: 254-710-2746
Patrick_Farmer@baylor.edu

Dr. Jeffrey W. Hudgens
NIST
100 Bureau Dr.
Gaithersburg, MD 20899
Phone: 301-975-2512
jeffrey.hudgens@nist.gov

ACKNOWLEDGEMENTS

During my time at MIT I have had the privilege of meeting and interacting with many bright minds and inspiring people. Many of them deserve recognition for all their help, advice, moral support, and good company.

First of all, I would like to thank my advisor, Professor Richard R. Schrock, who provided me with guidance, advice, a path to follow when I found myself lost, and freedom to explore areas of my own interest. I would also like to thank Professor Stephen J. Lippard for all the helpful discussions and suggestions he had about my research during our annual meetings. Professor Christopher C. Cummins has always put time aside to advice and help me whenever I sought for his aid. Most recently he helped the entire Schrock lab manage a spill, which ensured that nobody would get ill or affected by it. I express my complete gratitude for all his help and support. I thank Professor Daniel Nocera for helping me keep composure during 2nd and 3rd year examinations and for being completely honest with me when I was first deciding which laboratory to join my first year. Last, but not least I want to thank Professor Mircea Dincă for joining my thesis committee during my last year.

Many people within the department of Chemistry have been of invaluable assistance and support, but three individuals deserve special recognition. Macall Coombs, the administrative assistant of the Schrock laboratory, who just became a mother (congratulations!!!), has always made sure that everything runs smoothly in the group and without her the group would have probably crumbled to its knees. Susan Brighton, who recently retired and who worked within the Chemistry Education Office, was always a happy and kind person to interact with. I had the privilege of attending two SACNAS conferences with her to talk to undergraduate students about life at MIT. She certainly lifted the spirits of anyone she interacted with and she will be greatly missed in this department. Melinda Cerny, who is about to retire as well, had nothing but kind words and thanks to her Dr. Maggie Flook and I had the opportunity to complete our teaching requirements during IAP within our first year at MIT.

In my time as a member of the Schrock group, I've come to know many wonderful people. Dr. Rojendra Singh, Dr. Zachary Tonzetich, Dr. Tatiana Pilyugina, Dr. Brian Hanna, Dr. Andrea Garbert, Dr. Annie King, and Dr. Jia Min Chin served as my initial mentors within the lab and helped me become a competent synthetic chemist throughout the years.

When I joined the group, Dr. Rojendra Singh, Dr. Stefan Arndt, Dr. Thorsten Kreickmann, and Dr. Corina Striban were very welcoming and formed my first circle of friends within the group. Later on, Dr. Dennis Hetterscheid would join the inner circle of "international" researchers within the group. Together we enjoyed free wings on Wednesday nights at The Muddy Charles Pub. Dr. Dmitry Peryshkov and Dr. Jian Yuan are the two remaining international chemists in the group and they make synthesis look like a trivial ordeal. They have inspired me to become a better chemist and I thank them for that.

Dr. Brad Bailey, Dr. Brian Hanna, and Daniel Kozera are three people who always made sure to make everyone's days a little brighter by reminding us all that laughing is sometimes the best medicine to a stressful day.

Dr. Stephan Kilyanek is a tenacious and dedicated chemist with whom I had many intellectual and personal conversations and I thank him for that, but most of all for being a good friend.

Dr. Matt Cain is the last person to share a glove-box with me and I thank him for accommodating me and helping me maintain the box.

Dr. Janna Böerner, Dr. Smaranda Marinescu, and Dr. Annie King are three great chemists who are also amazing dance partners. Together, we danced many nights away. Of course, a dance party would not be justified if Dr. Maggie Flook was not mentioned because she was always the life of the party and the reason why the Schrock lab had some of the best Halloween parties in the whole city of Cambridge.

Laura Gerber, Erik Townsend, Daniel Kozera, Jon Axtell, Hyangsoo Jeong, and Dr. Graham Dobereiner are amazing chemists and my collegues. They have stimulated my learning and

curiosity for inorganic synthesis. In particular, I thank Jon and Hyangsoo for all our discussions about chemistry and for proofreading portions of this dissertation.

Dr. Loi Do, Dr. Woon Ju Song, and Dr. Maggie Flook are the oldest friends that I made while at MIT. Together we have shared many moments and their presence has always been a bright spot, even during stressful and discouraging moments at the lab. I cannot thank them enough for being my support group and for truly caring about a Bolivian chemist.

Finally, while a graduate student at MIT, I have had the good fortune of collaborating with many wonderful people and it would be a dishonor not to acknowledge Dr. Peter Müller, Dr. Michael K. Takase and Dr. Bo Li for all their contributions to solving the crystal structures that were presented in this thesis. Without a doubt, their hard work and expertise have contributed a great deal to the overall esthetic of my dissertation. Professor Amir H. Hoveyda of Boston College deserves special recognition for always providing interesting ideas and research paths to follow. Without him, none of Chapter 4 would have come to existence.

I want to thank my siblings, Carmen, C.J., and Nela Lichtscheidl, as well as my dad Carlos Lichtscheidl for their moral support and love of Chemistry :) From the time when my siblings and I came to America, my uncle Bernard and my aunt Rocio gave us the greatest gift of all, to have the opportunity to succeed and move forward. Although the road has not always been smooth and straightforward, their undying love and support were reason enough to continue the journey. There is no one word that can describe how thankful and grateful I am for all their help and doing more than anyone else would have done in their situation. Even though it is somewhat understood, I want to state for the record that they make me more proud of being part of their family than I can ever make them feel proud with my achievements. Thank you!!!

Also, I would like to thank Tammy Somasundaran and her family for all their support, help, and for planning a great congratulations party. The cake was awesome!

Lastly, many people helped me along the way to get here and I give special thanks to the MESA, SURF, and MSP programs, and my undergraduate advisors (Professor Patrick Farmer and Dr. Jeffrey Hudgens) for preparing me to become a scientist.